RADIOTRACER STUDIES OF ADSORPTION ON METHANOL SYNTHESIS CATALYSTS

THESIS

SUBMITTED FOR THE DEGREE

OF

DOCTOR OF PHILOSOPHY

OF THE

UNIVERSITY OF GLASGOW

BY

SUSAN EVITT, B.Sc.

OCTOBER, 1986

ProQuest LLC.
789 East Eisenhower Parkway
P.O. Box 1346
Ann Arbor, MI 48106 – 1346

I dedicate this work,

to my husband, Thomas Andrew Kinnaird,

for his patience and encouragement

over the past three years.

ACKNOWLEDGEMENTS

I would like to express my sincere thanks to Dr. G. Webb, my supervisor, and to Mr. G.C. Chinchen, my industrial supervisor, for proposing the topic for the thesis and for their advice and co-operation over the last three years.

I am indebted to Mr. R.A. Hadden and the rest of my colleagues in surface chemistry for their encouragement and advice and to Mr. T. Boyle and Mr. R. Kennedy for their technical assistance.

Thanks are also due to Mr. C.R. Plant and Mr. M. Shann for their assistance during my industrial visit and to both I.C.I. Agricultural Division and the Science and Engineering Research Council for the award of a C.A.S.E. Studentship.

I gratefully acknowledge the assistance of Dr. D. Parker (Physics and Radioisotopes Group, I.C.I. Petrochemicals and Plastics Division) and for the provision of radioactive materials used in this study.

SUMMARY

The adsorption of carbon dioxide and carbon monoxide on a $Cu/ZnO/Al_2O_3$ methanol synthesis catalyst and the ZnO and Al_2O_3 components of this catalyst, at ambient temperature, has been investigated using a [14-C]radiotracer technique. Before adsorption of the various gases, the catalysts were activated in a stream of 6% hydrogen in argon at 463K.

The relative strengths of adsorption of carbon dioxide and carbon monoxide, on the various catalysts, have been investigated by evacuation and molecular exchange experiments. Exchange between one of the [14-C]labelled carbon oxides pre-adsorbed on each of the catalysts and the other non labelled carbon oxide in the gas phase, together with adsorption measurements for each of the [14-C]carbon oxides after admission of the other non labelled gas, was used to examine the degree of competitive adsorption between the two adsorbates.

The effects, both separate and combined, of oxygen (from nitrous oxide) adsorbed on the copper surface and of hydrogen on the adsorption of carbon dioxide and carbon monoxide on $Cu/ZnO/Al_2O_3$, have also been examined using both the radiotracer method and a microreactor system coupled to a mass spectrometer.

It has been shown that, carbon dioxide adsorbs both weakly and relatively strongly on each of the components of the catalyst. On the copper component, carbon dioxide

dissociates at high energy sites to give adsorbed carbon monoxide and surface oxygen. This adsorbed carbon monoxide is different to that from the species obtained by adsorption of gaseous carbon monoxide in that it is strongly adsorbed and perhaps multiply bonded to the surface. Further slow adsorption of carbon dioxide takes place with oxygen atoms, formed by the dissociative adsorption of carbon dioxide, as well as with surface oxygen remaining after the reduction process to form a carbonate species. Similarly, a slow adsorption of carbon dioxide occurs on the support, forming a more strongly adsorbed species.

A limited amount of surface oxygen on the copper component, does not affect the amount of carbon dioxide adsorbed on the catalyst, although its strength of adsorption is increased. In sharp contrast, when the copper component is fully oxidised, sites for the adsorption of carbon dioxide are initially blocked, adsorption of this gas on fully oxidised copper being a very slow process.

Although hydrogen has little effect on the adsorption of carbon dioxide on reduced $Cu/ZnO/Al_2O_3$, complex formation takes place between carbon dioxide and hydrogen adsorbed on partially oxidised $Cu/ZnO/Al_2O_3$. Hydrogen adsorbs at Cu^+ - Cu^o sites to form hydroxyl groups which react with carbon dioxide possibly to form surface formate species.

In sharp contrast with carbon dioxide, carbon monoxide adsorbs, almost exclusively, on the copper component of the catalyst, where it is adsorbed relatively weakly. Although

CONTENTS

		Page
ACKNOWLEDGEMENTS		
SUMMARY		
CHAPTER ONE	INTRODUCTION	
1.1	Background to the Catalytic Synthesis of Methanol	1
1.1.1	Background to the Role of Copper in Methanol Synthesis Catalysts	3
1.1.2	Background to the Role of ZnO in Methanol Synthesis Catalysts	5
1.1.3	Background to the Role of Al_2O_3 in Methanol Synthesis Catalysts	7
1.1.4	The Active Component(s) of the $Cu/ZnO/Al_2O_3$ "Low Pressure" Methanol Synthesis Catalyst	11
1.2	The Adsorption of Carbon Monoxide, Carbon Dioxide and Hydrogen on $Cu/ZnO/Al_2O_3$ and the Role of Each Gas in the Synthesis of Methanol	22
CHAPTER TWO	OBJECTIVES OF THE PRESENT WORK	53
CHAPTER THREE	EXPERIMENTAL	
3.1	The Vacuum System	54
3.2	The Geiger-Müller System	56
3.3	The Pressure Transducer	58
3.4	The Gas Chromatography System	58
3.5	Catalysts	60
3.5.1	Preparation of a High Surface Area ZnO	62
3.5.2	Preparation of 80% Cu/Al_2O_3	62
3.6	Materials	63
3.6.1	Preparation of [14-C]Carbon Monoxide	64
3.7	Experimental Procedure	65
3.7.1	Catalyst Activation	65
3.7.2	Preparation of Oxidised $Cu/ZnO/Al_2O_3$ Catalyst Samples	65
3.7.2.1	Preparation of Fully Oxidised $Cu/ZnO/Al_2O_3$ Samples	66
3.7.2.2	Preparation of Partially Oxidised $Cu/ZnO/Al_2O_3$ Samples	67

		Page
3.7.3	Corrections to the Observed Count Rates	67
3.7.4	Adsorption Isotherms	69
3.8	Adsorption Studies in a Flow System	70
3.8.1	Experimental	70
3.8.1.1	Materials	71
3.8.2	Experimental Procedure	71
3.8.2.1	Catalyst Activation	71
3.8.2.2	Measurement of Copper Surface Area	72
CHAPTER FOUR	RESULTS	
4.1	Adsorption of [14-C]Carbon Dioxide on Reduced $Cu/ZnO/Al_2O_3$	73
4.1.1	Adsorption of [14-C]Carbon Dioxide on Unreduced $Cu/ZnO/Al_2O_3$	76
4.1.2	The Reversibility of Adsorption of Carbon Dioxide on Reduced $Cu/ZnO/Al_2O_3$	76
4.1.3	Successive Adsorptions/Evacuations of [14-C]Carbon Dioxide on the Same Reduced $Cu/ZnO/Al_2O_3$ Catalyst Sample	79
4.1.4	The Effects of Hydrogen on the Adsorption of Carbon Dioxide on Reduced $Cu/ZnO/Al_2O_3$	79
4.1.5	Adsorption of [14-C]Carbon Dioxide on Reduced $Cu/ZnO/Al_2O_3$ Over a Long Time Period	80
4.2	Adsorption of [14-C]Carbon Monoxide on Reduced $Cu/ZnO/Al_2O_3$	82
4.2.1	Adsorption of [14-C]Carbon Monoxide on Unreduced $Cu/ZnO/Al_2O_3$	82
4.2.2	The Reversibility of Adsorption of Carbon Monoxide on Reduced $Cu/ZnO/Al_2O_3$	82
4.2.3	Successive Adsorptions/Evacuations of [14-C]Carbon Monoxide on the Same Reduced $Cu/ZnO/Al_2O_3$ Catalyst Sample	85
4.2.4	The Effects of Hydrogen on the Adsorption of Carbon Monoxide on Reduced $Cu/ZnO/Al_2O_3$	85
4.2.5	Adsorption of [14-C]Carbon Monoxide on Reduced $Cu/ZnO/Al_2O_3$ Over a Long Time Period	86
4.3	Co-Adsorption of Carbon Dioxide, and Carbon Monoxide on Reduced $Cu/ZnO/Al_2O_3$	86

		Page
4.3.1	Adsorption of [14-C]Carbon Dioxide Followed by the Adsorption of [14-C]Carbon Monoxide on $Cu/ZnO/Al_2O_3$	86
4.3.2	Adsorption of [14-C]Carbon Monoxide Followed by the Adsorption of [14-C] Carbon Dioxide on Reduced $Cu/ZnO/Al_2O_3$	87
4.3.3	Adsorption of [14-C]Carbon Dioxide on a [12-C]Carbon Monoxide Precovered $Cu/ZnO/Al_2O_3$ Surface	87
4.3.4	Adsorption of [14-C]Carbon Monoxide on a [12-C]Carbon Dioxide Precovered $Cu/ZnO/Al_2O_3$ Surface	87
4.3.5	Exchange Between Carbon Dioxide Adsorbed on $Cu/ZnO/Al_2O_3$ and Gas Phase Carbon Monoxide	88
4.3.6	Exchange Between Carbon Monoxide Adsorbed on $Cu/ZnO/Al_2O_3$ and Gas Phase Carbon Dioxide	90
4.4	Adsorption of [14-C]Carbon Dioxide and [14-C]Carbon Monoxide on Cu/Al_2O_3	91
4.4.1	The Reversibility of Adsorption of Carbon Dioxide and Carbon Monoxide on Cu/Al_2O_3	91
4.5	Adsorption of [14-C]Carbon Dioxide and [14-C]Carbon Monoxide on ZnO - A	93
4.5.1	The Reversibility of Adsorption of Carbon Dioxide and Carbon Monoxide on ZnO - A	93
4.5.2	The Effects of Hydrogen on the Adsorption of Carbon Dioxide and Carbon Monoxide on ZnO - A	96
4.5.3	Adsorption of [14-C]Carbon Dioxide on ZnO - A Over a Long Time Period	96
4.5.4	Co-Adsorption of Carbon Dioxide and Carbon Monoxide on ZnO - A	97
4.5.4.1	Adsorption of [14-C]Carbon Dioxide on ZnO - A Followed by the Adsorption of [14-C]Carbon Monoxide and the Adsorption of [14-C]Carbon Monoxide on ZnO - A Followed by the Adsorption of [14-C]Carbon Dioxide	97
4.5.4.2	Exchange Between Carbon Dioxide Adsorbed on ZnO - A and Gas Phase Carbon Monoxide and Exchange Between Carbon Monoxide Adsorbed on ZnO - A and Gas Phase Carbon Dioxide	98

		Page
4.6	Adsorption of [14-C]Carbon Dioxide and [14-C]Carbon Monoxide on ZnO - B	99
4.7	Adsorption of [14-C]Carbon Dioxide and [14-C]Carbon Monoxide on Al_2O_3	100
4.7.1	The Reversibility of Adsorption of Carbon Dioxide on Al_2O_3	101
4.7.2	Adsorption of [14-C]Carbon Dioxide on Al_2O_3 Over a Long Time Period	102
4.8	Adsorption of [14-C]Carbon Dioxide and [14-C]Carbon Monoxide on Oxidised $Cu/ZnO/Al_2O_3$	103
4.8.1	Adsorption of [14-C]Carbon Dioxide and [14-C]Carbon Monoxide on Fully Oxidised $Cu/ZnO/Al_2O_3$	103
4.8.1.1	The Reversibility of Adsorption of Carbon Dioxide and Carbon Monoxide on Fully Oxidised $Cu/ZnO/Al_2O_3$	104
4.8.1.2	The Effects of Hydrogen on the Adsorption of Carbon Dioxide and Carbon Monoxide on Fully Oxidised $Cu/ZnO/Al_2O_3$	105
4.8.1.3	Adsorption of [14-C]Carbon Dioxide and Adsorption of [14-C]Carbon Monoxide on Fully Oxidised $Cu/ZnO/Al_2O_3$ Over a Long Time Period	106
4.8.2	Adsorption of [14-C]Carbon Dioxide and [14-C]Carbon Monoxide on 30% Partially Oxidised $Cu/ZnO/Al_2O_3$	107
4.8.2.1	The Reversibility of Adsorption of Carbon Dioxide and Carbon Monoxide on 30% Partially Oxidised $Cu/ZnO/Al_2O_3$	108
4.8.2.2	The Effects of Hydrogen on the Adsorption of Carbon Dioxide and Carbon Monoxide on 30% Partially Oxidised $Cu/ZnO/Al_2O_3$	109
4.9	Adsorption Studies in a Flow System	110
4.9.1	Adsorption of Carbon Dioxide on $Cu/ZnO/Al_2O_3$	111
4.9.2	Adsorption of Hydrogen on Fully Oxidised $Cu/ZnO/Al_2O_3$	113
CHAPTER FIVE	DISCUSSION	118
5.1	The Adsorption of Carbon Dioxide and Carbon Monoxide on Cu/Al_2O_3	119
5.2	The Adsorption of Carbon Dioxide and Carbon Monoxide on Reduced $Cu/ZnO/Al_2O_3$	120

		Page
5.3	The Adsorption of Carbon Dioxide and Carbon Monoxide on Partially Oxidised and Fully Oxidised $Cu/ZnO/Al_2O_3$	136
5.3.1	The Effects of Hydrogen on the Adsorption of Carbon Dioxide and Carbon Monoxide on Partially Oxidised and Fully Oxidised $Cu/ZnO/Al_2O_3$	140
5.4	General Conclusions.	145

REFERENCES

CHAPTER ONE

1. INTRODUCTION

1.1 Background to the Catalytic Synthesis of Methanol

Methanol is of major industrial importance both as a solvent and as a starting material in a number of chemical processes, for example, in the production of formaldehyde. However, recent developments involving the conversion of methanol to aromatic (1) and aliphatic (2) hydrocarbons have placed even greater emphasis on methanol synthesis in attempts to find an alternative fuel source.

In 1924 methanol was produced almost exclusively by the destructive distillation of wood wastes, the world production of methanol, at this time, being 45,000 tons per annum (3). For the past six decades, however, methanol has been synthesised under various conditions via the hydrogenation of carbon monoxide and carbon dioxide over a variety of ZnO containing catalysts. As a result of the development of the catalytic synthesis, production of methanol in the United States in 1953 exceeded 480,000 tons (4). The relatively cheap and plentiful supply of coal and natural gas favours this process compared to the manufacture of methanol from crude oil.

Although the catalytic hydrogenation of carbon monoxide and carbon dioxide to methanol is a highly selective process, exhibiting greater than 99% selectivity, methanol is one of the least thermodynamically stable products in the reaction. The standard free energies of formation of a number of

hydrocarbons and alcohols from the reaction of carbon monoxide with hydrogen as a function of temperature are shown in Figure 1.1. From this, it can be seen that, at kinetically favourable temperatures, the formation of higher alcohols and hydrocarbons is thermodynamically preferred to that of methanol. However, the products formed in the reaction of carbon monoxide with hydrogen can be controlled kinetically by careful selection of temperature and pressure and by the use of an appropriate catalyst. Figures 1.2 and 1.3 summarise the conditions and catalysts employed in the synthesis of a variety of products from the reaction of carbon monoxide with hydrogen.

The hydrogenation of both carbon monoxide and carbon dioxide to methanol are exothermic processes:

$$CO + 2H_2 \rightleftharpoons CH_3OH \qquad \Delta H_{600K} = -100.46 \text{ KJ mol}^{-1}$$

$$CO_2 + 3H_2 \rightleftharpoons CH_3OH + H_2O \qquad \Delta H_{600K} = -61.59 \text{ KJ mol}^{-1}$$

and hence are more favourable at lower temperatures. In practice, methanol synthesis is performed by operating at low temperatures, high pressures, high carbon monoxide: hydrogen ratios and high space velocities, which minimise the side reactions. The catalysts used in this process have been developed largely through empirical research, with no real understanding of the mechanism of the reaction or of the nature of the active centres involved in the conversion.

The first large scale catalytic synthesis of methanol was carried out by Badische Anilin and Soda Fabrik (B.A.S.F.)

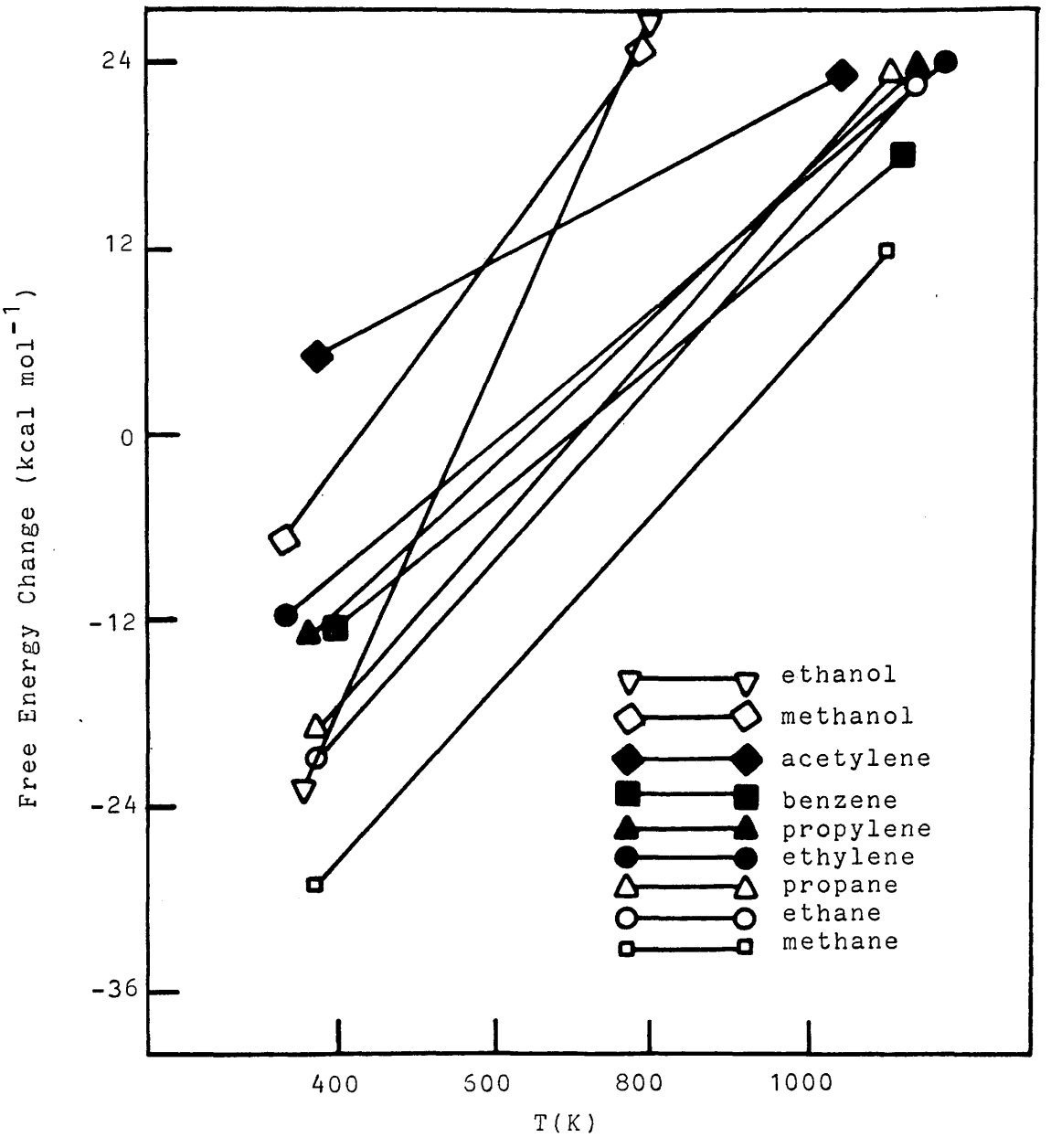

Figure 1.1 Standard Free Energies of Formation for Synthesis of Hydrocarbons and Alcohols from Carbon Monoxide and Hydrogen with Water as Byproduct (5).

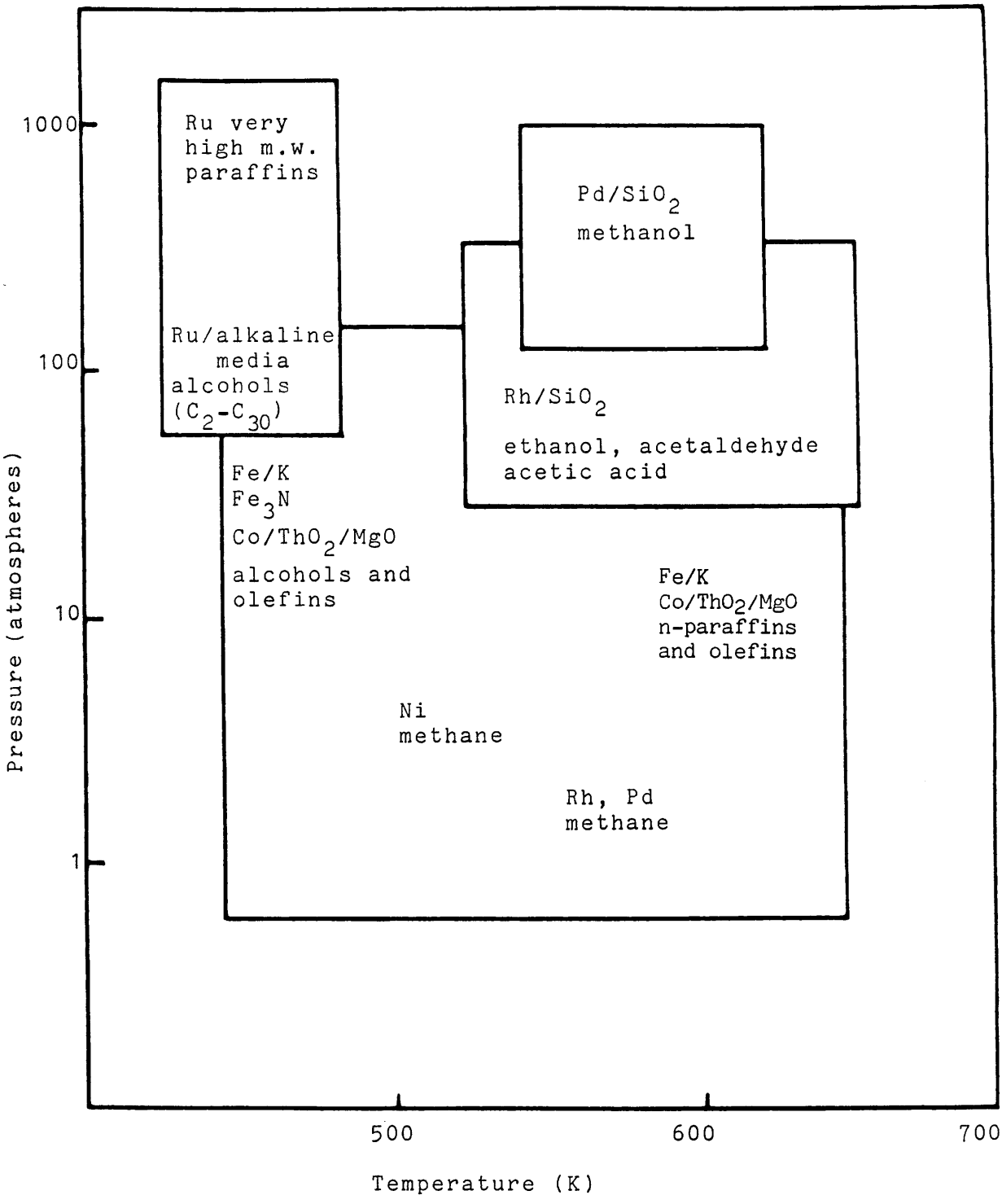

Figure 1.2 Products from the Reaction of Carbon Monoxide with Hydrogen over Transition Metals at Various Temperatures and Pressures (5).

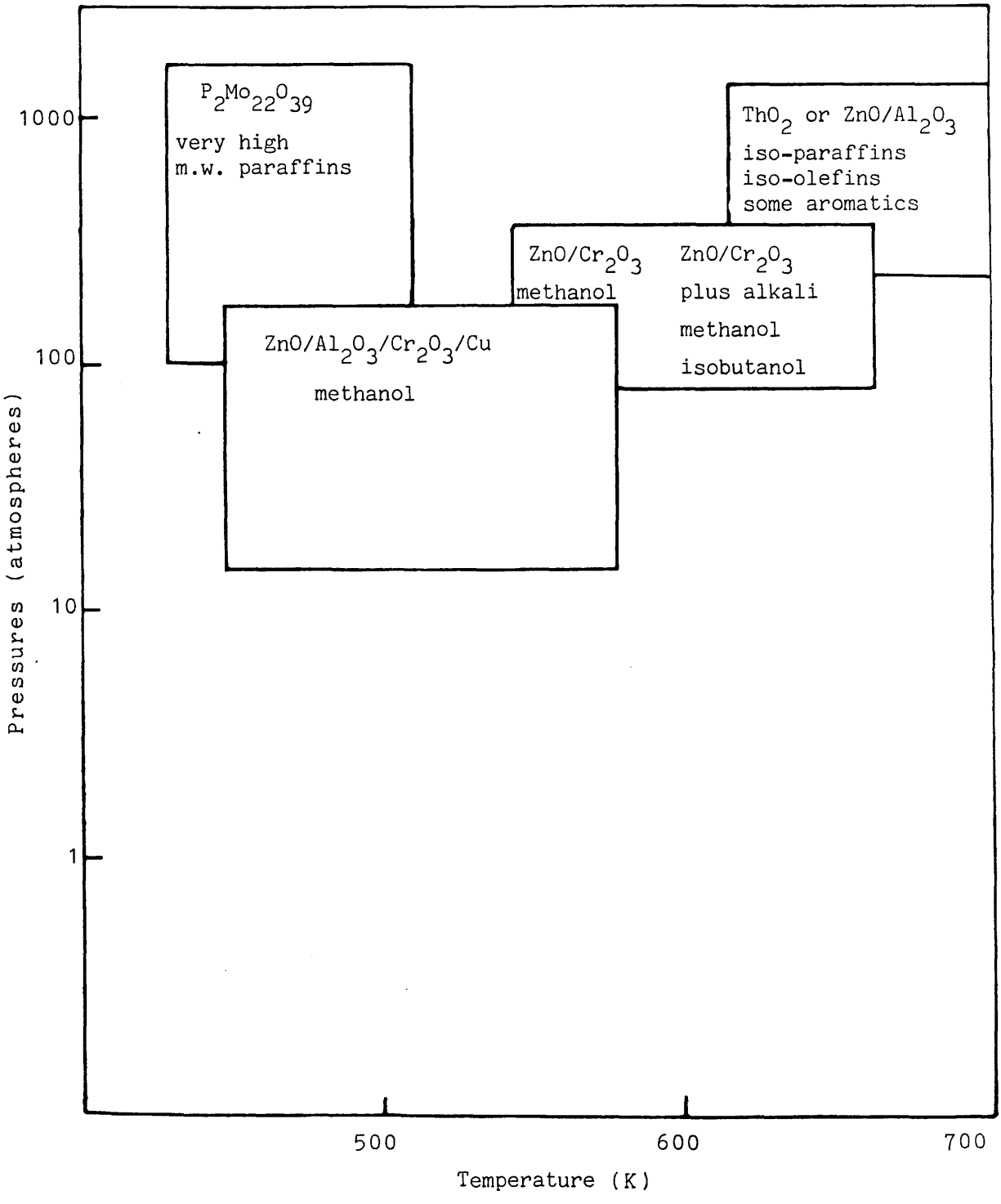

Figure 1.3 Products from the Reaction of Carbon Monoxide with Hydrogen Over Oxide Catalysts at Various Temperatures and Pressures (5).

(6) in 1923. This "high pressure" process operated at pressures of 200 - 350 atmospheres and temperatures of 573 - 673K and employed a catalyst based on ZnO and Cr_2O_3. The development of this process was reviewed by Natta in 1955 (7).

Between 1920 and 1930 B.A.S.F. patented a large number of catalysts for methanol synthesis. The catalysts found to be most active were based on ZnO or CuO. Despite its high activity CuO was not a component of the catalysts used in the "high pressure" process. Indeed, as late as 1955, Natta (7) maintained that the use of copper-containing catalysts was impractical due to their rapid ageing and their high sensitivity to poisons.

A major development in the synthesis of methanol from synthesis gas (carbon monoxide, carbon dioxide and hydrogen), came in the 1960's with the invention, by I.C.I., of the "low pressure" process operating at pressures of ca. 50 atmospheres. The "low pressure" catalysts contain copper and have higher activities than those based on ZnO. Hence they can be used at lower temperatures (473 - 523K), where the thermodynamics of methanol synthesis are more favourable. In addition to copper these catalysts contain ZnO and a structural promoter such as Cr_2O_3 or more commonly, Al_2O_3.

1.1.1 Background to the Role of Copper in Methanol Synthesis Catalysts

The promotion of methanol synthesis catalysts by copper

was first discovered by M. Patart (8), who, in the 1920's, patented these catalysts for the synthesis of methanol at pressures of 150 - 200 atmospheres and temperatures of 573 - 873K. Despite this discovery, it was not demonstrated until much later that the Cu/ZnO catalysts would operate at lower temperatures and pressures.

A number of conflicting reports have been published concerning the activity of unsupported copper for methanol synthesis. Audibert and Raineau (9) found that copper was active for the synthesis of methanol, but stressed that the method by which it was prepared was important. Cuprous oxide and cupric oxide were both found to be active, after reduction with hydrogen, when prepared from the nitrate salt or by the thermal decomposition of the unstable copper salts of inorganic acids. However, cuprous oxide prepared from chloride or sulphate solutions was found to be totally inactive. These authors also pointed out the importance of keeping the reduction temperature as low as possible, emphasising the sensitivity of this single component catalyst to heat. Klier (10), in a more recent study, found that a copper catalyst prepared from $[Cu_2(OH)_3NO_3]$, which had been precipitated from the reaction of copper nitrate with sodium carbonate and calcined at temperatures less than 623K, was inactive for methanol synthesis.

Friedrich et al (11), however, found that a Raney copper catalyst, with a BET surface area of $17m^2\ g^{-1}$, had good catalytic activity for methanol synthesis and suggested that the lack of activity observed by Klier could have been

due to sintering of the copper which was not observed, in the short term, with the Raney copper catalysts.

1.1.2 Background to the Role of ZnO in Methanol Synthesis Catalysts

ZnO, as well as being an important component of the "low pressure" process catalysts is the basis of catalysts used in the "high pressure" process. Indeed, Natta (7) reported ZnO to be the most selective of all catalysts for the synthesis of methanol under "high pressure" conditions.

Pure ZnO is both active in the synthesis (12, 13, 14) and decomposition (15, 16, 17, 18) of methanol. However, highly active forms of ZnO have a short life and, as such, have never been used in the industrial process. The activity of ZnO depends critically upon its method of preparation. Natta (7) proposed that the different activity of ZnO prepared by the combustion of metallic zinc compared with that of ZnO prepared from Zn^{2+} salts, whose anion has a reducing action e.g. $Zn(CH_3COO)_2$ was related to the different number of anionic deficiencies in the two samples. ZnO prepared from $Zn(CH_3COO)_2$ was found to be more active and this was attributed to the greater number of anionic deficiencies in this form of ZnO due to the presence of metallic zinc. Recent work by Bowker et al (14) reported that the rate of methanol synthesis from carbon dioxide and hydrogen increased initially tenfold on a "more highly defective" form of ZnO. This particular form of ZnO was prepared by the interaction of carbon monoxide and hydrogen

on polycrystalline ZnO at temperatures of 523K and 543K. They concluded, therefore, that the increased number of anion defects created by this interaction were the sites responsible for carbon dioxide adsorption and its conversion to methanol.

Studies carried out on the decomposition of methanol on ZnO have produced a similar correlation between activity and stoichiometry of ZnO. Dandy (16) tested two samples of ZnO which had been thermally decomposed under different atmospheres and concluded that methanol decomposition on ZnO involved zinc sites, differing amounts of which were created in the different thermal pretreatments. Morelli et al (18), using ZnO pelleted at various pressures, suggested that the increase in activation energy for the decomposition of methanol, exhibited by samples pelleted at high pressures, was attributable to the increase in oxygen content observed with these samples. These reports tend to suggest a correlation between the synthesis and decomposition of methanol. However, Natta (7) pointed out that there was a lack of "satisfactory similarity" between the catalytic activity for the reaction of synthesis and that of decomposition of methanol on ZnO. This was borne out by the observation that ZnO produced by the combustion of metallic zinc was a very poor catalyst for the synthesis of methanol, but was active in the decomposition reaction. Frolich et al (19), working with copper based catalysts found that $Cu(OH)_2$ precipitated by NaOH was very active in methanol

decomposition only if not washed free of its impurities. However, a catalyst precipitated by NH_4OH was not very active. In contrast to this, the $Cu(OH)_2$ catalysts obtained by NaOH precipitation showed lower activities for the synthesis of methanol than those precipitated by NH_4OH. Natta (7) concluded that earlier studies of the catalytic decomposition of methanol, which involved measuring the carbon monoxide and hydrogen released in the reaction, gave inaccurate results due to the formation of other products in the reaction, for example, formaldehyde.

1.1.3 Background to the Role of Al_2O_3 in Methanol Synthesis Catalysts

As well as CuO and ZnO components, methanol synthesis catalysts contain promoters, generally in the form of high melting oxides which are difficult to reduce. Examples of such promoters include Cr_2O_3 and Al_2O_3. The catalysts for the "high pressure" process are promoted with Cr_2O_3, although many other substances have been reported to be promoters in this system. These promoters have the common property of being, themselves, poor hydrogenation catalysts and their main function is to inhibit the sintering of ZnO and therefore stabilise the vacant lattice sites, which are present to a greater or lesser degree in ZnO depending upon its method of preparation.

Some promoters form solid solutions with ZnO. An example is cadmium, which is often present as a solid

solution in Smithsonite (mineral $ZnCO_3$). The high activity of Smithsonite for the synthesis of methanol (20) was believed to be due to this solid solution. In general, those zinc minerals which give rise to the most active catalysts, contain small amounts of divalent oxides, which are believed to behave as promoters. Other substances which have a promotional effect on ZnO and ZnO/Cr_2O_3 for methanol synthesis include MgO (7), ThO_2 (21), ZrO_2 (21), TaO_2 (21) and V_2O_5 (6).

The most important promoter of ZnO in "high pressure" process catalysts is Cr_2O_3. Although Cr_2O_3 is active for the synthesis of methanol, its activity is very low and, as with zinc oxide, dependent upon its method of preparation. Various types of Cr_2O_3 have been tested for catalytic activity (12, 22, 23, 24). However, only a few varieties of Cr_2O_3, for example, that from $Cr(OH)_3$ which was precipitated from $Cr(NO_3)_3$ with ammonia, were found to possess a relatively high catalytic activity (24). Many investigators have studied the ZnO/Cr_2O_3 system in an attempt to discover the reasons for the promotional effect of Cr_2O_3 on ZnO.

Huttig et al (25, 26, 27, 28) in a study of ZnO/Cr_2O_3 catalysts, concluded that a solid state reaction took place at 873K with the formation of spinel. Natta (7) reported that a mixture of ZnO and amorphous zinc chromite ($ZnCr_2O_4$), produced by the low temperature reduction of zinc chromate ($ZnCrO_4$), was found to exhibit high catalytic activity. Zinc chromite alone was reported to have low catalytic

activity and hence Natta (7) suggested that zinc chromite was not a good catalyst for methanol synthesis but was a good promoter with the promotional effects being due to prevention of the sintering of ZnO. Further evidence for zinc chromite acting purely as a promoter in this system was reported by Natta, who found that the activation energy for the synthesis of methanol on a catalyst containing 11% by weight of chromium, 7 kcal mol^{-1}, was equal to the activation energy for the synthesis on pure ZnO.

In contrast with these reports, Ogino et al (29) reported that the activity and selectivity of a ZnO/Cr_2O_3 catalyst could be elevated by increasing the surface concentration of zinc chromite. Similar conclusions were drawn by Ogino and Nakajima (30), who studied the decomposition of methanol on ZnO/Cr_2O_3 catalysts. These authors concluded that the activity of the ZnO/Cr_2O_3 catalyst was closely related to the surface structure of the zinc chromite.

Natta (7) reported that Al_2O_3 had a similar effect to Cr_2O_3, combining with ZnO to give a spinel ($ZnAl_2O_4$). He concluded that the promotional effect of Al_2O_3 was less than that of Cr_2O_3 and, because Al_2O_3 favoured the dehydration of methanol to dimethyl ether at high temperatures, it was rendered impractical as a promoter of ZnO based catalysts.

In spite of Natta's conclusion, the development of copper based catalysts for the synthesis of methanol has enabled the system to operate at relatively low temperatures

and Al_2O_3 is now widely used as a structural promoter in catalysts for the synthesis of methanol.

Although the effects of Al_2O_3 in the $Cu/ZnO/Al_2O_3$ catalyst have been accepted by the various investigators as being purely secondary to that of copper and ZnO, several roles have been attributed to Al_2O_3 in this system.

Andrew (31) pointed out the importance of crystalline zinc aluminate spinel ($ZnAl_2O_4$), which is deliberately added to I.C.I. catalysts in order to stabilise the catalyst for long-term performance. He suggested that the function of the zinc aluminate was to maintain the copper particles in a finely dispersed state.

Other preparations of $Cu/ZnO/Al_2O_3$ catalysts result in the formation of Al_2O_3 which is in an X-ray amorphous form. Herman et al (32) suggested that the role of amorphous Al_2O_3 was to stabilise the highly dispersed Cu/ZnO binary catalyst. These authors compared the activity of a $Cu/ZnO/Al_2O_3$ catalyst containing 52.4% copper, 24.3% ZnO and 23.3% Al_2O_3 with the activities of Cu/ZnO binary catalysts of different compositions and concluded that the only effect of Al_2O_3 appeared to be structural promotion.

In contrast to Herman et al, Fischer et al (33) reported that the role of amorphous alumina was the induction of surface defects by "endotactic" inclusion of Al_2O_3 clusters in copper.

Klier (10) has concluded that all of these effects may take place to varying degrees in the commercial catalysts.

1.1.4 The Active Component(s) of the $Cu/ZnO/Al_2O_3$ "Low Pressure" Methanol Synthesis Catalyst

Considerable debate still exists between the various investigators concerning the active component(s) of the $Cu/ZnO/Al_2O_3$ catalyst in the synthesis of methanol from carbon monoxide, carbon dioxide and hydrogen.

Several investigators noted that the activity of pure copper and pure zinc oxide was enhanced when mixtures of the two were formed. Kostelitz and Hüttig (34) reported that, in the decomposition of methanol, mixed catalysts of CuO/ZnO exhibited higher activities than the two separate components. These authors concluded that a "synergic promotion" took place in the zinc oxide rich catalysts, which also displayed the highest activity. They believed this "synergic promotion" was a promotion due to chemical and physical interactions of the catalyst components, as opposed to "structural promotion", which is associated with increasing or maintaining the surface area of the active phase.

As in the case of ZnO, the question still arose, however, as to whether or not it was valid to assess the activity of CuO/ZnO catalysts for activity for methanol synthesis by studying the decomposition reaction. Sabatier et al (35, 36) found that many catalysts, including copper, were active for the decomposition of methanol, but copper was reported to be inactive for the synthesis of methanol(6). Frolich et al (37, 38, 39) studied the decomposition and synthesis of methanol over a variety of CuO/ZnO catalysts and postulated

that there was a close relationship between the synthesis and decomposition of methanol. Pure copper was found to decompose methanol to give predominantly formaldehyde, whilst addition of a small percentage of zinc oxide to copper caused the formation of methyl formate. Further addition of ZnO led to the formation of carbon monoxide. He concluded that those catalysts which decomposed methanol to carbon monoxide, that is, beyond formaldehyde and formate stages, were good catalysts for the synthesis of methanol by the reverse reaction involving the high pressure reduction of carbon monoxide. The authors also reported that pure ZnO was active in the synthesis and decomposition of methanol, but pure copper, although active for the decomposition, was inactive for methanol synthesis.

Although the mutual promotion effect of CuO and ZnO was agreed upon by the various investigators, much conflict existed concerning the optimum amounts of each component for maximum activity. Patart (7) reported that maximum activity for the synthesis and decomposition of methanol was exhibited by a CuO/ZnO catalyst containing 10% ZnO and this was later confirmed by Fleury (40). Frolich et al (37, 38, 39) however, reported that the most efficient catalysts contained between 30% and 40% CuO. In order to explain this observation Frolich et al (39) carried out a study of a variety of CuO/ZnO catalysts involving X-ray determination of the lattice constants of copper and ZnO over the entire range. The authors found that the rate of decomposition of methanol to

carbon monoxide correlated with changes in the lattice constant of ZnO and that the decomposition of methanol to methyl formate correlated with changes in the lattice constant of copper. The authors concluded that the mechanism by which methanol decomposed on the catalysts was strongly influenced by the composition of the catalysts but they did not offer further interpretation of these results.

In an attempt to elucidate the nature of the active site, which is responsible for the enhanced activity observed when pure CuO and ZnO are intimately mixed, Herman et al (41, 42, 43) carried out a study of $CuO/ZnO/Al_2O_3$, $CuO/ZnO/Cr_2O_3$, CuO/ZnO catalysts, pure CuO and ZnO. These studies were undertaken using a variety of surface physics techniques as well as electron microscopy. The two and three component catalysts were prepared from basic 1 M solutions of $Cu(NO_3)_2$ and $Zn(NO_3)_2$ by the dropwise addition of Na_2CO_3 and calcination at temperatures less than 623K. The precipitates formed were $Cu_2(OH)_3NO_3$, $Zn_5(OH)_6(CO_3)_2$ and $(Cu,Zn)_2(OH)_2CO_3$.

X-ray diffraction measurements of the calcined binary and ternary catalysts revealed between 2 and 4% less than the theoretical amount of CuO. This percentage of CuO has been attributed to a Cu^I species dissolved in the ZnO matrix. Further evidence for this was obtained from X-ray fluorescence analysis in a Scanning Transmission Electron Microscope. An optical absorbance in the near infrared has also been assigned to Cu^I in the ZnO lattice. Upon reduction of these

binary and ternary catalysts the amount of Cu^{I} dissolved in ZnO was reported to have increased to 12% in the binary- and 16% in the ternary-catalysts.

Herman et al pointed out that dissolution of Cu^{I} in ZnO is favoured by the fact that Cu^{I} is isoelectronic with Zn^{II} and assumes, like Zn^{II}, a tetrahedral coordination in many of its inorganic compounds. The limitation of this dissolution is the requirement of electroneutrality upon substitution of some Zn^{II} by Cu^{I}, which must be maintained either by oxygen loss or by the presence of interstitial cations. However, a further increase in the concentration of dissolved Cu^{I} ions could be obtained upon the simultaneous dissolution of trivalent ions. This may account for the greater amount of dissolved Cu^{I} observed in the reduced $Cu/ZnO/Al_2O_3$ catalyst, compared to that in the Cu/ZnO binary catalyst.

The precipitates formed during the precipitation of these catalysts, $Cu_2(OH)_3NO_3$, $Zn_5(OH)_6(CO_3)_2$ and $(Cu,Zn)_2(OH)_2CO_3$, were found not to influence the phase composition of the calcined CuO/ZnO, or the reduced Cu/ZnO samples. However, they did effect the catalyst dispersion and morphology. Indeed, Herman observed a completely different morphology for the binary catalysts between 40% and 60% CuO to that found in catalysts containing between 2% and 30% CuO although, within any one range, no major differences in morphology were observed. It was also found that the ternary systems, 60% $CuO/ZnO/Cr_2O_3$ and 60%

$Cu/ZnO/Cr_2O_3$, exhibited the same morphological features as those found in the 67% CuO/ZnO and 67% Cu/ZnO catalysts respectively.

Herman et al found that the particles of the components of the calcined binary catalysts, CuO/ZnO, containing between 40% and 67% CuO were larger than those of catalysts containing between 2% and 30% CuO and the interconnected network of ZnO crystallites, characteristic of the latter range of catalysts, was not present. The CuO particles were found to be of a similar morphology to those in pure CuO. Upon reduction, these particles changed shape and formed irregular crystallites of copper metal, similar to those observed in the reduction of pure CuO. In addition, some preferential orientation of copper was revealed, which indicated a frequent orientation of the Cu(110) planes parallel to the surface of the supporting film. Herman et al proposed that the CuO dispersion produced as a final result of the calcination and the dispersion of the subsequently reduced copper, was determined by the decomposition of the precursor precipitates $(Cu,Zn)_2(OH)_2CO_3$ and $Cu_2(OH)_3NO_3$, the latter predominating for copper concentrations in excess of 40%. $(Cu,Zn)_2(OH)_2CO_3$ was found to give rise to fine dispersions, while $Cu_2(OH)_3NO_3$ gave larger crystals of CuO. Hence, after reduction, large crystals of copper occurred in the 40% to 67% copper catalysts. Addition of Cr_2O_3, after precipitation, was found to have no effect on the catalyst morphology and

structure.

The ZnO particles in those catalysts, containing between 40% and 67% CuO, were found to be separate crystals of platelet appearance, with hexagonal outline and major dimension of the order 70 - 120 nm. There was evidence for a preferential formation of Zn (0001) basal planes at the surface and no significant changes were observed upon reduction. An electron exchange was proposed to occur between the interface of the Cu (211) and the preferentially formed Zn ($10\bar{1}0$) planes for those catalysts containing between 5% and 30% copper. This electron exchange was believed to be much less significant for those catalysts containing between 40% and 67% copper due to the limited contact between the copper particles and the ZnO crystallites in this range of catalysts.

Herman et al compared the activity of the catalysts for methanol synthesis with the morphology of the various components within these systems and concluded that, because the activity of the binary catalysts was much greater than that of the pure components and because the only new interaction observed in all of these catalysts was a Cu^{I}/ZnO phase, the promotional effect could only come from this species. Thus, the activity and selectivity of the "low pressure" methanol synthesis catalyst was proposed to be due to the simultaneous presence of copper and ZnO, the effects of Al_2O_3 and Cr_2O_3 being purely secondary.

The observation of a copper solution within the ZnO

lattice has since been reported by a number of investigators using a variety of techniques, including XRD (44) and XPS (45). The XPS study (45) also provided evidence for a zinc solution within the CuO lattice. XANES (46) and EXAFS (47) studies by Vlaic et al failed to confirm the presence of $Cu^{I}(ZnO)$, within the detection limits of these techniques.

Amenomiya and Tagawa (48) concluded that, since methanol was not detected by the reaction of carbon dioxide and hydrogen over a 12% ZnO/Al_2O_3 catalyst at temperatures below 545K, copper was an essential component of the active site in $Cu/ZnO/Al_2O_3$ catalysts for the low temperature synthesis of methanol from carbon dioxide and hydrogen. They reported that the methanol synthesis activity of the catalyst increased with ZnO content, until a plateau was reached at an atom ratio of Cu:ZnO of 1 and suggested that this provided evidence in support of conclusions reached by Klier and co-workers (41 - 43) who maintained that the active site was associated with a pair of Cu and Zn sites. Further evidence in support of the argument that the activity of the low temperature methanol synthesis catalyst requires the simultaneous existence of copper and zinc has been provided by Bridgewater et al (49). These authors studied the synthesis of methanol from carbon monoxide, carbon dioxide and hydrogen over Raney Cu-Zn catalysts. They found that Raney copper and Raney zinc both showed low or undetectable activity for methanol synthesis at 513K. For each alloy the aluminium and zinc levels dropped with

increasing extraction time, the latter being the length of time which the catalyst was in contact with the sodium hydroxide leaching solution. In general the authors found that, for any one alloy the overall conversion of carbon monoxide and carbon dioxide to methanol measured after 3 hours on stream, rose and passed through a maximum with increasing extraction time.

Several investigators have reported that copper is the active component in low temperature methanol synthesis catalysts. Andrew (31) studied the synthesis of methanol from carbon monoxide, carbon dioxide and hydrogen over $Cu/ZnO/Al_2O_3$ catalysts and reported a correlation between activity and copper surface area. This work was later confirmed by Chinchen et al (50), who stated that only the copper surface was implicated in the rate determining step in the synthesis of methanol under industrial conditions. They also concluded that no unique synergy exists in the Cu/ZnO system, similar effects having been obtained for supports as diverse as MgO and SiO_2. Andrew (31) proposed that the ZnO merely acted as a scavenger of poisons present in the synthesis gas and that Al_2O_3 prevented sintering of the catalyst.

Friedrich et al (11) reported that, in a study of methanol synthesis over fully extracted Raney Cu-Zn catalysts, maximum activity was exhibited by catalysts containing approximately 97 wt % copper. These catalysts consisted of copper crystallites of similar size to those

(50 - 70 Å diameter) which Andrew (31) concluded were highly active in methanol synthesis. Both Raney copper and Cu/SiO_2 catalysts, with BET surface areas of $17m^2\ g^{-1}$ and $41.5m^2\ g^{-1}$ respectively, were active in the production of methanol from carbon monoxide and hydrogen and it was concluded that copper was the active component for the hydrogenation of carbon monoxide on fully extracted Raney Cu-Zn catalysts.

Work has been carried out to reveal the chemical state of copper in the low temperature methanol synthesis catalyst both after reduction and during operation. Okamoto et al (51,52), using XPS, have studied the surface state of CuO/ZnO catalysts reduced at 523K with hydrogen. Catalysts with < 25 wt % CuO were found to contain a monovalent copper species at the surface. In high copper content catalysts (> 25 wt % CuO), the copper was present predominantly as copper metal particles. In contrast, in the low copper content catalysts (< 10 wt % CuO) the major metallic copper species was a two dimensional epitaxial copper layer over the ZnO. It was concluded that both the two dimensional copper metal layer and the monovalent copper species were formed from the reduction of Cu^{2+} dissolved in the ZnO lattice, whereas the well-dispersed copper particles originated from crystalline and amorphous copper oxide phases. The two dimensional copper species was found to be preferentially reoxidised to Cu^{+} when exposed to air at room temperature and it was suggested that

the two dimensional Cu^{o} - Cu^{+} species was the species active in methanol synthesis from carbon monoxide and hydrogen.

In a similar study, using XPS, Apai et al (53) provided evidence that, in Cu/Cr_2O_3 catalysts, a monovalent copper species was extant and was stable to hydrogen reduction at 523K. The authors correlated the amount of surface stable Cu^{+} species and activity for methanol synthesis from carbon monoxide and hydrogen. They concluded that this was the first direct evidence for Cu^{+} as the associative carbon monoxide and, consequently, alcohol producing site on these catalysts.

Fleisch and Mieville (54), using XPS, found that complete reduction of CuO in $CuO/ZnO/Al_2O_3$ took place at 413K. These authors also studied the catalyst surface after reaction with a stream of carbon dioxide/carbon monoxide/ hydrogen (2/25/73) and found that the surface was composed entirely of metallic copper and ZnO. There was no evidence for the presence of Cu^{+} on the surface within the detection limits of the technique (> 2%).

Chinchen and Waugh (55) measured the copper area of a $Cu/ZnO/Al_2O_3$ catalyst before and after treatment with various compositions of synthesis gas using nitrous oxide and the technique of frontal chromatography (56). The authors found that, during operation, the copper was in a partially oxidised state and that the extent of oxidation depended on the carbon dioxide:carbon monoxide ratio in the synthesis gas, a maximum oxygen coverage (ca. 40%)

having been recorded for a ratio of carbon dioxide:carbon monoxide::1:3. They explained the lack of Cu^{+} species, reported by Fleisch and Mieville (54), as being a result of the low carbon dioxide:carbon monoxide ratio (ca. 0.08) used in the latter author's study. By extrapolation from the results obtained by Chinchen and Waugh, a carbon dioxide:carbon monoxide ratio of 0.08 would have produced an oxygen coverage of less than 2%, which was below the detection limits of the apparatus used by Fleisch and Mieville. Chinchen et al (57) proposed that methanol synthesis occurred at Cu/Cu^{I} sites which, as previously mentioned, Okamoto et al (51,52) concluded to be the active site.

Further evidence in support of the argument that, during operation, copper is in a partially oxidised state was provided by Gusi et al (44), who determined the copper surface area of $Cu/ZnO/Al_2O_3$ catalysts after reaction with synthesis gas, by nitrous oxide decomposition. They provided evidence for three different types of copper containing species in the spent catalysts namely, metallic copper, CuO and copper which could not be detected by XRD. The latter was attributed to Cu^{+} dissolved in the ZnO lattice. They concluded that a form of easily reoxidisable copper and the copper species inside the ZnO lattice were the active species in methanol synthesis.

1.2 The Adsorption of Carbon Monoxide, Carbon Dioxide and Hydrogen on $Cu/ZnO/Al_2O_3$ and the Role of Each Gas in the Synthesis of Methanol

Methanol is produced industrially via the following process:-

$$CO/CO_2/H_2 \rightleftharpoons[Cu/ZnO/Al_2O_3] CH_3OH$$

A mixture of carbon monoxide, carbon dioxide and hydrogen (10% carbon monoxide, 10% carbon dioxide and 80% hydrogen) is passed over a $Cu/ZnO/Al_2O_3$ (60/30/10) catalyst at a space velocity of 40,000 hr^{-1} to produce methanol with greater than 99% selectivity (58). The use of a copper-based catalyst allows the synthesis to be carried out under the relatively low temperature and pressure conditions of ca. 523K and ca. 50 atmospheres respectively. This is a well established industrial process, although the mechanism whereby such conversion occurs is still a matter of considerable debate. In particular, the nature and role of the adsorbed carbon monoxide and carbon dioxide in the hydrogenation reaction is not well understood.

Kagan et al studied the synthesis of methanol from carbon dioxide and hydrogen (59) and carbon monoxide and hydrogen (60) over $Cu/ZnO/Al_2O_3$ and concluded that methanol was synthesised via the direct hydrogenation of carbon dioxide and not through the intermediate formation of carbon monoxide which had been previously assumed by various investigators. In the first of these studies (59) the

authors pointed out the difficulty involved in assessing which of the gases, carbon monoxide or carbon dioxide was hydrogenated to methanol because of the water-gas shift reaction which rapidly became established on the surface:-

$$CO + H_2O \rightleftharpoons CO_2 + H_2 \qquad (1)$$

To avoid the formation of this equilibrium the authors carried out the synthesis at a high space velocity which reduced the contact time of the reactants with the surface.

In the second of these reports (60), Kagan et al studied the hydrogenation of carbon monoxide over $Cu/ZnO/Al_2O_3$. They found that when the carbon monoxide and hydrogen mixture was subjected to purification from carbon dioxide and water (which prevented the formation of carbon dioxide from carbon monoxide via reaction (1)) methanol synthesis ceased and recommenced only after the purification was stopped. The authors concluded that methanol synthesis from carbon monoxide and hydrogen took place only through the formation of carbon dioxide as an intermediate product and that no direct pathway existed for the hydrogenation of carbon monoxide.

Kagan et al (61) further demonstrated that the source of carbon in methanol was from carbon dioxide and not carbon monoxide using [14-C] labelled carbon monoxide and [14-C] labelled carbon dioxide. They believed that, at high space velocities, if methanol was produced via reaction (2):-

$$CO + 2H_2 \longrightarrow CH_3OH \qquad (2)$$

then the specific radioactivity of methanol would have been equal to that of carbon monoxide averaged over the experiment. However, if methanol was produced via reaction (3):-

$$CO + H_2O \longrightarrow CO_2 + H_2 \xrightarrow{2H_2} CH_3OH + H_2O \qquad (3)$$

then the specific radioactivity of methanol would have been equal to that of carbon dioxide averaged over the experiment. Their results indicated that the specific radioactivity of the methanol produced was between the initial and final values of that of carbon dioxide and hence they concluded that even with a predominance of carbon monoxide in the reaction mixture, the main direction for the synthesis of methanol was from carbon dioxide via equation (3).

This work has recently been repeated and confirmed by Chinchen et al (57). These authors studied the synthesis of methanol from synthesis gas containing equal moles of carbon monoxide and carbon dioxide over $Cu/ZnO/Al_2O_3$ under standard methanol synthesis conditions. In order to distinguish the two carbon oxides, the authors used [14-C] labelled carbon dioxide and prevented 'scrambling' of the radioactivity via reaction (1) by using high space velocities. They reported that at very high space velocities the [14-C] activity of methanol was the same as that in the inlet carbon dioxide (Figure 1.4) and hence deduced that methanol synthesis proceeded via carbon dioxide. Using these results and results obtained from temperature

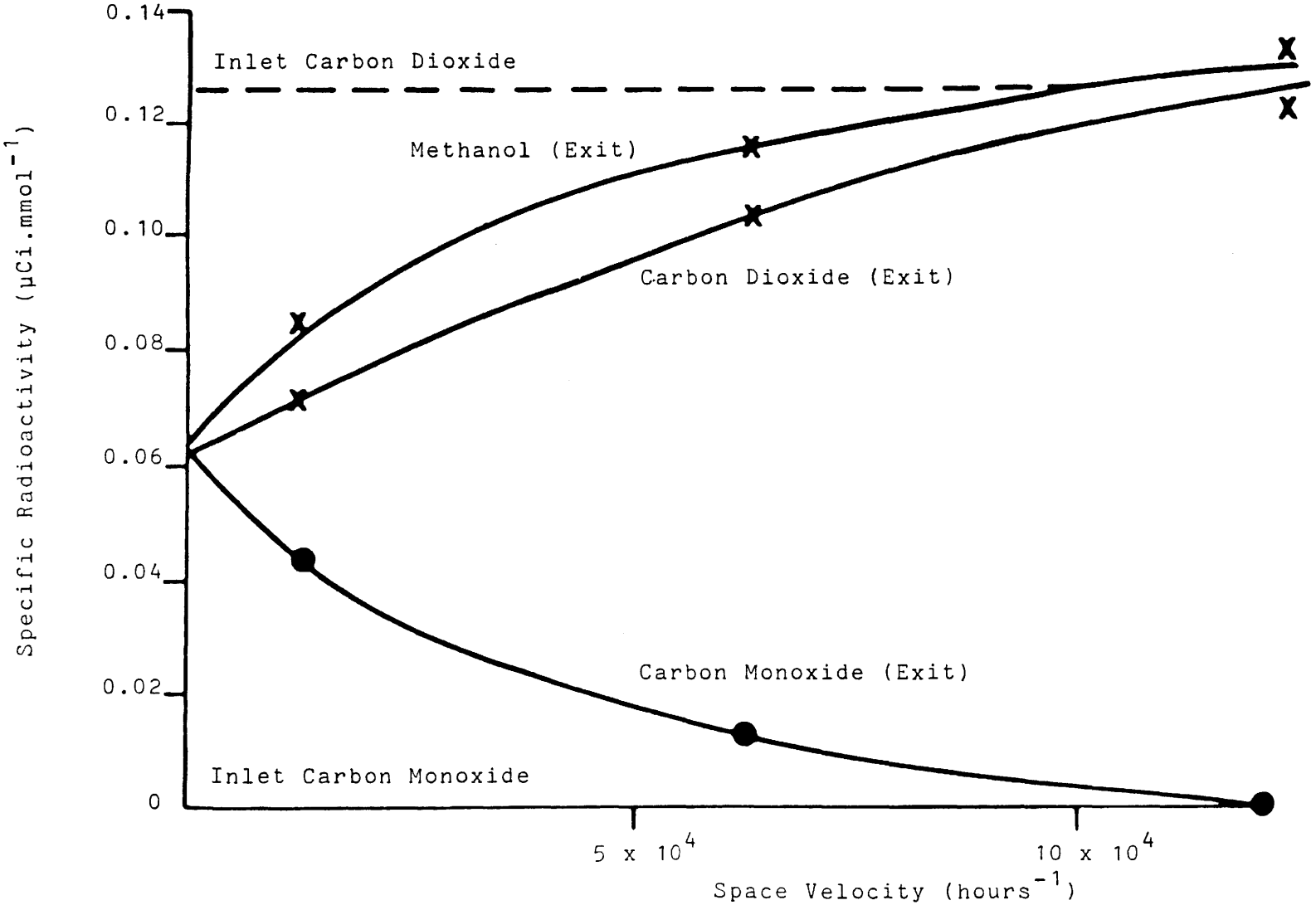

Figure 1.4 Specific Radioactivities of the Products Formed in the Reaction between [14-C]Carbon Dioxide, Carbon Monoxide and Hydrogen on $Cu/ZnO/Al_2O_3$ as a Function of Space Velocity (57)

programmed desorption (TPD) and temperature programmed reaction spectroscopy (TPRS) studies, the authors concluded that carbon dioxide, adsorbed on the support or on the partially oxidised copper surface, reacted with hydrogen atoms at the support/copper interface forming a formate species, the rate determining step being the hydrogenolysis of the adsorbed formate. They suggested that, based on ab initio molecular orbital calculations, no energy barrier existed for the reaction of hydrogen atoms with CO_2^- and proposed that the overall mechanism may be written as

$$CO_2^-(a) + H(a) \longrightarrow HCO_2^-(a) \qquad (4)$$

$$HCO_2^-(a) + 3H(a) \longrightarrow CH_3OH(a) + O^-(a) \qquad (5)$$

where the negative charge on the adsorbed carbon dioxide and formate species may be less than unity. The authors stated that copper became oxidised via reaction (5) and that this accounted for the catalyst being in a 30% partially oxidised state during methanol synthesis, the steady state being maintained by the reactions of carbon monoxide and hydrogen with the adsorbed oxygen atoms.

However, Klier (10) has argued that methanol is synthesised via the hydrogenation of carbon monoxide and not carbon dioxide. Parris and Klier (62) studied the adsorption of carbon monoxide and oxygen on a range of Cu/ZnO catalysts and found that irreversible chemisorption of carbon monoxide was induced in the Cu/ZnO catalysts, while pure copper adsorbed carbon monoxide only reversibly and pure

zinc oxide did not adsorb this gas at all at ambient temperature. The amount of carbon monoxide reversibly adsorbed on the Cu/ZnO catalysts was found to show good linearity with irreversible oxygen chemisorption on these catalysts. They concluded that both irreversible oxygen and reversible carbon monoxide adsorb on the copper metal surface and the irreversible carbon monoxide chemisorption was attributed to solute copper in zinc oxide. It was shown that, for each zinc oxide morphology reported previously (42) (concluding that Cu/Zn $\lesssim$ 30/70 had prism ($10\bar{1}0$) morphology and Cu/ZnO $\gtrsim$ 40/60 basal (0001) morphology), a linear relationship existed between the amount of irreversibly adsorbed carbon monoxide and the concentration of copper solute sites on the ZnO surface (Figure 1.5). From this it can be seen that, if the irreversibly bound carbon monoxide molecules titrate the surface copper solute sites, then these sites are accumulated more by the ZnO (0001) planes. This was attributed by Parris and Klier (62) to the electrostatic charge, which was present in the basal plane, but not in the prism plane of zinc oxide. Hence, the copper species which were also charged tended to neutralise the excess charge on the (0001) planes.

Klier (10) correlated the turnover rates of methanol synthesis over sites binding carbon monoxide irreversibly upon the concentration of these sites on the surface of a range of Cu/ZnO catalysts for each zinc oxide morphology (Figure 1.6). He concluded that the methanol synthesis

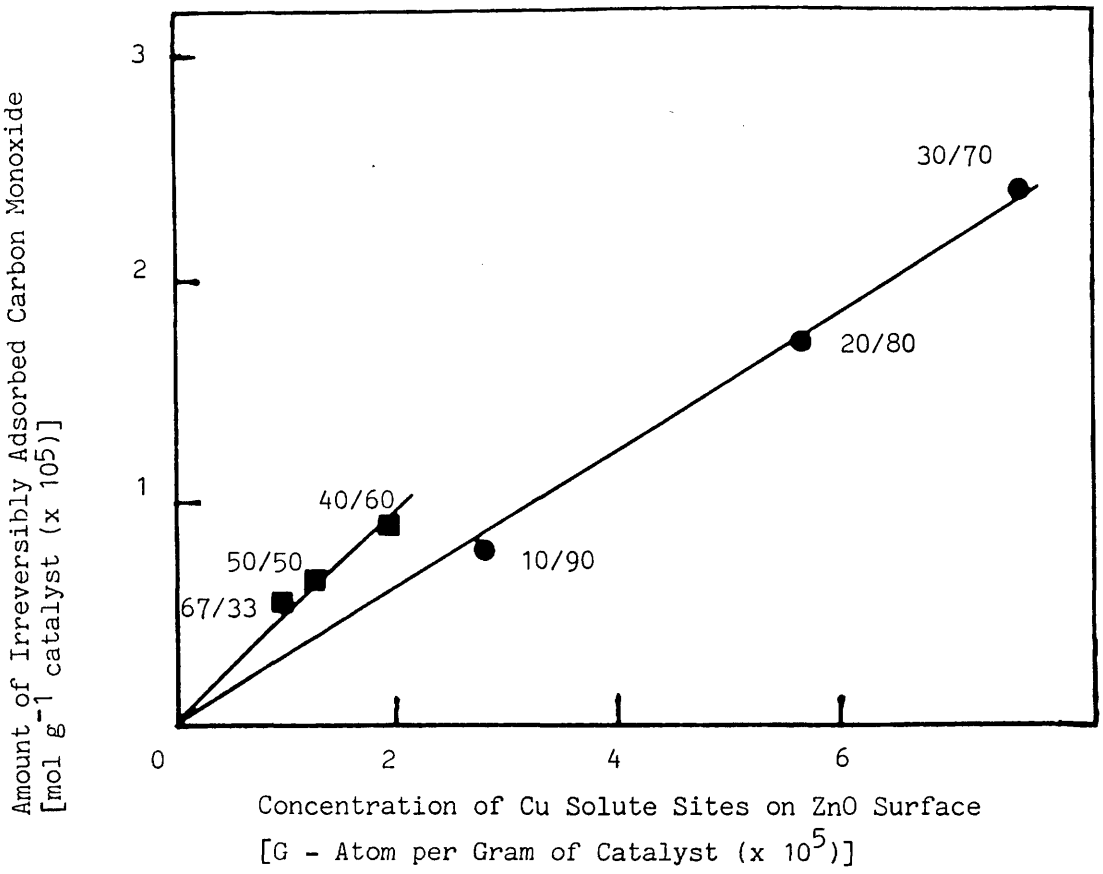

Figure 1.5 The Dependence of the Amount of Irreversibly Chemisorbed Carbon Monoxide on the Concentration of Amorphous Copper (62).

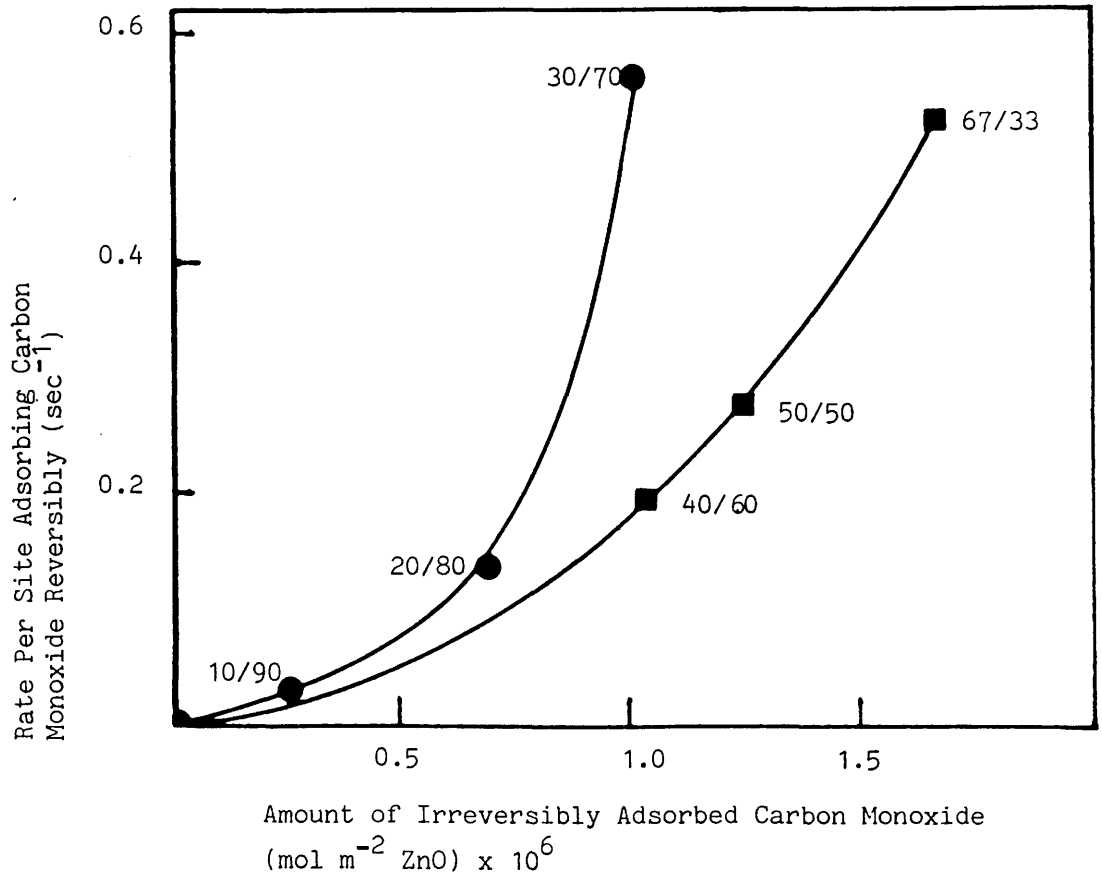

Figure 1.6 The Dependence of Turnover Rates of Methanol Synthesis (at 523K, 75 atm) over Sites Binding Carbon Monoxide Irreversibly upon the Concentration of These Sites on the ZnO Surface (10).

activity in Cu/ZnO catalysts appeared to be linked to sites which also irreversibly chemisorbed carbon monoxide rather than sites which adsorbed carbon monoxide reversibly.

Klier et al (63) reported that carbon dioxide had a true promotional effect on the rate of methanol synthesis from carbon monoxide and hydrogen rather than increasing it by the direct hydrogenation of this gas to methanol. The authors reported that 95% of the yield of methanol was produced by the hydrogenation of carbon monoxide and 5% by the hydrogenation of carbon dioxide and put forward a kinetic model based on the following observations:-

(1) The methanol conversion rates from carbon monoxide and hydrogen increased substantially upon the addition of carbon dioxide and prolonged exposure of the catalyst to carbon dioxide-free carbon monoxide and hydrogen, resulted in irreversible deactivation of the catalyst.

(2) Further reduction of a catalyst, which had been reduced in hydrogen at 523K, could be obtained by carbon monoxide with the appearance of carbon dioxide. When this carbon monoxide reduced catalyst was exposed to carbon dioxide, it was reoxidised and carbon dioxide was converted to carbon monoxide.

(3) The activity of the catalyst increased as the concentration of copper solute species in the zinc oxide phase increased.

(4) Carbon dioxide was adsorbed relatively strongly, the reactant adsorption strengths being estimated to decrease

in the order:

carbon dioxide > carbon monoxide > hydrogen.

Based on these observations the authors proposed that the catalyst could exist in a reduced state, A_{red}, which was inactive, and in an oxidised state, A_{ox}, which was active. The proportion of A_{ox} and A_{red} was suggested to be controlled by the ratio of carbon dioxide and carbon monoxide in the synthesis gas via:-

$$A_{ox} + CO(g) \rightleftharpoons A_{red} + CO_2(g).$$

Klier postulated that A_{red} was metallic copper and A_{ox} was monovalent copper in zinc oxide. Therefore, in the presence of carbon dioxide Cu^{I}/ZnO was formed but, in its absence, inactive copper (A_{red}) was formed. This explained the deactivation of the catalyst by carbon dioxide-free carbon monoxide and hydrogen (63). Klier et al (41) explained that the carbon dioxide:carbon monoxide and water:hydrogen ratios employed in the industrial synthesis were sufficient to prevent the reduction of Cu^{I} to fine copper dispersions, but were insufficient to prevent the reduction of Cu^{I} to bulk copper metal. Hence the deactivation mechanism was irreversible once large crystallites of copper were produced from the Cu^{I}/ZnO phase.

The stabilisation of Cu^{I} species by carbon dioxide was also reported by Ruggeri et al (64), who studied the reduction of $Cu/ZnO/Al_2O_3$ with hydrogen and nitrogen at various temperatures and reported that reduction was

delayed, even in the presence of small concentrations of carbon dioxide in the hydrogen and nitrogen mixture.

Klier and co-workers (41) concluded that the initial step in the synthesis of methanol over Cu/ZnO binary catalysts was the activation of carbon monoxide on Cu^{I} and of hydrogen on the surrounding ZnO surface. The total mechanism for the reaction, as proposed by these authors, is given in Figure 1.7.

Lui et al (65) rationalised the conflicting reports of Klier (10), Kagan et al (59 - 61) and Chinchen et al (57) using [18-O] labelled carbon dioxide. Lui et al (65) concluded that methanol could be produced primarily by two independent pathways, one involving the hydrogenation of carbon monoxide, the other involving the hydrogenation of carbon dioxide. They reported that, in the absence of water, methanol was produced from both carbon monoxide and carbon dioxide, the hydrogenation of carbon dioxide being very competitive with that of carbon monoxide, even although the pressure of carbon dioxide was only $^{1}/_{20}$th that of carbon monoxide. This was in good agreement with other authors who had reported that, under reaction conditions, carbon dioxide was hydrogenated faster than carbon monoxide. In the presence of water, Lui et al (65) reported that the production of [18-O]-methanol decreased whereas the yields of [16-O]-methanol and [18-O]-carbon monoxide remained unaffected. From these results it was proposed that water was so strongly adsorbed that the

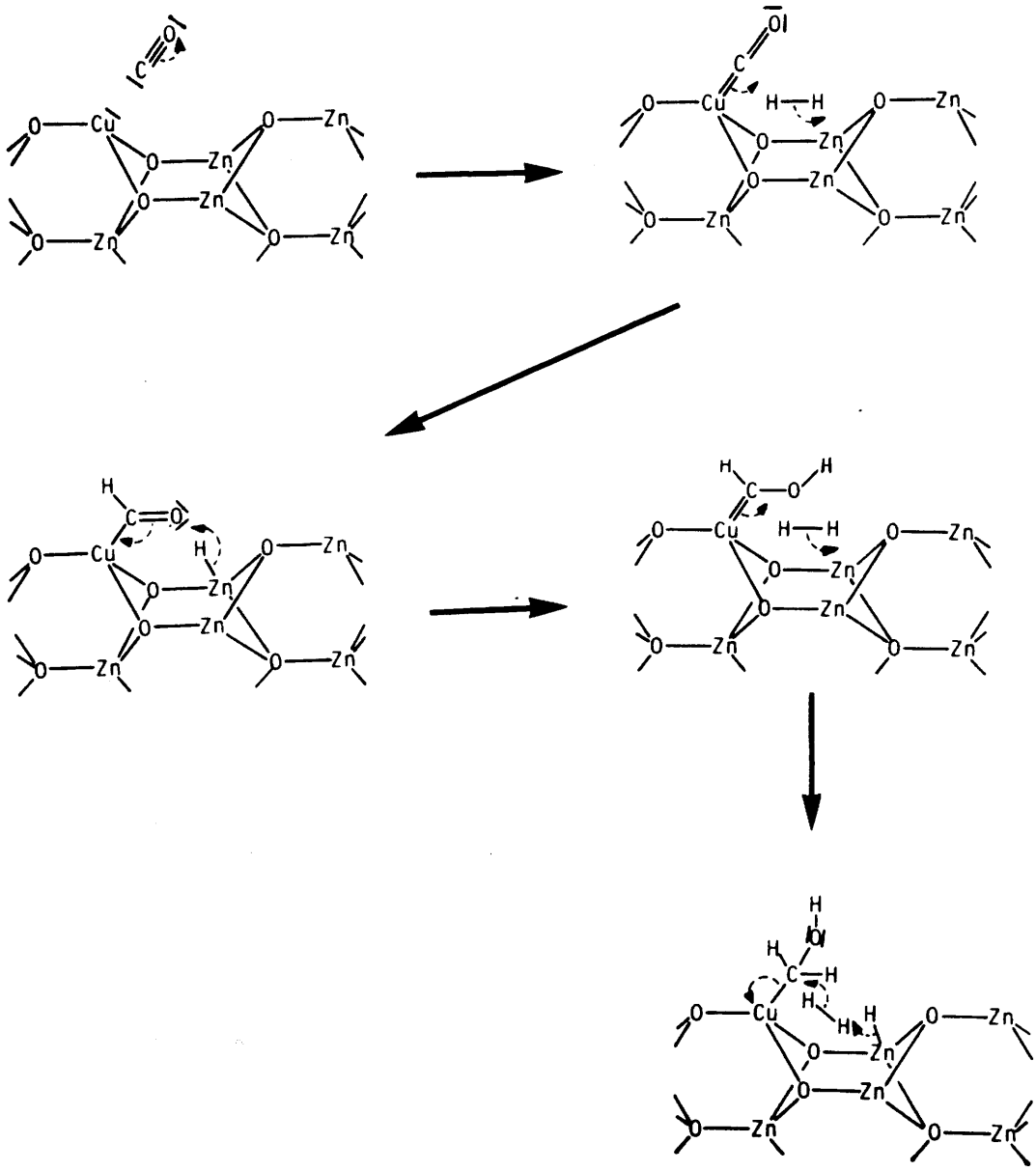

Figure 1.7 Mechanism for the Synthesis of Methanol from Carbon Monoxide and Hydrogen on $Cu/ZnO/Al_2O_3$ as Proposed by Klier et al (41).

carbon dioxide hydrogenation site was blocked. It was also concluded that the synthesis of methanol from carbon dioxide did not involve the dissociation of carbon dioxide to carbon monoxide and the subsequent hydrogenation of this to methanol. They believed that in the synthesis of methanol from carbon dioxide, carbon monoxide and hydrogen at low conversions and low temperatures, methanol was produced primarily via the hydrogenation of carbon dioxide, because it was faster than the hydrogenation of carbon monoxide, thus explaining the results of Kagan et al (59 - 61) and Chinchen et al (57). Alternatively, at high conversions when significant amounts of water were produced by the hydrogenation of carbon dioxide and the reverse water-gas shift reaction, water preferentially suppressed carbon dioxide hydrogenation and methanol was synthesised largely from carbon monoxide.

However, of greater relevance to the present study is the debate which exists as to the catalyst sites responsible for the adsorption and subsequent reaction of the reactants carbon monoxide, carbon dioxide and hydrogen during methanol synthesis.

In the case of "high pressure" catalysts based on ZnO, Natta (7) reported that carbon monoxide, carbon dioxide and hydrogen were strongly adsorbed on ZnO and that carbon monoxide adsorbed at ZnO defect sites was the precursor to methanol.

Many investigators have studied the adsorption of

carbon monoxide, carbon dioxide and hydrogen on ZnO. Garner (66) studied the adsorption of carbon monoxide and carbon dioxide on ZnO at various temperatures. He reported that carbon monoxide could be adsorbed on ZnO in two ways; at room temperature reversible adsorption of carbon monoxide occurred with an isosteric heat of ca. 13 kcal mol^{-1} and no carbonates were formed. The reversible adsorption of carbon monoxide at room temperature was attributed to the formation of $CO^{\delta+}$ in association with a surface metal ion. At temperatures greater than 373K carbon monoxide was found to adsorb irreversibly, being recoverable as carbon dioxide at 673K. Carbon dioxide was found to adsorb on ZnO and form carbonate ions with an activation energy of ca. 20 kcal mol^{-1}. This gas was reported to desorb at room temperature.

Similar studies were carried out by Winter (67), who reported an isosteric heat of adsorption of carbon monoxide on ZnO of 9 kcal mol^{-1} between 250K and 293K. In addition, carbon monoxide was found to exchange oxygen atoms with the surface between 473K and 553K with an activation energy of 14.5 kcal mol^{-1}. Similarly carbon dioxide was found to exchange oxygen atoms with the ZnO surface between 293K and 553K with zero activation energy.

The adsorption of hydrogen on ZnO has been extensively covered in the literature and was reviewed by C.S. John (68) in 1980. In general, there is evidence for four types of hydrogen adsorbed on ZnO (the ZnO used in these studies was largely Kadox 25 which had been pretreated thermally to ca. 700K):-

Type I: rapid and reversible at room temperature, this first type has been attributed (69) to two species:-

Zn ——— H and O ——— H

and is thought not to be dependent upon surface non-stoichiometry.

Type II: irreversible at room temperature, attributed (70) to:-

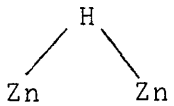

and O - H ----O

bridged structures. This adsorption is believed to occur on sites that are independent of those associated with Type I species.

Type III: occurs at low temperatures (77K), hydrogen is adsorbed reversibly and non-dissociatively and is believed to be associated with the same sites as Type I.

Type IV: occurs at high temperatures and also to varying extents at room temperature.

However in more recent reports involving the adsorption of hydrogen on Raney zinc at temperatures between 203K and 473K (11) and ZnO at a temperature of 123K (71), no evidence for hydrogen adsorption was obtained.

Bowker et al (15) reported the adsorption of a number of gases on analar ZnO, which had been pre-treated at 550K in hydrogen to produce surface defects. The authors reported that the total amount of carbon dioxide adsorbed on ZnO increased with temperature and believed that this adsorption

was associated with surface defect sites. Two types of adsorbed carbon dioxide were reported. One was activated and attributed to CO_3^{2-} formation, the other non activated and believed to occur on defect sites (V_o) thus:-

$$CO_2 + V_o(s) + e^- \longrightarrow CO_2^-(a)$$

$$CO_2^-(a) \longrightarrow CO(g) + O^-(s)$$

The authors proposed that the activation energy for adsorption into the high energy, activated sites, derived from a combination of the need to segregate the defect to the surface and also for the carbon dioxide to overcome a small energy barrier to adsorb at that site. Hydrogen adsorption on this ZnO was found to be relatively small and again associated with defect sites.

The authors reported that carbon dioxide and hydrogen co-adsorption on ZnO at temperatures greater than 450K resulted in complex formation which was attributed to formate. No carbon monoxide was found to adsorb on the defected ZnO although it did adsorb on "less" defected ZnO. During the co-adsorption of carbon monoxide and hydrogen on ZnO no evidence for formate formation was obtained. Indeed, in a more recent report Bowker et al (14), studied the adsorption of carbon monoxide and carbon dioxide at temperatures greater than 300K on ZnO pre-reduced in hydrogen and reported that carbon monoxide was weakly held by ZnO (ΔH_{ads} = 3.8 kcal mol^{-1}) and that the amount of this gas adsorbed on ZnO was reduced when co-adsorbed with hydrogen.

The authors also studied the reactions of carbon monoxide and hydrogen and carbon dioxide and hydrogen on ZnO and concluded that between 523K and 573K methanol was formed on ZnO, by the hydrogenation of carbon dioxide and that carbon monoxide and hydrogen produced defect sites for the adsorption of carbon dioxide and its transformation to methanol.

However a number of investigators (72,73) have studied the co-adsorption of hydrogen and carbon monoxide on ZnO and reported a mutual enhancement in the adsorption of these gases.

Nagarjunan et al (72) concluded that this mutual enhancement was due to additional site creation, as well as complex formation:-

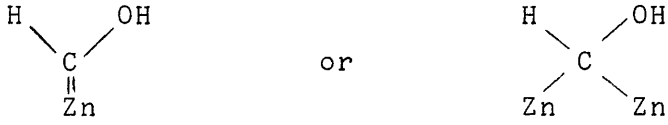

In a study of carbon monoxide adsorbed on hydrogen precovered ZnO at ambient temperature, Boccuzzi et al (74) concluded that carbon monoxide was adsorbed via the carbon atom to exposed zinc ions, and that the molecule was strongly polarised with the negative and positive ends on the carbon and oxygen atoms respectively. From infrared spectra they suggested that the following process took place:-

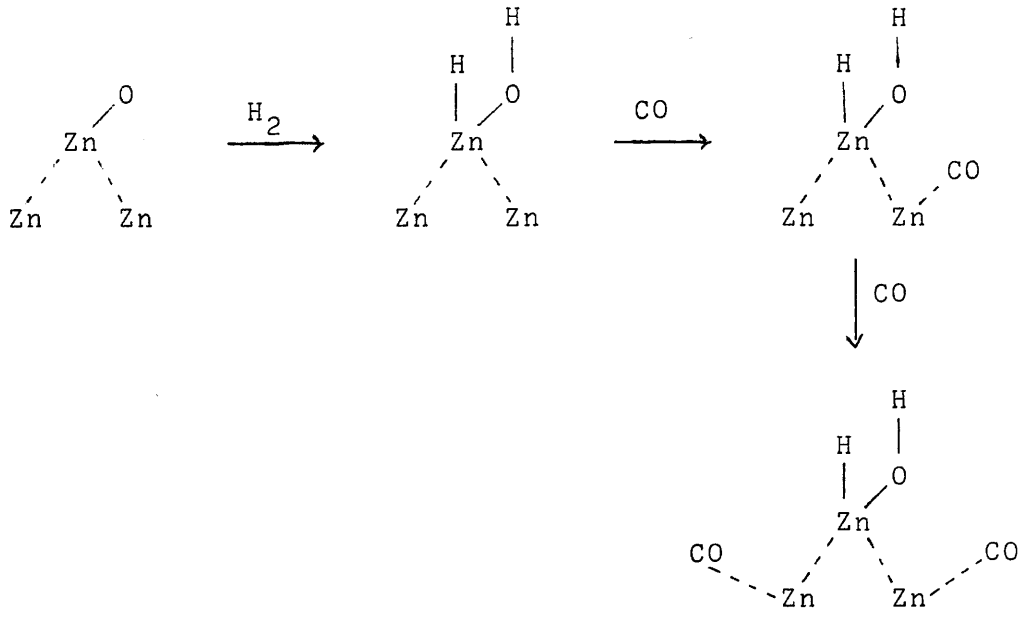

Addition of copper to ZnO based catalysts in the "low pressure" process has led to greater conflict among the various investigators regarding the active sites for the adsorption and subsequent reaction of the reactants. However, although many investigators have reported the adsorption of carbon monoxide, carbon dioxide and hydrogen on the individual components, namely copper, ZnO, Al_2O_3 and the Cu/ZnO binary system, few studies have been reported on the catalyst itself.

Waugh et al (58) reported that the isosteric heats of adsorption of carbon monoxide on $Cu/ZnO/Al_2O_3$ of 12 kcal mol^{-1} as determined by gas adsorption chromatography, were the same as that on polycrystalline copper and concluded that carbon monoxide resided to a greater extent on the copper component of the catalyst. The authors believed that carbon

dioxide, which was found to be only weakly held by polycrystalline copper with isosteric heats of 4 kcal mol^{-1}, was adsorbed on the partially reduced ZnO component and reacted with hydrogen at the Cu/ZnO interface to form a formate species.

The adsorption of carbon monoxide, carbon dioxide and hydrogen on Cu/ZnO binary catalysts was studied by Klier (10), who reported that there was no evidence that the addition of Al_2O_3 to the binary systems caused significant synergic promotion. Although carbon dioxide is known to adsorb on Al_2O_3 (75) no evidence exists regarding its contribution to methanol synthesis. As mentioned previously, in the study of Cu/ZnO binary systems Klier reported that carbon monoxide was reversibly adsorbed on the copper component of the catalyst and irreversibly adsorbed on the copper solute species (Cu^I) dissolved in the ZnO lattice, the latter being the precursor to methanol. Indeed Cu^I is better suited for bonding carbon monoxide than any other valence states of copper (76). Cu^I is free from 4s screening electrons and therefore the 3d orbitals are available for back bonding to the π^* orbitals of carbon monoxide.

Klier et al (63) deduced the heats of adsorption of carbon monoxide, carbon dioxide and hydrogen on the Cu/ZnO binary catalyst from kinetic models. Klier (10) reported these to decrease:-

$$-\Delta H_a(CO_2) > -\Delta H_a(CO) > -\Delta H_a(H_2)$$

In combination with the corresponding adsorption entropy

values it was concluded that carbon monoxide and hydrogen were bonded to the binary catalyst with intermediate strength and retained some mobility in the adsorbed phase, whereas carbon dioxide was relatively strongly bound and immobile, which accounted for the retarding effect of carbon dioxide at high carbon dioxide:carbon monoxide ratios. Klier proposed that the sites which strongly adsorbed carbon dioxide were most likely located on the ZnO surface and may have been associated with the basicity of the ZnO:-

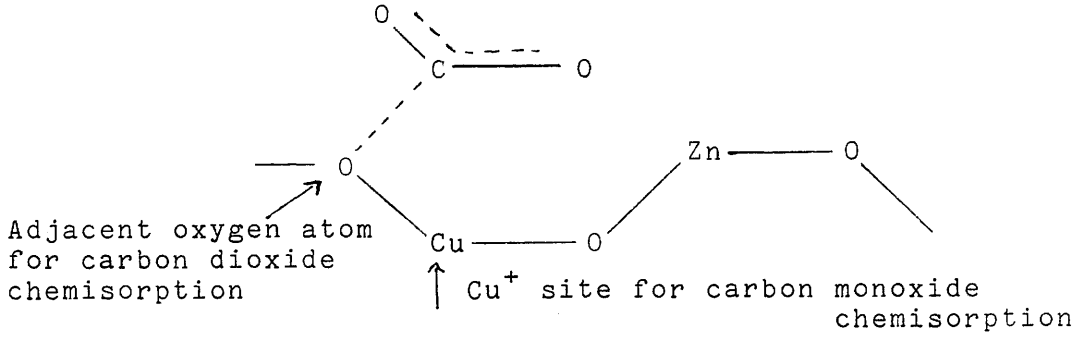

The strongly adsorbed carbon dioxide molecule which is fairly immobile, thus blocks the site which activates carbon monoxide.

Boccuzzi et al (77) studied the adsorption of carbon monoxide on small particles of copper dispersed on micro-crystalline ZnO at 77K and 300K. They reported that when the catalyst was oxidised with oxygen before admission of carbon monoxide at 77K, in addition to other bands, bands at 2143 cm^{-1} and 2116 cm^{-1} were recorded by infrared spectroscopy. The authors assigned the 2143 cm^{-1} band to carbon monoxide adsorbed on oxidised corner and edge atoms and the band at 2116 cm^{-1} to carbon monoxide adsorbed on copper atoms directly bonded to adsorbed oxygen:-

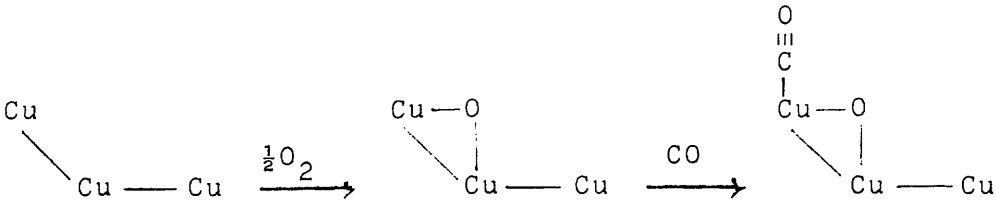

However, the carbon monoxide spectra recorded from the catalyst oxidised with nitrous oxide was different to that oxidised with oxygen. The authors concluded that the surface produced after oxidation with nitrous oxide was different to that oxidised with oxygen and proposed that the former process could be summarised as:-

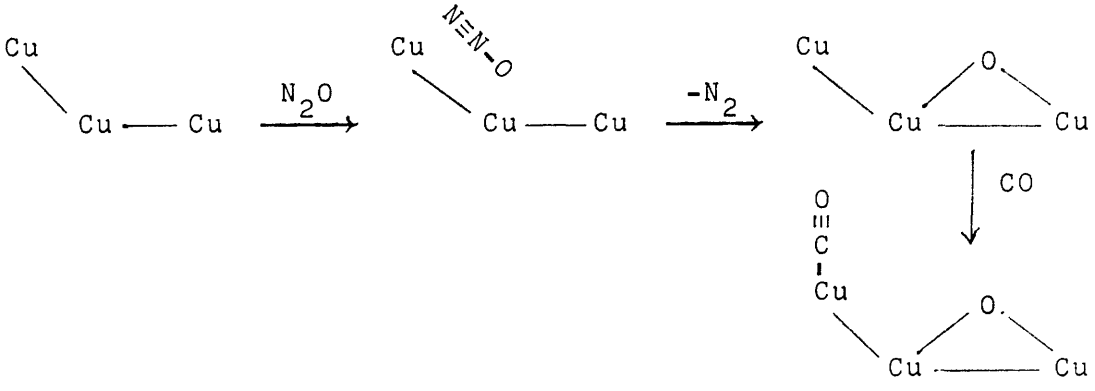

The 2143 cm^{-1} band reported by Boccuzzi et al (77) for carbon monoxide adsorbed on a copper surface oxidised with oxygen was supported by the earlier work of Hollins and Pritchard (78). These authors studied the adsorption of carbon monoxide at 82K on Cu(111) and Cu(110) single crystals oxidised with oxygen using reflection-absorption infrared spectroscopy (RAIRS). They reported a band at 2140 cm^{-1} from carbon monoxide adsorbed on the oxidised Cu(110) surface. In contrast with Cu(110), the main features in the spectra obtained from carbon monoxide adsorbed on oxidised Cu(111) were found at frequencies close to those for carbon monoxide

on clean copper surfaces. They concluded that the sites involved in the adsorption of carbon monoxide on oxidised Cu(111) could be copper atoms not directly bonded to oxygen and therefore little changed by the oxidation process. Wachs and Madix (79), studied the influence of surface oxygen upon the adsorption behaviour of carbon monoxide and carbon dioxide on Cu(110) and concluded that, the presence of oxygen atoms on the surface diminished the sticking probabilities of carbon monoxide and carbon dioxide adsorbed at 180K. They proposed that this may reflect the decreased number of adsorption sites available to carbon monoxide and carbon dioxide.

Many investigators have studied the adsorption of carbon monoxide and carbon dioxide on Cu_2O at various temperatures. Hierl et al (80) studied the adsorption of carbon monoxide on Cu_2O by infrared spectroscopy; bands at 2125 cm^{-1}, assigned to a stretching vibration of carbon monoxide coordinated to Cu^+ and at 2170 cm^{-1}, assigned to $Cu - CO^+$, were recorded. The $Cu - CO^+$ was easily removed by evacuation.

Winter (67) reported that both carbon monoxide and carbon dioxide readily exchanged their oxygen atoms with the whole of a Cu_2O surface at room temperature. The activation energy for the adsorption of carbon monoxide was found to be 10 kcal mol^{-1}, the formation of carbon dioxide during this exchange being negligible. The activation energy for the adsorption of carbon dioxide was reported as 4 kcal mol^{-1}.

Stone and Tiley (81) studied the adsorption of carbon dioxide on metallic copper coated with a thin oxide film. They reported no appreciable adsorption of carbon dioxide at 293K on a reduced or baked out surface. However, after oxygen had been preadsorbed on the reduced surface, carbon dioxide was rapidly adsorbed with a heat of adsorption of 23 kcal mol^{-1}. These authors concluded that carbon dioxide was stabilised on the surface via the formation of a surface complex with adsorbed oxygen. They attributed this species to a CO_3(ads), which may have been negatively charged.

Garner et al (82) found that considerable quantities of carbon monoxide were adsorbed at room temperature by a Cu_2O/CuO surface which had been evacuated at 473K, no carbon dioxide was evolved. It was concluded that a surface complex was formed which was stable at room temperature. These authors also reported that when the evacuated Cu_2O/CuO surface was oxygenated ca. 50% of the adsorbed oxygen was converted to carbon dioxide upon reaction with carbon monoxide. The activation energy for the reaction of carbon monoxide with adsorbed oxygen from oxygen or nitrous oxide, on Cu(111) and Cu(100) has been reported as ca. 19 kcal mol^{-1} by Habraken et al (83). These workers concluded that the reaction proceeds between two chemisorbed reactants by a Langmuir-Hinshelwood mechanism.

The importance of oxidised copper in methanol synthesis was emphasised by Chinchen et al (57), who proposed that carbon dioxide may adsorb on partially oxidised copper, as opposed to ZnO, and react with hydrogen producing a formate

species, which is then hydrogenated to methanol. The importance of surface oxygen has been reported by other investigators studying the decomposition of methanol (79,84) and ethanol (85) on copper single crystals. Russell et al (84) found that clean Cu(111) was inert for the decomposition of methanol at temperatures between 190K and 700K and that high oxygen coverage inhibited surface reactivity. However, maximum activity for methanol decomposition was recorded when the oxygen coverage was about 0.26 O atom/Cu atom. The same authors also reported complete scrambling between [18-O] labelled oxygen adsorbed on Cu(111) and [16-O]-methanol giving rise to $C^{16}O_2$, $C^{16}O^{18}O$, $C^{18}O_2$ products for an oxygen atom:copper atom ratio of 0.5. Wachs and Madix (85) reported that in the decomposition of deuterated ethanol (CH_3CH_2OD) on Cu(110), the clean surface was relatively inert. However, the ability of Cu(110) to dissociatively chemisorb ethanol was found to be enhanced by surface oxygen.

Roberts and Griffin (71) studied the adsorption of hydrogen on Cu/ZnO binary catalysts using TPD. The hydrogen was adsorbed by exposing the catalyst samples to hydrogen at 300K then cooling the samples in the presence of hydrogen to 123K. They found that hydrogen adsorbed on the binary catalysts but did not adsorb on pure ZnO and concluded that, since the hydrogen desorption energies obtained (21 and 30 kcal mol^{-1}) were higher than those reported in the literature for hydrogen desorption from copper crystal surfaces, as measured using pre-dissociated hydrogen atoms, hydrogen

adsorption occurred on copper cations dissolved in the ZnO lattice.

Hydrogen adsorption on oxidised Cu(111) was studied by Mesters et al (86) using low energy electron diffraction (LEED), Auger electron spectroscopy (AES) and ellipsometry at crystal temperatures between 513K and 703K. These authors maintained that hydrogen dissociation occurred on pure copper sites, since an initial slow rate of reaction was obtained at high oxygen coverages and, in consequence, oxygen blocked sites for hydrogen dissociation. The authors proposed that the interaction of hydrogen with oxygen adsorbed on Cu(111) could be summarised as:-

$$H_2(g) \rightleftharpoons H_2(a) \rightleftharpoons 2H(a)$$

$$H(a) + O(a) \rightleftharpoons OH(a)$$

$$H(a) + OH(a) \rightleftharpoons H_2O(a)$$

$$H_2O(a) \longrightarrow H_2O(g)$$

It was found that an operating pressure gauge accelerated the reaction, which was attributed to the ion gauge facilitating the dissociation of hydrogen. The overall activation energy for the reaction in the presence of the gauge was given as 1.2 kcal mol^{-1} which was less than the activation energy for the dissociative hydrogen chemisorption on copper, 2.9 kcal mol^{-1}, reported by Balooch et al (87).

Molecular and atomic hydrogen adsorption on poly-crystalline copper and copper single crystals has been well reviewed in the literature. Although the adsorption

of atomic hydrogen has been observed on copper films at low temperatures, that of molecular hydrogen has not been observed to any appreciable extent. Considerable debate still exists between the various investigators as to whether hydrogen dissociatively chemisorbs on copper at low temperatures.

A number of investigators have reported that hydrogen does not dissociatively chemisorb on copper (88,89,90). In a study (88) of hydrogen/deuterium exchange on copper prepared from CuO and a high purity copper from electro-deposition, the nature of the hydrogen adsorbed was indicated by the ability of the samples to exchange hydrogen. The authors reported that the purified copper samples were unable to dissociatively chemisorb hydrogen at 273K, although the other copper samples, which were less pure, did dissociate hydrogen and this was attributed to the presence of transition metal impurities.

Eberhardt et al (89) studied the photoemission of mono-layers and thick films of hydrogen molecules condensed onto Cu(100) cleaned in situ by Argon ion bombardment. They reported that molecular hydrogen adsorbed on Cu(100) at 4K. However, no evidence was obtained for the dissociation of hydrogen upon contact with the metal. The hydrogen adsorbed at 4K was found to be very weakly held and desorbed upon warming to 15K. The authors concluded that since atomic hydrogen adsorbed on copper, then a "dissociation barrier" existed on noble metals with filled d bands, which hydrogen could not overcome, even though the gas was at room

temperature before adsorption. Similar conclusions were drawn in a study (90) of hydrogen adsorption on Cu(111) between 15 - 300K using angle resolved photoemission and thermal desorption.

In a study of hydrogen/deuterium exchange on a copper foil Mikovsky et al (91) reported that hydrogen dissociated on copper at temperatures greater than 573K, and the activation energy for the rate of hydrogen/deuterium exchange was given as 23 kcal mol^{-1}. They compared these results with those of previous investigators who concluded that hydrogen did not chemisorb on copper below 573K and proposed that the inactivity of copper compared to nickel, with respect to hydrogen adsorption, was attributed to the d — s promotional energy in copper. The authors suggested that when the bonding energy gained as a result of promotion of an electron from 3d to 4s was sufficient then an excited or active copper atom was produced, which resembled nickel and was able to adsorb hydrogen with sufficient strength.

A number of investigators have reported that hydrogen dissociatively chemisorbs on copper (87,92,93). Balooch et al (87) studied the adsorption and desorption of hydrogen on (100), (110) and stepped (310) crystal faces of copper at temperatures above 800K. The crystal faces were exposed simultaneously to a molecular beam of hydrogen and a highly dissociated beam of deuterium. The majority of the hydrogen molecules did not adsorb, but some did adsorb dissociatively and they were found to react catalytically with adsorbed deuterium atoms to give hydrogen deuteride molecules. However,

there was evidence for the existence of substantial energy barriers for the adsorption depending on the crystallographic orientation. Activation energies for the adsorption of hydrogen on Cu(110) were estimated to be 3 kcal mol^{-1} and, on Cu(100) and Cu(310), to be 5 kcal mol^{-1}. The authors concluded that, since the energy dependence for the dissociative adsorption and the angular distribution of desorbed hydrogen deuteride was the same for stepped (310) and (100) faces, but both were different for (110) faces; ledge sites, boundaries and other defects on the surface were not the principal regions responsible for the adsorption of hydrogen on these crystals.

Using surface potential techniques at temperatures between 242K and 337K Alexander and Pritchard (92) reported that hydrogen dissociated on copper films with isosteric heats of adsorption of ca. 9.5 - 11.9 kcal mol^{-1}. In a subsequent report, Pritchard et al (93) showed that exposure of the low index Cu(100), Cu(111), Cu(110) faces to molecular hydrogen at room temperature led to no measureable change of surface potential, although this result was inconclusive. In contrast, marked negative surface potentials appeared when the high index Cu(211), Cu(311) and Cu(755) faces were examined. The isosteric heats of adsorption for hydrogen on Cu(311) were found to be ca. 9.6 kcal mol^{-1}. The fact that the high index faces and polycrystalline films were both active in hydrogen chemisorption led the authors to conclude that polycrystalline copper surfaces often consisted of mainly high index faces.

The adsorption of carbon monoxide on polycrystalline copper and copper single crystals has also been extensively reported in the literature. Bonding in the isolated carbon monoxide molecule is regarded as resulting from an sp_z-hybrid orbital of the carbon atom combining with the p_z-orbital of the oxygen atom to produce a σ-bond, while the p_x- and p_y-orbitals of the carbon and oxygen atoms combine to produce two π-bonds. The valence electronic configuration of carbon monoxide is thus $4\sigma_u^2\ 1\pi_u^4\ 5\sigma_g^2\ 2\pi_g^0$ and it bonds to metal atoms by means of stabilisation of the $5\sigma_g$ orbital, on mixing with the metal molecular orbitals. It had been assumed that this interaction was with metal 'd' orbitals only, on several metal surfaces. However, Anderson (94) in a molecular orbital study of the interaction of carbon monoxide with Cu(100) showed that the metal 4s orbitals played a partial role in binding with the carbon monoxide $5\sigma_g$ orbital. The interaction of the $5\sigma_g$ orbital with the metal molecular orbitals creates a σ-bond between the carbon atom and the metal atom putting a large formal negative charge on the metal atom. In order to remove this excess negative charge and hence stabilise the bond, "back donation" of electrons, from a metal d-orbital to the antibonding π^*-molecular orbital of the carbon monoxide occurs.

When carbon monoxide is adsorbed on copper at 77K, two stages of adsorption are known to take place (95), which correlate with structural developments in the overlayer observed by LEED. On the low index faces of copper, the first stage in the adsorption of carbon monoxide at 77K,

as revealed by LEED, gives rise to an ordered overlayer structure with unit meshes that are related to the unit meshes of the metal surfaces. The first ordered structures to appear on Cu(100), Cu(111) and Cu(110) are c(2 x 2), $(\sqrt{3} \times \sqrt{3}) - 30^{\circ}$ and p(2 x 1) respectively. The second stage which initiates after approximately half monolayer coverage leads, at saturation, to diffraction patterns which have been attributed to an overlayer of carbon monoxide molecules, more or less close packed, but whose spacings are not simply related to the unit meshes of the metal surface. In this case the molecules are not restricted to specific sites and a lack of registry exists between the overlayer and the metal atoms. This uniform compression model for the second stage in the adsorption of carbon monoxide on copper fits in well with infrared spectra, which show no evidence for any marked frequency changes, or for the appearance of new species at the second stage. However, it does not explain large changes in the surface potential as the second stage develops. Pritchard (95) re-interpreted these results in terms of an alternative site (terminal and bridged) adsorption model. He concluded that adsorption of carbon monoxide on linear and bridged sites was consistent with LEED patterns for the high coverage carbon monoxide overlayer structures on Cu(100) and Cu(111), although copper favoured linearly bound carbon monoxide and carbon monoxide would be held less strongly, therefore, at bridged sites.

Barber et al (96) studied the adsorption of carbon monoxide on polycrystalline copper by Secondary Ion Mass

Spectrometry between 77K and 390K and reported that only a linear structure was observed at 77K, and only a bridged structure at 295K. They found that 20 Langmuir doses of carbon monoxide at 77K caused a build-up of $CuCO^+$ peaks. Apart from Cu^+ and $CuCO^+$, the only peaks appearing in the spectrum were due to Cu_2^+. The authors proposed that $CuCO^+$ was derived from the surface structure:-

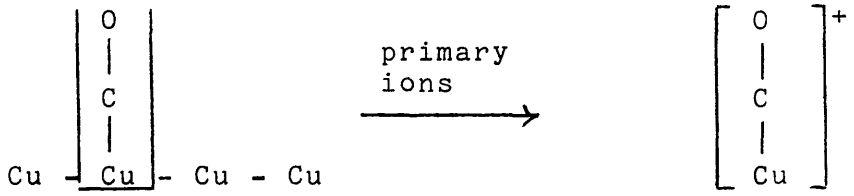

secondary ion

After the surface had been saturated with carbon monoxide at 77K the temperature was raised to 295K and the signal due to $CuCO^+$ continuously monitored. The desorption curve indicated two distinct surface species, both of which were completely desorbed at room temperature. Barber explained these results together with previous results obtained by LEED, infrared and surface potential measurements. He suggested that up to $\theta = \frac{1}{2}$ one species was present, at $\theta > 0.5$ a second type of adsorption occurred which was desorbed first upon warming. This second species was desorbed completely at 195K.

The authors also reported the presence of the secondary ion species Cu_2CO^+ after adsorption of carbon monoxide at room temperature which they proposed derived from the surface

structure:-

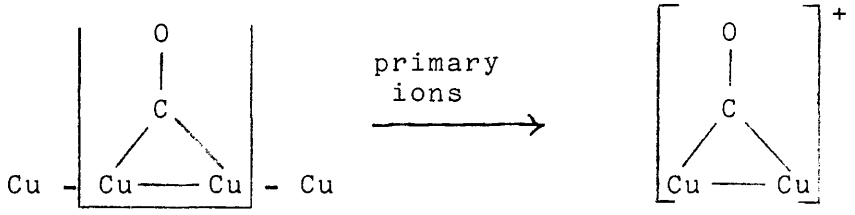

secondary ion

When the sample was treated in a flow of carbon monoxide at 390K, several carbide species were detected on the surface. This was attributed to the disproportionation reaction:-

$$2CO(a) \longrightarrow C(a) + CO_2(a) \longrightarrow C(a) + CO_2(g)$$

since $Cu_2CO_2^+$ was detected as a weak signal in some of the spectra. However, Chatikavanij (97) found no evidence for carbon present on the surface of Cu/ZnO catalysts during reaction with carbon monoxide and hydrogen, since methane, which would be expected to form by the hydrogenation of surface carbon, could not be detected.

Dell et al (98) studied the adsorption of carbon monoxide on reduced copper in the form of a granular powder at 195K and 293K. The amount of carbon monoxide adsorbed was 20 - 25% of a monolayer at both temperatures and this correlated well with the measured area of copper active in the decomposition of nitrous oxide at 293K. The authors proposed that, if the surface was homogeneous, changes in the activity and surface area would be expected to parallel each other. If, however, the surface was heterogeneous and

portions of the surface were particularly active, then variations in coverage would be expected if the method of preparation of the surface was modified. An experiment involving the sintering of copper at 593K resulted in reductions in the surface area of 35% and in the activity for carbon monoxide adsorption of 60%. In consequence, the authors concluded that the copper surface was heterogeneous. The heat of adsorption of carbon monoxide on copper at low coverages was measured calorimetrically and found to be between 16 and 17 kcal mol^{-1}.

Other investigators have measured the heats of adsorption of carbon monoxide on various forms of copper. Joyner et al (99) reported that carbon monoxide adsorbs on Cu(100) at 295K with a heat of adsorption of ca. 19.1 kcal mol^{-1}. However, carbon monoxide is held less tightly by Cu(111). Hollins and Pritchard (100) studied the adsorption of carbon monoxide on Cu(111) at low temperatures. They determined an initial heat of adsorption of 11.9 kcal mol^{-1}, which was maintained until $\frac{1}{3}$ coverage, at which point it dropped abruptly to 9.1 kcal mol^{-1}.

Pritchard et al (93) compared the infrared spectra obtained in a study of carbon monoxide chemisorbed on polycrystalline copper and copper single crystals. They deduced that, since most of the polycrystalline copper surface gave infrared bands in the same range as those observed on Cu(211), Cu(311) and Cu(755) faces, this was further evidence that polycrystalline copper surfaces often consisted of mainly high index faces.

Waugh et al (58) reported that carbon monoxide was relatively strongly held on polycrystalline copper (compared to zinc oxide) with isosteric heats of adsorption of ca. 12 kcal mol^{-1}; these were unaffected by the co-adsorption of carbon monoxide with hydrogen.

In contrast with carbon monoxide, studies of the adsorption of carbon dioxide on copper have been minimal. This may be a direct result of earlier studies which claimed that carbon dioxide did not chemisorb on copper. Stone and Tiley (81), as mentioned previously, studied the adsorption of carbon dioxide on metallic copper coated with a thin oxide film. They reported that no appreciable amount of carbon dioxide was adsorbed on a reduced surface at 293K. However, more recent studies have shown that carbon dioxide does adsorb, albeit weakly, on copper.

Waugh et al (58) reported that, in contrast with carbon monoxide, carbon dioxide was weakly held on copper. The authors found that the isosteric heats of adsorption of carbon dioxide on reduced polycrystalline copper were ca. 4 kcal mol^{-1} as determined by frontal chromatography.

Anderson (94) reported that carbon dioxide was weakly held on Cu(100). He estimated the binding energy to be 11 kcal mol^{-1} in a molecular orbital study of the system. Anderson also concluded that carbon dioxide bonded in a μ-bridging position through mixing of the copper d-orbitals with carbon dioxide π^* orbitals. He pointed out that stabilisation of the $6a_1$ orbital prevented dissociation of carbon dioxide at transition metal surfaces including copper.

However, Wachs and Madix (79) have reported that the adsorption of carbon dioxide on Cu(110) at 180K results in 99% dissociation of carbon dioxide to carbon monoxide and surface oxygen as revealed by desorption spectra. The magnitude of the carbon monoxide peak after adsorption of carbon dioxide was found to greatly diminish when the copper surface was predosed with 1 to 3 Langmuirs of oxygen.

Further evidence for the dissociation of carbon dioxide on copper was provided by Grabke (101), who measured the rate of oxygen transfer from carbon dioxide to the copper surface at ca. 1273K in a flow apparatus using [14-C] labelled carbon dioxide. The activation energy for the reaction was reported as 60.6 ± 0.3 kcal mol^{-1}.

CHAPTER TWO

2. OBJECTIVES OF THE PRESENT WORK

The work described in this thesis comprises of a detailed study of the adsorption of carbon dioxide and carbon monoxide on $Cu/ZnO/Al_2O_3$ and related catalysts using static radiotracer and microreactor flow adsorption techniques.

The main objectives of the work were:-

(a) to investigate the separate and competitive adsorption of carbon dioxide and carbon monoxide on a $Cu/ZnO/Al_2O_3$ catalyst system.

(b) to investigate the effects of evacuation and molecular exchange on the species formed during the adsorption processes.

(c) to examine the effects of surface oxygen on the adsorption of carbon dioxide and carbon monoxide.

(d) to examine the effects of hydrogen on the adsorption of carbon dioxide and carbon monoxide.

From these studies it was intended to obtain further information regarding (i) the nature of the surface sites responsible for the adsorption and subsequent reaction of each species; (ii) the relative strengths of adsorption and the nature of the adsorbed carbon oxides on each component of the catalyst; (iii) the role that carbon dioxide and carbon monoxide play both in the hydrogenation reaction and in the conditioning of the catalyst surface and (iv) the effect of surface adsorbed oxygen on the adsorption and subsequent reaction of carbon dioxide and carbon monoxide at the copper surface.

CHAPTER THREE

3. EXPERIMENTAL

3.1 The Vacuum System

The apparatus was a conventional high vacuum system (Figure 3.1) maintained at a pressure of $\leqslant 10^{-4}$ torr by means of a mercury-diffusion pump backed by a rotary oil pump. Two liquid nitrogen traps were connected in series with the mercury-diffusion pump in order to increase e efficiency of the vacuum and to trap any mercury vapour, which may otherwise have poisoned the catalyst.

The gases used in this study were stored in four $1000cm^3$ storage bulbs (B - E) and a $2000cm^3$ storage bulb (A) connected via 4mm taps to the secondary manifold and via 2mm taps to a part of the system close to the reaction vessel. Ampoules could be attached to bulb D which was used to store [14-C]carbon dioxide, similarly a [14-C]carbon dioxide to [14-C]carbon monoxide converter (Section 3.6.1) was attached to bulb E, in which [14-C]carbon monoxide was stored.

Pressures of gases in the system were measured by a mercury manometer; to allow smaller changes in pressure to be monitored a differential pressure transducer (Section 3.3) was used to measure pressures in the reaction vessel.

The volumes of various parts of the apparatus were determined using a bulb of known volume ($135.0195cm^3$). The bulb was attached to the vacuum system and filled with a known pressure of dry air. This was expanded into various

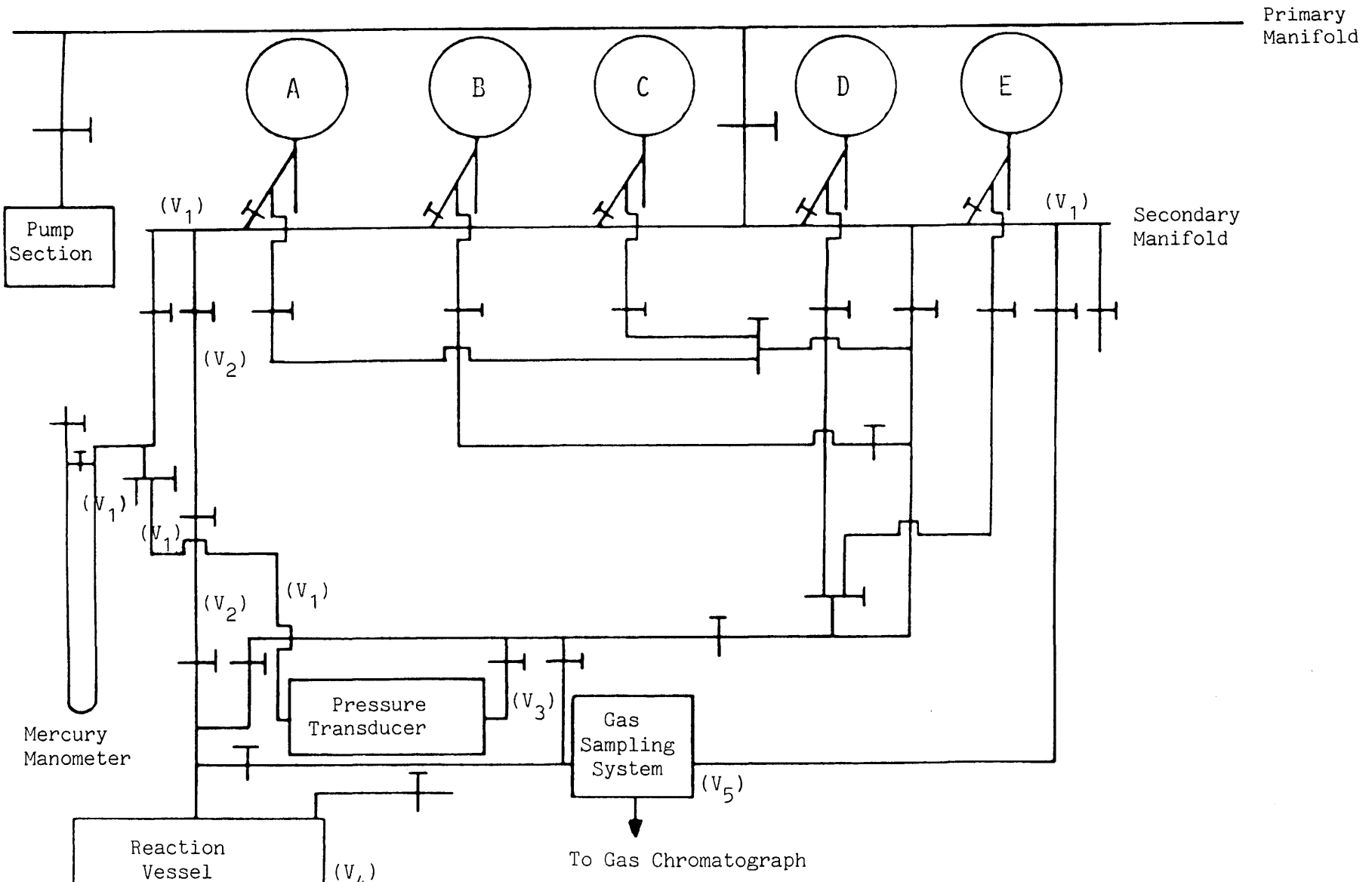

Figure 3.1 The Vacuum System .

parts of the apparatus and the pressure in each measured using a two-limbed mercury manometer; a cathetometer being used to measure the height of mercury in each limb. Each volume was determined as an average of three separate determinations. These are shown in Table 3.1.

Table 3.1

Volumes of Various Sections of the Apparatus

	Volume (cm^3)
Secondary manifold, pressure transducer-reference side and manometer (V_1)	430.1 ± 0.5
Connection between secondary manifold and reaction vessel (V_2)	13.0 ± 0.2
Pressure transducer-measuring side (V_3)	3.4 ± 0.2
Reaction vessel (with boat and G.-M. tubes in position) (V_4)	392.3 ± 0.9
Sample loop to gas chromatograph (V_5)	11.7 ± 0.1

The reaction vessel (volume 392.3cm^3) used in this study is shown in Figure 3.2. This allowed the direct observation of the adsorbed species, both during the adsorption and subsequent surface processes, via two inter-calibrated Geiger-Müller tubes (Section 3.2). These were sealed into B34 cones with Araldite, which were then sealed into the B34 sockets of the reaction vessel with Apiezon 'N'

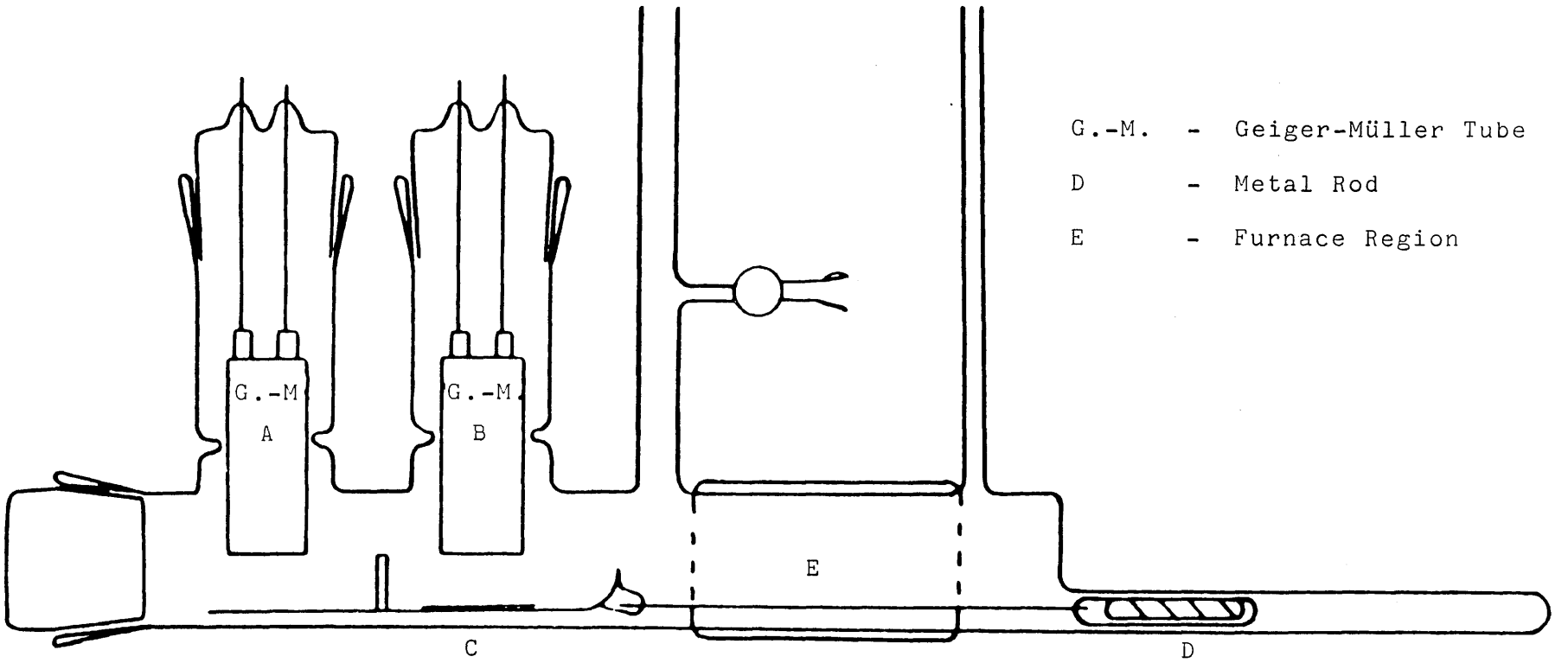

Figure 3.2 The Reaction Vessel.

grease. The catalyst was uniformly spread on the surface of one half of the boat (C) by slurrying with distilled water and drying on top of an oven, before the boat was placed in the reaction vessel. By the application of an external magnet to the glass enclosed metal rod (D), the boat was positioned in the furnace region (E) for catalyst reduction/ activation, or under the Geiger-Müller tubes during the adsorption measurements.

Geiger-Müller tube (A) monitored the radioactivity in the gas phase, while Geiger-Müller tube (B) monitored the radioactivity on the surface and in the gas phase. Equal volumes of gas were seen by each tube and therefore surface activity could be obtained by subtraction. A glass partition was positioned in the centre of the boat to prevent radioactivity from the surface being registered by Geiger-Müller tube (A).

To facilitate the analysis of the gas phase in contact with the surface during the adsorption or subsequent surface processes, the reaction vessel was coupled via a gas sampling system to a gas chromatograph (Section 3.4).

3.2 The Geiger-Müller System

The Geiger-Müller tubes used in this study were Müllard MX168/01. These had mica windows of thickness ca. 3 mg cm^{-2}.

Each of the Geiger-Müller tubes was connected to a Nuclear Enterprises SR7 scalar ratemeter. The optimum voltage setting for each Geiger-Müller (G.-M.) tube was

determined by placing a solid [14-C]polymethyl-methacrylate source under the tube and measuring the count rate as a function of applied voltage. A typical graph is shown in Figure 3.3. The count rate rose rapidly with increasing voltage until a plateau was reached (indicated by a gradient $\leq$ 5%). After the plateau the count rate increased rapidly again with increasing voltage and the tube moved into a region of continuous discharge. The mid-point of the plateau was selected as the operating voltage.

After determination of the operating voltages an estimate was made of the reliability of the counter performance by taking 20 separate counts of the source at the operating voltage. The mean, $\bar{N}$, and the standard deviation, σ, were determined, where

$$\sigma = \sqrt{\frac{\Sigma(\bar{N} - N_i)^2}{n - 1}}$$

According to statistical theory, for a normal distribution of N_i values about the mean $\bar{N}$, 68.3% of the N_i values should fall within the range $\bar{N} \pm \sigma$; 95.1% within $\bar{N} \pm 2\sigma$ and > 99% within $\bar{N} \pm 3\sigma$.

The results for this apparatus were as follows:-

	G.-M. 1	G.-M. 2	Theoretical
$\bar{N} \pm \sigma$	75%	70%	68.3%
$\bar{N} \pm 2\sigma$	95%	95%	95.1%
$\bar{N} \pm 3\sigma$	100%	100%	99%

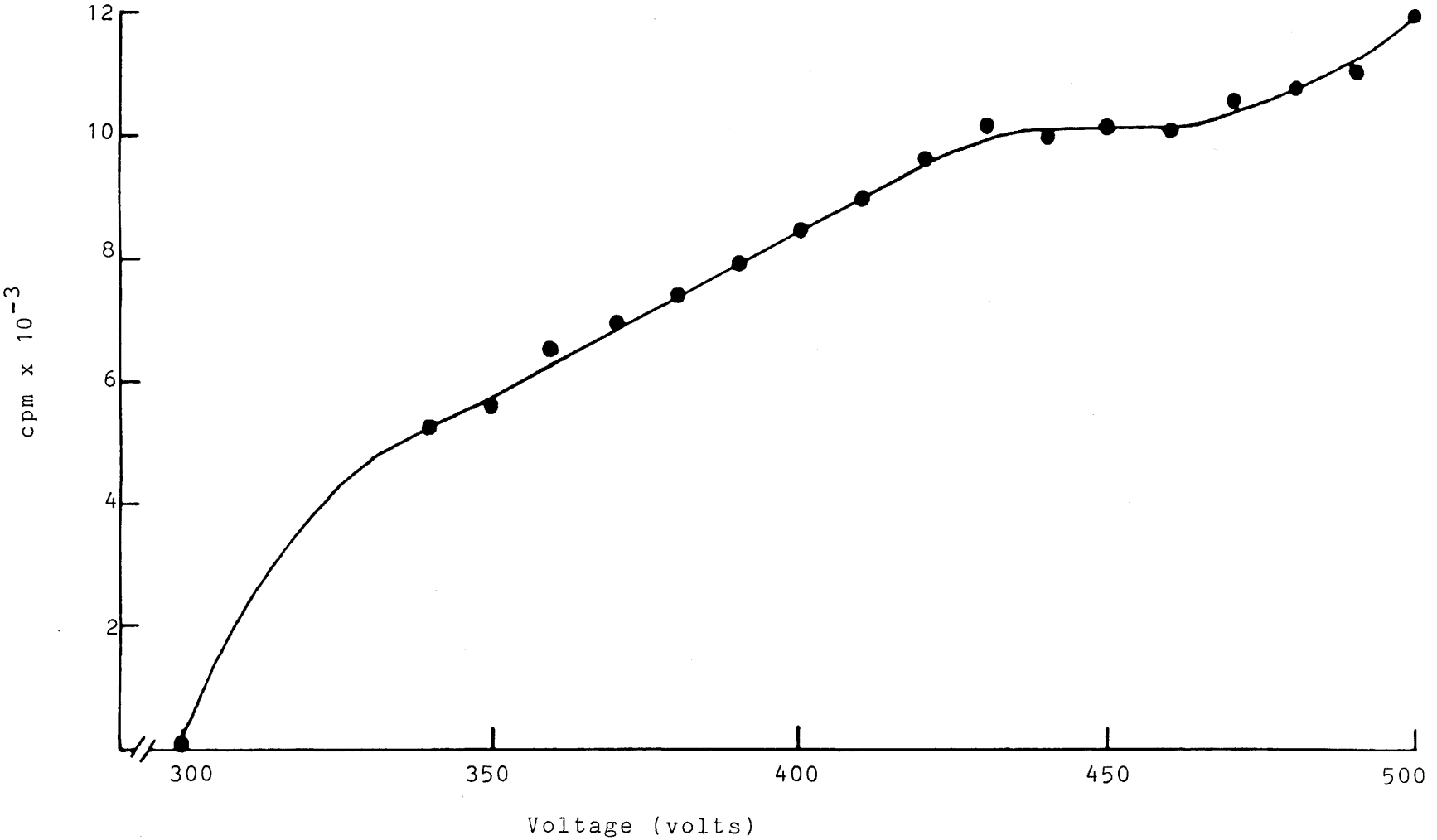

Figure 3.3 Geiger-Müller Tube Plateau .

Although twenty determinations of a count rate is a small sample for the application of statistical theory the results suggest that the system is reliable.

3.3 The Pressure Transducer

The Pressure Transducer used in this study was supplied by Thorn EMI Datatech Ltd (Type: SE/V/10D). Calibration of the pressure transducer was carried out using the mercury manometer and a cathetometer to measure the height of the mercury columns. The transducer output was fed to a Servoscribe chart recorder set at 20 mV. At this voltage, calibration of the pressure transducer showed that full-scale deflection corresponded to a pressure of 2 torr. Under these conditions the transducer was capable of accurately recording pressure changes $\geq$ 0.01 torr.

3.4 The Gas Chromatography System

Analysis of the gas phase during the adsorption or subsequent reaction of the gases on the catalyst surface was obtained using a gas chromatograph coupled to the reaction vessel via a gas sampling system. The sampling system is shown in Figure 3.4. This consisted of a U-tube (volume 11.7cm^3) which could either be flushed with carrier gas or evacuated depending on the position of the three-way taps T_1 and T_2 (Whitey SS 41 XS1). Another three-way tap T_3 permitted the carrier gas to flow through the column, by-passing the sample loop. Samples to be analysed were

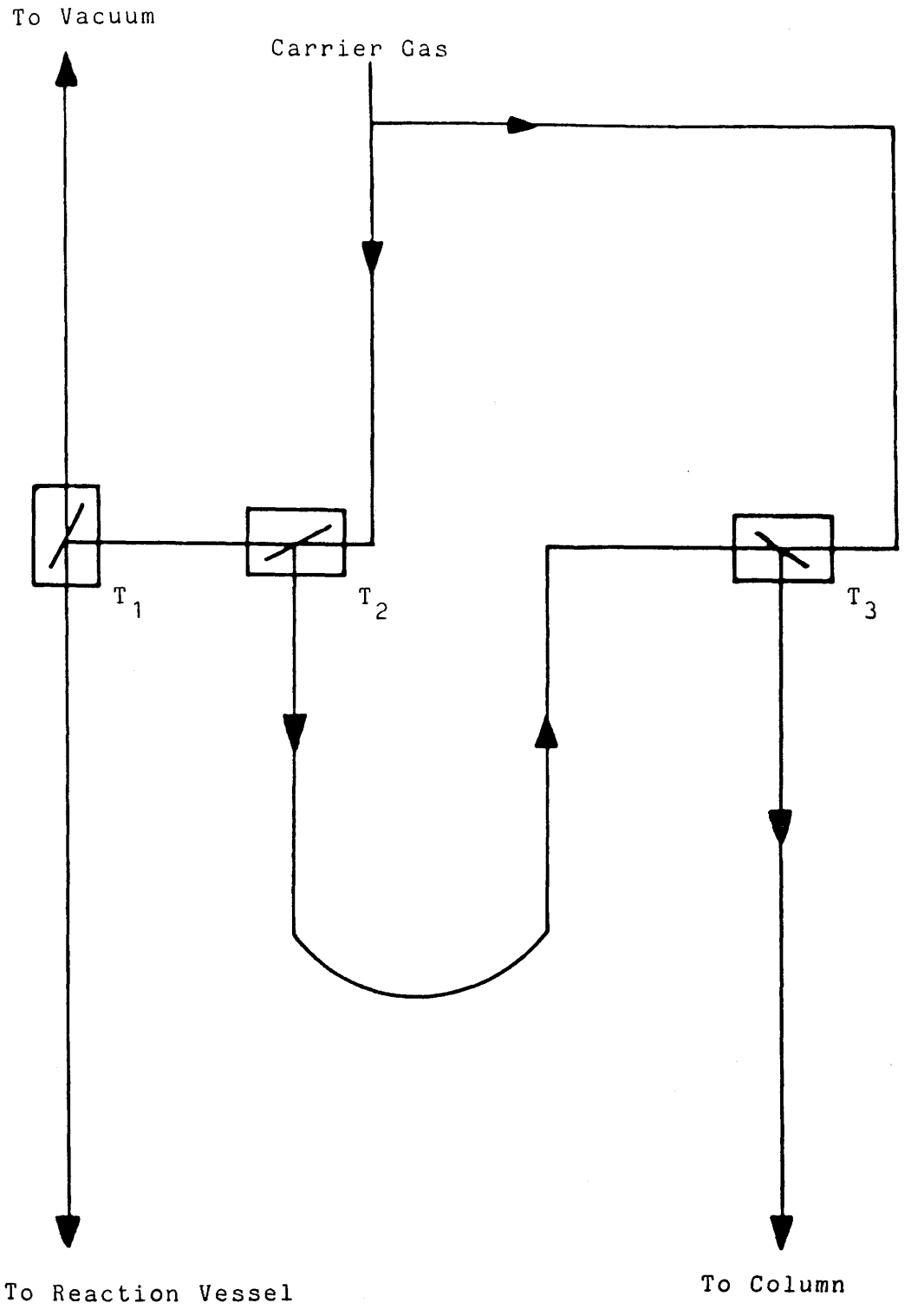

Figure 3.4 The Gas Sampling System ·

introduced into the sample loop via taps T_1 and T_2. By turning taps T_2 and T_3 simultaneously, the carrier gas was diverted from the by-pass through the sample loop carrying the sample on to the column.

Gas mixtures were separated using a 1.5 metre (2.3mm i.d.) stainless steel column packed with 80 - 100 mesh Carbosieve 'S' (supplied by Phase Sep. Ltd). The column was operated at 413K with helium as carrier gas at a flow rate of 26.6 ml min^{-1}. The detector used was a Gow-Mac thermal conductivity detector (Field Instruments Co. Ltd.) [Model 10 - 285] operated at a filament current of 200 mV via a supply unit (Stirling Control System Ltd.) [Model No. GUGC2]. The output from the supply unit was fed to a Servoscribe chart recorder operating at a full scale deflection of 10 mV. A typical trace is shown in Figure 3.5.

This system gave good separation of the gas mixtures (carbon monoxide, carbon dioxide, hydrogen, nitrous oxide and nitrogen) although it was unable to separate nitrogen and air. The retention times are given in Table 3.2.

Table 3.2

Retention Times

	Retention time (minutes)
Carbon Monoxide	1.35
Carbon Dioxide	4.90
Hydrogen	0.65
Nitrous Oxide	8.80
Nitrogen	1.15

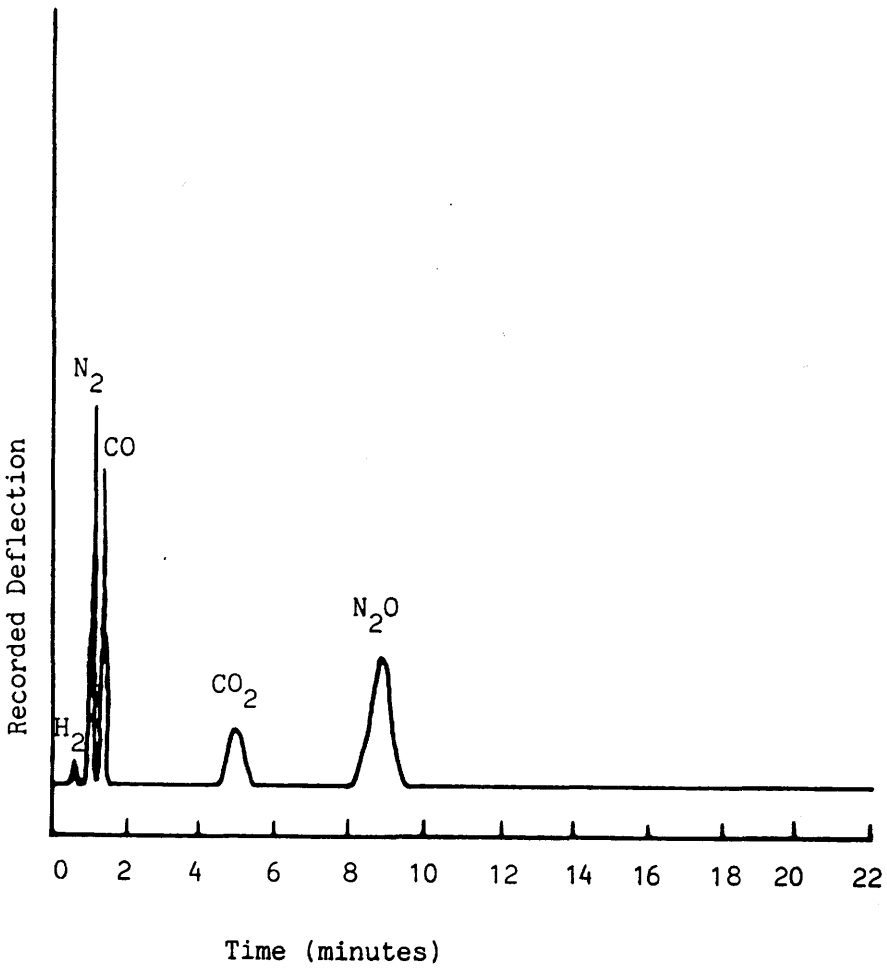

Figure 3.5 Gas Chromatography Trace

A response factor (S_A) for each gas was determined by admitting different pressures of gas into the chromatograph and measuring the height of each peak (this was found to be more reproducible than calculating the area under a given peak). The response factor is given by

$$S_A = \frac{\text{peak height}}{\text{pressure of gas}} \quad \text{mm torr}^{-1}$$

The sensitivity of the detector varied slightly from day to day and, therefore, the response factors were determined before each experiment.

3.5 Catalysts

The catalysts used in this study were $Cu/ZnO/Al_2O_3$, Cu/Al_2O_3, Al_2O_3 (from the same stock as that used in the preparation of the catalysts), a high surface area ZnO and ZnO (Analar B.D.H.).

Throughout this and subsequent sections, the high surface area ZnO is referred to as ZnO - A and ZnO (Analar B.D.H.) as ZnO - B.

The BET areas, copper surface areas, pore diameters and Na_2O impurity levels of the catalysts were measured by I.C.I. The results are shown in Table 3.3.

Table 3.3

Micromeritics, Copper Surface Areas and Na_2O Impurity Levels of the Catalysts

Catalyst	BET area ($m^2 g^{-1}$)	Copper surface area ($m^2 g^{-1}$)	Pore diameter (Å)	Na_2O level (ppm)
$Cu/ZnO/Al_2O_3$ (60/30/10)	67.8	32.1	< 36	460
Cu/Al_2O_3 (80/20)	81.1	12.0	< 36	190
ZnO - A	50.2	-	< 36	110
ZnO - B	5.1	-	< 36	< 10
Al_2O_3	308	-	< 36	630

3.5.1 Preparation of a High Surface Area ZnO

2400ml 1M $Zn(NO_3)_2$ (I.C.I. plc) and 1.5M Na_2CO_3 (I.C.I. plc) were heated to 358K in separate flasks. The $Zn(NO_3)_2$ solution was added to a large vessel (fitted with a mechanical stirrer) at the rate of 8 litres hr^{-1}, the pH was adjusted to 6.5 using the Na_2CO_3 solution.

The slurry was aged for 1 hour at 338K with continuous stirring, it was then filtered, washed with 30 litres of distilled water and dried in an oven at 383K for 16 hours before calcination at 573K for 6 hours.

3.5.2 Preparation of 80% Cu/Al_2O_3

655ml 1M $Al(NO_3)_3$ (B.D.H.), 1742ml 1M $Cu(NO_3)_2$ (I.C.I. plc) and 1M Na_2CO_3 were heated to 358K in separate flasks. The $Al(NO_3)_3$ and $Cu(NO_3)_3$ solutions were added to a large vessel (fitted with a mechanical stirrer) at a rate of 8 litres hr^{-1}, the pH was adjusted to 6.5 using the Na_2CO_3 solution.

The slurry was aged for 1 hour at 338K with continuous stirring, it was then filtered, washed with distilled water and dried in an oven at 383K for 16 hours before calcination at 573K for 6 hours.

3.6 Materials

[14-C]carbon dioxide was obtained as the gas (I.C.I. plc) or was prepared from barium [14-C]carbonate (Radiochemical Centre, Amersham) by the following method. Using the apparatus shown in Figure 3.6, concentrated hydrochloric acid, contained in part A of the apparatus was added dropwise to a suspension of 5mCi barium [14-C]-carbonate and water contained in part B. [14-C]carbon dioxide was evolved in the reaction. The reaction was assumed complete when the effervescence had stopped. The [14-C]carbon dioxide was then condensed into a tube containing magnesium perchlorate using a liquid nitrogen trap, this process was repeated again to remove water from the sample. The [14-C]carbon dioxide was then warmed and condensed into a receiving flask then sealed in ampoules each containing 1mCi [14-C]carbon dioxide ready for use. Before use the [14-C]carbon dioxide was diluted to the required specific activity with non-radioactive carbon dioxide (Air Products Ltd.).

Carbon dioxide and carbon monoxide (B.O.C. Ltd.) were found to contain no impurities detectable by gas chromatography and were used as supplied.

Nitrous oxide (B.D.H.) contained air which was removed by three successive bulb-to-bulb distillations.

Helium (B.O.C. Ltd.) was used as the carrier gas in the gas chromatography system without further purification.

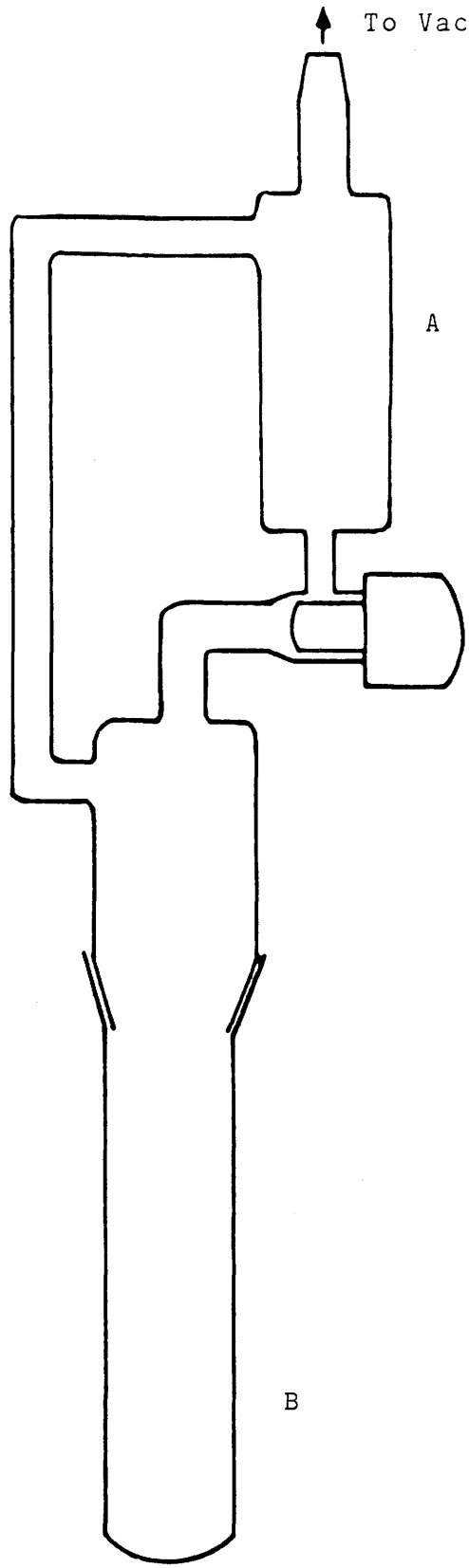

Figure 3.6 Reaction Vessel for the Preparation of [14-C]Carbon Dioxide from Barium [14-C] Carbonate .

3.6.1 Preparation of [14-C]Carbon Monoxide

[14-C]Carbon monoxide was prepared by the reduction of [14-C]carbon dioxide using metallic zinc after the method described by Bernstein and Taylor (102).

Zinc pellets (ca. 5mm diameter) were prepared from a moistened mixture containing 95% by weight zinc dust (Analar) and 5% Aerosil silica (Degussa). The pellets were dried in an air oven at 393K for 24 hours. They were then placed in the carbon dioxide converter (Figure 3.7) made up of a Pyrex loop with a furnace region (C), a B14 cone (D) for attachment to the bulb and a B14 socket (B) via which the [14-C]carbon dioxide ampoule was attached. The zinc pellets were degassed by pumping continuously for 24 hours at 593K. After raising the temperature of the furnace to 673K the break-seal on the ampoule was fractured using ball bearings contained in part A of the converter and the [14-C]carbon dioxide admitted. The [14-C]carbon dioxide was converted to [14-C]carbon monoxide by convection circulation within the converter for 48 hours. Any unconverted [14-C]carbon dioxide was then removed by freezing out using a liquid nitrogen trap placed around the cold finger (E) before the [14-C]carbon monoxide was allowed to expand into a storage bulb.

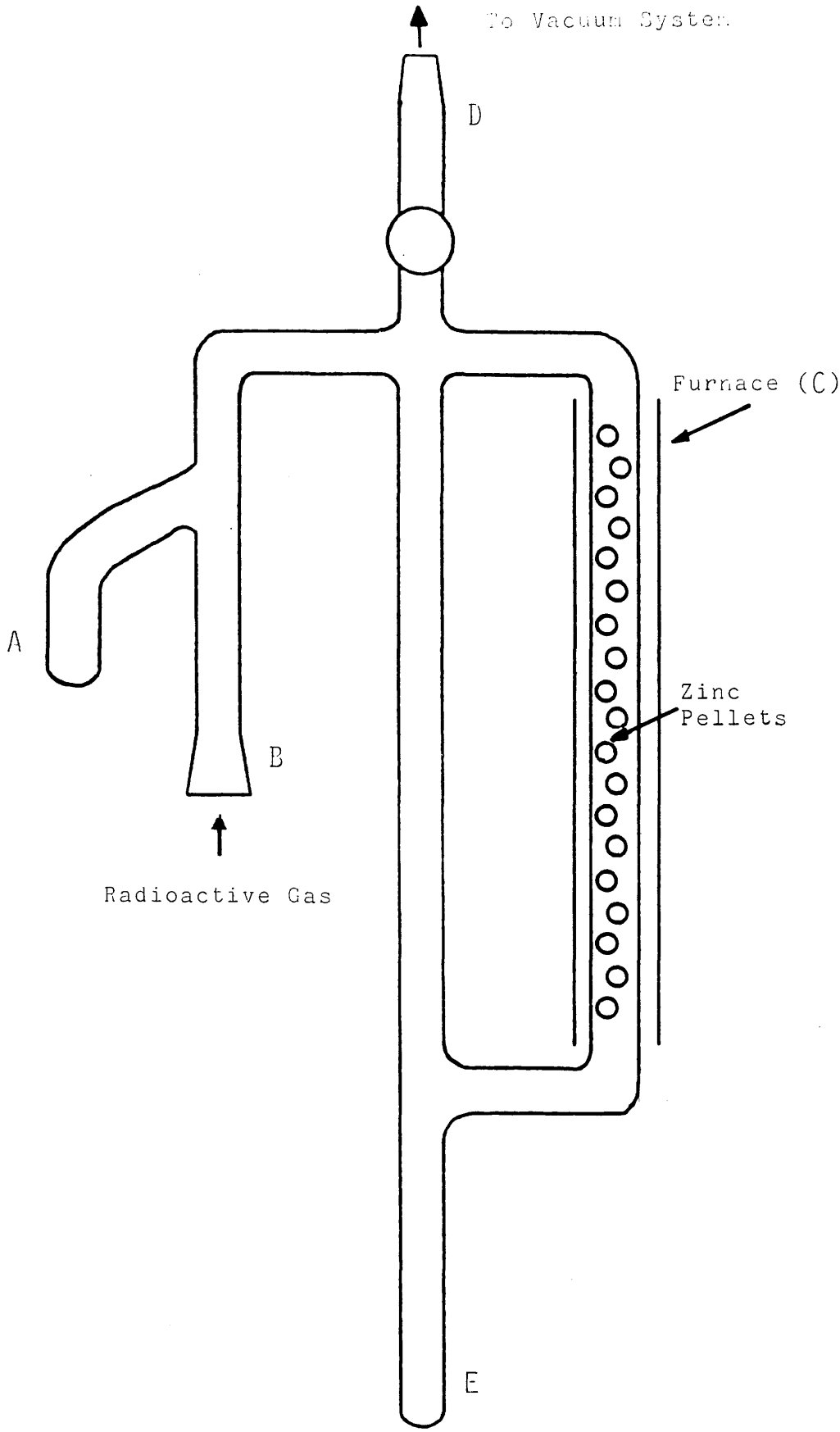

Figure 3.7 Reaction Vessel for Reduction of [14-C]Carbon Dioxide.

3.7 Experimental Procedure

3.7.1 Catalyst Activation

The catalysts ($Cu/ZnO/Al_2O_3$, Cu/Al_2O_3, ZnO and Al_2O_3) were activated in a similar manner. A sample (ca. 0.2g) in a finely divided form (60 - 100 B.S.S. mesh), was uniformly spread on one half of the boat and reduced in the furnace region of the reaction vessel with a flow of 6% hydrogen in argon (ca. 15ml min^{-1}). The temperature of the catalyst was raised over 15 minutes to 463K and maintained at this value until no further uptake of hydrogen occurred. The hydrogen uptake was monitored by a thermal conductivity detector operating at a filament current of 100 mV, the detector output being monitored on a Servoscribe chart recorder operating at a full scale deflection of 500 mV and 30mm hr^{-1} chart speed. A typical reduction profile, for $Cu/ZnO/Al_2O_3$, is shown in Figure 3.8.

When hydrogen uptake ceased the temperature was raised over 10 minutes to 513K for 2 hours without interruption of the hydrogen/argon flow. The hydrogen/argon flow was then turned off and the taps connecting the reaction vessel to the vacuum pump opened, the catalyst was then cooled to ambient temperature under continuous pumping.

3.7.2 Preparation of Oxidised $Cu/ZnO/Al_2O_3$ Catalyst Samples

Fully oxidised and partially oxidised samples of $Cu/ZnO/Al_2O_3$ were prepared using nitrous oxide. Nitrous

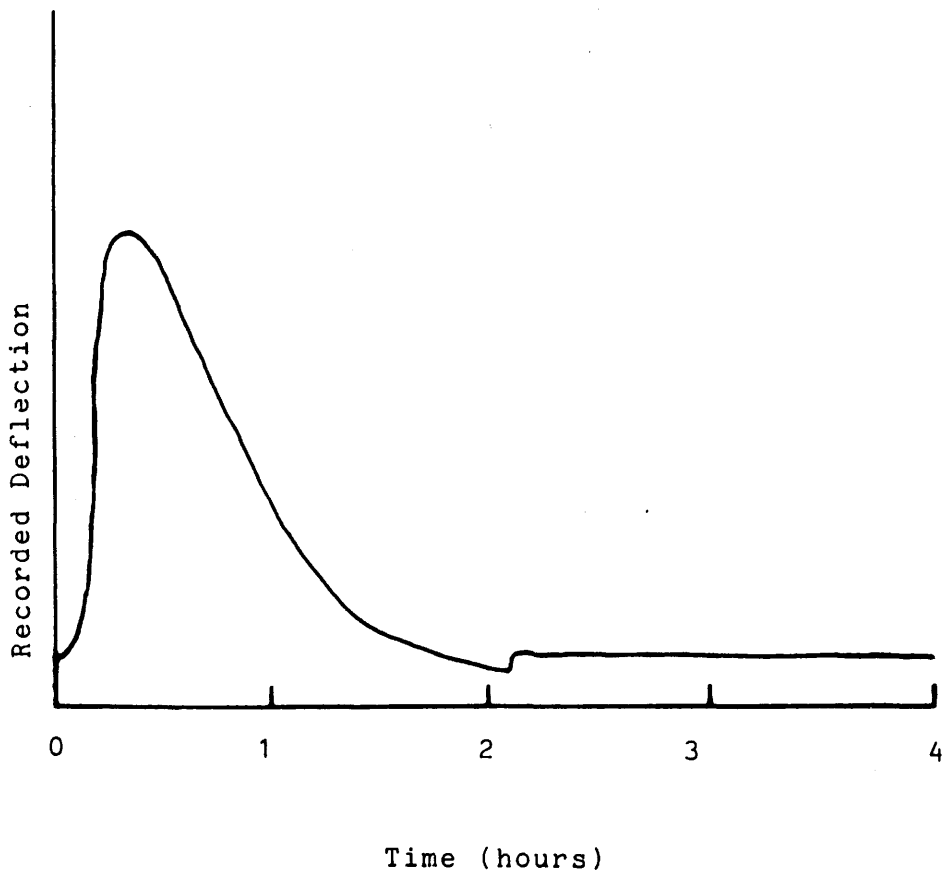

Figure 3.8 $Cu/ZnO/Al_2O_3$ Reduction Profile.

oxide reacts with the surface copper component of the $Cu/ZnO/Al_2O_3$ catalyst at temperatures below 373K to produce chemisorbed oxygen atoms and gas phase nitrogen according to the process:-

$$N_2O(g) + 2Cu(s) \longrightarrow N_2(g) + (Cu - O - Cu)_s \qquad (1)$$

where s denotes surface atoms (103). The copper surface area of the $Cu/ZnO/Al_2O_3$ catalyst was determined by measuring the amount of nitrous oxide consumed or the amount of nitrogen generated in the reaction, by gas chromatography. In addition, by controlled addition of nitrous oxide to the catalyst samples, fully oxidised and partially oxidised samples were prepared.

3.7.2.1 Preparation of Fully Oxidised $Cu/ZnO/Al_2O_3$ Samples

The approximate volume of nitrous oxide required to fully oxidise samples of $Cu/ZnO/Al_2O_3$ by equation (1) was calculated as follows. The approximate copper surface area of the catalyst was taken to be ca. $30m^2\ g^{-1}$ (quoted by the suppliers), it was assumed that an equal distribution of Cu(111), Cu(110) and Cu(100) planes existed at the surface giving an average site density on the surface of 1.46×10^{19} atom m^{-2} (104). From this value the approximate number of surface copper atoms in ca. 0.2g of sample was calculated (8.8×10^{19} atoms) and thus the volume of nitrous oxide required for full surface oxidation to Cu^I deduced (ca. 3.4 torr).

The fully oxidised samples were prepared by the *in situ* reduction of ca. 0.2g $Cu/ZnO/Al_2O_3$ as previously described (Section 3.7.1), the catalyst was then heated to 353K and excess nitrous oxide (ca. 5.0 torr) added and left overnight.

After ca. 12 hours samples of gas were taken from the reaction vessel and analysed by gas chromatography. The copper surface area of the $Cu/ZnO/Al_2O_3$ catalyst was found to be 32.1m^2 g^{-1}. The reaction vessel was then evacuated and the catalyst cooled to ambient temperature under continuous pumping.

3.7.2.2 Preparation of Partially Oxidised $Cu/ZnO/Al_2O_3$ Samples

Experiments were also carried out on 30% oxidised $Cu/ZnO/Al_2O_3$ samples. These were prepared by a similar method to that used in the preparation of fully oxidised samples using an amount of nitrous oxide (ca. 1.0 torr) such that 30% oxidation had occurred when no nitrous oxide could be detected in the gas phase.

3.7.3 Corrections to the Observed Count Rates

Three corrections were made to the observed count rates. These will be discussed separately:

(a) dead time corrections,

(b) background corrections,

and (c) multiplication of one of the G.-M. tube count rates by the intercalibration factor.

a) Dead Time

The dead time of a counter is the time after a particle has been detected before another can be detected. This factor becomes more important with increasing count rate. The dead time for each counter was determined. Various pressures of [14-C]carbon dioxide were admitted to the reaction vessel and, after each addition the number of counts after 600 seconds, recorded on each Geiger-Müller tube (N_{obs}). The theoretical number of counts (N_T) for each pressure of [14-C]carbon dioxide was then calculated from a graph of N_{obs} against pressure (Figure 3.9). N_T, the number of counts recorded by the Geiger-Müller tube after correction for dead-time effects is assumed negligible at low pressures (counts) and therefore a straight line correlation is drawn through the first few points on the graph. N_T for each value of N_{obs} is given by the projection of N_{obs} on to this straight line. The dead time was then determined by:

$$t_d = \frac{(N_T - N_{obs})}{N_T N_{obs}} \times 600 \text{ sec. count}^{-1}$$

The Geiger-Müller tubes had a dead time ca. 0.06 μ sec. $count^{-1}$.

(b) Background

Before each experiment the activity due to external radiation was determined (background count rate). This was then corrected for dead time and subtracted from all subsequently determined experimental count rates.

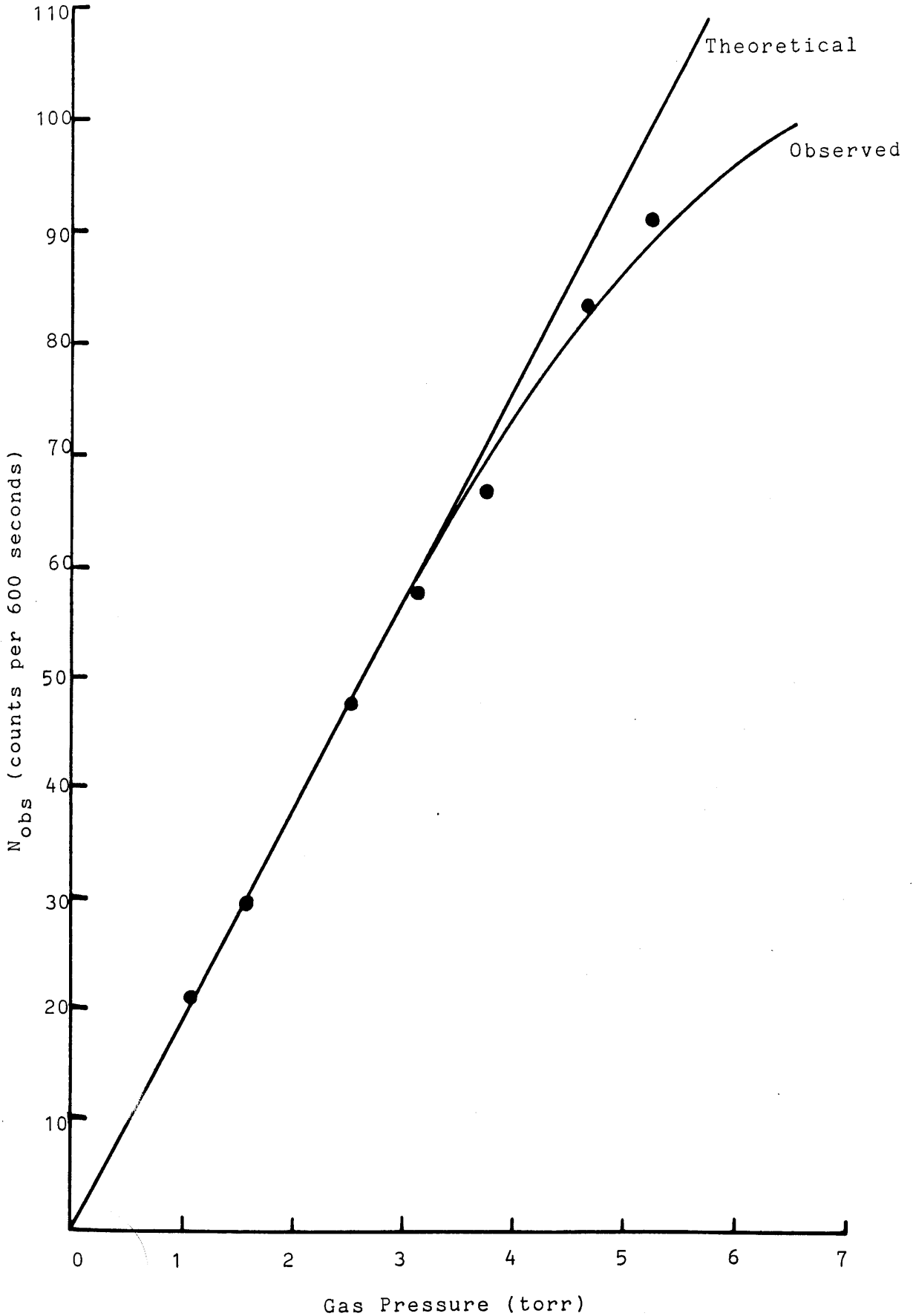

Figure 3.9 N_{obs} as a Function of Gas Pressure .

(c) Intercalibration

The efficiency of the G.-M. tubes was slightly different and thus it was necessary to obtain a relationship between the counts registered by G.-M. (A) and those registered by G.-M. (B).

Increasing pressures of radioactive gas were admitted to the reaction vessel with the boat in position (with no catalyst present) under the G.-M. tubes and the count rates determined. Figure 3.10 shows a graph of G.-M. (B) count rate (corrected for background and dead-time losses) against the corresponding count rate for G.-M. (A). The inter-calibration factor was determined from the gradient of this graph and all count rates subsequently measured by G.-M. (B) were multiplied by this factor before determination of the surface count rate by subtraction of the two corrected count rates.

3.7.4 Adsorption Isotherms

Adsorption of [14-C]labelled species was carried out by admitting small aliquots (ca. 0.2 torr) of the relevant gas to the reaction vessel containing the activated catalyst (Sections 3.5 and 3.7.1) with the boat situated under the G.-M. tubes. After admission of each aliquot, three separate determinations of the count rates were made over a period of 30 minutes, two identical count rates being taken as an indication of the attainment of surface-gas equilibrium.

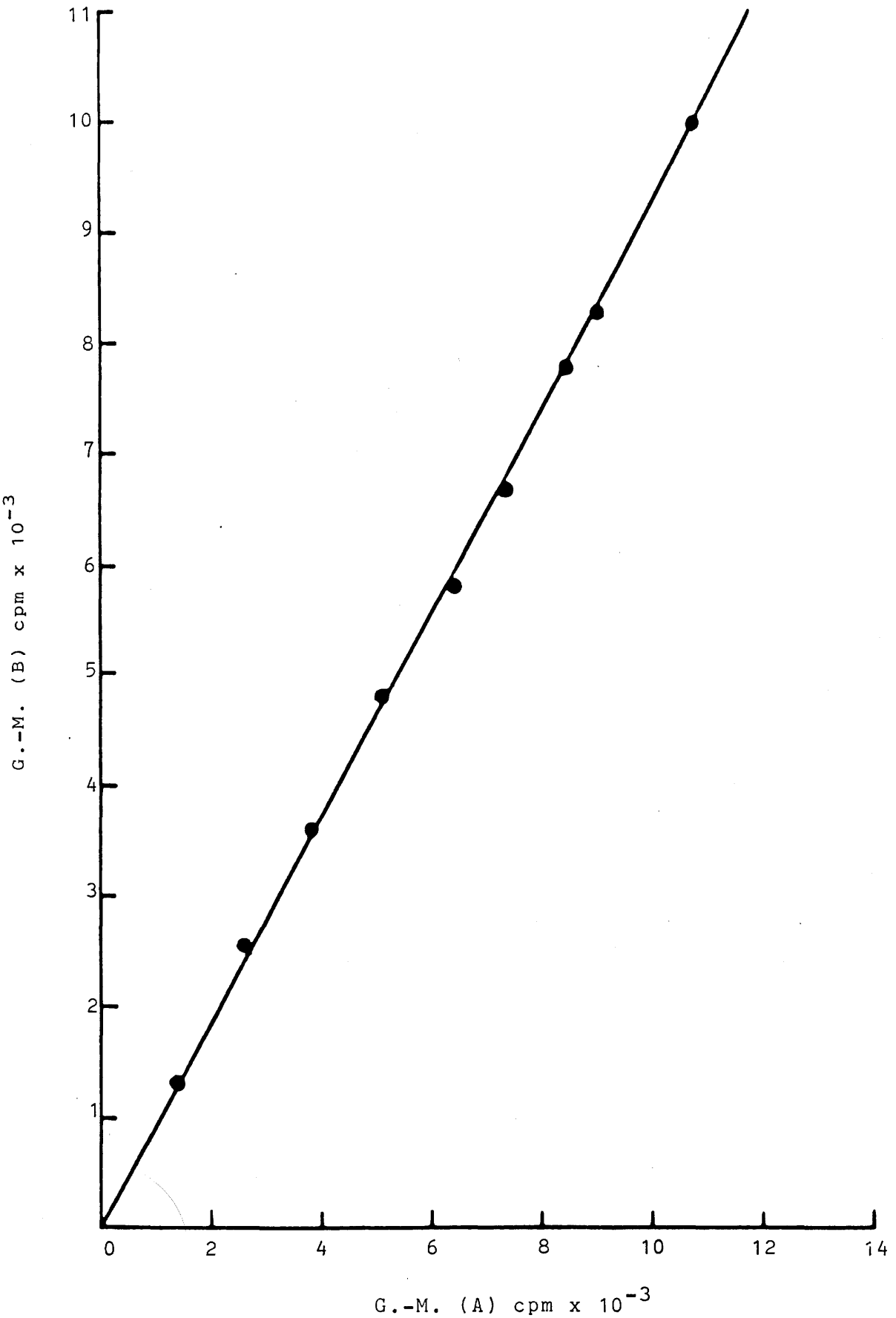

Figure 3.10 Intercalibration Plot for G.-M. Tubes.

The adsorption isotherm was stopped at a total pressure of ca. 2 torr in the reaction vessel.

3.8 Adsorption Studies in a Flow System

The methods described in this section refer to the results reported in Section 4.9.

3.8.1 Experimental

The apparatus (Figure 3.11) consisted of a microreactor system (A) coupled to a mass spectrometer (Type VG Micromass QX 200), the output from which was fed to a Chessel flat-bed chart recorder.

The microreactor system was made up of a 10cm long stainless steel tube (6mm i.d.) mounted in an oven. Catalyst samples were placed in the stainless steel tube and held in position with glass wool. Helium, 2.5% hydrogen in nitrogen, carbon monoxide in helium and argon (11/80/9) or carbon dioxide was passed over a Deoxo column depending on the position of the three-way taps T_1 and T_2. By positioning the three-way taps T_3 and T_4 correctly, one of these gases or 3.3% nitrous oxide in helium was passed over the catalyst sample or admitted directly to the mass spectrometer. The mass spectrometer was heated to temperatures in excess of 373K to prevent water condensing in the system. The various gases were monitored by recording the following masses: $^{m}/_{e}$ = 17 (H_2O), $^{m}/_{e}$ = 2 (H_2), $^{m}/_{e}$ = 14 (CO), $^{m}/_{e}$ = 44 (N_2O), $^{m}/_{e}$ = 28 (N_2), $^{m}/_{e}$ = 22 (CO_2).

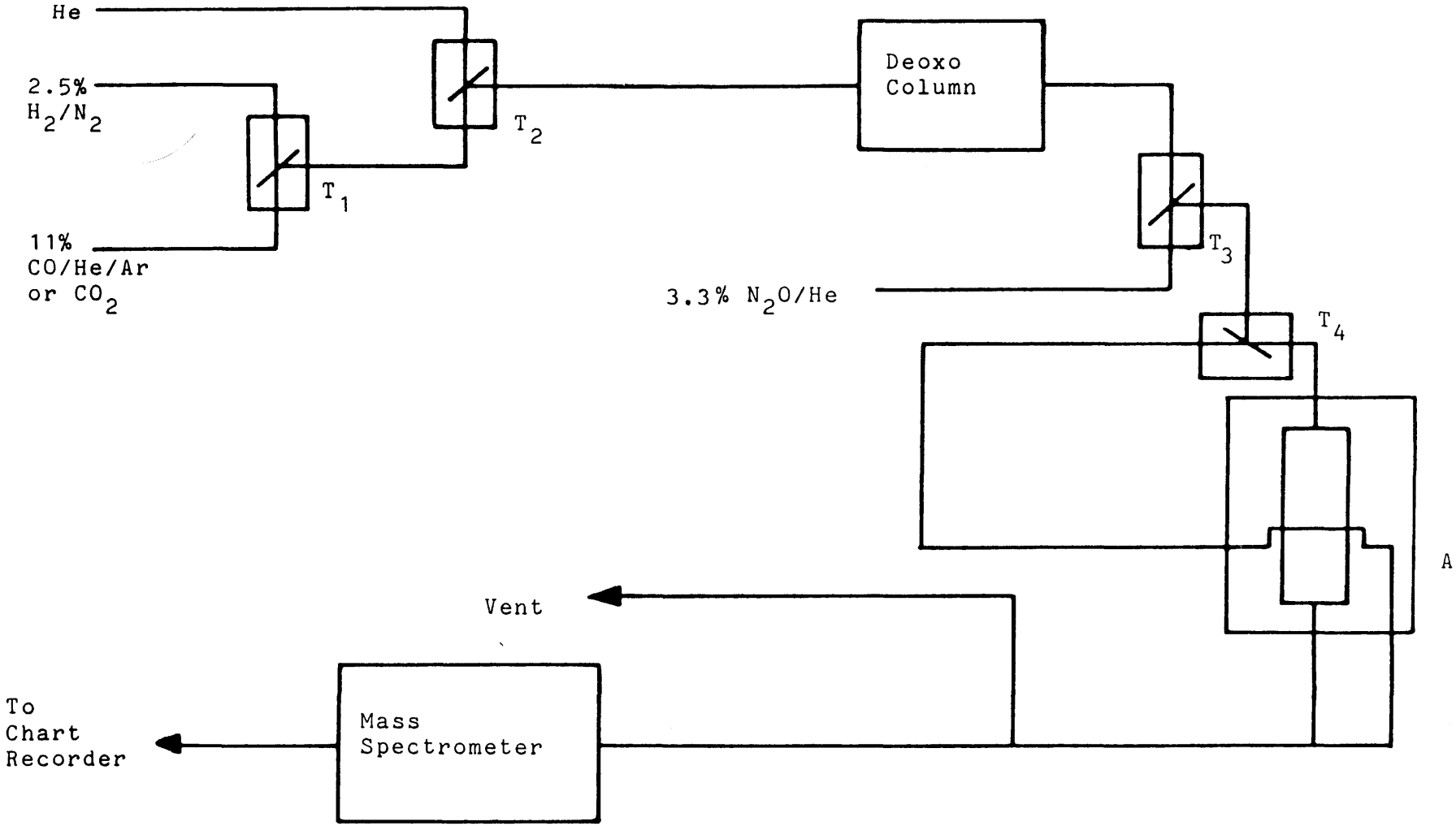

Figure 3.11 The Microreactor/Mass Spectrometer System.

3.8.1.1 Materials

The catalyst used in this study was $Cu/ZnO/Al_2O_3$, as described previously (Section 3.5).

Carbon dioxide, helium, carbon monoxide in helium and argon (11/80/9) and 2.5% hydrogen in nitrogen were supplied by I.C.I. Agricultural Division, these gases contained traces of oxygen, which was removed by a Deoxo column supplied by Phase Sep. Ltd.

For the oxidation of catalysts, 3.3% nitrous oxide in helium (I.C.I. Agricultural Division) was used without further purification.

3.8.2 Experimental Procedure

3.8.2.1 Catalyst Activation

A sample of $Cu/ZnO/Al_2O_3$ catalyst (ca. 3.0g) in a finely divided form (18 - 25 B.S.S. mesh) was placed in the stainless steel reactor tube and held in position with glass wool.

A stream of 2.5% hydrogen in nitrogen (flow rate = 200ml min^{-1}) was passed over the catalyst and the temperature ramped up to 503K at a rate of 16^{o} min^{-1}. The catalyst was then reduced at 503K for four hours. After reduction, the gas was switched to helium and the catalyst cooled in a flow of helium to ambient temperature before the adsorption studies were carried out.

3.8.2.2 Measurement of Copper Surface Area

The copper surface area of the $Cu/ZnO/Al_2O_3$ catalysts was determined *in situ* by frontal chromatography as described by Chinchen and Waugh (105). This involved sweeping out the reduction/reactant gases with helium and cooling to ambient temperature. A flow of 3.3% nitrous oxide in helium was then passed over the catalyst and the nitrogen front produced, monitored by the mass spectrometer. The copper surface area was then calculated from the volume of nitrogen produced. Fully oxidised samples of $Cu/ZnO/Al_2O_3$ could, therefore, be prepared using this technique.

CHAPTER FOUR

4. RESULTS

All adsorption measurements were made at 293 ± 2K by the method described in Section 3.7.4.

4.1 Adsorption of [14-C]Carbon Dioxide on Reduced $Cu/ZnO/Al_2O_3$

Figure 4.1 shows two adsorption isotherms obtained when successive aliquots of [14-C]carbon dioxide were admitted to freshly reduced samples of $Cu/ZnO/Al_2O_3$, activated as described in Section 3.7.1. After each addition of [14-C]-carbon dioxide, a slow adsorption or reaction on the catalyst sample was indicated by a slow, continuous decrease in pressure in the reaction vessel measured by the pressure transducer. Each point on the isotherm was determined after admission of each aliquot by taking three separate determinations of the count rates over a period of 30 minutes, two identical count rates being taken as an indication of the attainment of surface-gas equilibrium.

Gas chromatographic analysis of the gas phase in contact with the surface during the adsorption process, revealed that, carbon dioxide was the only gas present.

In order to facilitate the comparison in the amount of radiolabelled gas adsorbed by catalyst samples after different treatments, adsorptions on the same catalyst sample were attempted. In this way, changes in the counting geometry which took place when the sample was changed would have been minimised. However, attempts to regenerate the catalyst surface by re-reduction in a stream of 6% hydrogen

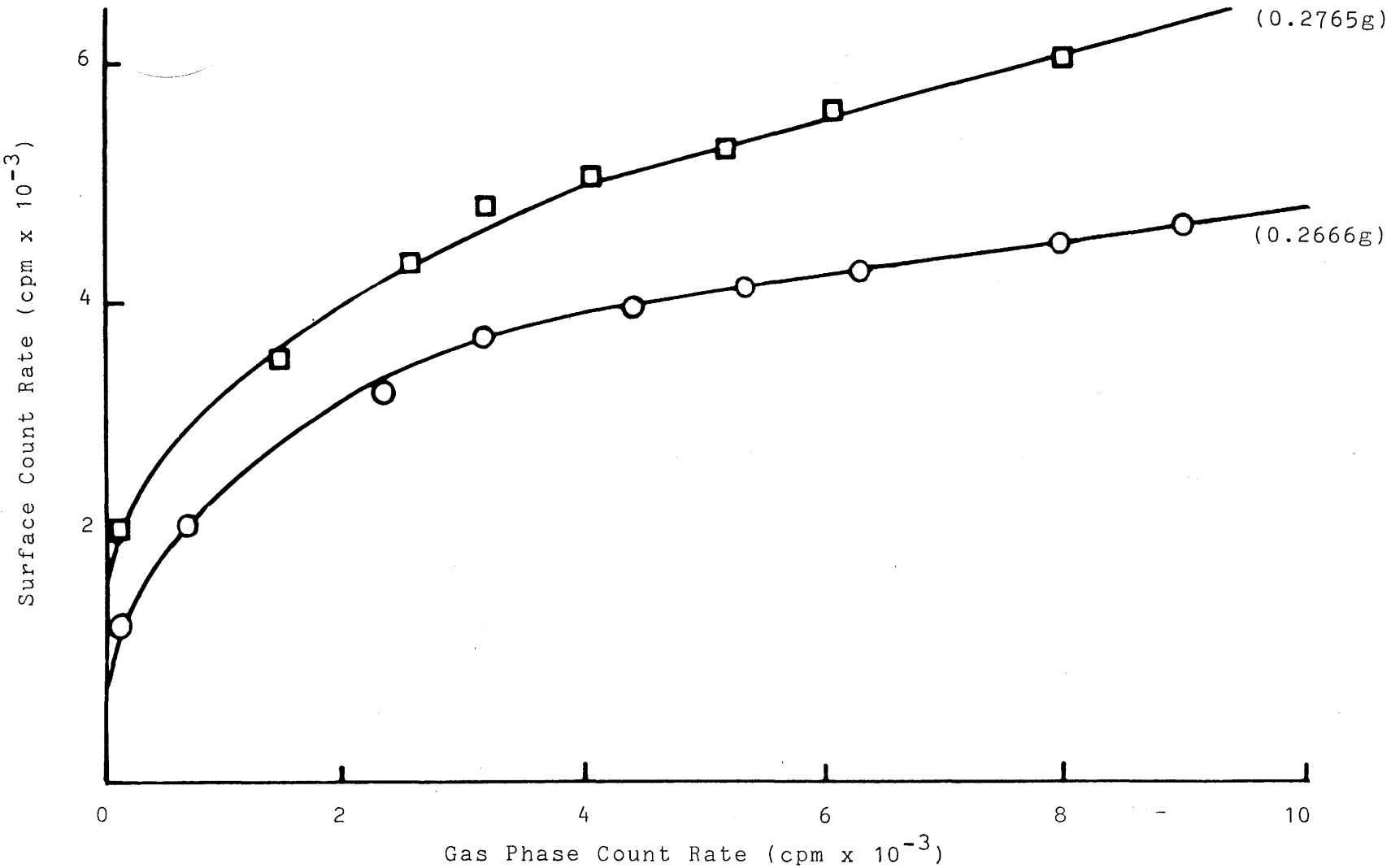

Figure 4.1 Adsorption Isotherms for [14-C]Carbon Dioxide (sp. acty = 0.130 mCi $mmol^{-1}$) on $Cu/ZnO/Al_2O_3$.

in argon (flow rate = 15ml min^{-1}) at 463K for 2 hours, after [14-C]carbon dioxide had been adsorbed on a freshly reduced sample of $Cu/ZnO/Al_2O_3$ and evacuated for 10 minutes, indicated that, although nearly all of the surface radioactivity had been removed, the amount of [14-C]carbon dioxide subsequently adsorbed on the catalyst had decreased. No reduction was found to take place during the treatment of the [14-C]carbon dioxide precovered catalyst with 6% hydrogen in argon at 463K, as indicated by the thermal conductivity detector. When following the adsorption of [14-C]carbon dioxide, the same catalyst sample was treated at 463K with helium for 2 hours, a similar effect to that of 6% hydrogen in argon was observed, nearly all of the surface radioactivity being removed. The amount of [14-C]carbon dioxide subsequently adsorbed on the catalyst was less than that which was adsorbed after the 6% hydrogen in argon thermal pretreatment. The results are shown in Table 4.1. In order to determine the reason for the reduction in the amount of [14-C]carbon dioxide adsorbed on the catalyst surface after the thermal treatments, the copper surface area of a $Cu/ZnO/Al_2O_3$ catalyst was determined using nitrous oxide (Section 3.7.2) after adsorption of [14-C]carbon dioxide and treatment with helium at 463K for 2 hours. The copper surface area was found to have decreased by 51% compared to that of a freshly reduced catalyst. An experiment carried out in the absence of [14-C]carbon dioxide indicated a loss in copper area of 22% compared to that of a freshly reduced catalyst.

Table 4.1 Adsorption of [14-C]Carbon Dioxide on $Cu/ZnO/Al_2O_3$ After Different Thermal Pre-Treatments

Specific Activity of [14-C]carbon dioxide = 0.106mCi $mmol^{-1}$

Weight of catalyst = 0.2482g

Procedure	Surface count rate (cpm)	% Change
Adsorption of [14-C]carbon dioxide to gas pressure of 1.89torr	3510	-
Evacuation for 10 minutes followed by 6% hydrogen in argon at 463K for 2 hours	-	-
Adsorption of [14-C]carbon dioxide to gas pressure of 1.89torr	3162	9.9
Evacuation for 10 minutes followed by helium at 463K for 2 hours	-	-
Adsorption of [14-C]carbon dioxide to gas pressure of 1.89torr	2534	27.8

4.1.1 Adsorption of [14-C]Carbon Dioxide on Unreduced $Cu/ZnO/Al_2O_3$

Figure 4.2 shows an adsorption isotherm obtained when successive aliquots of [14-C]carbon dioxide were admitted to an unreduced $Cu/ZnO/Al_2O_3$ catalyst sample.

The adsorption of [14-C]carbon dioxide on unreduced $Cu/ZnO/Al_2O_3$ was similar to that on reduced $Cu/ZnO/Al_2O_3$ in that a pressure decrease in the reaction vessel was recorded during the adsorption process, however, the isotherm obtained is not similar to those in Figure 4.1.

4.1.2 The Reversibility of Adsorption of Carbon Dioxide on Reduced $Cu/ZnO/Al_2O_3$

The reversibility of adsorption of carbon dioxide on reduced $Cu/ZnO/Al_2O_3$ was measured in 2 ways.

(1) Evacuation

Small aliquots of [14-C]carbon dioxide were admitted to the reaction vessel containing a freshly reduced catalyst sample and an adsorption isotherm obtained in the usual manner. The reaction vessel was evacuated for 10 minutes and the surface count rate determined. The results are shown in Table 4.2.

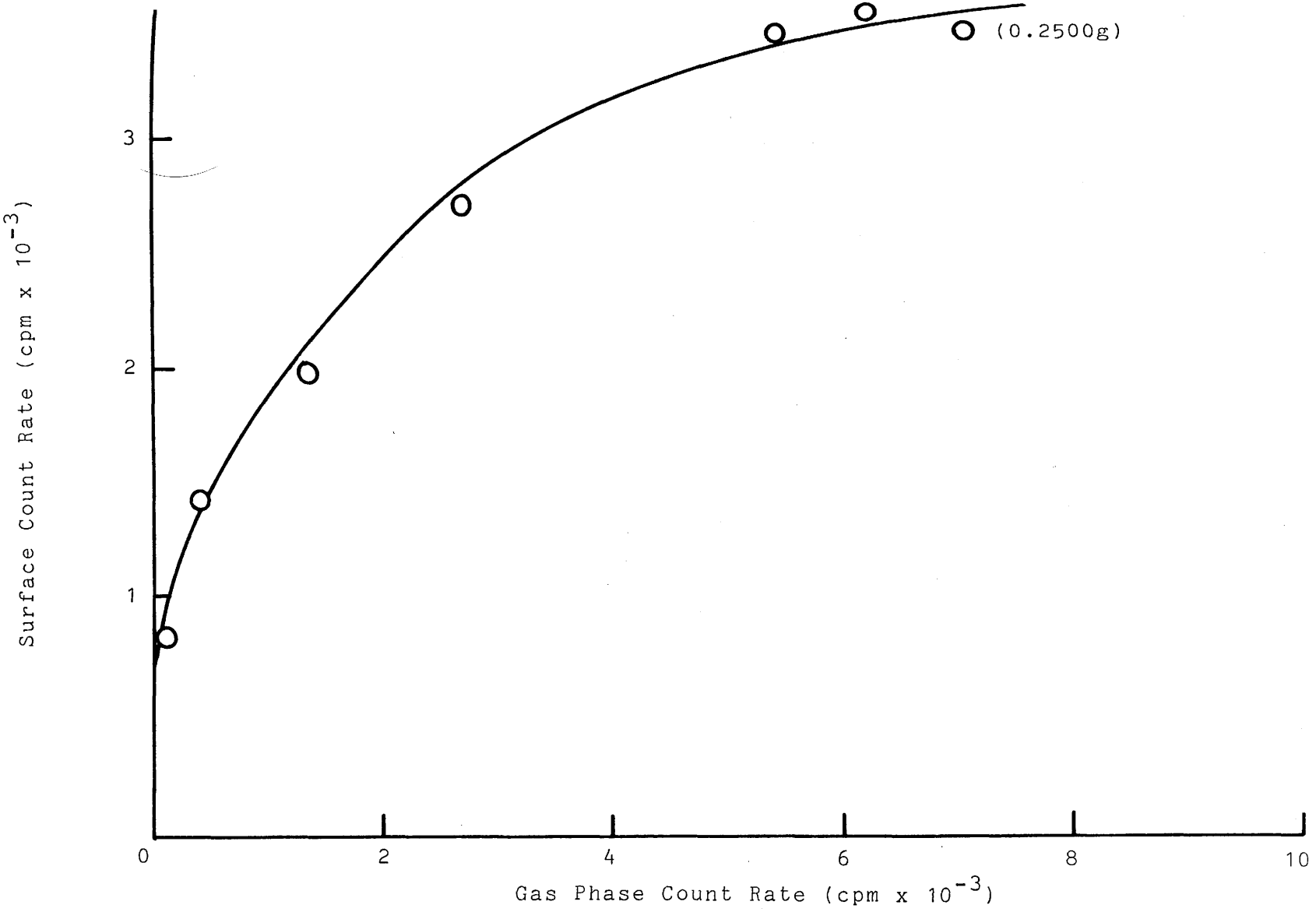

Figure 4.2 Adsorption Isotherm for [14-C]Carbon Dioxide (sp. acty = 0.106 mCi $mmol^{-1}$) on Unreduced $Cu/ZnO/Al_2O_3$.

Table 4.2 Effects of Evacuation on Carbon Dioxide Adsorbed on $Cu/ZnO/Al_2O_3$

Specific activity of [14-C]carbon dioxide = 0.045mCi $mmol^{-1}$

Weight of catalyst = 0.2250g

Procedure	Surface count rate (cpm)	% Change
Adsorption of [14-C]carbon dioxide to gas pressure of 1.89torr	1452	-
Evacuation for 10 minutes	964	-33.6

(2) Molecular Exchange

The exchange between preadsorbed [14-C]carbon dioxide and [12-C]carbon dioxide in the gas phase both (a) before and (b) after evacuation of the precovered surface was determined as follows. Successive aliquots of [14-C]carbon dioxide were admitted to a freshly reduced catalyst sample until the pressure in the gas phase was ca. 2 torr, then (a) without evacuation, 4.72 torr [12-C]carbon dioxide was admitted to the reaction vessel and the surface count rate determined after various time intervals, or, (b) the reaction vessel was evacuated for 10 minutes and the surface count rate determined. 4.67 torr [12-C]carbon dioxide was then admitted and the surface count rate determined after various time intervals. The results are shown in Tables 4.3(a) and 4.3(b).

Table 4.3(a) Effects of Molecular Exchange on Carbon Dioxide Adsorbed on $Cu/ZnO/Al_2O_3$ Without Evacuation

Specific activity of [14-C]carbon dioxide = 0.045mCi $mmol^{-1}$

Weight of catalyst = 0.2296g

Procedure	Surface count rate (cpm)	% Change
Adsorption of [14-C]carbon dioxide to gas pressure of 1.96torr	1529	-
Admission of 4.72torr [12-C]carbon dioxide		
for 10 minutes	1321	-13.6
for 12 hours	1248	-18.4

Table 4.3(b) Effects of Molecular Exchange on Carbon Dioxide Adsorbed on $Cu/ZnO/Al_2O_3$ after Evacuation

Specific activity of [14-C]carbon dioxide = 0.045mCi $mmol^{-1}$

Weight of catalyst = 0.2250g

Procedure	Surface count rate (cpm)	% Change
Adsorption of [14-C]carbon dioxide to gas pressure of 1.89torr	1452	-
Evacuation for 10 minutes	964	-33.6
Admission of 4.67torr [12-C]carbon dioxide		
for 10 minutes	629	-56.7
for 12 hours	479	-67.0

4.1.3 Successive Adsorptions/Evacuations of [14-C]Carbon Dioxide on the Same Reduced $Cu/ZnO/Al_2O_3$ Catalyst Sample

Figure 4.3 shows a series of isotherms obtained when successive aliquots of [14-C]carbon dioxide were admitted to a reduced catalyst sample until a pressure ca. 2 torr was obtained in the reaction vessel. The reaction vessel was then evacuated for 10 minutes and the surface count rate determined before further aliquots of [14-C]carbon dioxide were admitted. After the last point on the second adsorption isotherm had been measured, the reaction vessel was evacuated for a further 10 minutes and the surface count rate again determined before a third isotherm for [14-C]carbon dioxide was established on the surface. From Figure 4.3, it can be seen that the shapes of isotherms 2 and 3 are similar but are different to isotherm 1. The amount which was evacuated after the last point had been determined on each isotherm was 31%, 25% and 21% for isotherms 1, 2 and 3 respectively.

4.1.4 The Effects of Hydrogen on the Adsorption of Carbon Dioxide on Reduced $Cu/ZnO/Al_2O_3$

The adsorption isotherm obtained when [14-C]carbon dioxide was adsorbed on a freshly reduced $Cu/ZnO/Al_2O_3$ catalyst sample in the presence of hydrogen is shown in Figure 4.4. This was obtained when 3.62 torr hydrogen was admitted to a reduced catalyst sample and left for 45 minutes. During this time a gradual decrease in pressure (0.44 torr)

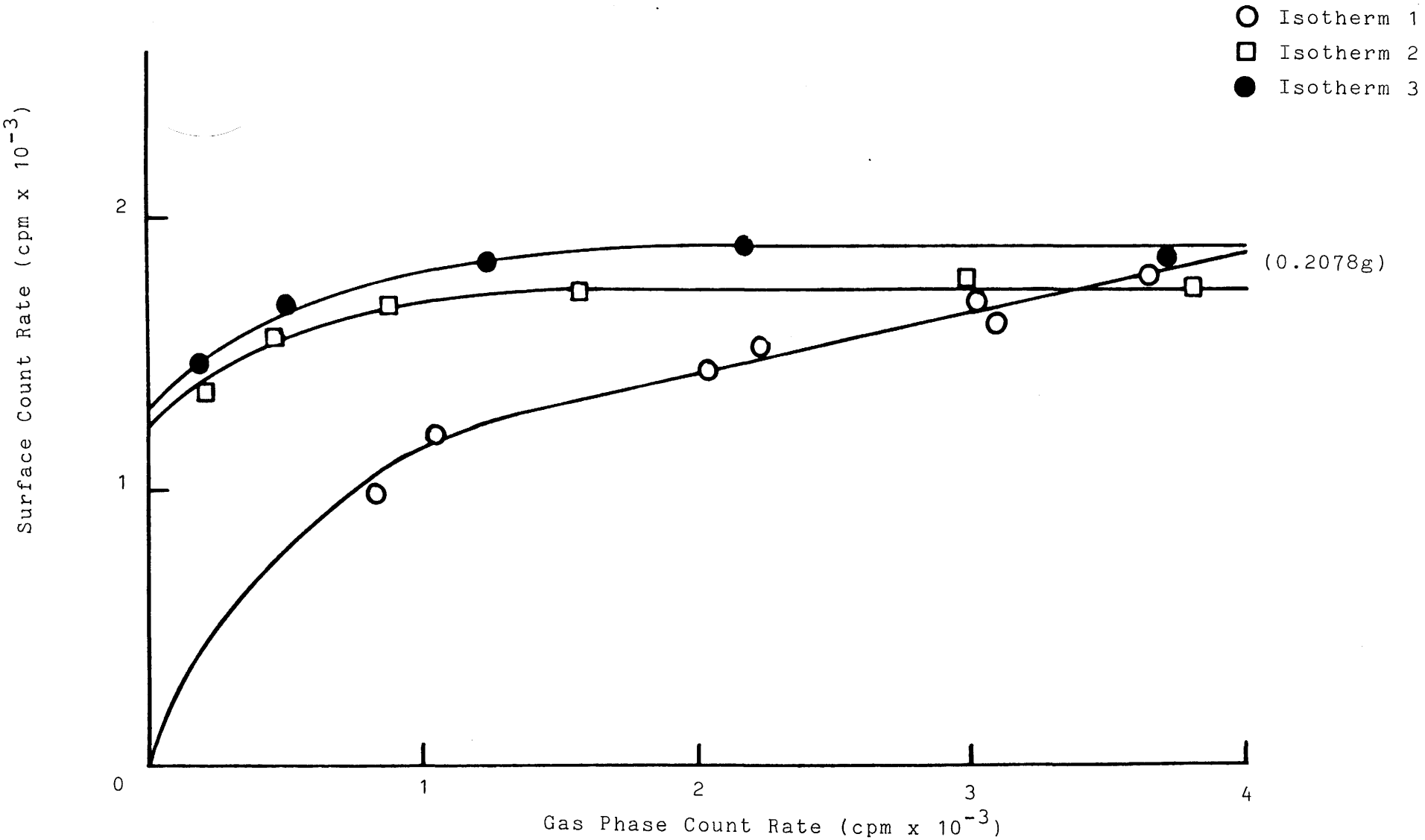

Figure 4.3 Adsorption Isotherms for [14-C]Carbon Dioxide (sp. acty = 0.062 mCi $mmol^{-1}$) on the Same $Cu/ZnO/Al_2O_3$ Catalyst Sample.

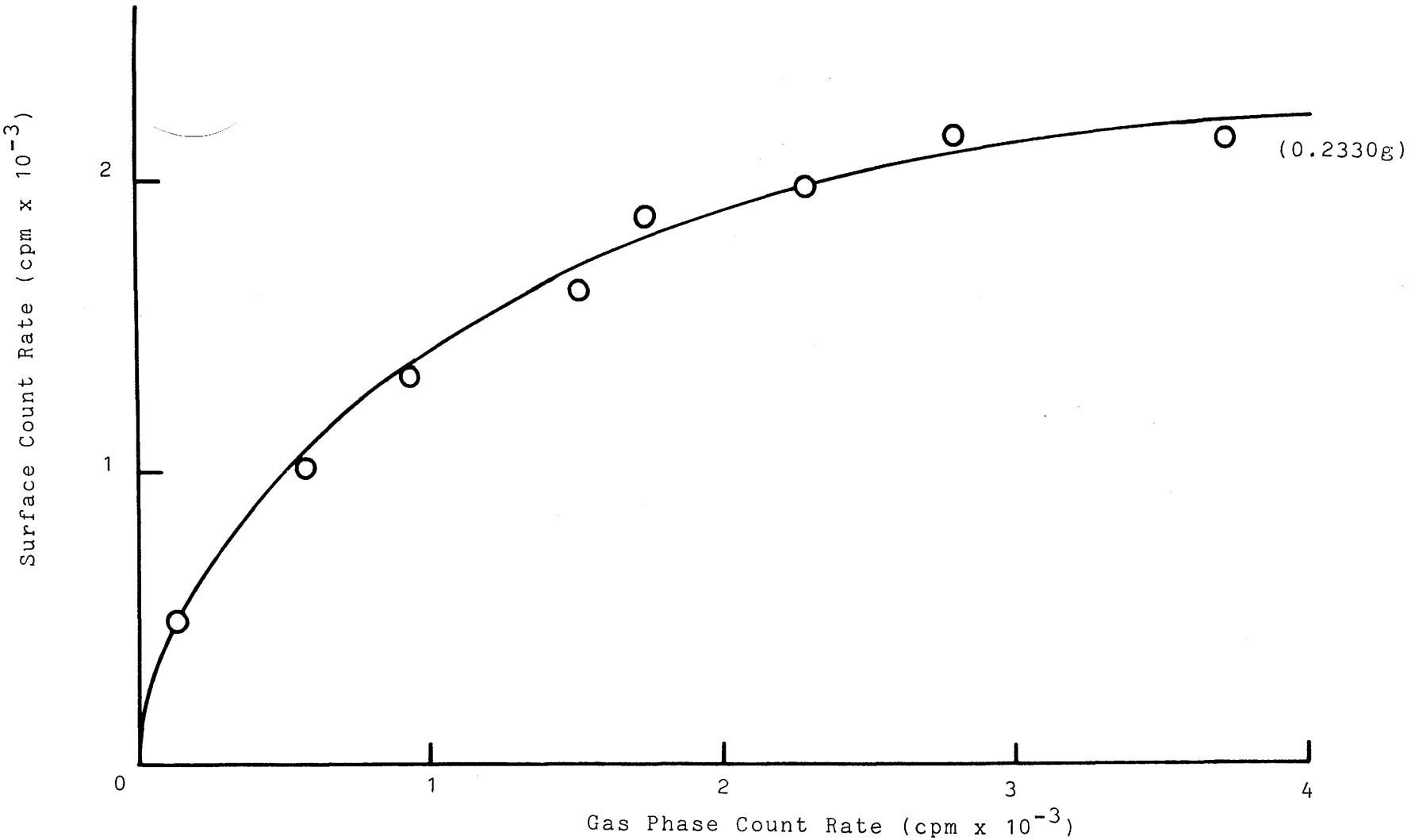

Figure 4.4 Adsorption Isotherm for [14-C]Carbon Dioxide (sp. acty = 0.062 mCi $mmol^{-1}$) on $Cu/ZnO/Al_2O_3$ in the Presence of 3.62 torr Hydrogen.

in the reaction vessel was recorded by the pressure transducer. Without evacuation, successive aliquots of [14-C]carbon dioxide were admitted to the reaction vessel until ca. 2 torr [14-C]carbon dioxide had been admitted. The reaction vessel was then evacuated over a period of 10 minutes and the surface count rate determined. 23% of the adsorbed species was evacuated.

4.1.5 Adsorption of [14-C]Carbon Dioxide on Reduced $Cu/ZnO/Al_2O_3$ Over a Long Time Period

From the decrease in pressure in the reaction vessel recorded during the adsorption of [14-C]carbon dioxide on reduced $Cu/ZnO/Al_2O_3$, reported in Section 4.1, it became apparent that carbon dioxide, adsorbed or reacted slowly on the catalyst surface. In order to determine the time taken for a sample of carbon dioxide to reach equilibrium with the surface, a large aliquot (2.61 torr) of [14-C]carbon dioxide was admitted to a freshly reduced catalyst sample and the surface count rate determined over a period of 39 hours.

Gas chromatographic analysis during the adsorption indicated the presence of a small amount of carbon monoxide (ca. 5×10^{17} molecules) in the gas phase after 25 hours.

A graph of surface count rate against time for the adsorption of 2.61 torr [14-C]carbon dioxide on reduced $Cu/ZnO/Al_2O_3$ is shown in Figure 4.5. From Figure 4.5, it can be seen that, 2.61 torr [14-C]carbon dioxide took 26

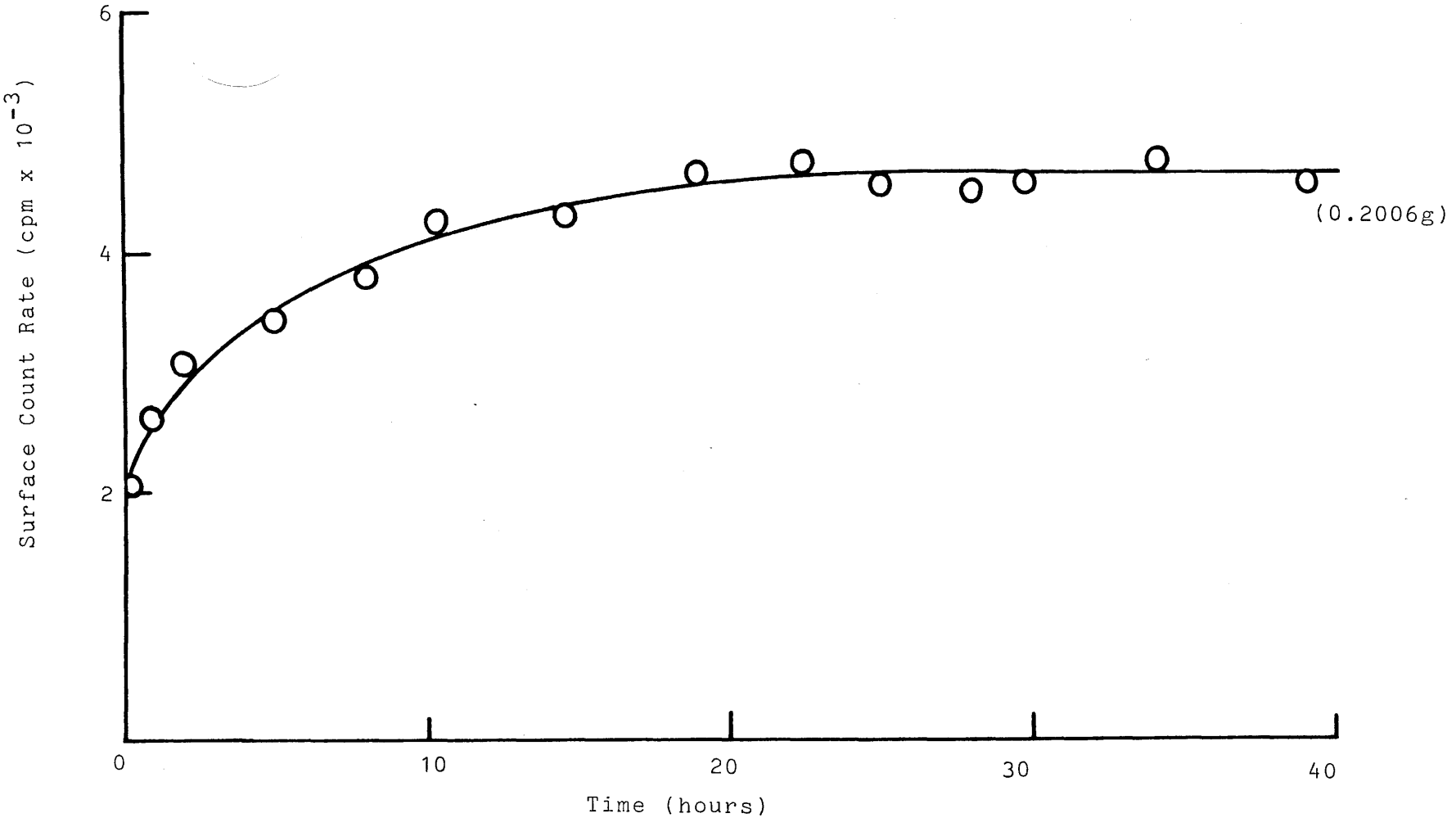

Figure 4.5 Adsorption of 2.61 torr [14-C]Carbon Dioxide (sp. acty = 0.045 mCi $mmol^{-1}$) on $Cu/ZnO/Al_2O_3$ Over a Long Time Period .

hours to reach surface saturation. By comparison of the graph in Figure 4.5 with the isotherms for the adsorption of [14-C]carbon dioxide on reduced $Cu/ZnO/Al_2O_3$ in Figure 4.1, where each point was a "pseudo" equilibrium point, obtained by taking an average of two constant count rates over a period of 30 minutes, it would appear that the adsorption of carbon dioxide on reduced $Cu/ZnO/Al_2O_3$ is a two-stage process. The first stage involves a relatively fast adsorption of carbon dioxide on the catalyst and the second stage a slow adsorption or reaction of carbon dioxide.

The strength of adsorption of [14-C]carbon dioxide adsorbed on reduced $Cu/ZnO/Al_2O_3$ over a long time period was investigated by molecular exchange (Section 4.1.2). The results are shown in Table 4.4.

Table 4.4 Effects of Molecular Exchange on Carbon Dioxide Adsorbed on $Cu/ZnO/Al_2O_3$ (at surface equilibrium) Without Evacuation

Specific activity of [14-C]carbon dioxide = 0.045mCi $mmol^{-1}$

Weight of catalyst = 0.2291g

Procedure	Surface count rate (cpm)	% Change
Adsorption of 2.00 torr [14-C]carbon dioxide over a period of 26 hours	3502	-
Admission of 5.29 torr [12-C]carbon dioxide		
for 10 minutes	2934	-16.2
for 12 hours	2280	-34.9

4.2 Adsorption of [14-C]Carbon Monoxide on Reduced $Cu/ZnO/Al_2O_3$

Two adsorption isotherms obtained for the adsorption of [14-C]carbon monoxide on samples of reduced $Cu/ZnO/Al_2O_3$ are shown in Figure 4.6. These were obtained when small aliquots of [14-C]carbon monoxide were admitted to freshly reduced catalyst samples. In contrast with the adsorption of [14-C]-carbon dioxide on reduced $Cu/ZnO/Al_2O_3$, no decrease in pressure in the reaction vessel was recorded by the pressure transducer upon admission of the [14-C]carbon monoxide. This suggests that, in contrast with carbon dioxide, carbon monoxide is adsorbed relatively quickly on the catalyst surface and no subsequent slow adsorption takes place.

Analysis of the gas phase in contact with the surface during the adsorption process showed that the adsorbate, carbon monoxide, was the only species present.

4.2.1 Adsorption of [14-C]Carbon Monoxide on Unreduced $Cu/ZnO/Al_2O_3$

Carbon monoxide did not adsorb on an unreduced sample of $Cu/ZnO/Al_2O_3$.

4.2.2 The Reversibility of Adsorption of Carbon Monoxide on Reduced $Cu/ZnO/Al_2O_3$

This was determined in the following ways.

(i) Evacuation

Successive aliquots of [14-C]carbon monoxide were admitted to a freshly reduced catalyst sample until the pressure in the reaction vessel was ca. 2 torr. The reaction

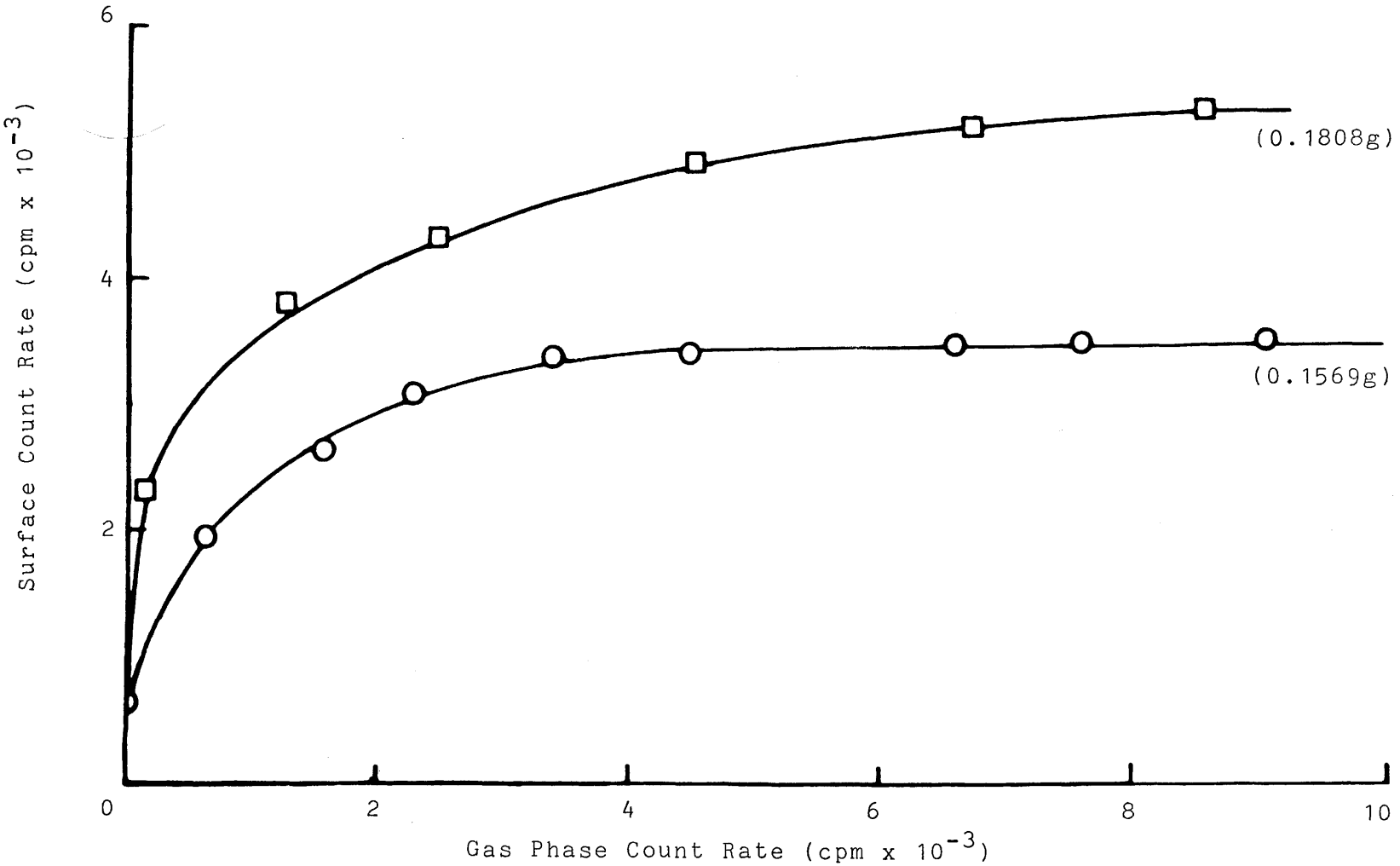

Figure 4.6 Adsorption Isotherms for [14-C]Carbon Monoxide (sp. acty = 0.163 mCi $mmol^{-1}$) on $Cu/ZnO/Al_2O_3$.

vessel was then connected to the vacuum and evacuated for 10 minutes. The surface count rate was determined before and after evacuation. The results are shown in Table 4.5.

Table 4.5 Effects of Evacuation on Carbon Monoxide Adsorbed on $Cu/ZnO/Al_2O_3$

Specific activity of [14-C]carbon monoxide = 0.070mCi $mmol^{-1}$

Weight of catalyst = 0.2711g

Procedure	Surface count rate (cpm)	% Change
Adsorption of [14-C]carbon monoxide to gas pressure of 2.12 torr	3004	-
Evacuation for 10 minutes	538	-82.1

(ii) Molecular Exchange

Small aliquots of [14-C]carbon monoxide were admitted to a freshly reduced catalyst sample until the pressure in the reaction vessel was ca. 2 torr, then (a) without evacuation, 4.17 torr [12-C]carbon monoxide was admitted to the reaction vessel and the surface count rate determined after various time intervals, or, (b) the reaction vessel was evacuated for 10 minutes and the surface count rate determined. 4.32 torr [12-C]carbon monoxide was then admitted to the reaction vessel and the surface count rate determined after various time intervals. The results are shown in Tables 4.6(a) and 4.6(b).

Table 4.6(a) Effects of Molecular Exchange on Carbon Monoxide Adsorbed on $Cu/ZnO/Al_2O_3$ Without Evacuation

Specific activity of [14-C]carbon monoxide = 0.070mCi $mmol^{-1}$

Weight of catalyst = 0.1747g

Procedure	Surface count rate (cpm)	% Change
Adsorption of [14-C]carbon monoxide to gas pressure of 2.43 torr	2050	-
Admission of 4.17 torr [12-C]carbon monoxide		
for 10 minutes	1226	-40.2
for 12 hours	1279	-37.6

Table 4.6(b) Effects of Molecular Exchange on Carbon Monoxide Adsorbed on $Cu/ZnO/Al_2O_3$ After Evacuation

Specific activity of [14-C]carbon monoxide = 0.070mCi $mmol^{-1}$

Weight of catalyst = 0.2711g

Procedure	Surface count rate (cpm)	% Change
Adsorption of [14-C]carbon monoxide to gas pressure of 2.12 torr	3004	-
Evacuation for 10 minutes	538	-82.1
Admission of 4.32 torr [12-C]carbon monoxide		
for 10 minutes	408	-86.4
for 12 hours	397	-86.8

4.2.3 Successive Adsorptions/Evacuations of [14-C]Carbon Monoxide on the Same Reduced $Cu/ZnO/Al_2O_3$ Catalyst Sample

A series of isotherms for the adsorption of [14-C]carbon monoxide on a reduced $Cu/ZnO/Al_2O_3$ sample are shown in Figure 4.7. These were obtained when small aliquots of [14-C]carbon monoxide were admitted to a reduced catalyst sample until a pressure of ca. 2 torr was obtained in the reaction vessel. After evacuation of the reaction vessel for 10 minutes and determination of the residual surface count rate, further aliquots of [14-C]carbon monoxide were admitted to the reaction vessel. This procedure was repeated until three successive adsorption isotherms/evacuations were determined using the same catalyst sample.

From the isotherms in Figure 4.7, it can be seen that, in contrast with the successive adsorptions/evacuations of [14-C]carbon dioxide on reduced $Cu/ZnO/Al_2O_3$ (Figure 4.3), isotherms 1, 2 and 3 are very similar in shape. The amount of [14-C]carbon monoxide which was evacuated after the last point had been determined on each isotherm was 77%, 82% and 76% for isotherms 1, 2 and 3 respectively.

4.2.4 The Effects of Hydrogen on the Adsorption of Carbon Monoxide on Reduced $Cu/ZnO/Al_2O_3$

The adsorption isotherm obtained when [14-C]carbon monoxide was adsorbed on a freshly reduced $Cu/ZnO/Al_2O_3$ catalyst sample in the presence of 3.82 torr hydrogen, as described previously (Section 4.1.4), is shown in Figure 4.8.

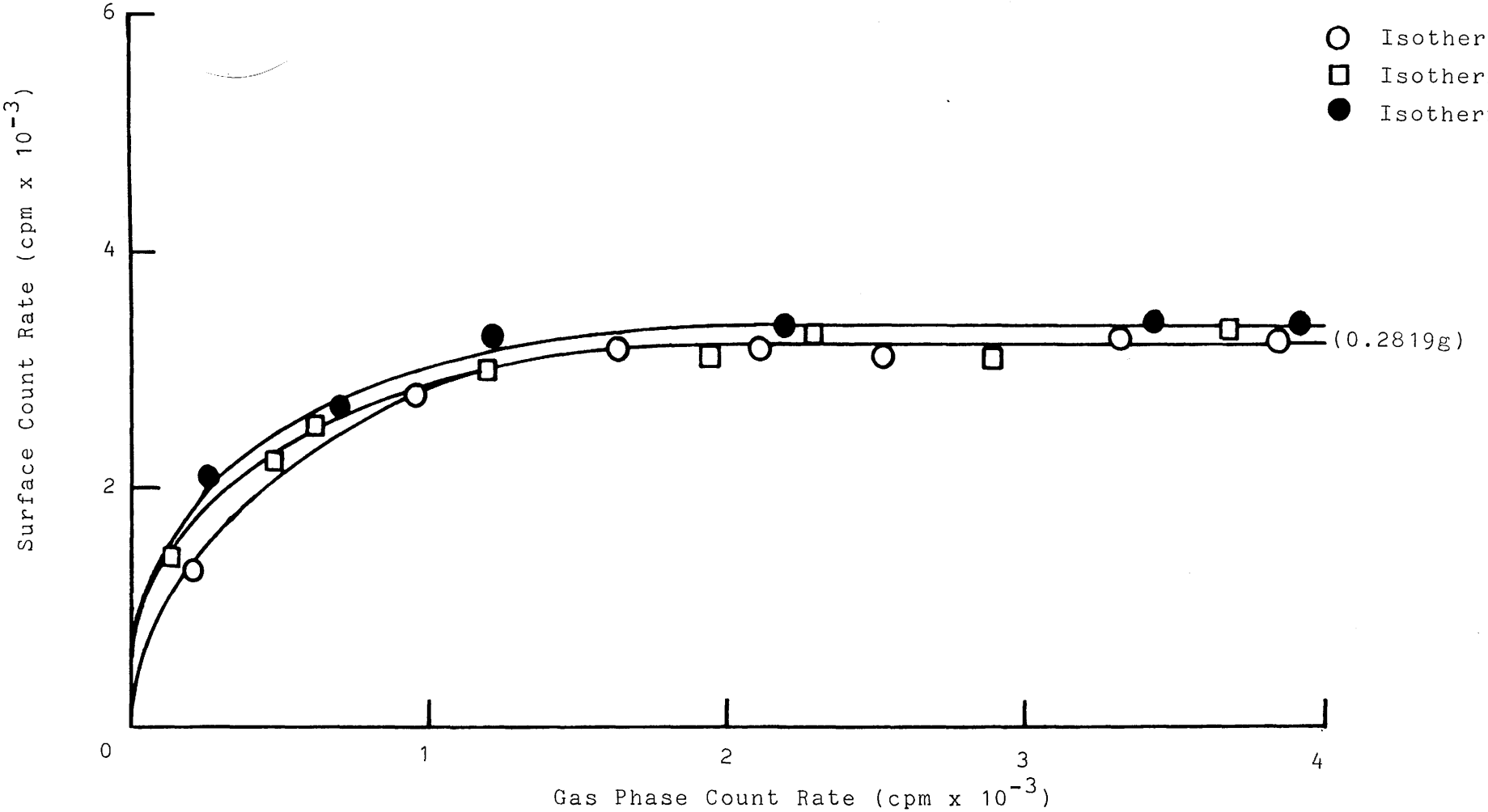

Figure 4.7 Adsorption Isotherms for [14-C]Carbon Monoxide (sp. acty = 0.061 mCi $mmol^{-1}$) on the Same $Cu/ZnO/Al_2O_3$ Catalyst Sample.

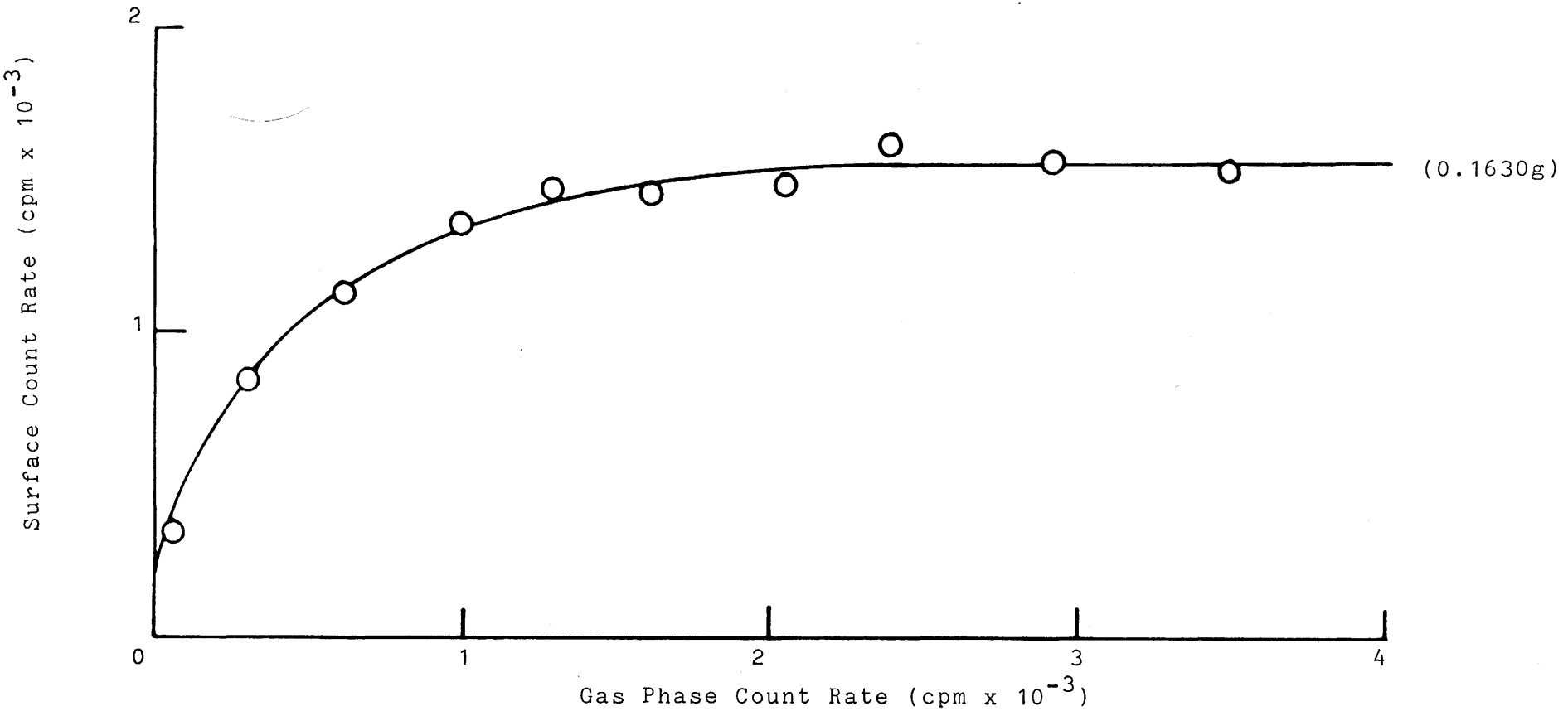

Figure 4.8 Adsorption Isotherm for [14-C]Carbon Monoxide (sp. acty = 0.058 mCi $mmol^{-1}$) on $Cu/ZnO/Al_2O_3$ in the Presence of 3.82 torr Hydrogen.

The amount of [14-C] labelled species which was evacuated after the last point on the isotherm was measured, was 80%.

4.2.5 Adsorption of [14-C]Carbon Monoxide on Reduced $Cu/ZnO/Al_2O_3$ Over a Long Time Period

A large aliquot (2.71 torr) of [14-C]carbon monoxide was admitted to a freshly reduced catalyst sample and the surface count rate determined over a period of 4 hours. The results are shown in Figure 4.9. From this, it can be seen that, in contrast with carbon dioxide adsorption on reduced $Cu/ZnO/Al_2O_3$, (Figure 4.5), equilibrium was reached with the surface almost immediately.

Analysis of the gas phase in contact with the surface during the adsorption process showed that carbon monoxide was the only species present. The fraction of the adsorbed species which was evacuated over a period of 10 minutes after the last point was measured, was 78%.

4.3 Co-Adsorption of Carbon Dioxide and Carbon Monoxide on Reduced $Cu/ZnO/Al_2O_3$

The effects of the presence of carbon dioxide on the adsorption of carbon monoxide and vice-versa was investigated in a number of ways.

4.3.1 Adsorption of [14-C]Carbon Dioxide Followed by the Adsorption of [14-C]Carbon Monoxide on Reduced $Cu/ZnO/Al_2O_3$

Figure 4.10(a) shows the adsorption isotherms obtained when small aliqots of [14-C]carbon dioxide were admitted to

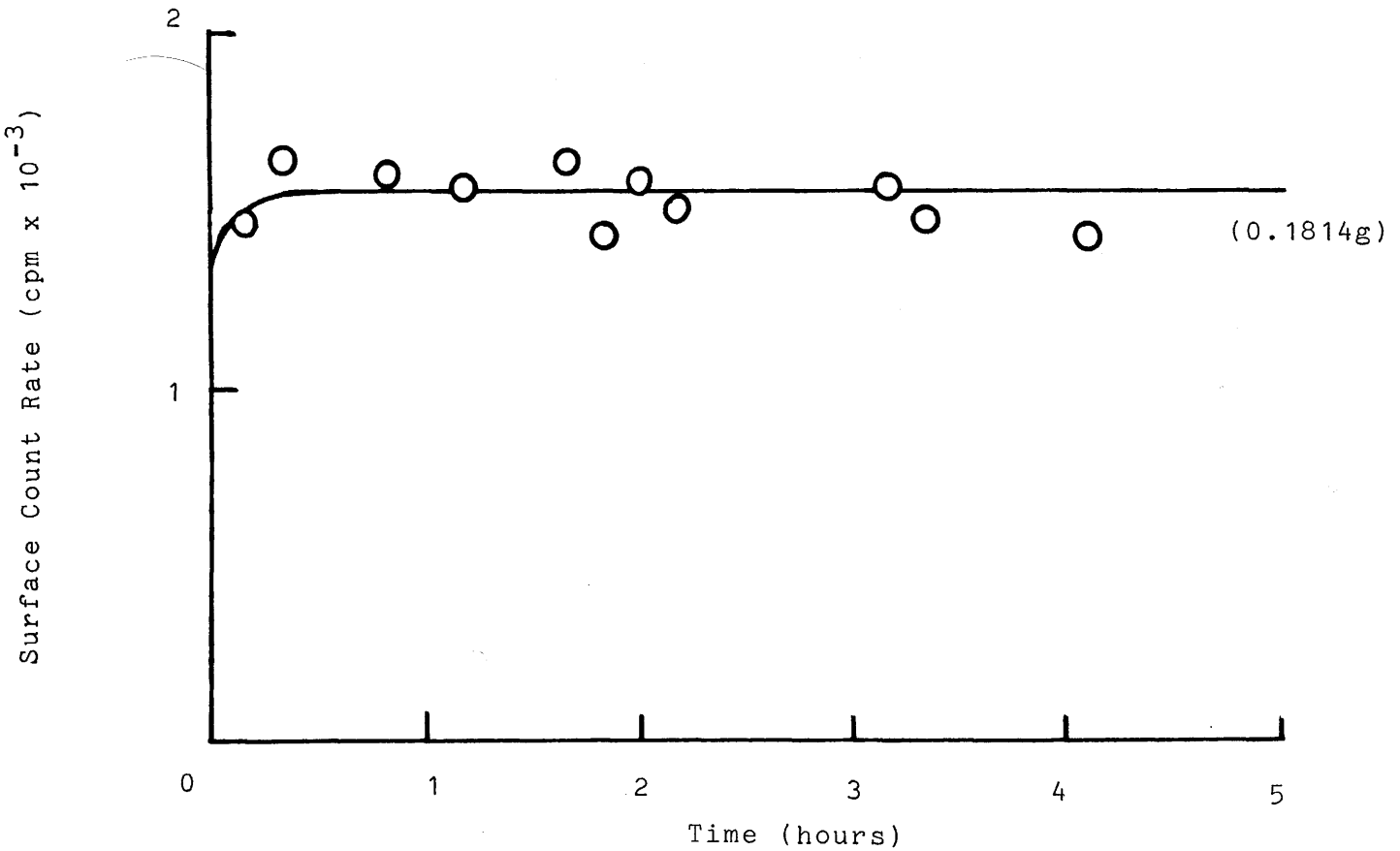

Figure 4.9 Adsorption of 2.71 torr [14-C]Carbon Monoxide (sp. acty = 0.061 mCi $mmol^{-1}$) on $Cu/ZnO/Al_2O_3$ Over a Long Time Period.

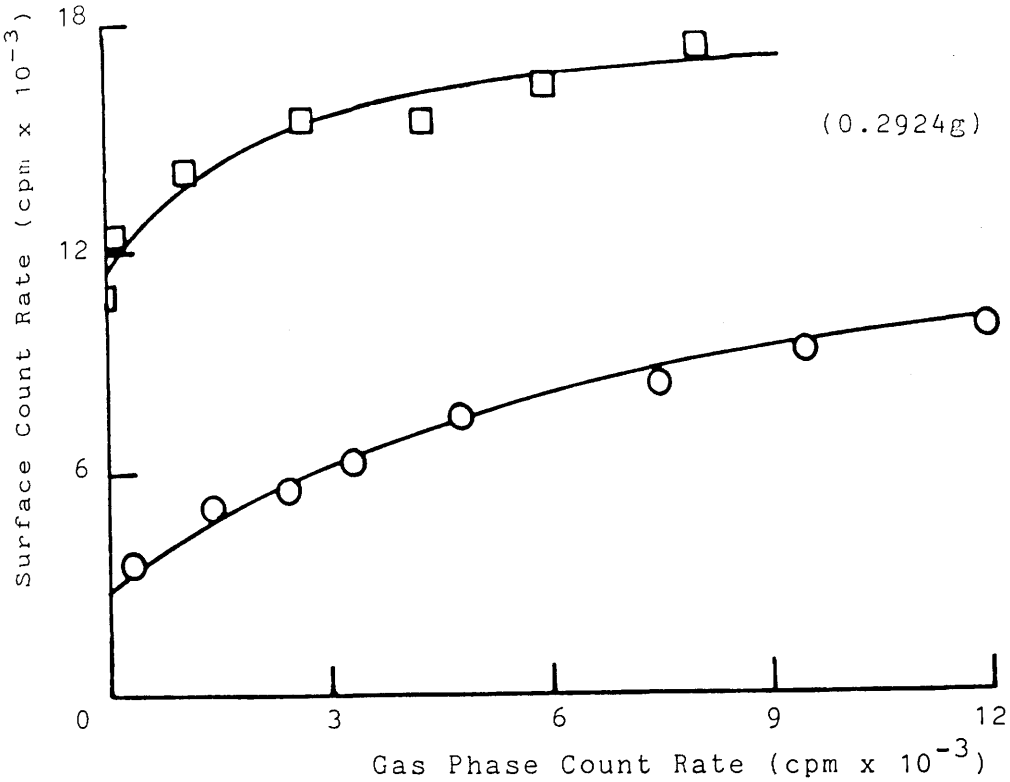

Figure 4.10(a) Adsorption Isotherm for [14-C]Carbon Dioxide (sp. acty = 0.192 mCi $mmol^{-1}$) Followed by Adsorption Isotherm for [14-C]Carbon Monoxide (sp. acty = 0.214 mCi $mmol^{-1}$) on $Cu/ZnO/Al_2O_3$.

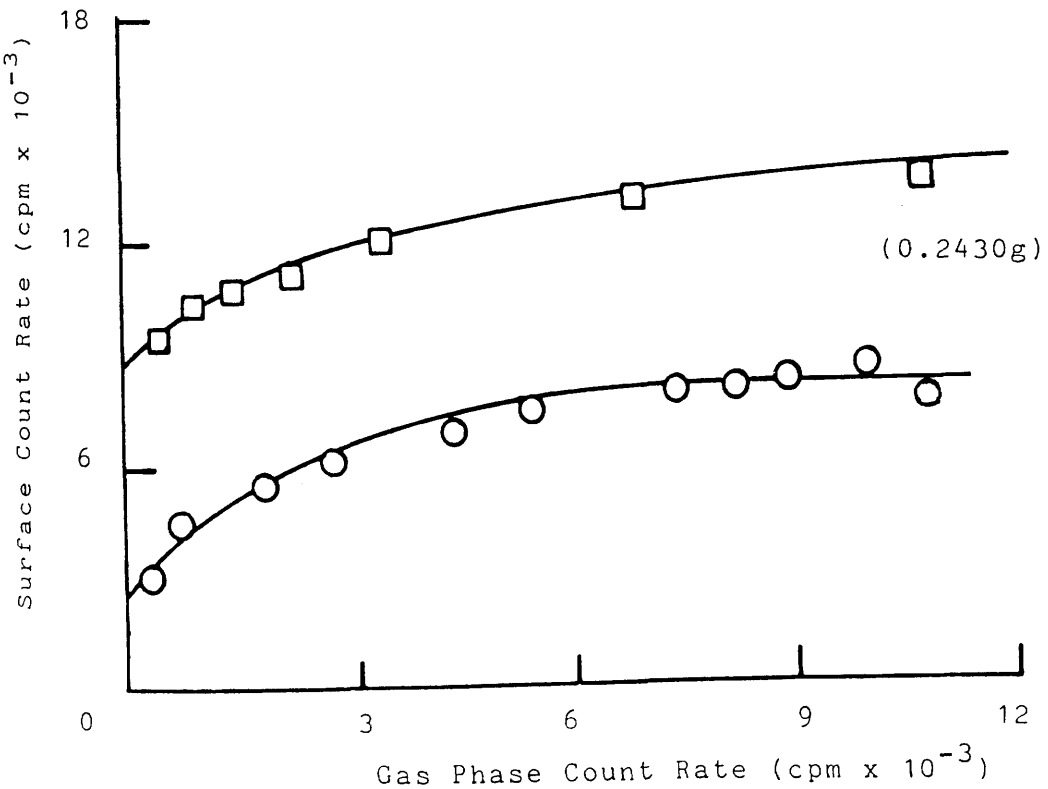

Figure 4.10(b) Adsorption Isotherm for [14-C]Carbon Monoxide (sp. acty = 0.214 mCi $mmol^{-1}$) Followed by Adsorption Isotherm for [14-C]Carbon Dioxide (sp. acty = 0.192 mCi $mmol^{-1}$) on $Cu/ZnO/Al_2O_3$.

a freshly reduced catalyst sample until the pressure in the gas phase was 1.70 torr and then, without evacuation, aliquots of [14-C]carbon monoxide were admitted.

4.3.2 Adsorption of [14-C]Carbon Monoxide Followed by the Adsorption of [14-C]Carbon Dioxide on Reduced $Cu/ZnO/Al_2O_3$

The isotherms obtained when the radiolabelled gases were admitted in a similar manner but in reverse order to that described in Section 4.3.1 that is, [14-C]carbon monoxide followed by [14-C]carbon dioxide are shown in Figure 4.10(b).

4.3.3 Adsorption of [14-C]Carbon Dioxide on a [12-C]Carbon Monoxide Precovered $Cu/ZnO/Al_2O_3$ Surface

In order to obtain more quantitative information, the adsorption of [14-C]carbon dioxide on a [12-C]carbon monoxide precovered surface and of [14-C]carbon monoxide on a [12-C]carbon dioxide precovered surface (Section 4.3.4) was investigated. Figure 4.11(a) shows the adsorption isotherm obtained when 3.82 torr of [12-C]carbon monoxide was admitted to a freshly reduced $Cu/ZnO/Al_2O_3$ catalyst sample and left for 30 minutes, then, without evacuation, small aliquots of [14-C]carbon dioxide were admitted to the reaction vessel.

4.3.4 Adsorption of [14-C]Carbon Monoxide on a [12-C]Carbon Dioxide Precovered $Cu/ZnO/Al_2O_3$ Surface

Figure 4.11(b) shows the adsorption isotherm obtained

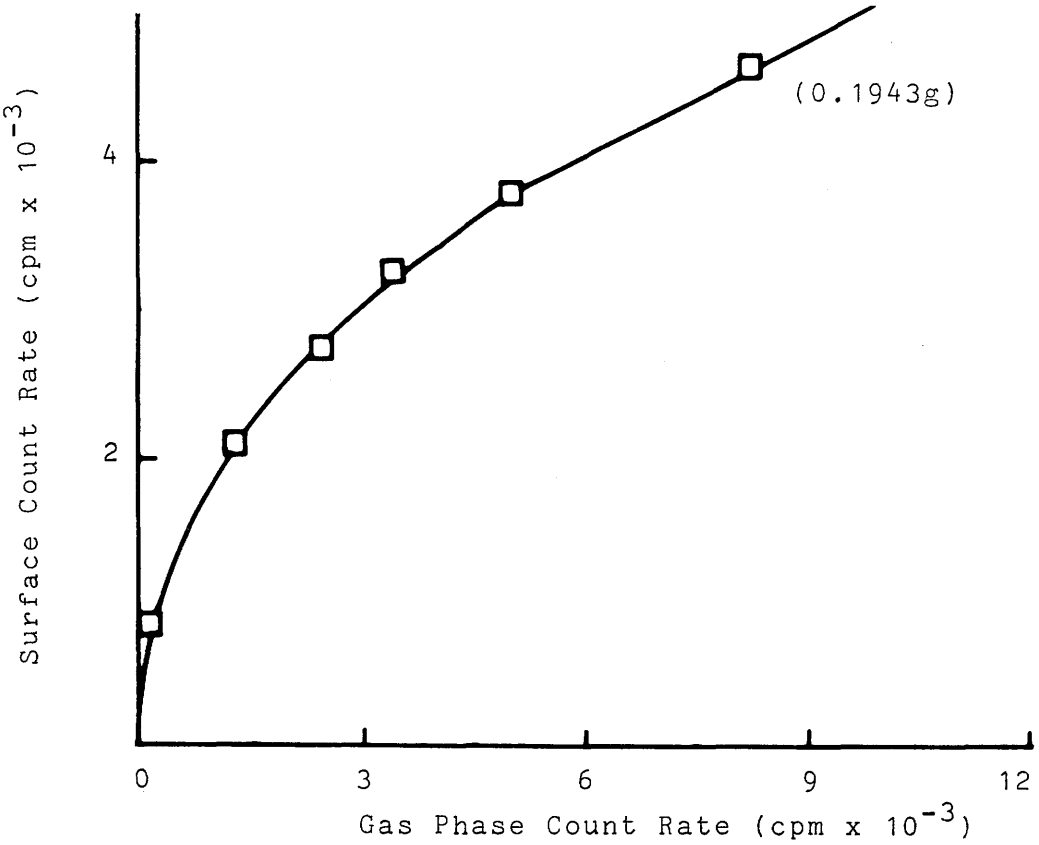

Figure 4.11(a) Adsorption Isotherm for [14-C]Carbon Dioxide (sp. acty = 0.165 mCi $mmol^{-1}$) on $Cu/ZnO/Al_2O_3$ in the Presence of 3.82 torr [12-C]Carbon Monoxide.

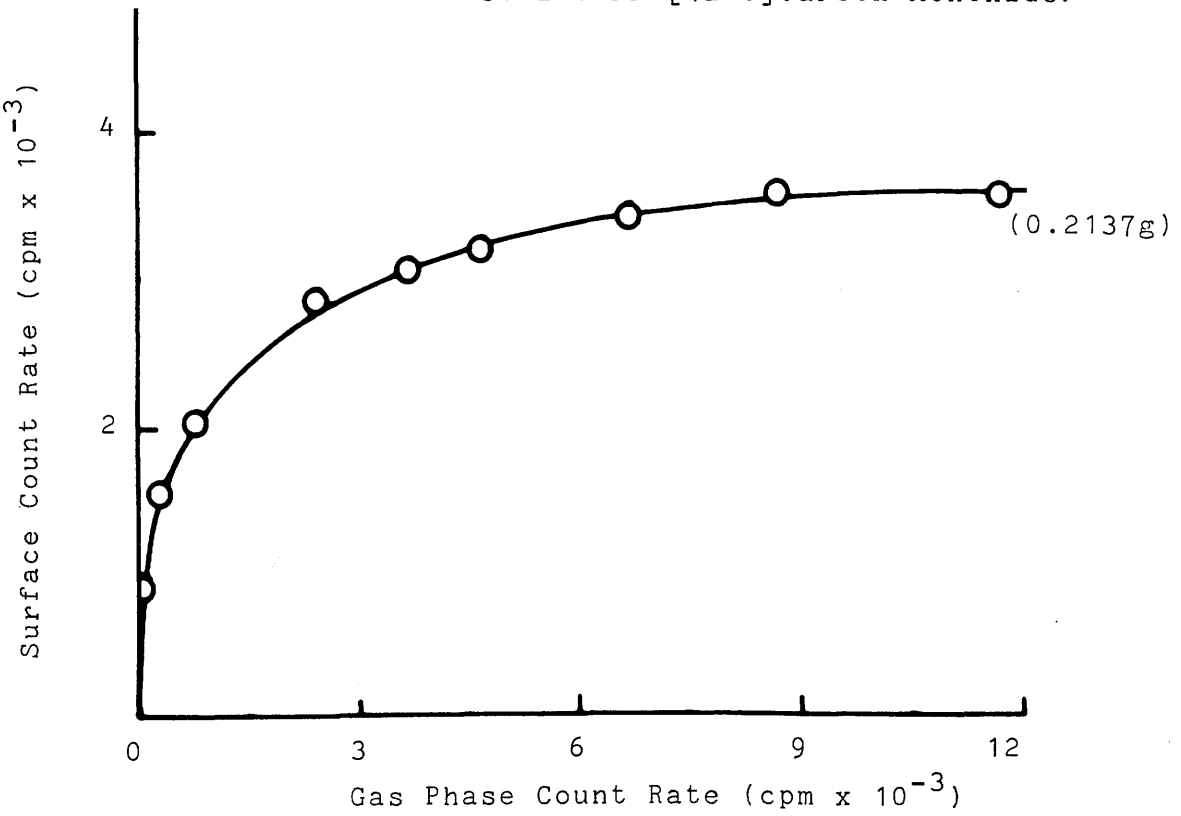

Figure 4.11(b) Adsorption Isotherm for [14-C]Carbon Monoxide (sp. acty = 0.163 mCi $mmol^{-1}$) on $Cu/ZnO/Al_2O_3$ in the Presence of 4.86 torr [12-C]Carbon Dioxide.

when successive [14-C] labelled aliquots of carbon monoxide were admitted to a freshly reduced $Cu/ZnO/Al_2O_3$ sample which was precovered with 4.86 torr [12-C]carbon dioxide for 30 minutes, without evacuation.

4.3.5 Exchange Between Carbon Dioxide Adsorbed on $Cu/ZnO/Al_2O_3$ and Gas Phase Carbon Monoxide

The amount of exchange between adsorbed carbon dioxide and gas phase carbon monoxide was investigated as follows. Successive aliquots of [14-C]carbon dioxide were admitted to a freshly reduced catalyst sample until a pressure of 1.79 torr was obtained in the gas phase, then, without evacuation, a large aliquot (5.52 torr) of [12-C]carbon monoxide was admitted to the reaction vessel. The surface count rate was determined after various time intervals. The results are summarised in Table 4.7.

Table 4.7 Exchange Between Carbon Dioxide Adsorbed on $Cu/ZnO/Al_2O_3$ and Gas Phase Carbon Monoxide

Specific activity of [14-C]carbon dioxide = 0.056mCi $mmol^{-1}$

Weight of catalyst = 0.2242g

Procedure	Surface count rate (cpm)	% Change
Adsorption of [14-C]carbon dioxide to gas pressure of 1.79torr	1256	-
Admission of 5.52torr [12-C]carbon monoxide		
for 10 minutes	1702	+35.5
for 12 hours	1532	+22.0

The slow adsorption of [14-C]carbon dioxide on the reduced catalyst (Section 4.1.5) thus appeared to disguise the exchange (if any) between adsorbed [14-C]carbon dioxide and gas phase [12-C]carbon monoxide. In order to check if any exchange occurred between these gases on $Cu/ZnO/Al_2O_3$ after surface equilibrium of carbon dioxide had been attained, an adsorption of [14-C]carbon dioxide (2.61 torr) over a long time period was carried out, then, after surface saturation had been obtained, a large aliquot (2.58 torr) of [12-C]carbon monoxide was admitted to the reaction vessel and the surface count rate determined after various time intervals. The results are shown in Table 4.8.

Table 4.8 Exchange Between Carbon Dioxide Adsorbed on $Cu/ZnO/Al_2O_3$ (at surface equilibrium) and Gas Phase Carbon Monoxide

Specific activity of [14-C]carbon dioxide = 0.045mCi $mmol^{-1}$
Weight of catalyst = 0.2006g

Procedure	Surface count rate (cpm)	% Change
Adsorption of 2.61 torr [14-C]carbon dioxide over a period of 50 hours	4894	-
Admission of 2.58 torr [12-C]carbon monoxide		
for 10 minutes	4659	-4.8
for 12 hours	4800	-1.9

4.3.6 Exchange Between Carbon Monoxide Adsorbed on $Cu/ZnO/Al_2O_3$ and Gas Phase Carbon Dioxide

Table 4.9 summarises the results obtained when the exchange between adsorbed carbon monoxide and gas phase carbon dioxide was investigated as follows. Small aliquots of [14-C]carbon monoxide were admitted to a freshly reduced catalyst sample until a pressure of 1.88 torr was obtained in the gas phase. Without evacuation, a large aliquot (4.80 torr) of [12-C]carbon dioxide was admitted to the reaction vessel and the surface count rate determined after various time intervals.

Table 4.9 Exchange Between Carbon Monoxide Adsorbed on $Cu/ZnO/Al_2O_3$ and Gas Phase Carbon Dioxide

Specific activity of [14-C]carbon monoxide = 0.058mCi $mmol^{-1}$
Weight of catalyst = 0.2083g

Procedure	Surface count rate (cpm)	% Change
Adsorption of [14-C]carbon monoxide to gas pressure of 1.88torr	2010	-
Admission of 4.80torr [12-C]carbon dioxide		
for 10 minutes	1778	-11.5
for 12 hours	584	-70.9
for 24 hours	311	-84.5

4.4. Adsorption of [14-C]Carbon Dioxide and [14-C]Carbon Monoxide on Cu/Al_2O_3

Figures 4.12(a) and 4.12(b) show a series of adsorption isotherms observed for the adsorption of [14-C]carbon dioxide and [14-C]carbon monoxide respectively, on samples of Cu/Al_2O_3, pretreated under conditions described in Section 3.7.1. Similar to [14-C]carbon dioxide adsorption on reduced $Cu/ZnO/Al_2O_3$ (Section 4.1), a pressure decrease in the reaction vessel was recorded during the adsorption of [14-C]carbon dioxide on Cu/Al_2O_3.

From Figure 4.12(a), it can be seen that, the adsorption isotherms for [14-C]carbon dioxide adsorption on Cu/Al_2O_3 are not similar in shape to those obtained for the adsorption of [14-C]carbon dioxide on reduced $Cu/ZnO/Al_2O_3$ (Figure 4.1). The form of the isotherms for the adsorption of [14-C]carbon monoxide on Cu/Al_2O_3 (Figure 4.12(b)) are similar to those obtained for the adsorption of [14-C]carbon monoxide on reduced $Cu/ZnO/Al_2O_3$ (Figure 4.6).

Analysis of the gas phase in contact with the surface during each of the adsorption processes, indicated that, the adsorbate gas was the only gas present.

4.4.1 The Reversibility of Adsorption of Carbon Dioxide and Carbon Monoxide on Cu/Al_2O_3

The reversibility of adsorption of carbon dioxide and carbon monoxide on reduced Cu/Al_2O_3 was investigated by evacuation experiments as described in Sections 4.1.2 and 4.2.2. The results for carbon dioxide and carbon monoxide

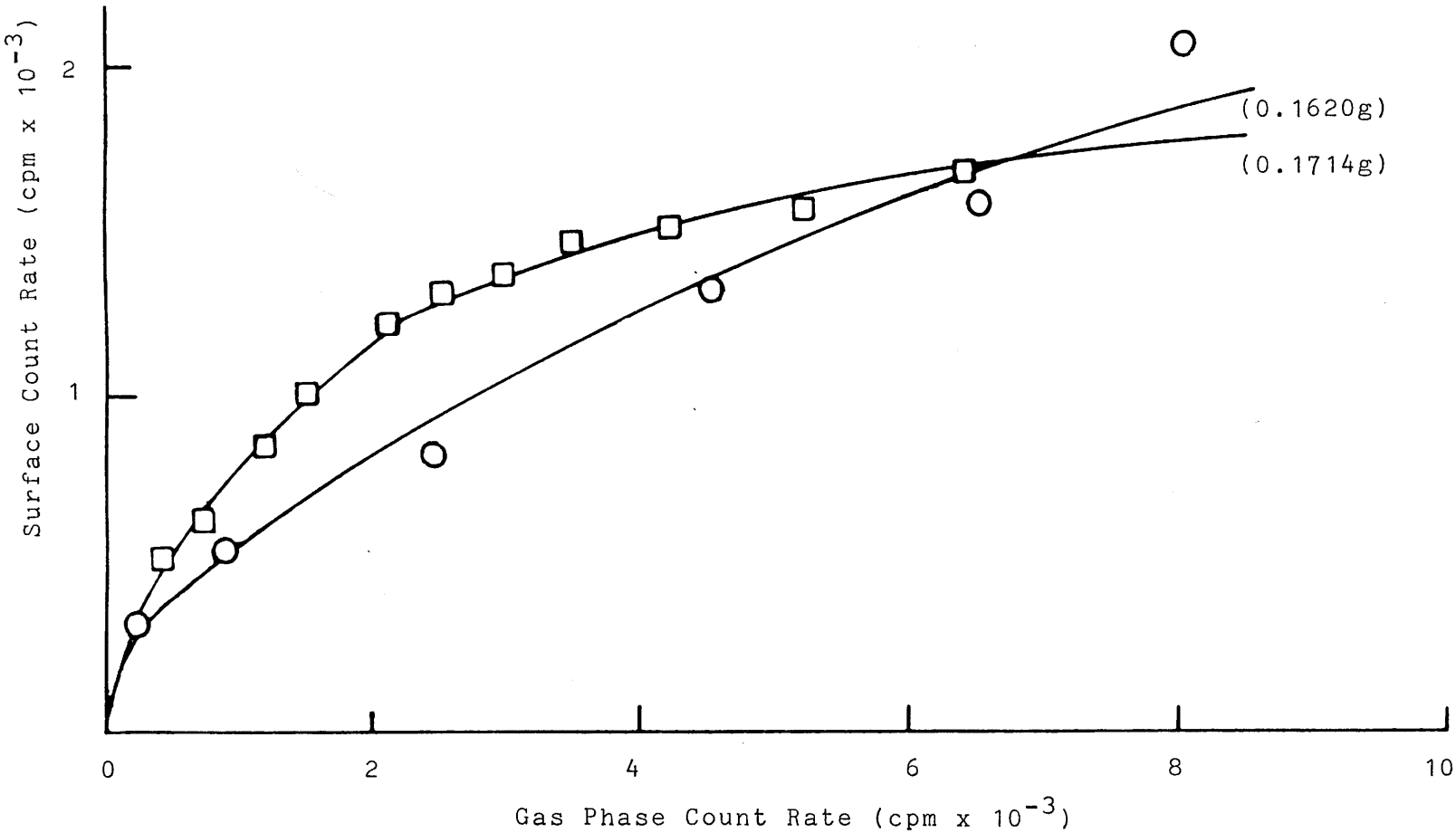

Figure 4.12(a) Adsorption Isotherms for [14-C]Carbon Dioxide (sp. acty = 0.130 mCi $mmol^{-1}$) on Cu/Al_2O_3.

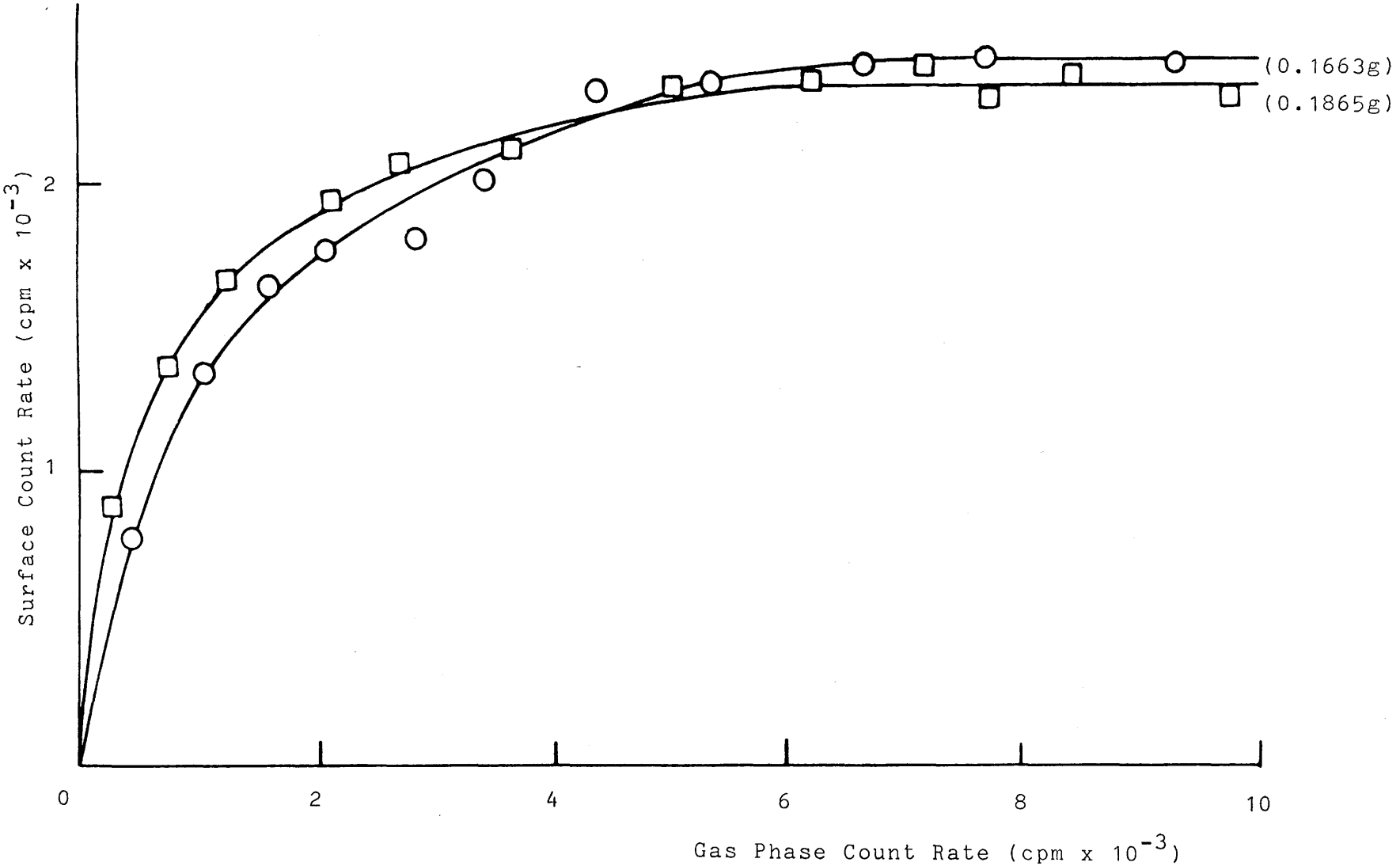

Figure 4.12(b) Adsorption Isotherms for [14-C]Carbon Monoxide (sp. acty = 0.085 mCi $mmol^{-1}$) on Cu/Al_2O_3.

are summarised, respectively, in Tables 4.10(a) and 4.10(b).

Table 4.10(a) Effects of Evacuation on Carbon Dioxide Adsorbed on Cu/Al_2O_3

Specific activity of [14-C]carbon dioxide = 0.066mCi $mmol^{-1}$

Weight of catalyst = 0.1351g

Procedure	Surface count rate (cpm)	% Change
Adsorption of [14-C]carbon dioxide to gas pressure of 1.65torr	725	-
Evacuation for 10 minutes	403	-44.4

Table 4.10(b) Effects of Evacuation on Carbon Monoxide Adsorbed on Cu/Al_2O_3

Specific activity of [14-C]carbon monoxide = 0.058mCi $mmol^{-1}$

Weight of catalyst = 0.1500g

Procedure	Surface count rate (cpm)	% Change
Adsorption of [14-C]carbon monoxide to gas pressure of 1.42torr	1150	-
Evacuation for 10 minutes	111	-90.3

4.5 Adsorption of [14-C]Carbon Dioxide and [14-C]Carbon Monoxide on ZnO-A

Figures 4.13(a) and 4.13(b) show a number of adsorption isotherms obtained for the adsorption of [14-C]carbon dioxide and [14-C]carbon monoxide, respectively, on samples of ZnO-A, pretreated under conditions described in Section 3.7.1. Similar to [14-C]carbon dioxide adsorption on reduced $Cu/ZnO/Al_2O_3$ (Section 4.1) and Cu/Al_2O_3 (Section 4.4) a pressure decrease in the reaction vessel, although smaller, was recorded during the adsorption of [14-C]carbon dioxide on ZnO-A.

From Figure 4.13(a), it can be seen that, the isotherms for the adsorption of [14-C]carbon dioxide on ZnO-A are different in shape to those obtained for the adsorption of [14-C]carbon dioxide on reduced $Cu/ZnO/Al_2O_3$ (Figure 4.1). Similar to the results obtained for [14-C]carbon dioxide, Figure 4.13(b) shows that the adsorption isotherms obtained for the adsorption of [14-C]carbon monoxide on ZnO-A are of a different form to those obtained for the adsorption of this gas on reduced $Cu/ZnO/Al_2O_3$ (Figure 4.6).

Analysis of the gas phase in contact with the surface during the adsorption process, in each case, indicated that, the adsorbate gas was the only gas present.

4.5.1 The Reversibility of Adsorption of Carbon Dioxide and Carbon Monoxide on ZnO-A

The reversibility of adsorption of carbon dioxide and carbon monoxide on ZnO-A was studied by evacuation and

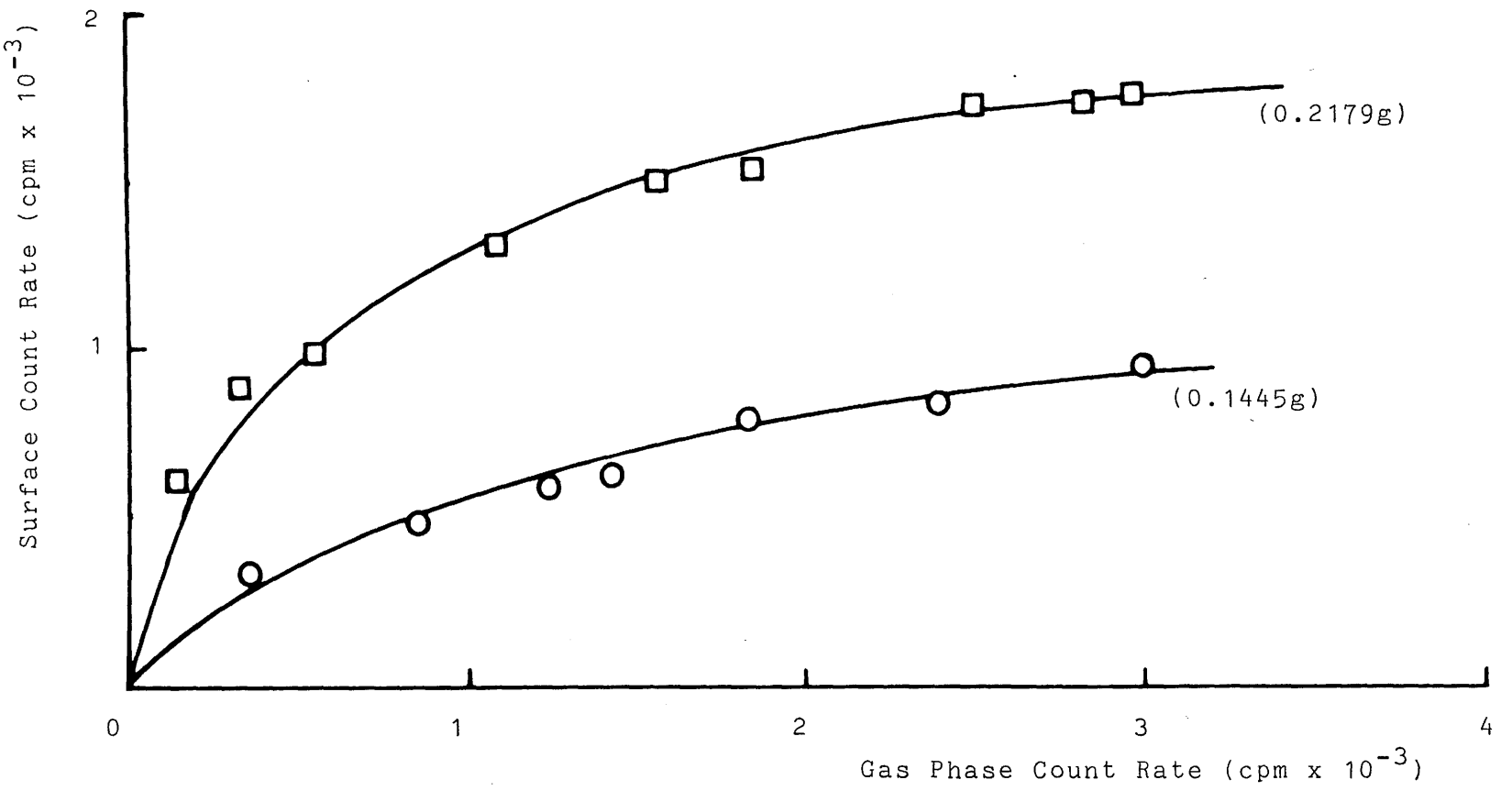

Figure 4.13(a) Adsorption Isotherms for [14-C]Carbon Dioxide (sp. acty = 0.045 mCi $mmol^{-1}$) on ZnO-A.

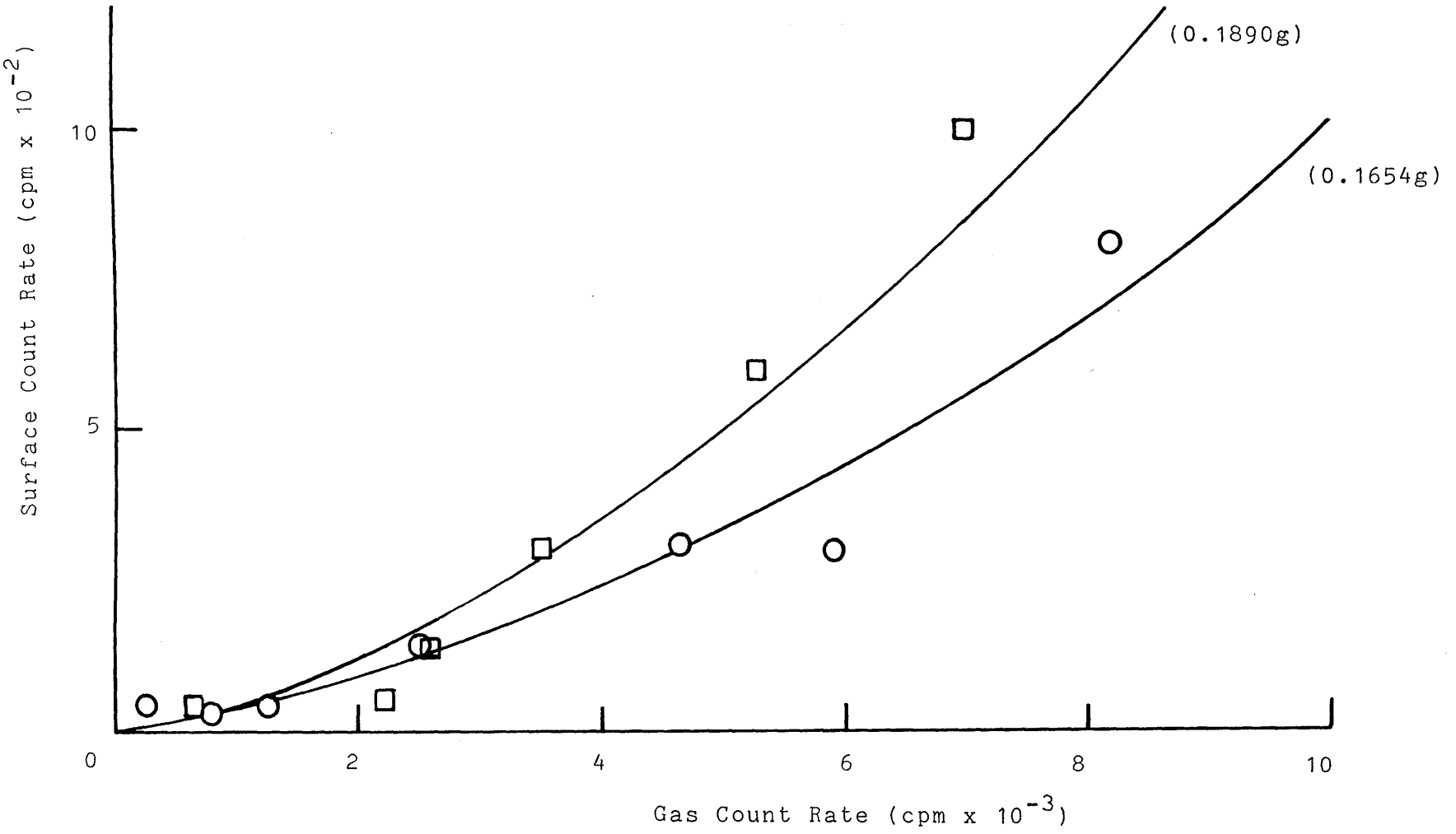

Figure 4.13(b) Adsorption Isotherms for [14-C]Carbon Monoxide (sp. acty = 0.085 mCi $mmol^{-1}$) on ZnO-A .

molecular exchange.

Tables 4.11(a) and 4.11(b) summarise the results obtained for evacuation experiments with [14-C]carbon dioxide and [14-C]carbon monoxide respectively, as previously described in Sections 4.1.2 and 4.2.2.

The effects of molecular exchange (Sections 4.1.2 and 4.2.2.) on a precovered [14-C]carbon dioxide surface and a precovered [14-C]carbon monoxide surface, without evacuation, are shown in Tables 4.12(a) and 4.12(b) respectively.

Table 4.11(a) Effects of Evacuation on Carbon Dioxide Adsorbed on ZnO-A

Specific activity of [14-C]carbon dioxide = 0.045mCi $mmol^{-1}$
Weight of catalyst = 0.2179g

Procedure	Surface count rate (cpm)	% Change
Adsorption of [14-C]carbon dioxide to gas pressure of 2.00torr	1747	-
Evacuation for 10 minutes	1040	-40.5

Table 4.11(b) Effects of Evacuation on Carbon Monoxide Adsorbed on ZnO-A

Specific activity of [14-C]carbon monoxide = 0.058mCi $mmol^{-1}$
Weight of catalyst = 0.1865g

Procedure	Surface count rate (cpm)	% Change
Adsorption of [14-C]carbon monoxide of to gas pressure of 1.54torr	326	-
Evacuation for 10 minutes	6	-98.2

Table 4.12(a) Effects of Molecular Exchange on Carbon Dioxide Adsorbed on ZnO-A Without Evacuation

Specific activity of [14-C]carbon dioxide = 0.066mCi $mmol^{-1}$

Weight of catalyst = 0.1051g

Procedure	Surface count rate (cpm)	% Change
Adsorption of [14-C]carbon dioxide to gas pressure of 1.72torr	789	-
Admission of 4.99torr [12-C]carbon dioxide		
for 10 minutes	324	-58.9
for 12 hours	313	-60.3

Table 4.12(b) Effects of Molecular Exchange on Carbon Monoxide Adsorbed on ZnO-A Without Evacuation

Specific activity of [14-C]carbon monoxide = 0.058mCi $mmol^{-1}$

Weight of catalyst = 0.1367g

Procedure	Surface count rate (cpm)	% Change
Adsorption of [14-C]carbon monoxide to gas pressure of 1.92torr	312	-
Admission of 4.23torr [12-C]carbon monoxide		
for 10 minutes	318	+1.9
for 12 hours	217	-30.4

4.5.2 The Effects of Hydrogen on the Adsorption of Carbon Dioxide and Carbon Monoxide on ZnO-A

The adsorption of [14-C]carbon dioxide (sp. acty = 0.066mCi $mmol^{-1}$) in the presence of hydrogen (3.84 torr) and the adsorption of [14-C]carbon monoxide (sp. acty = 0.058mCi $mmol^{-1}$) in the presence of hydrogen (5.30 torr) was investigated by the method described in Section 4.1.4. In comparison to the pressure decrease recorded for hydrogen in contact with reduced $Cu/ZnO/Al_2O_3$, 0.44 torr (Section 4.1.4), a smaller decrease in pressure in the reaction vessel, 0.04 torr, was recorded upon admission of hydrogen to the ZnO-A samples. The amount of adsorbed species which was evacuated after the adsorption of [14-C]carbon dioxide on ZnO-A in the presence of hydrogen, 25%, was reduced compared to the amount which was evacuated after the adsorption of this gas on ZnO-A in the absence of hydrogen (40.5%). In contrast with carbon dioxide, the amount of surface species which was evacuated after the adsorption of [14-C]carbon monoxide on ZnO-A in the presence of hydrogen, 100%, was the same as that after the adsorption of this gas on ZnO-A in the absence of hydrogen.

4.5.3 Adsorption of [14-C]Carbon Dioxide on ZnO-A Over a Long Time Period

The small decrease in pressure in the reaction vessel recorded during the adsorption of [14-C]carbon dioxide on ZnO-A, reported in Section 4.5, suggested that carbon dioxide

adsorbed or reacted slowly on the catalyst surface. The time taken for a sample of carbon dioxide to reach equilibrium with the surface was investigated. A large aliquot (2.87 torr) of [14-C]carbon dioxide was admitted to a sample of ZnO-A and the surface count rate determined over a period of 26 hours.

Gas chromatographic analysis during the adsorption indicated that the adsorbate gas, carbon dioxide, was the only gas present in the gas phase.

A graph of surface count rate against time for the adsorption of 2.87 torr [14-C]carbon dioxide is shown in Figure 4.14. From Figure 4.14, it can be seen that, 2.87 torr [14-C]carbon dioxide took 8 hours to reach surface-gas equilibrium. The amount of [14-C]carbon dioxide which was removed by evacuation over a period of 10 minutes, after the last point on the graph was determined, was 28%.

4.5.4 Co-Adsorption of Carbon Dioxide and Carbon Monoxide on ZnO-A

The co-adsorption of carbon monoxide and carbon dioxide on ZnO-A was studied in two ways.

4.5.4.1 Adsorption of [14-C]Carbon Dioxide on ZnO-A Followed by the Adsorption of [14-C]Carbon Monoxide and the Adsorption of [14-C]Carbon Monoxide on ZnO-A Followed by the Adsorption of [14-C]Carbon Dioxide

Figure 4.15(a) shows the adsorption isotherms obtained when small aliquots of [14-C]carbon dioxide were admitted to

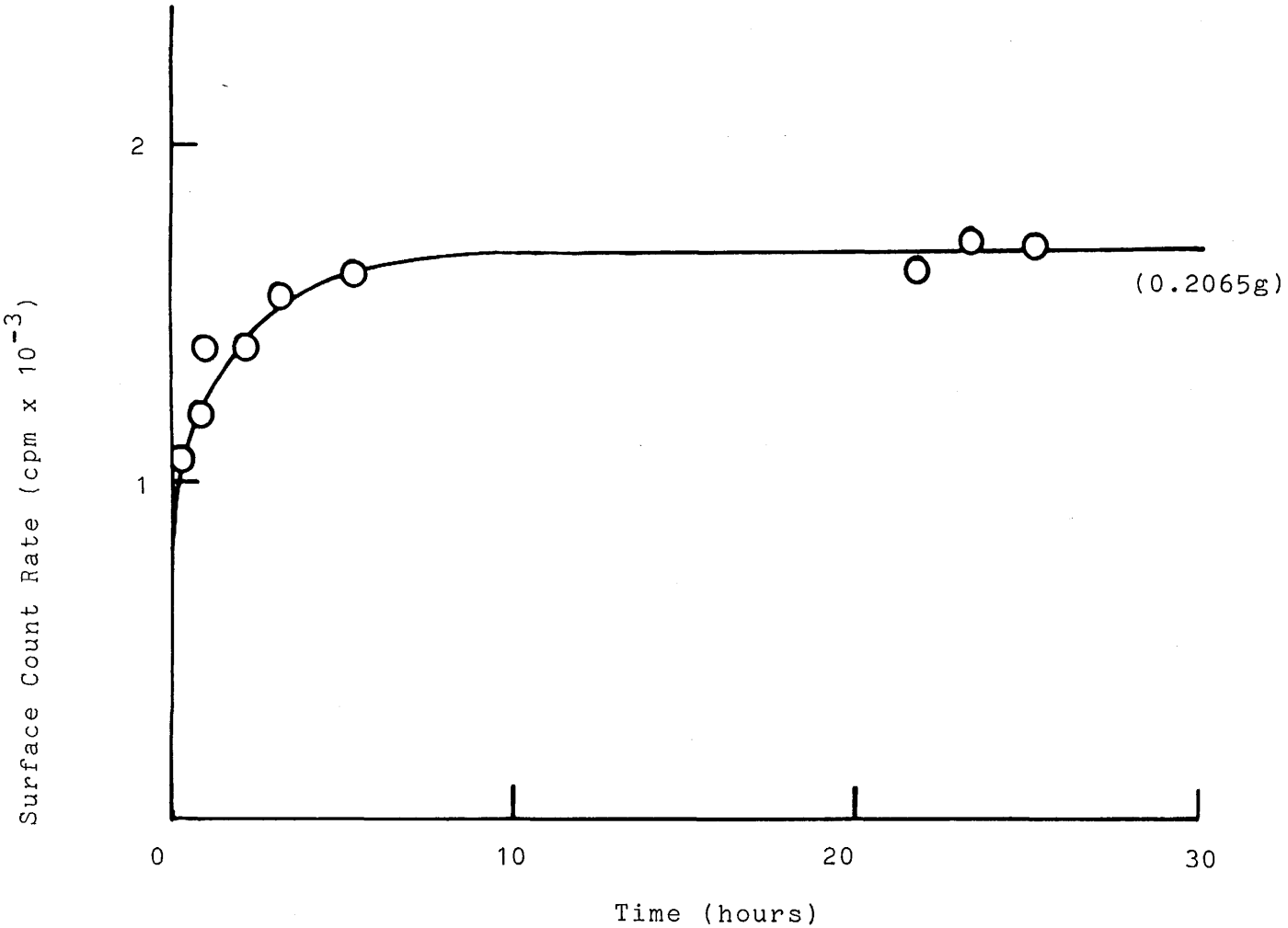

Figure 4.14 Adsorption of 2.87 torr [14-C]Carbon Dioxide (sp. acty = 0.062 mCi $mmol^{-1}$) on ZnO-A Over a Long Time Period.

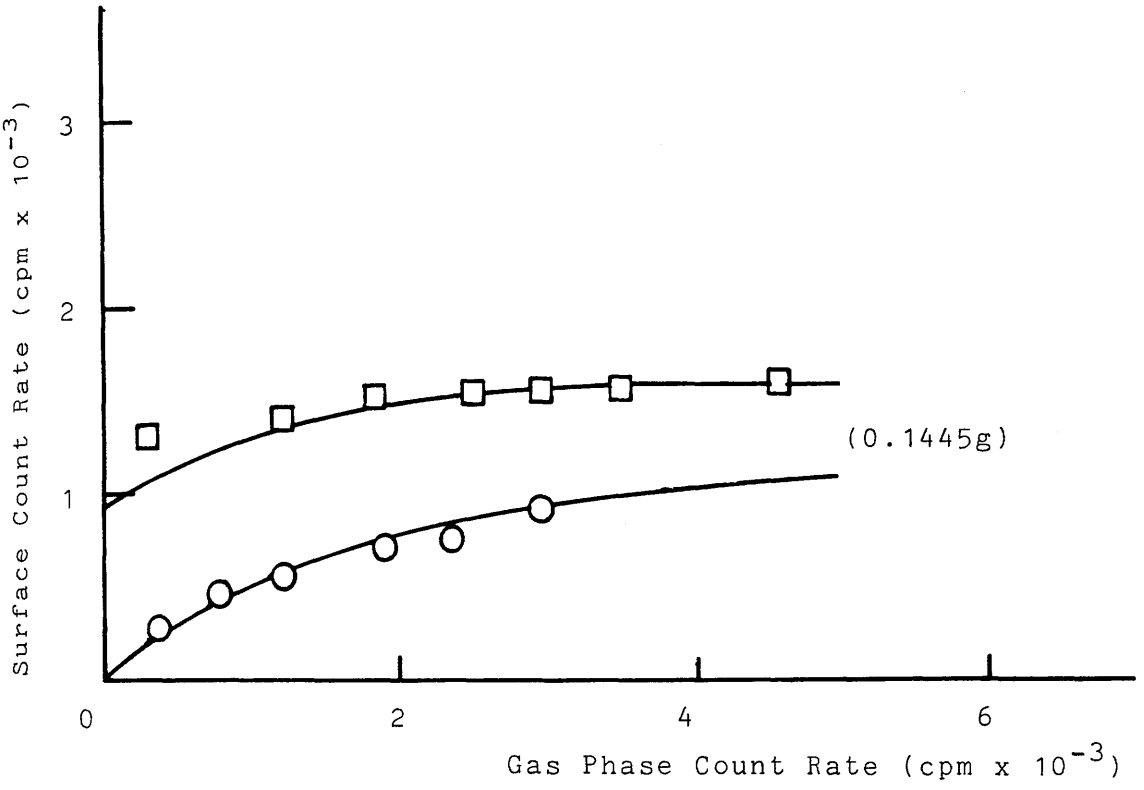

Figure 4.15(a) Adsorption Isotherm for [14-C]Carbon Dioxide (sp. acty = 0.045 mCi $mmol^{-1}$) Followed by Adsorption Isotherm for [14-C]Carbon Monoxide (sp. acty = 0.085 mCi $mmol^{-1}$) on ZnO-A.

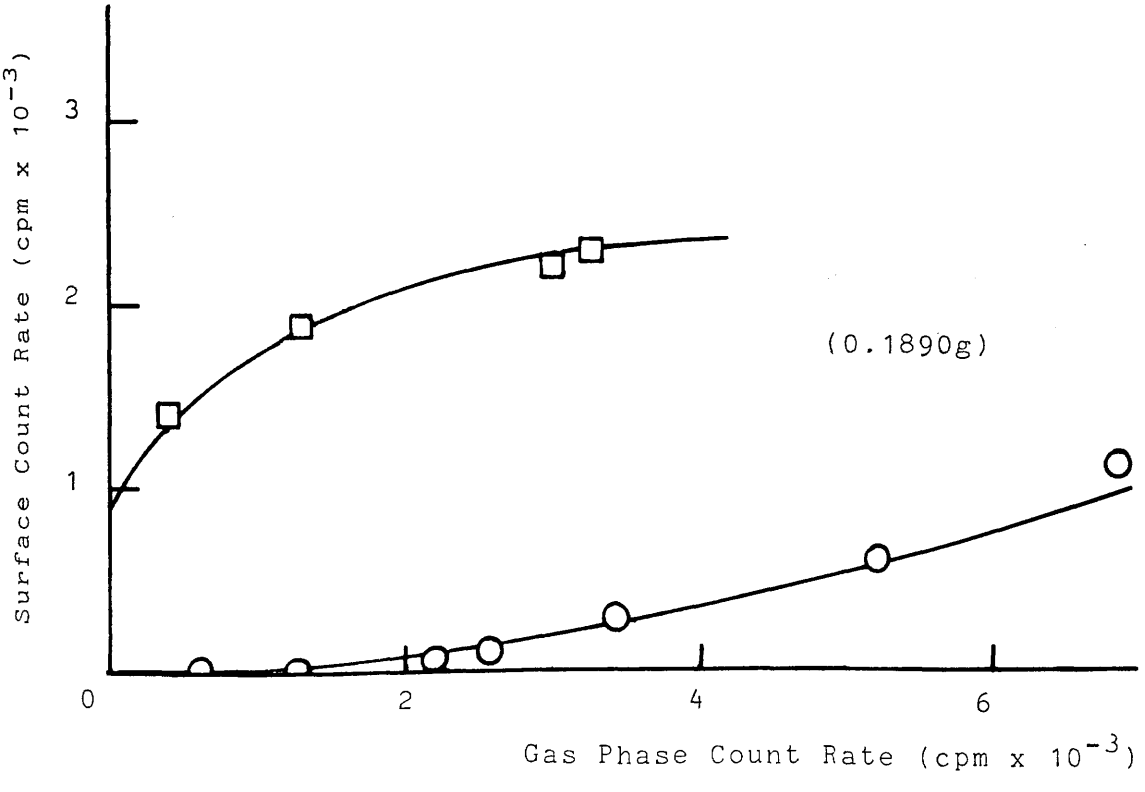

Figure 4.15(b) Adsorption Isotherm for [14-C]Carbon Monoxide (sp. acty = 0.085 mCi $mmol^{-1}$) Followed by Adsorption Isotherm for [14-C]Carbon Dioxide (sp. acty = 0.045 mCi $mmol^{-1}$) on ZnO-A.

the reaction vessel containing a sample of ZnO-A, to a total gas pressure of 1.81 torr. Without evacuation, small aliquots of [14-C]carbon monoxide were admitted to the reaction vessel. Figure 4.15(b) illustrates the isotherms produced when these gases were admitted in reverse order to that described above.

4.5.4.2 Exchange Between Carbon Dioxide Adsorbed on ZnO-A and Gas Phase Carbon Monoxide, and Exchange Between Carbon Monoxide Adsorbed on ZnO-A and Gas Phase Carbon Dioxide

The amount of exchange between adsorbed [14-C]carbon dioxide on ZnO-A and gas phase [12-C]carbon monoxide and the amount of exchange between adsorbed [14-C]carbon monoxide and gas phase [12-C]carbon dioxide was investigated by the method previously described in Sections 4.3.5 and 4.3.6. The results are summarised in Tables 4.13(a) and 4.13(b).

Table 4.13(a) Exchange Between Carbon Dioxide Adsorbed on ZnO-A and Gas Phase Carbon Monoxide

Specific activity of [14-C]carbon dioxide = 0.045mCi $mmol^{-1}$
Weight of catalyst = 0.1912g

Procedure	Surface count rate (cpm)	% Change
Adsorption of [14-C]carbon dioxide to a gas pressure of 1.50torr	1335	-
Admission of 2.26torr [12-C]carbon monoxide for 10 minutes	1347	+0.9
for 12 hours	1693	+26.8

Table 4.13(b) Exchange Between Carbon Monoxide Adsorbed on ZnO-A and Gas Phase Carbon Dioxide

Specific activity of [14-C]carbon monoxide = 0.058mCi $mmol^{-1}$

Weight of catalyst = 0.1585g

Procedure	Surface count rate (cpm)	% Change
Adsorption of [14-C]carbon monoxide to a gas pressure of 1.83torr	416	-
Admission of 5.73torr [12-C]carbon dioxide for 10 minutes	-231	-100
for 12 hours	-257	-100

4.6 Adsorption of [14-C]Carbon Dioxide and [14-C]Carbon Monoxide on ZnO-B

Figure 4.16 shows two adsorption isotherms on the same catalyst sample, obtained when small aliquots of [14-C]carbon dioxide were admitted to a sample of ZnO-B activated under conditions described in Section 3.7.1. The reaction vessel was then evacuated for 10 minutes; 50% of the adsorbed species were removed by this process, before further aliquots of [14-C]carbon dioxide were admitted to the reaction vessel. In contrast with the adsorption of [14-C]carbon dioxide on ZnO-A (Section 4.5), no decrease in pressure in the reaction vessel was recorded during the adsorption process. It seems evident, therefore, that unlike the adsorption of [14-C]-carbon dioxide on ZnO-A, the adsorption of [14-C]carbon dioxide on ZnO-B is immediate, with no subsequent slow

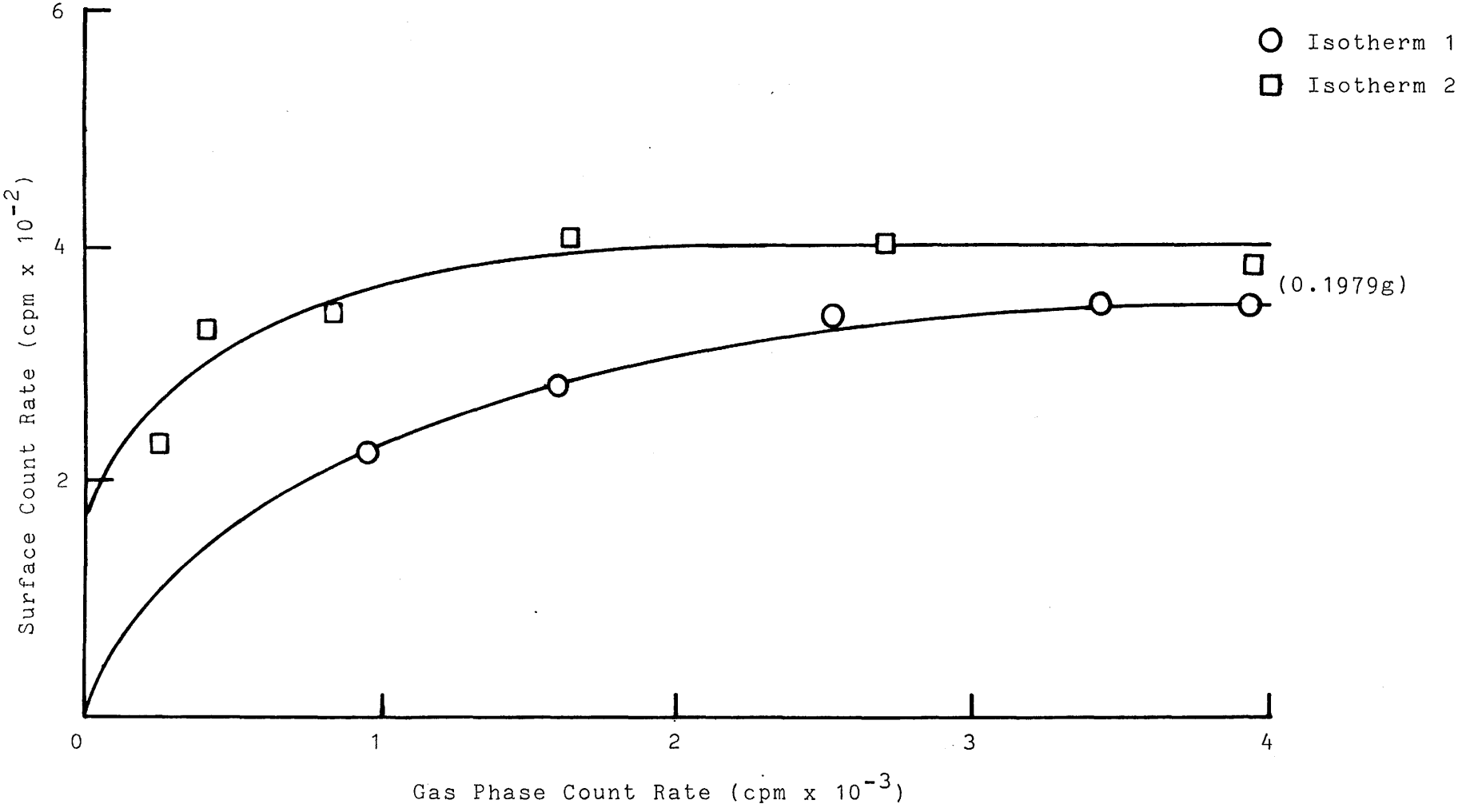

Figure 4.16 Adsorption Isotherms for [14-C]Carbon Dioxide (sp. acty = 0.062 mCi $mmol^{-1}$) on the Same ZnO-B Catalyst Sample.

adsorption or reaction on the catalyst.

From isotherm 1 in Figure 4.16, it can be seen that, the isotherm obtained for the adsorption of [14-C]carbon dioxide on ZnO-B is similar to the isotherms obtained for the adsorption of [14-C]carbon dioxide on ZnO-A (Figure 4.13(b)).

Analysis of the gas phase by gas chromatography during the adsorption process, indicated that carbon dioxide was the only gas present.

In contrast with carbon dioxide, no measurable amount of carbon monoxide was found to adsorb on ZnO-B.

4.7 Adsorption of [14-C]Carbon Dioxide and [14-C]Carbon Monoxide on Al_2O_3

Figure 4.17 shows two adsorption isotherms obtained for the adsorption of [14-C]carbon dioxide on two different samples of Al_2O_3, pretreated under conditions described in Section 3.7.1. During the adsorption process, a pressure decrease in the reaction vessel similar to that observed during the adsorption of [14-C]carbon dioxide on reduced $Cu/ZnO/Al_2O_3$ (Section 4.1), Cu/Al_2O_3 (Section 4.4) and ZnO-A (Section 4.5) was recorded.

From Figure 4.17, it can be seen that, the isotherms for the adsorption of [14-C]carbon dioxide on Al_2O_3 are dissimilar to those observed on reduced $Cu/ZnO/Al_2O_3$ (Figure 4.1).

Analysis of the gas phase by gas chromatography,

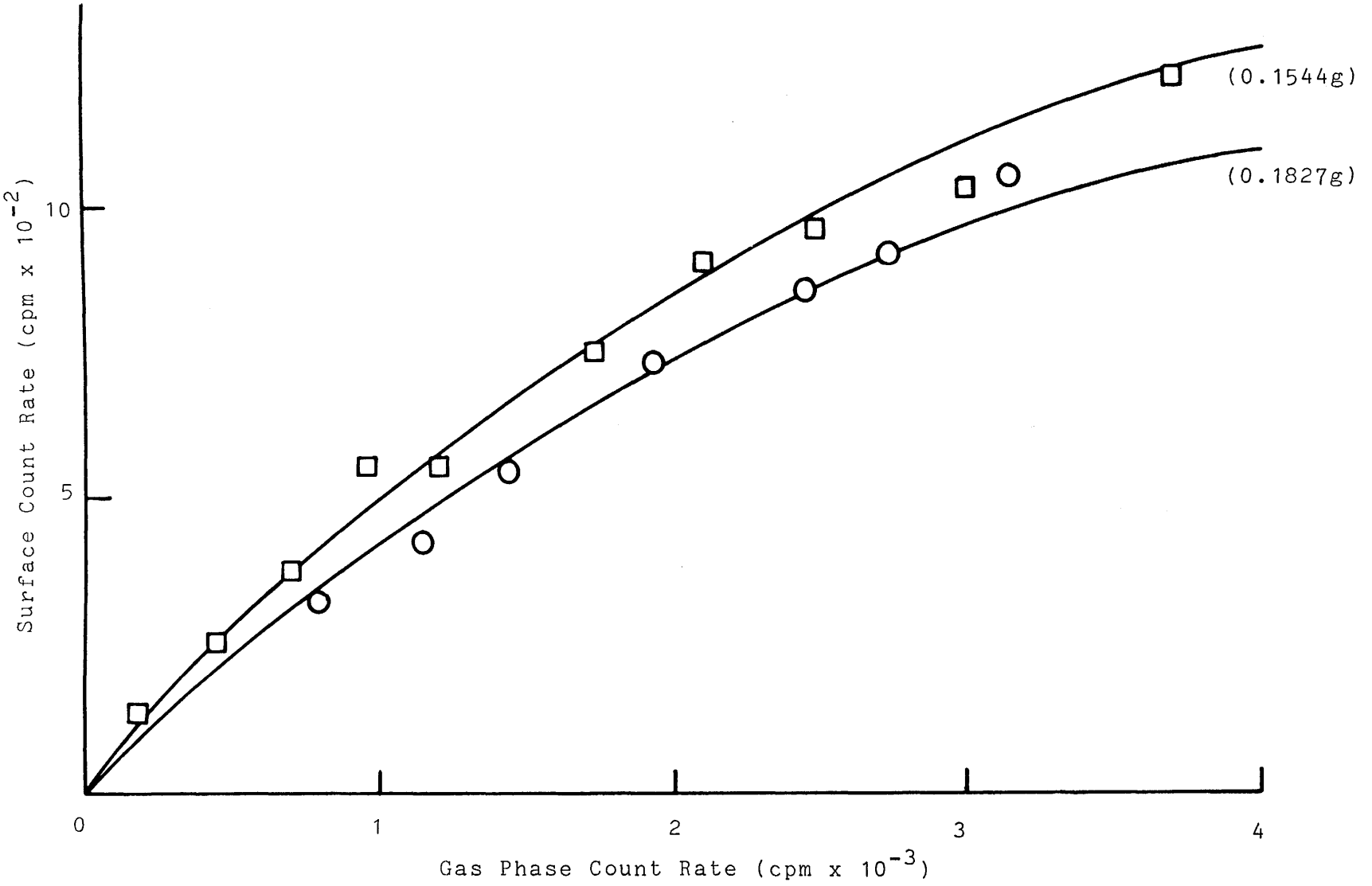

Figure 4.17 Adsorption Isotherms for [14-C]Carbon Dioxide (sp. acty = 0.045 mCi $mmol^{-1}$) on Al_2O_3.

indicated that, carbon dioxide was the only gas present.

In contrast with carbon dioxide, carbon monoxide was found not to adsorb on Al_2O_3.

4.7.1 The Reversibility of Adsorption of Carbon Dioxide on Al_2O_3

The reversibility of adsorption of carbon dioxide on Al_2O_3 was studied by evacuation and molecular exchange.

The effects of evacuation (Section 4.1.2) on a [14-C]carbon dioxide precovered Al_2O_3 sample are shown in Table 4.14.

Table 4.15 summarises the results obtained when adsorbed [14-C]carbon dioxide was exchanged with 4.02 torr gas phase [12-C]carbon dioxide without evacuation, as previously described in Section 4.1.2.

Table 4.14 Effects of Evacuation on Carbon Dioxide Adsorbed on Al_2O_3

Specific activity of [14-C]carbon dioxide = 0.045mCi $mmol^{-1}$
Weight of catalyst = 0.1827g

Procedure	Surface count rate (cpm)	% Change
Adsorption of [14-C]carbon dioxide to gas pressure of 1.90torr	1108	-
Evacuation for 10 minutes	686	-38.1

Table 4.1 5 Effects of Molecular Exchange on Carbon Dioxide Adsorbed on Al_2O_3 Without Evacuation

Specific activity of [14-C]carbon dioxide = 0.045mCi $mmol^{-1}$
Weight of catalyst = 0.1544g

Procedure	Surface count rate (cpm)	% Change
Adsorption of [14-C]carbon dioxide to gas pressure of 2.23torr	1223	-
Admission of 4.02torr [12-C]carbon dioxide for 10 minutes	1076	-12.0
for 12 hours	968	-20.8

4.7.2 Adsorption of [14-C]Carbon Dioxide on Al_2O_3 Over a Long Time Period

During the adsorption of [14-C]carbon dioxide on Al_2O_3, as previously reported in Section 4.7, a pressure decrease was monitored in the reaction vessel by the pressure transducer. To investigate the time taken for a sample of carbon dioxide to reach equilibrium with the surface, a large aliquot (2.93torr) of [14-C]carbon dioxide was admitted to the reaction vessel containing a sample of Al_2O_3 and the surface count rate determined over a period of 23 hours.

Analysis of the gas phase in contact with the surface during the adsorption process, indicated that, carbon dioxide was the only gas present.

A graph of surface count rate against time for the

adsorption of 2.93 torr [14-C]carbon dioxide is shown in Figure 4.18. From Figure 4.18, it can be seen that, 2.93 torr [14-C]carbon dioxide took 16 hours to reach surface saturation. The amount of [14-C]carbon dioxide which was removed by evacuation over a period of 10 minutes, after the last point on the graph was determined, was 18%.

4.8 Adsorption of [14-C]Carbon Dioxide and [14-C]Carbon Monoxide on Oxidised $Cu/ZnO/Al_2O_3$

The fully oxidised and partially oxidised $Cu/ZnO/Al_2O_3$ catalyst samples referred to in this section, were prepared using nitrous oxide by the methods described in Section 3.7.2.

4.8.1 Adsorption of [14-C]Carbon Dioxide and [14-C]Carbon Monoxide on Fully Oxidised $Cu/ZnO/Al_2O_3$

Small aliquots of [14-C]carbon dioxide were admitted to a fully oxidised sample of $Cu/ZnO/Al_2O_3$. The isotherm produced is shown in Figure 4.19(a). During the adsorption process a slow, continuous decrease in pressure in the reaction vessel was recorded by the pressure transducer.

Gas chromatographic analysis during the adsorption revealed that the adsorbate gas, carbon dioxide, was the only gas present.

Figure 4.19(b) shows an adsorption isotherm produced when successive aliquots of [14-C]carbon monoxide were admitted to a fully oxidised sample of $Cu/ZnO/Al_2O_3$. In

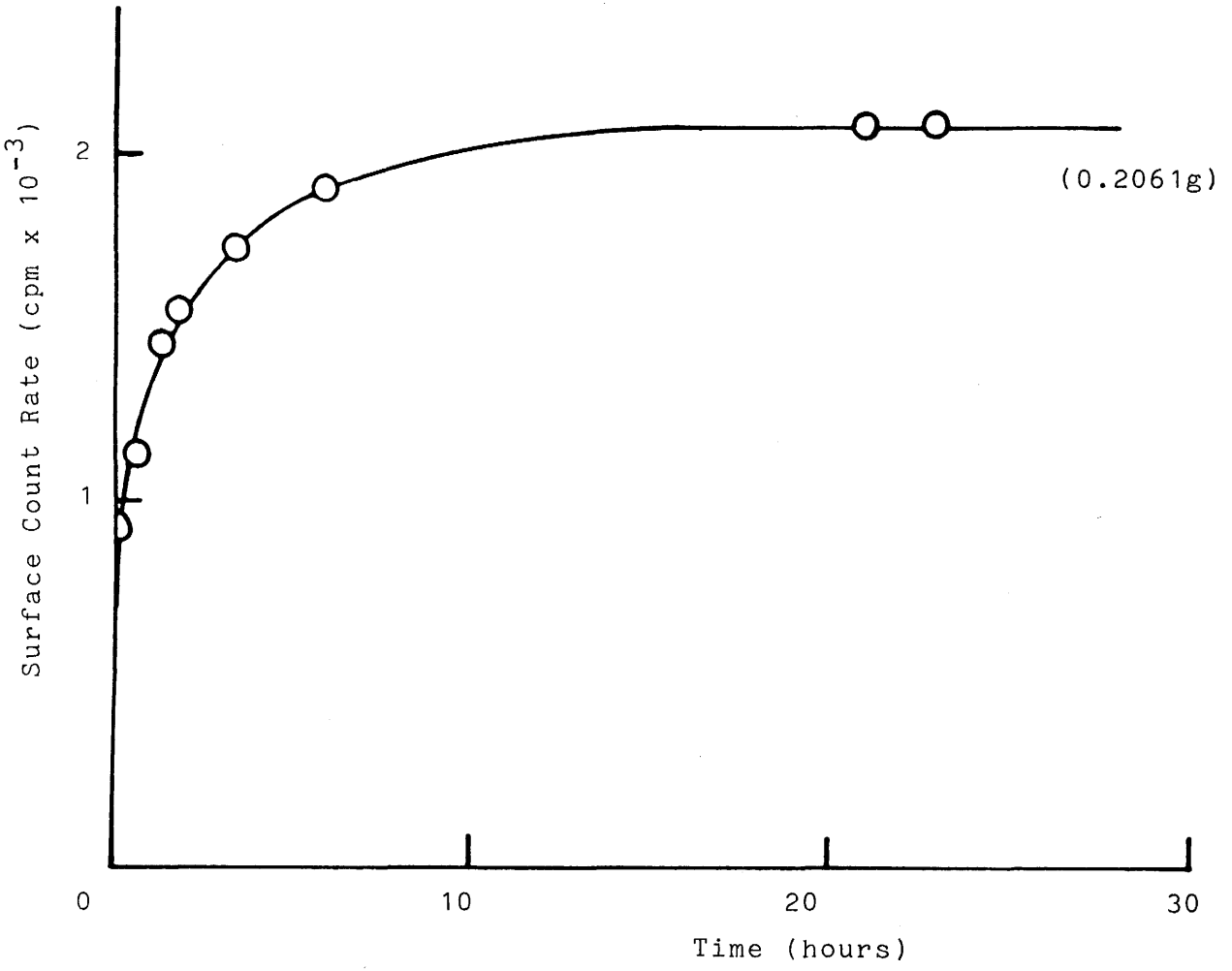

Figure 4.18 Adsorption of 2.93 torr [14-C]Carbon Dioxide (sp. acty = 0.062 mCi $mmol^{-1}$) on Al_2O_3 Over a Long Time Period.

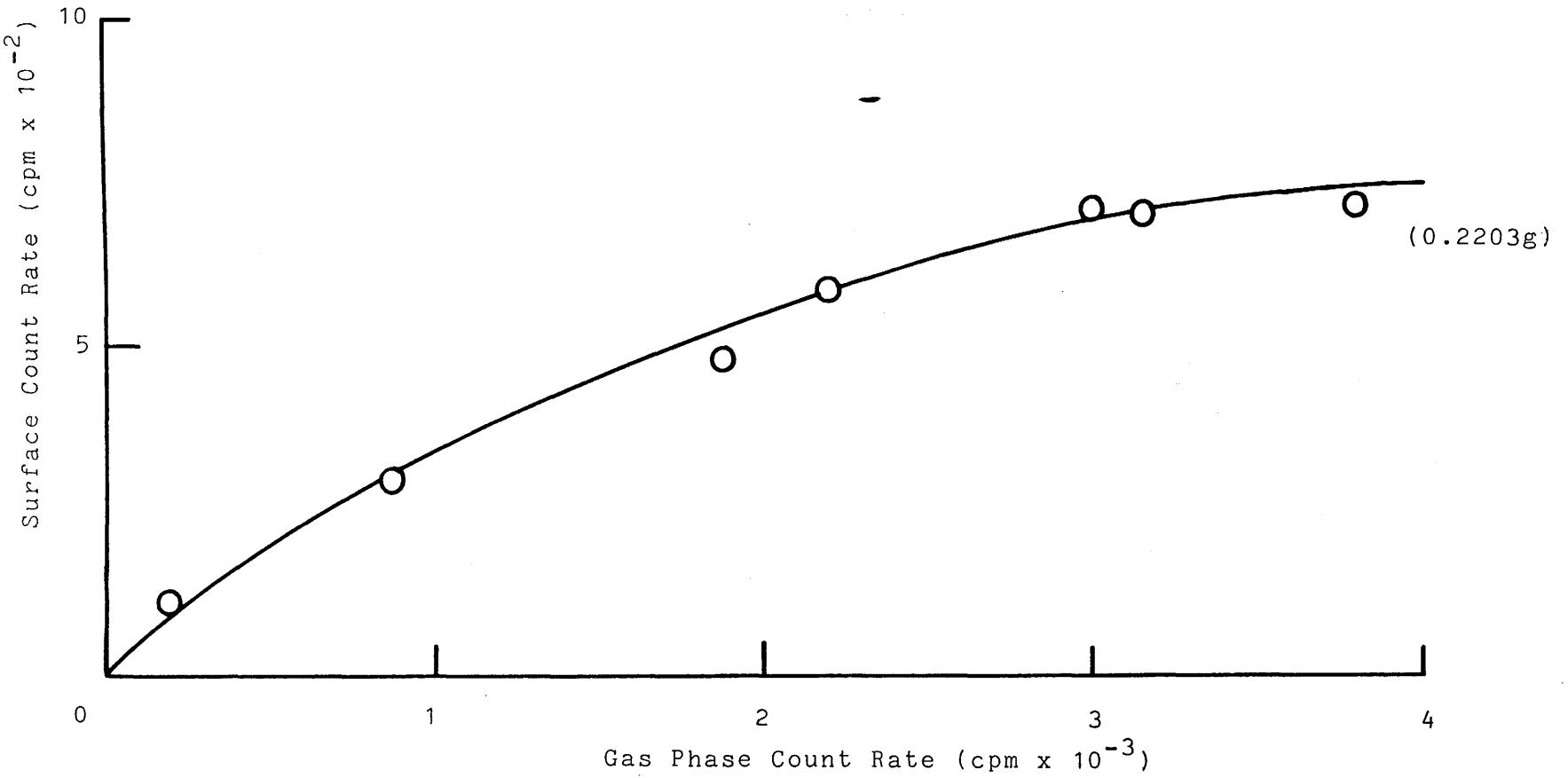

Figure 4.19(a) Adsorption Isotherm for [14-C]Carbon Dioxide (sp. acty = 0.066 mCi $mmol^{-1}$) on Fully Oxidised $Cu/ZnO/Al_2O_3$.

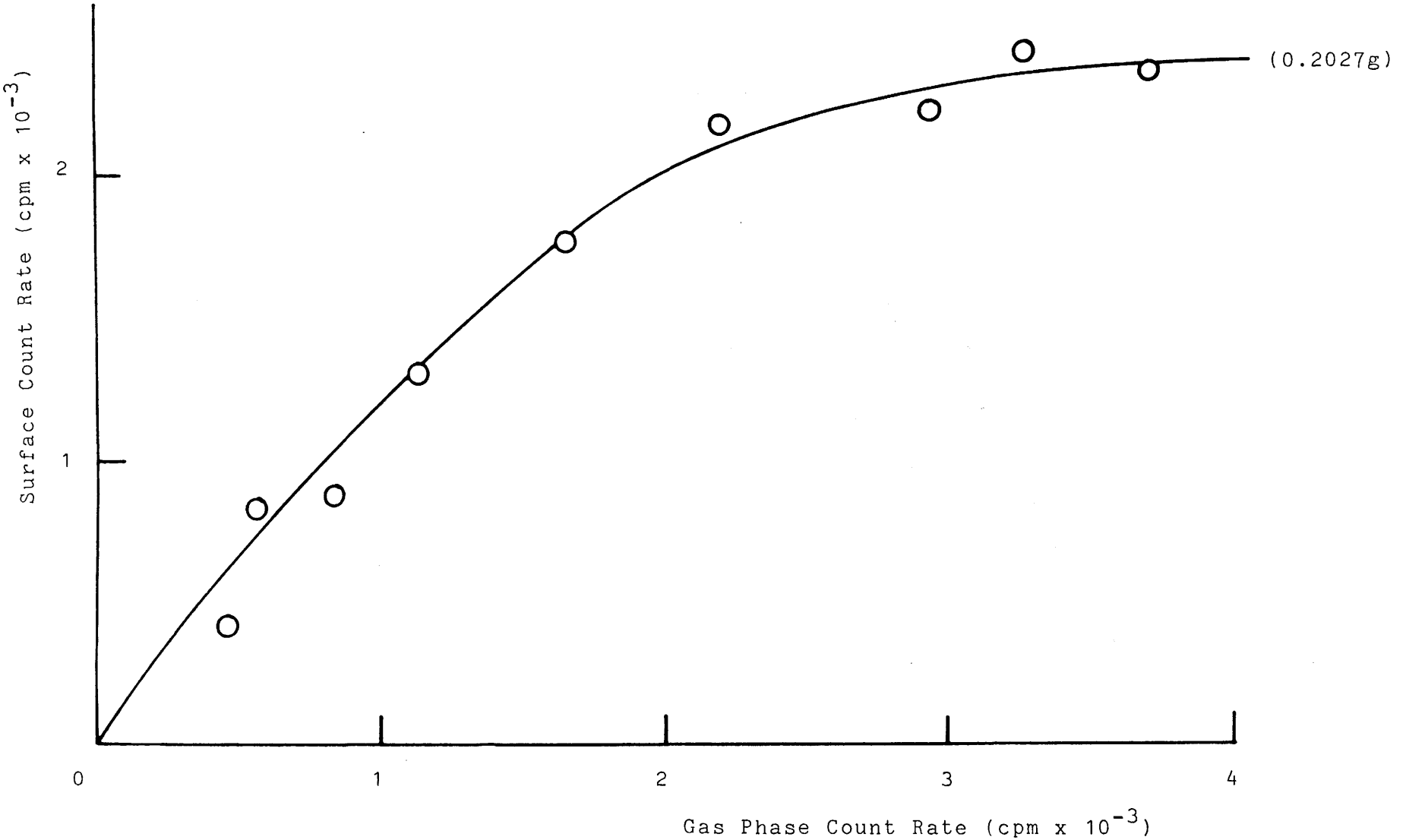

Figure 4.19(b) Adsorption Isotherm for [14-C]Carbon Monoxide (sp. acty = 0.058 mCi $mmol^{-1}$) on Fully Oxidised $Cu/ZnO/Al_2O_3$.

contrast with the adsorption of [14-C]carbon monoxide on reduced $Cu/ZnO/Al_2O_3$ (Section 4.2) a slow, continuous decrease in pressure (although smaller than that recorded for the adsorption of [14-C]carbon dioxide on reduced $Cu/ZnO/Al_2O_3$ (Section 4.1)), was recorded in the reaction vessel during the adsorption process.

During the adsorption of [14-C]carbon monoxide on fully oxidised $Cu/ZnO/Al_2O_3$, carbon dioxide (9×10^{18} molecules) was detected in the gas phase by gas chromatography.

4.8.1.1 The Reversibility of Adsorption of Carbon Dioxide and Carbon Monoxide on Fully Oxidised $Cu/ZnO/Al_2O_3$

The reversibility of adsorption of carbon dioxide and carbon monoxide on fully oxidised $Cu/ZnO/Al_2O_3$ was studied by evacuation (Sections 4.1.2 and 4.2.2). The results are shown in Tables 4.16(a) and 4.16(b).

Table 4.16(a) Effects of Evacuation on Carbon Dioxide Adsorbed on Fully Oxidised $Cu/ZnO/Al_2O_3$

Specific activity of [14-C]carbon dioxide = 0.066mCi $mmol^{-1}$
Weight of catalyst = 0.2203g

Procedure	Surface count rate (cpm)	% Change
Adsorption of [14-C]carbon dioxide to gas pressure of 1.70torr	712	-
Evacuation for 10 minutes	901	+26.5

Table 4.16(b) Effects of Evacuation on Carbon Monoxide Adsorbed on Fully Oxidised $Cu/ZnO/Al_2O_3$

Specific activity of [14-C]carbon monoxide = 0.058mCi $mmol^{-1}$
Weight of catalyst = 0.2027g

Procedure	Surface count rate (cpm)	% Change
Adsorption of [14-C]carbon monoxide to gas pressure of 1.90torr	2334	-
Evacuation for 10 minutes	1557	-33.3

4.8.1.2 The Effects of Hydrogen on the Adsorption of Carbon Dioxide and Carbon Monoxide on Fully Oxidised $Cu/ZnO/Al_2O_3$

The effects of hydrogen on the adsorption of [14-C]-carbon dioxide and on the adsorption of [14-C]carbon monoxide on fully oxidised $Cu/ZnO/Al_2O_3$ were investigated by the method described in Section 4.1.4. The isotherms produced are illustrated in Figures 4.20(a) and 4.20(b). In comparison with the addition of hydrogen to reduced $Cu/ZnO/Al_2O_3$ (Section 4.1.4), a relatively small decrease in pressure (0.04 torr) in the reaction vessel was recorded upon admission of hydrogen to the fully oxidised $Cu/ZnO/Al_2O_3$ samples. As with the adsorption of [14-C]carbon dioxide and [14-C]carbon monoxide on fully oxidised $Cu/ZnO/Al_2O_3$, a decrease in pressure in the reaction vessel was recorded during the adsorption of each of these gases on fully oxidised $Cu/ZnO/Al_2O_3$ in the presence of hydrogen.

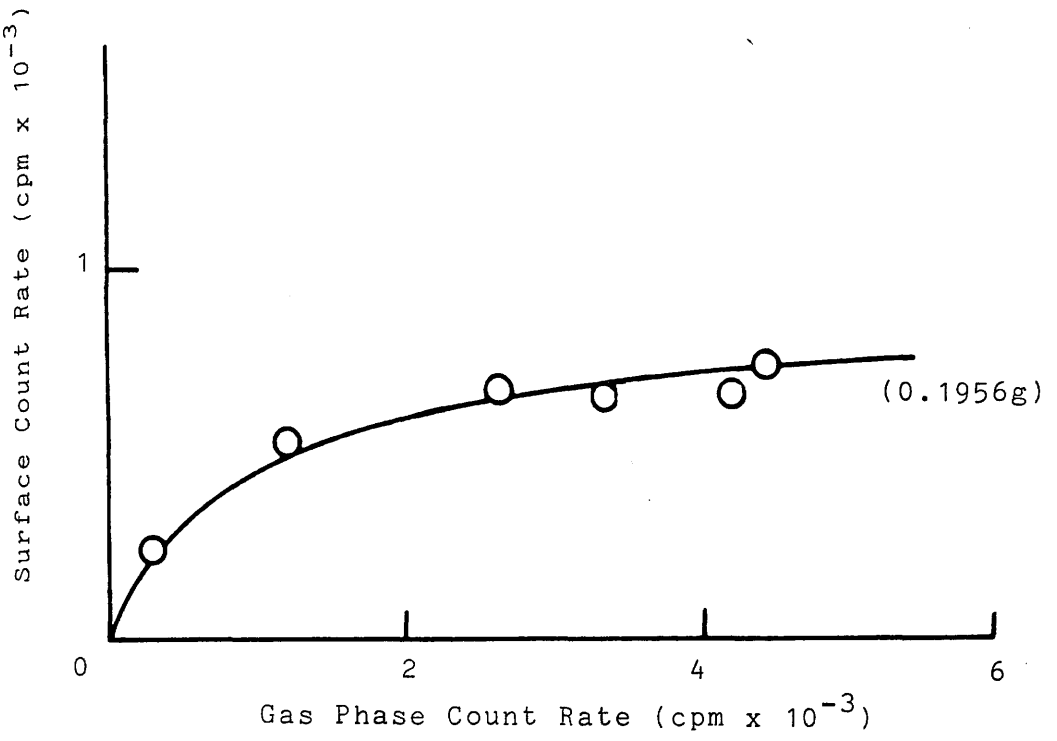

Figure 4.20(a) Adsorption Isotherm for [14-C]Carbon Dioxide (sp. acty = 0.062 mCi $mmol^{-1}$) on Fully Oxidised $Cu/ZnO/Al_2O_3$ in the Presence of 4.01 torr Hydrogen.

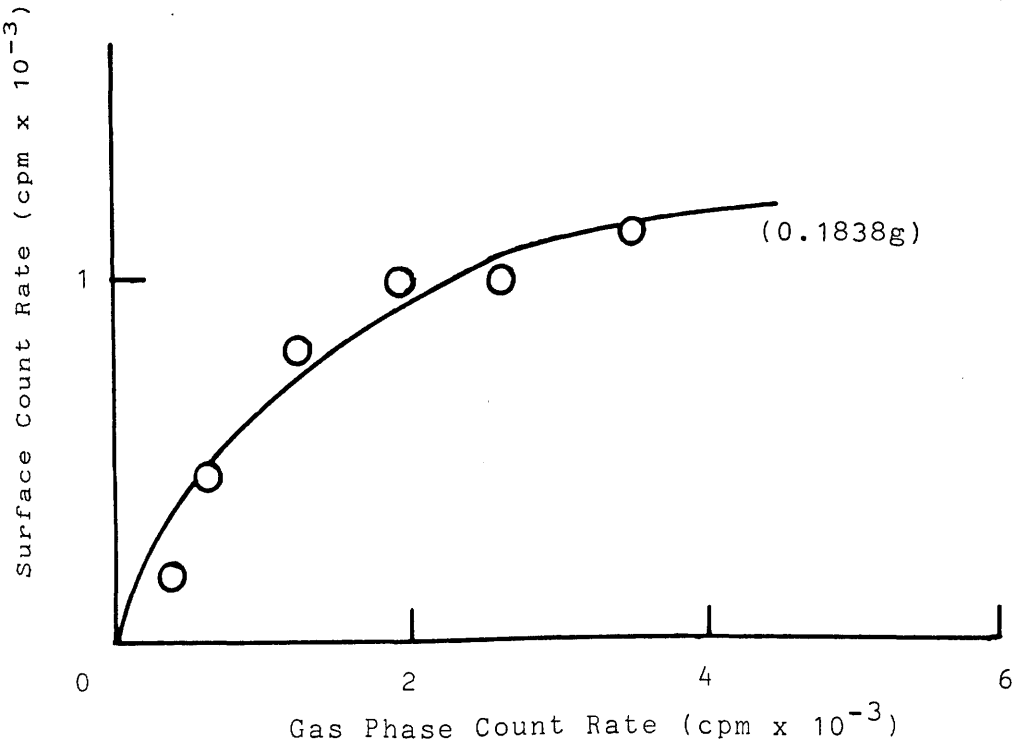

Figure 4.20(b) Adsorption Isotherm for [14-C]Carbon Monoxide (sp. acty = 0.058 mCi $mmol^{-1}$) on Fully Oxidised $Cu/ZnO/Al_2O_3$ in the Presence of 3.83 torr Hydrogen.

Analysis of the gas phase during the adsorption processes revealed that, during the adsorption of [14-C]-carbon dioxide on fully oxidised $Cu/ZnO/Al_2O_3$ in the presence of hydrogen, the adsorbate gas was the only gas present, and, in contrast with the adsorption of [14-C]carbon monoxide on fully oxidised $Cu/ZnO/Al_2O_3$ (Section 4.8.1), during the adsorption of [14-C]carbon monoxide on fully oxidised $Cu/ZnO/Al_2O_3$ in the presence of hydrogen, carbon dioxide was not detected in the gas phase.

After the last point had been measured on each of the isotherms in Figures 4.20(a) and 4.20(b), the fraction of adsorbed species which was evacuated from the surface was 4% for carbon dioxide and 25% for carbon monoxide.

4.8.1.3 Adsorption of [14-C]Carbon Dioxide and Adsorption of [14-C]Carbon Monoxide on Fully Oxidised $Cu/ZnO/Al_2O_3$ Over a Long Time Period

As with the adsorption of [14-C]carbon dioxide on fully oxidised $Cu/ZnO/Al_2O_3$, it became apparent from the adsorption measurements made with [14-C]carbon monoxide on fully oxidised $Cu/ZnO/Al_2O_3$ (Section 4.8.1), that carbon monoxide was being adsorbed slowly on the surface of this catalyst.

Figures 4.21(a) and 4.21(b) show graphs of surface count rate against time for the adsorption of 2.69 torr [14-C]carbon dioxide and for the adsorption of 2.72 torr [14-C]carbon monoxide, respectively, on fully oxidised $Cu/ZnO/Al_2O_3$.

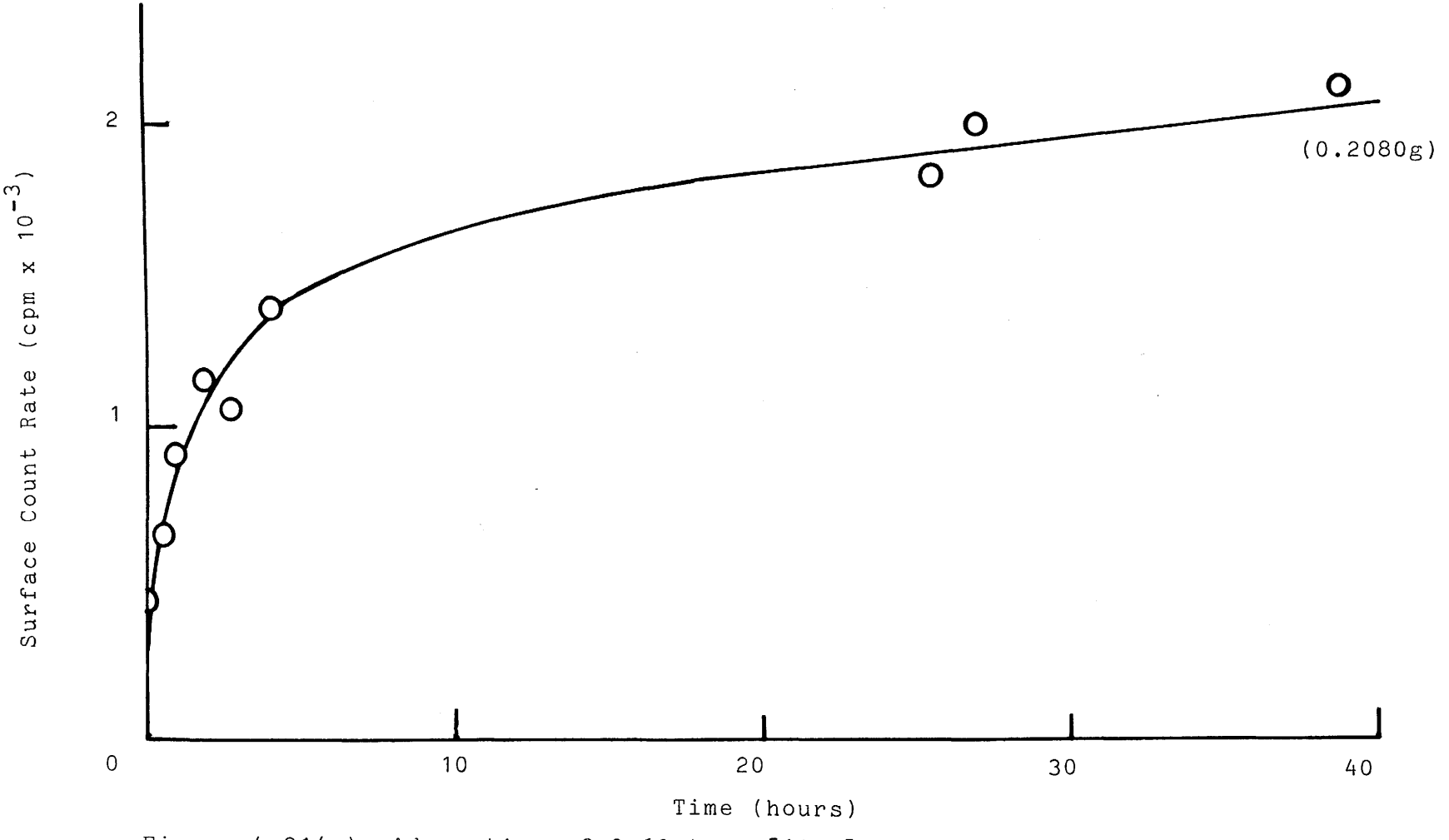

Figure 4.21(a) Adsorption of 2.69 torr [14-C]Carbon Dioxide (sp. acty = 0.062 mCi $mmol^{-1}$) on Fully Oxidised $Cu/ZnO/Al_2O_3$ Over a Long Time Period.

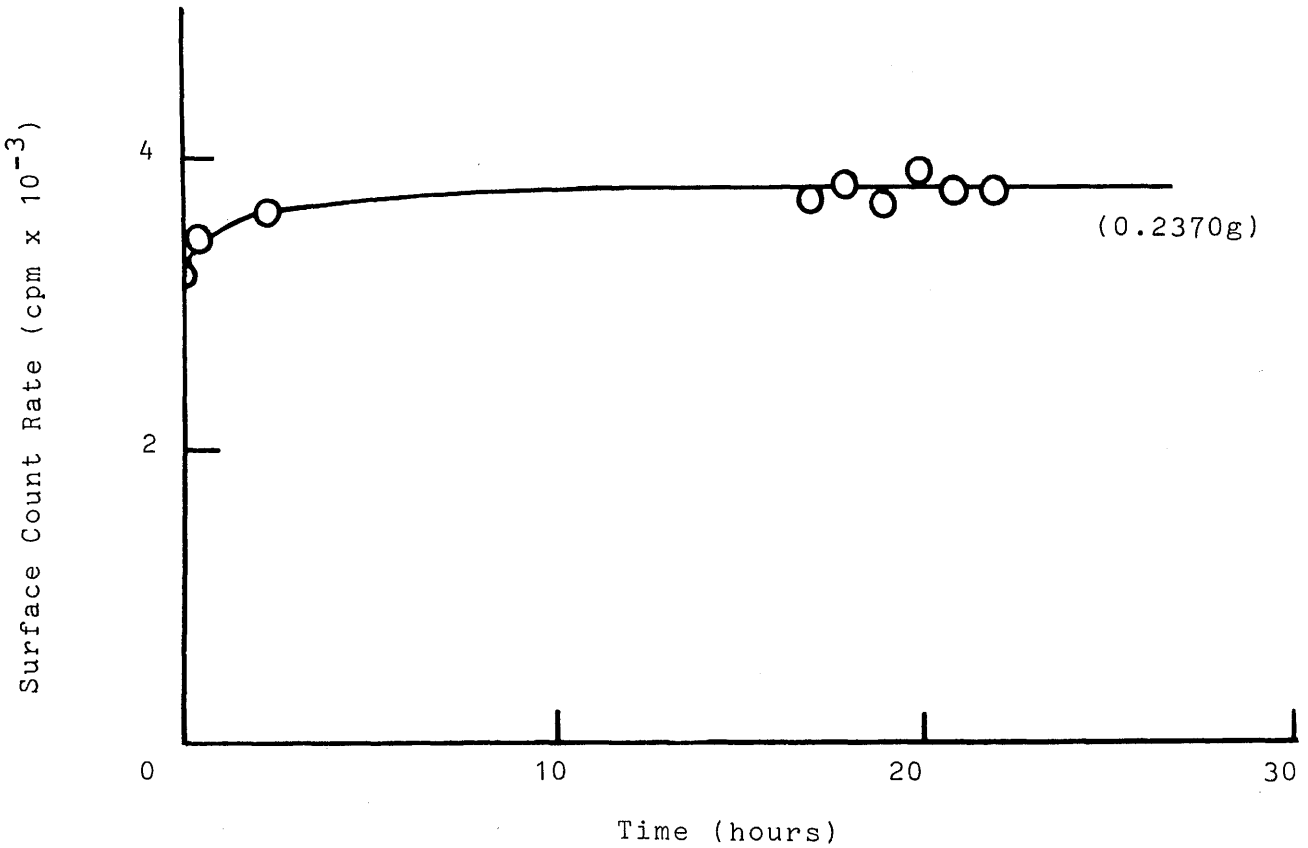

Figure 4.21(b) Adsorption of 2.72 torr [14-C]Carbon Monoxide (sp. acty = 0.061 mCi $mmol^{-1}$) on Fully Oxidised $Cu/ZnO/Al_2O_3$ Over a Long Time Period.

Analysis of the gas phase during the adsorption of [14-C]carbon dioxide on fully oxidised $Cu/ZnO/Al_2O_3$ over a long time period revealed that carbon dioxide was the only gas present, however, gas chromatographic analysis during the adsorption of [14-C]carbon monoxide on fully oxidised $Cu/ZnO/Al_2O_3$ over a long time period revealed that, carbon dioxide (1.55×10^{19} molecules after 22 hours) was present in the gas phase.

From Figure 4.21(a), it can be seen that, unlike the adsorption of [14-C]carbon dioxide on reduced $Cu/ZnO/Al_2O_3$, where equilibrium was reached after 26 hours (Figure 4.5), during the adsorption of [14-C]carbon dioxide on fully oxidised $Cu/ZnO/Al_2O_3$, equilibrium was not reached after 40 hours. Similarly from Figure 4.21(b), it can be seen that, unlike the adsorption of [14-C]carbon monoxide on reduced $Cu/ZnO/Al_2O_3$, where surface saturation was reached after 20 minutes (Figure 4.9), during the adsorption of [14-C]-carbon monoxide on fully oxidised $Cu/ZnO/Al_2O_3$, 10 hours were required for surface equilibrium to be attained.

The amount of each gas which was evacuated after the last point on each graph was determined, was 5% for carbon dioxide and 25% for carbon monoxide.

4.8.2 Adsorption of [14-C]Carbon Dioxide and [14-C]Carbon Monoxide on 30% Partially Oxidised $Cu/ZnO/Al_2O_3$

Figure 4.22(a) shows an adsorption isotherm produced when small aliqots of [14-C]carbon dioxide were admitted to a

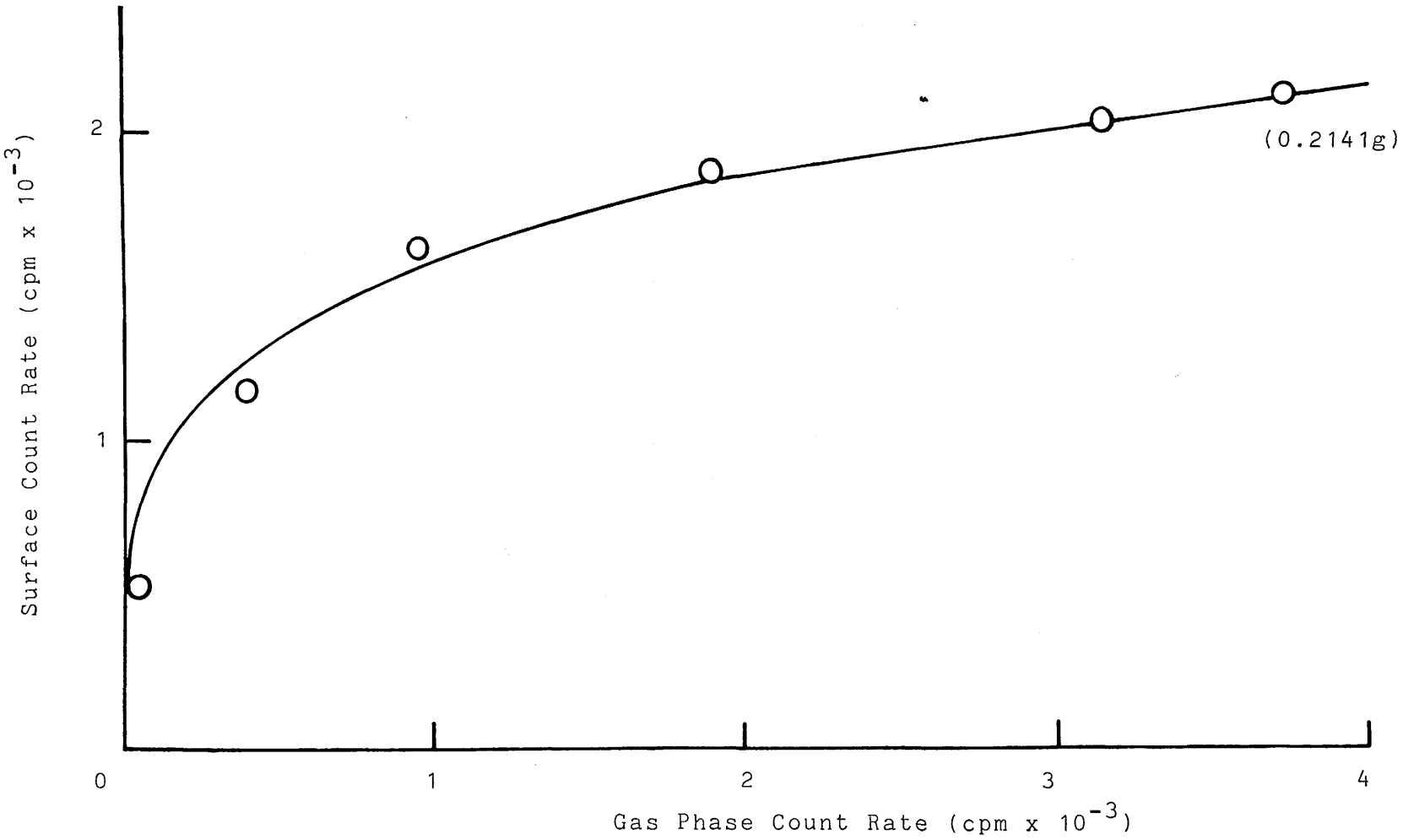

Figure 4.22(a) Adsorption Isotherm for [14-C]Carbon Dioxide (sp. acty = 0.062 mCi $mmol^{-1}$) on Partially Oxidised $Cu/ZnO/Al_2O_3$.

30% partially oxidised sample of $Cu/ZnO/Al_2O_3$. As with the adsorption of [14-C]carbon dioxide on reduced $Cu/ZnO/Al_2O_3$ (Section 4.1), a slow, continuous decrease in pressure in the reaction vessel was monitored by the pressure transducer.

Analysis of the gas phase in contact with the surface during the adsorption process, indicated that, carbon dioxide was the only gas present.

The adsorption isotherm produced when small aliquots of [14-C]carbon monoxide were admitted to a 30% partially oxidised sample of $Cu/ZnO/Al_2O_3$ is shown in Figure 4.22(b). As with the adsorption of [14-C]carbon monoxide on fully oxidised $Cu/ZnO/Al_2O_3$ (Section 4.8.1), a slow, continuous decrease in pressure was recorded in the reaction vessel after addition of each aliquot.

Gas chromatographic analysis of the gas phase during the adsorption process, revealed that, carbon dioxide as well as the adsorbate gas, carbon monoxide, was present.

4.8.2.1 The Reversibility of Adsorption of Carbon Dioxide and Carbon Monoxide on 30% Partially Oxidised $Cu/ZnO/Al_2O_3$

The reversibility of adsorption of carbon dioxide and carbon monoxide on partially oxidised $Cu/ZnO/Al_2O_3$ was studied by evacuation using the method described previously (Sections 4.1.2 and 4.2.2). The results are shown in Tables 4.17(a) and 4.17(b).

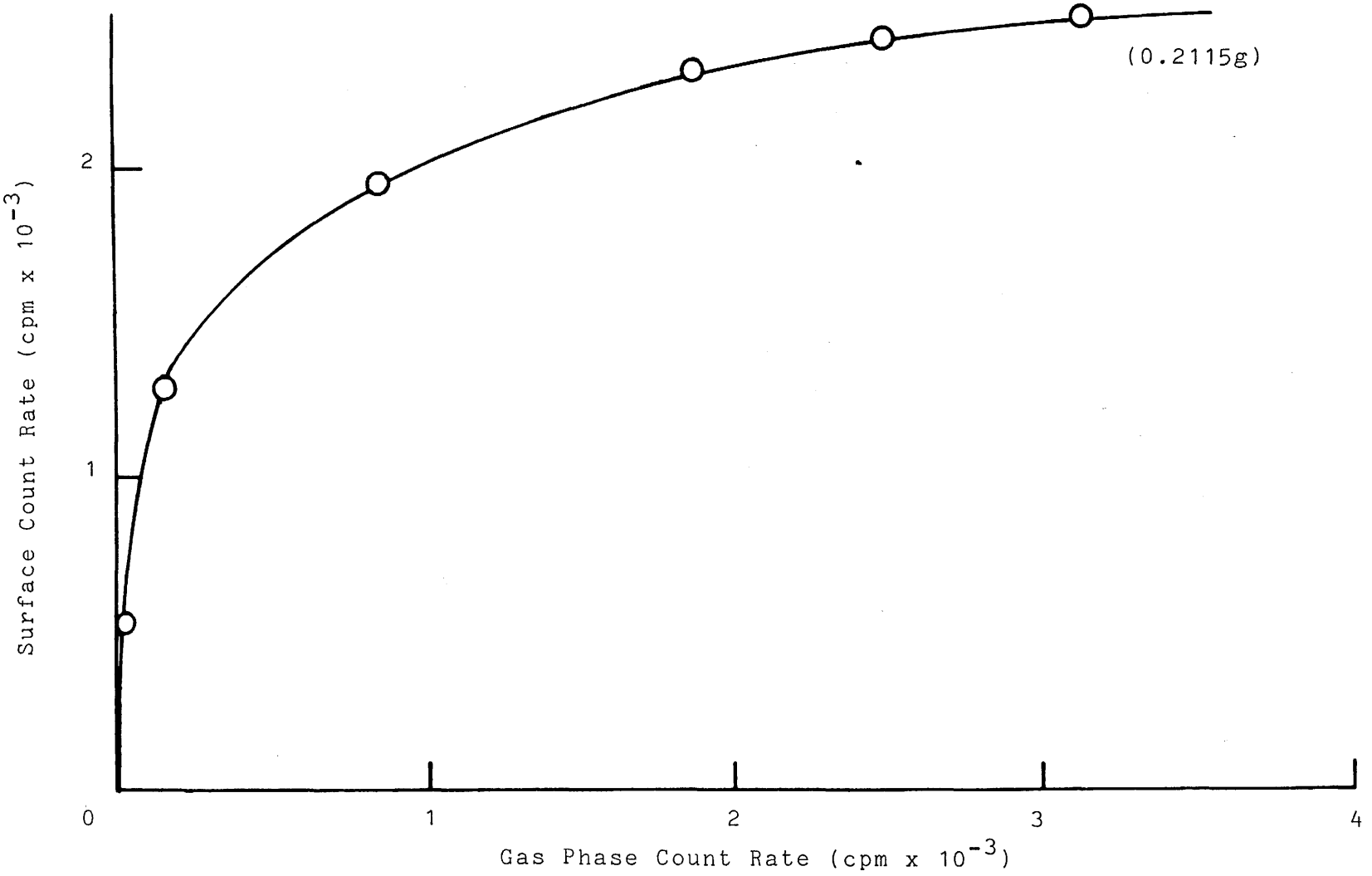

Figure 4.22(b) Adsorption Isotherm for [14-C]Carbon Monoxide (sp. acty = 0.058 mCi $mmol^{-1}$) on Partially Oxidised $Cu/ZnO/Al_2O_3$.

Table 4.17(a) Effects of Evacuation on Carbon Dioxide Adsorbed on Partially Oxidised $Cu/ZnO/Al_2O_3$

Specific activity of [14-C]carbon dioxide = 0.062mCi $mmol^{-1}$
Weight of catalyst = 0.1916g

Procedure	Surface count rate (cpm)	% Change
Adsorption of [14-C]carbon dioxide to gas pressure of 1.70torr	1689	-
Evaucation for 10 minutes	1553	-8.0

Table 4.17(b) Effects of Evacuation on Carbon Monoxide Adsorbed on Partially Oxidised $Cu/ZnO/Al_2O_3$

Specific activity of [14-C]carbon monoxide = 0.058mCi $mmol^{-1}$
Weight of catalyst = 0.2115g

Procedure	Surface count rate (cpm)	% Change
Adsorption of [14-C]carbon monoxide to gas pressure of 1.95torr	2411	-
Evacuation for 10 minutes	1318	-45.3

4.8.2.2 The Effects of Hydrogen on the Adsorption of Carbon Dioxide and Carbon Monoxide on 30% Partially Oxidised $Cu/ZnO/Al_2O_3$

The adsorption of [14-C]carbon dioxide on partially oxidised $Cu/ZnO/Al_2O_3$ in the presence of 4.09 torr hydrogen

and the adsorption of [14-C]carbon monoxide on partially oxidised $Cu/ZnO/Al_2O_3$ in the presence of hydrogen (3.63 torr) was investigated by the method described previously (Sections 4.1.4 and 4.2.4) and the isotherms shown in Figures 4.23(a) and 4.23(b). Similar to the addition of hydrogen to reduced $Cu/ZnO/Al_2O_3$ (Section 4.1.4), a decrease in pressure (0.18 torr) in the reaction vessel was recorded upon admission of hydrogen to the partially oxidised $Cu/ZnO/Al_2O_3$ samples.

Gas chromatographic analysis during each of the adsorption processes, revealed that, during the adsorption of [14-C]carbon dioxide on partially oxidised $Cu/ZnO/Al_2O_3$ in the presence of hydrogen, the adsorbate gas was the only gas present, and as with the adsorption of [14-C]carbon monoxide on fully oxidised $Cu/ZnO/Al_2O_3$ in the presence of hydrogen (Section 4.8.1.2) no carbon dioxide was detected in the gas phase during the adsorption of [14-C]carbon monoxide on partially oxidised $Cu/ZnO/Al_2O_3$ in the presence of hydrogen.

After the last point on each of the isotherms was measured, the amount of adsorbed species which was evacuated from the surface was 9% for carbon dioxide and 24% for carbon monoxide.

4.9 Adsorption Studies in a Flow System

The results described in this section refer to work carried out in the microreactor/mass spectrometer system described in Section 3.8.1.

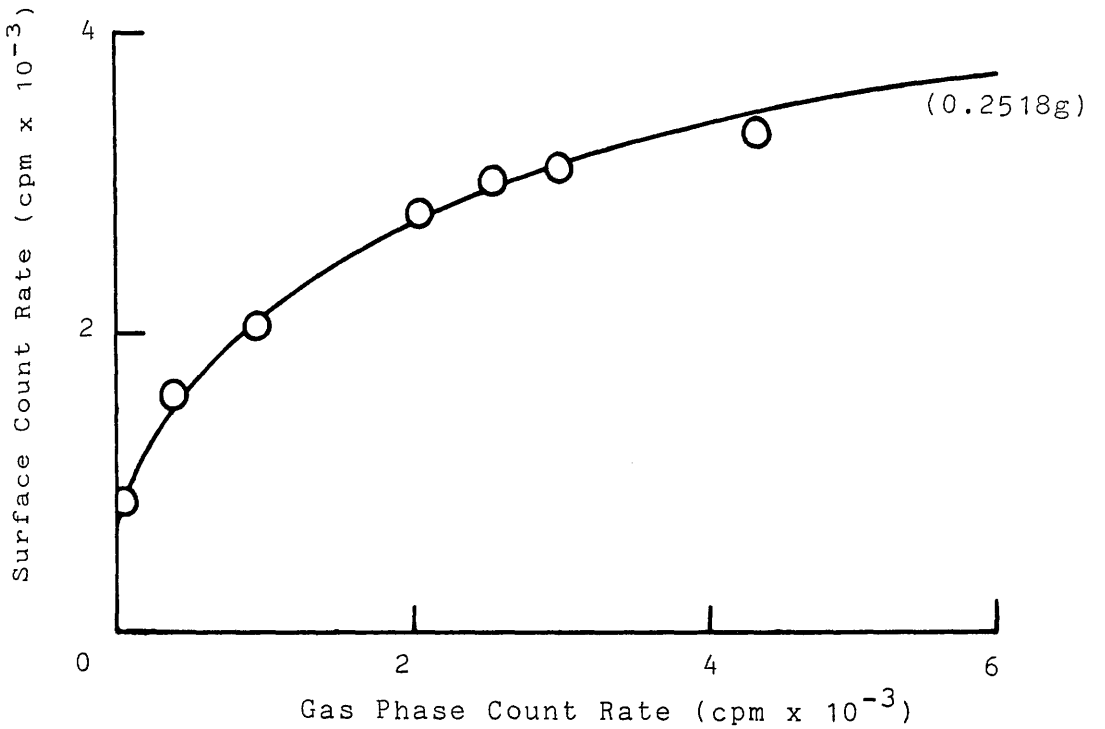

Figure 4.23(a) Adsorption Isotherm for [14-C]Carbon Dioxide (sp. acty = 0.062 mCi $mmol^{-1}$) on Partially Oxidised $Cu/ZnO/Al_2O_3$ in the Presence of 4.09 torr Hydrogen.

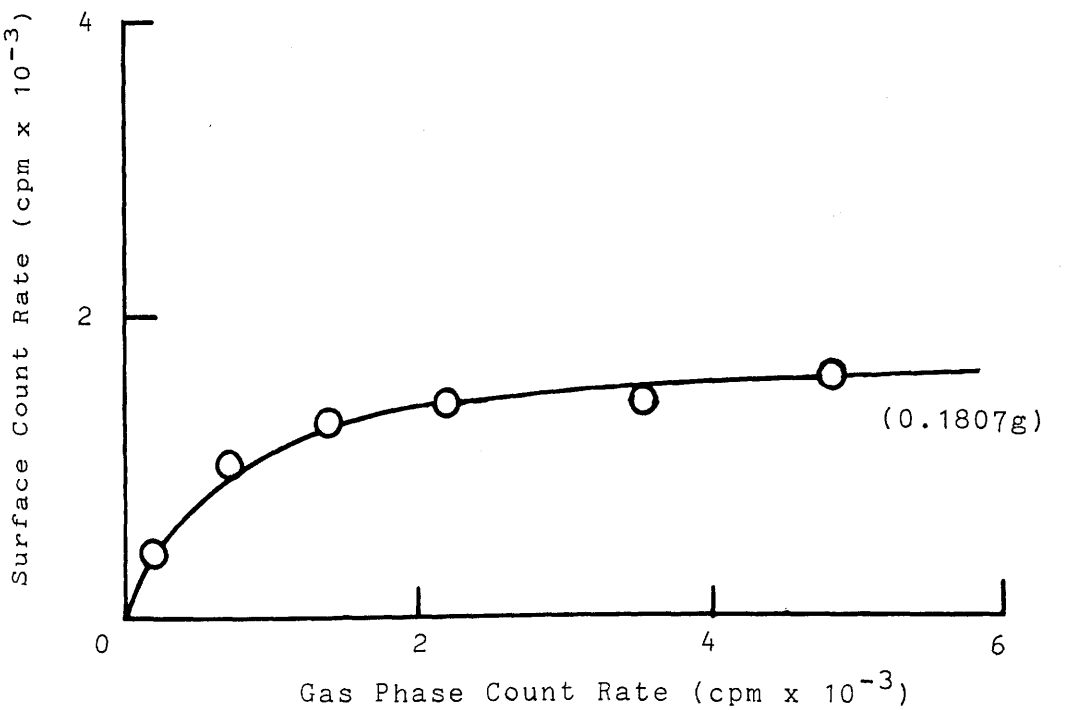

Figure 4.23(b) Adsorption Isotherm for [14-C]Carbon Monoxide (sp. acty = 0.058 mCi $mmol^{-1}$) on Partially Oxidised $Cu/ZnO/Al_2O_3$ in the Presence of 3.63 torr Hydrogen.

4.9.1 Adsorption of Carbon Dioxide on $Cu/ZnO/Al_2O_3$

A sample of $Cu/ZnO/Al_2O_3$ was activated as described in Section 3.8.2.1. The copper surface area of the sample was then determined using nitrous oxide before it was re-reduced at 503K and purged with helium for 10 minutes. A stream of carbon dioxide was passed over the catalyst at 503K (flow rate = 50ml min^{-1}) for 1½ hours and the level of carbon monoxide in the outlet stream measured by monitoring $^{m}/_{e}$ = 14 on the mass spectrometer. The trace obtained is shown in Figure 4.24. From this, it can be seen that, during treatment of the catalyst with carbon dioxide, the carbon monoxide level increased rapidly then reached a steady value which was above the level of carbon monoxide in the inlet stream of carbon dioxide. After treatment with carbon dioxide the catalyst sample was purged with helium at 503K. After cooling in helium to ambient temperature, the copper surface area was determined using nitrous oxide. The catalyst was then re-reduced and the copper surface area determined again following this re-reduction. The results are summarised in Table 4.18.

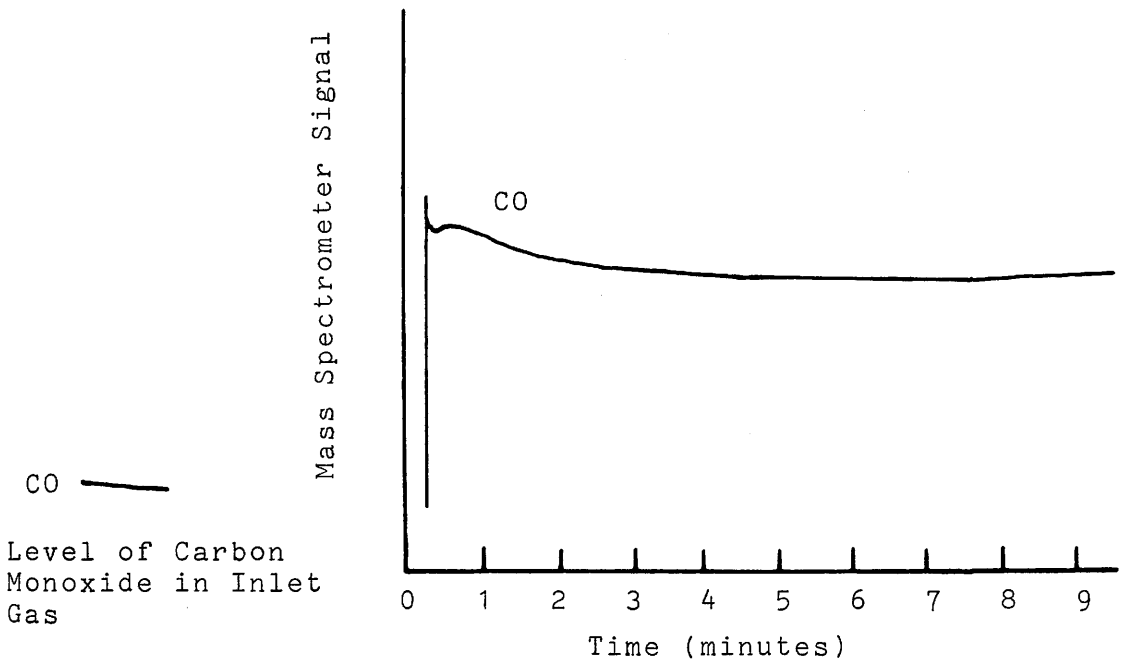

Figure 4.24 Adsorption of Carbon Dioxide on $Cu/ZnO/Al_2O_3$ at 503K - Level of Carbon Monoxide in Outlet Gas.

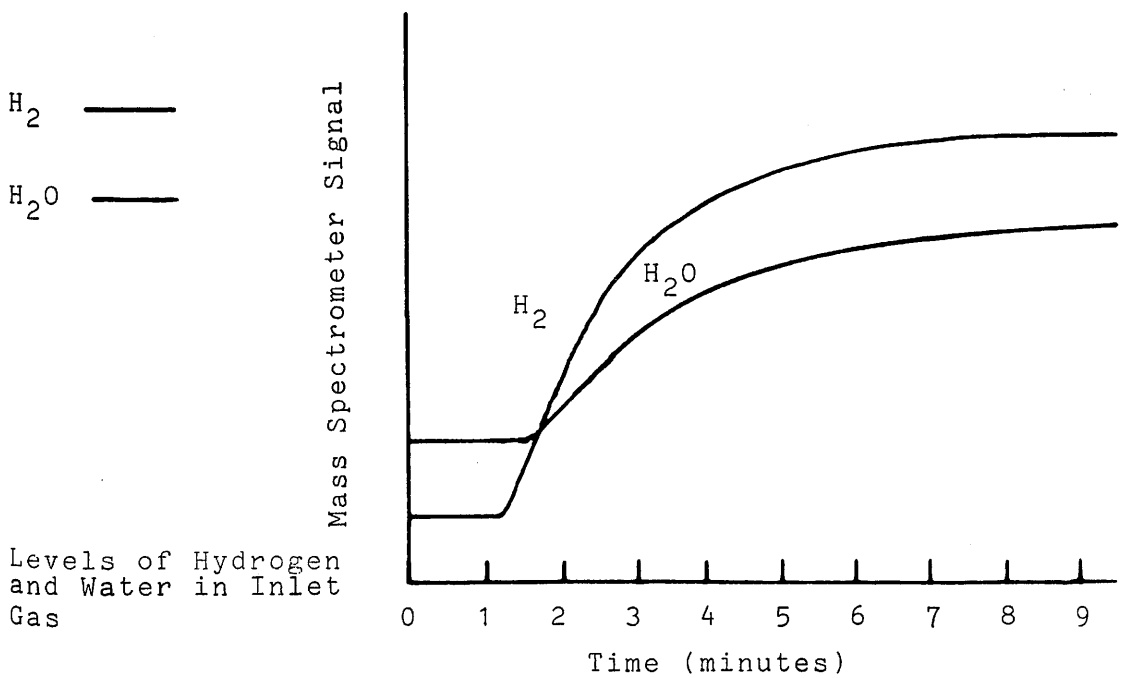

Figure 4.25 Adsorption of Hydrogen on $Cu/ZnO/Al_2O_3$ at Ambient Temperature after Treatment with Carbon Dioxide at 503K - Levels of Hydrogen and Water in Outlet Gas

Table 4.18 Adsorption of Carbon Dioxide on $Cu/ZnO/Al_2O_3$ at 503K.

Procedure	Copper surface area after treatment ($m^2\ g^{-1}$)	% Change
Catalyst reduced	29	-
Catalyst re-reduced, purged with helium for 10 minutes and carbon dioxide passed over the catalyst at 503K for $1\frac{1}{2}$ hours	18	-38
Catalyst re-reduced	27	-7

The adsorption of hydrogen on the catalyst sample after treatment with carbon dioxide at 503K for $1\frac{1}{2}$ hours was studied by the same experimental technique as that used above except that, after treatment with carbon dioxide, the catalyst was purged and cooled in helium to ambient temperature before a stream of 2.5% hydrogen in nitrogen (flow rate = 50ml min^{-1}) was passed over the catalyst for 1 hour. The copper surface area was then determined. The results are shown in Table 4.19. During treatment of the catalyst at ambient temperature with hydrogen, the amount of hydrogen and water in the outlet stream was measured by monitoring $^{m}/_{e}$ = 2 and $^{m}/_{e}$ = 17, respectively, on the mass spectrometer. The trace is shown in Figure 4.25. From this, it can be seen that, hydrogen was adsorbed by the catalyst immediately, but no water was produced during this time; the level of water in the outlet stream did not rise above

that in the inlet. The total amount of hydrogen adsorbed by the catalyst after 1 hour was $4cm^3$.

Table 4.19 Adsorption of Carbon Dioxide on $Cu/ZnO/Al_2O_3$ at 503K Followed by the Adsorption of Hydrogen at Ambient Temperature

Procedure	Copper surface area after treatment ($m^2\ g^{-1}$)	% Change
Catalyst reduced	27	-
Catalyst re-reduced, purged with helium for 10 minutes and carbon dioxide passed over the catalyst at 503K for 1½ hours then cooled in helium to ambient temperature and a stream of 2.5% hydrogen in nitrogen passed over the catalyst for 1 hour	21	-22
Catalyst re-reduced	25.5	-6

4.9.2 Adsorption of Hydrogen on Fully Oxidised $Cu/ZnO/Al_2O_3$

The same catalyst sample as that used in the study of the adsorption of carbon dioxide and hydrogen on $Cu/ZnO/Al_2O_3$ (Section 4.9.1) was used to study the adsorption of hydrogen on fully oxidised $Cu/ZnO/Al_2O_3$. After re-reduction, the catalyst was fully oxidised with nitrous oxide. During the oxidation process, the level of nitrous oxide and of nitrogen was measured by monitoring $^{m}/_{e}$ = 44 and $^{m}/_{e}$ = 28, respectively, on the mass spectrometer. The amount of nitrous oxide adsorbed by the catalyst was found to be $16cm^3$.

After purging with helium for 10 minutes, a stream of 2.5% hydrogen in nitrogen (flow rate = 50ml min^{-1}) was passed over the catalyst sample at ambient temperature for 20 minutes. During this period the levels of hydrogen and water in the outlet gas were measured by monitoring $^{m}/e = 2$ and $^{m}/e = 17$, respectively, on the mass spectrometer. The trace is shown in Figure 4.26. From this, it can be seen that, during treatment of the fully oxidised catalyst with hydrogen at ambient temperature, hydrogen was adsorbed by the catalyst after an induction period, but no water was produced. After treatment with hydrogen the inlet gas was switched to helium and the temperature ramped up to 503K at the rate of 16^{o} min^{-1}. During this time the outlet gas was monitored for hydrogen and water, respectively, on $^{m}/e = 2$ and $^{m}/e = 17$. The trace obtained is shown in Figure 4.27, from which, it can be seen that no hydrogen or water desorbed from the surface until 365K when the level of water in the exit stream began to rise above that in the inlet stream. After heating the sample under helium to 503K the copper surface area was re-determined and found to be $24m^2$ g^{-1}.

The adsorption of carbon monoxide on the same catalyst sample after full oxidation with nitrous oxide followed by treatment with hydrogen at ambient temperature for 40 minutes and a helium purge for 10 minutes was studied using the same experimental procedure as that used above, except that after treatment with hydrogen (flow rate = 66ml min^{-1}) and purging with helium, the gas was switched to carbon monoxide in

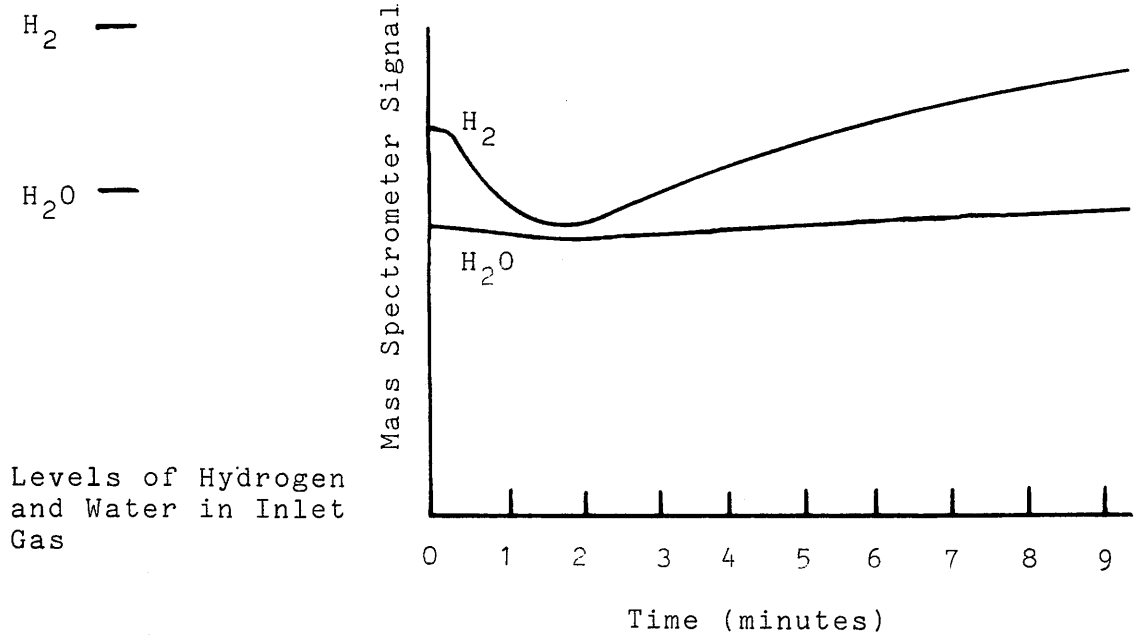

Figure 4.26 Adsorption of Hydrogen on Fully Oxidised $Cu/ZnO/Al_2O_3$ at Ambient Temperature - Levels of Hydrogen and Water in Outlet Gas.

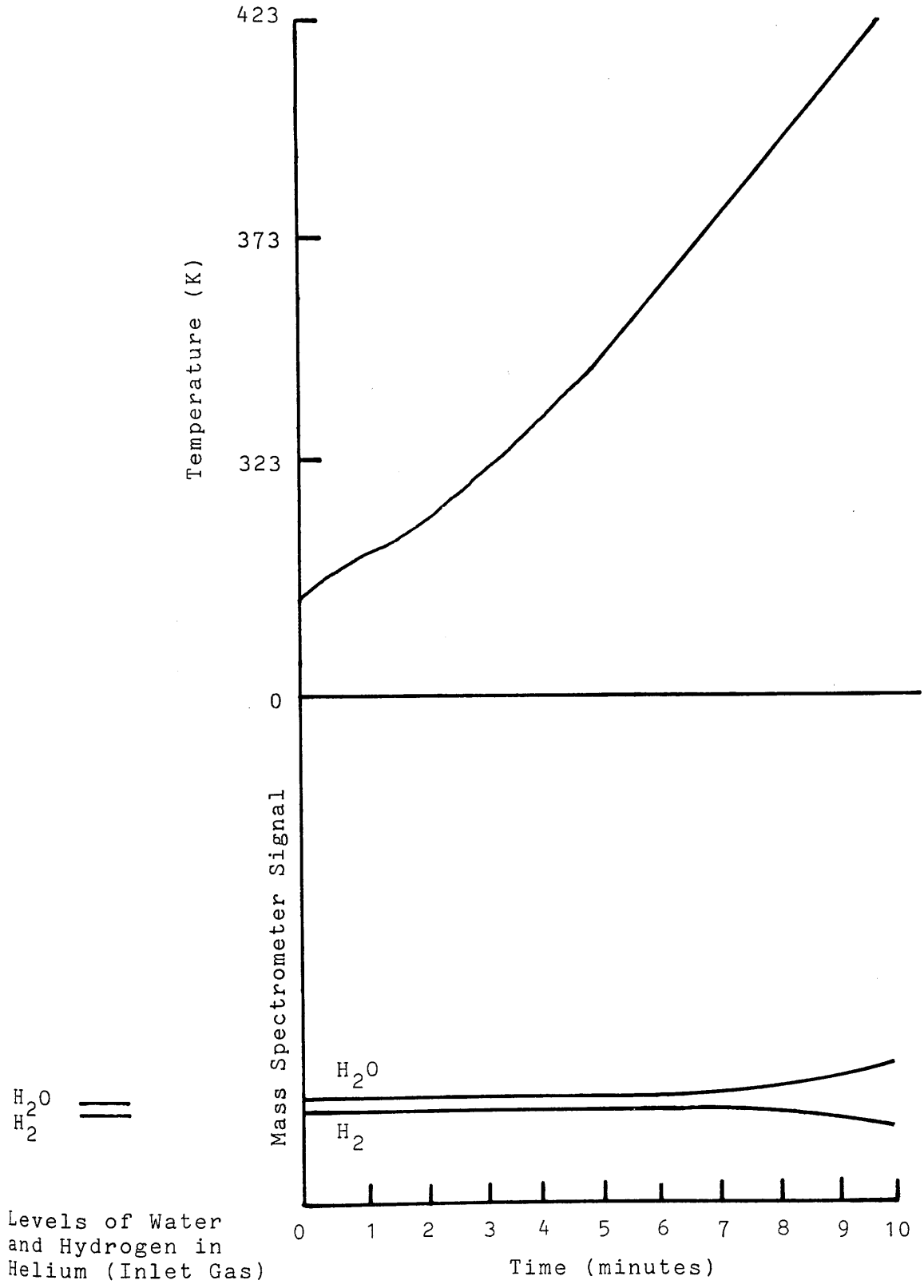

Figure 4.27 Thermal Desorption Spectrum of Hydrogen on Fully Oxidised $Cu/ZnO/Al_2O_3$.

helium and argon (11/80/9) at ambient temperature for 1 hour. As with the results reported in the previous experiment, after an induction period, hydrogen was adsorbed by the catalyst ($8cm^3$), as determined via the mass spectrometer. During treatment of the catalyst with carbon monoxide, the mass spectrometer measured the levels of carbon monoxide, carbon dioxide, hydrogen and water in the exit gas on $^{m}/e$ = 14, $^{m}/e$ = 22, $^{m}/e$ = 2 and $^{m}/e$ = 17, respectively. The trace shown in Figure 4.28, shows that carbon monoxide was adsorbed by the catalyst immediately ($10cm^3$) causing a desorption of hydrogen from the surface ($0.5cm^3$). No carbon dioxide was produced during this process. After treatment of the oxidised catalyst with hydrogen and carbon monoxide, the copper surface area was determined using nitrous oxide. The results are shown in Table 4.20.

Table 4.20 Adsorption of Hydrogen Followed by the Adsorption of Carbon Monoxide on Fully Oxidised $Cu/ZnO/Al_2O_3$ at Ambient Temperature

Procedure	Copper surface area after treatment ($m^2\ g^{-1}$)	% Change
Catalyst reduced	24	-
Hydrogen passed over the oxidised catalyst at ambient temperature for 40 minutes and purged with helium for 10 minutes, then carbon monoxide in helium and argon passed over the catalyst for 1 hour.	8.2	-66

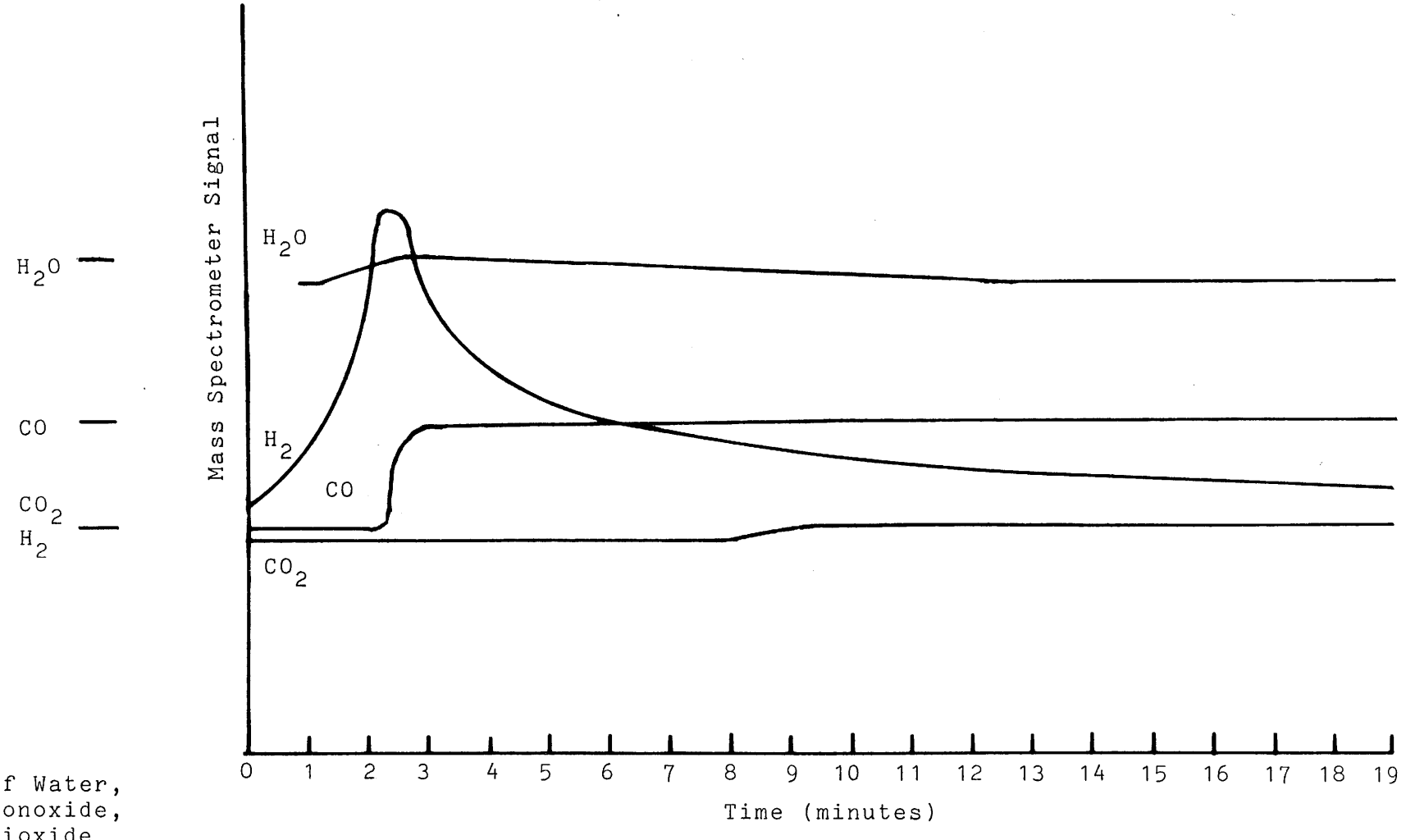

Figure 4.28 Adsorption of Carbon Monoxide on Fully Oxidised $Cu/ZnO/Al_2O_3$ After Treatment with Hydrogen at Ambient Temperature - Levels of Water, Carbon Monoxide, Carbon Dioxide and Hydrogen in Outlet Gas.

The copper surface area of a $Cu/ZnO/Al_2O_3$ catalyst after full oxidation and treatment with hydrogen at ambient temperature, was investigated using a fresh sample of catalyst and the same experimental procedure as described in the previous experiment, excluding treatment with carbon monoxide in helium and argon (11/80/9) for 1 hour at ambient temperature. The results are summarised in Table 4.21. The amount of hydrogen adsorbed by the oxidised catalyst at ambient temperature was measured using mass spectrometry and found to be $10cm^3$. During treatment of the catalyst with nitrous oxide (flow rate = 55ml min^{-1}) at ambient temperature (after full oxidation, treatment with hydrogen and a helium purge for 10 minutes) the levels of nitrous oxide, nitrogen, hydrogen and water were measured by monitoring $^m/_e = 44$, $^m/_e = 28$, $^m/_e = 2$ and $^m/_e = 17$ respectively, on the mass spectrometer. The trace is shown in Figure 4.29. From this, it can be seen that, nitrous oxide was adsorbed by the catalyst and nitrogen released in the exit gas, however, hydrogen ($3cm^3$) was also desorbed from the catalyst during this process. The level of water in the exit stream did not rise above that in the inlet stream.

Table 4.21 Adsorption of Hydrogen on Fully Oxidised $Cu/ZnO/Al_2O_3$ at Ambient Temperature

Procedure	Copper surface area after treatment ($m^2\ g^{-1}$)	% Change
Catalyst reduced	29.6	
Hydrogen passed over oxidised catalyst for 40 minutes followed by a helium purge for 10 minutes	20	-32

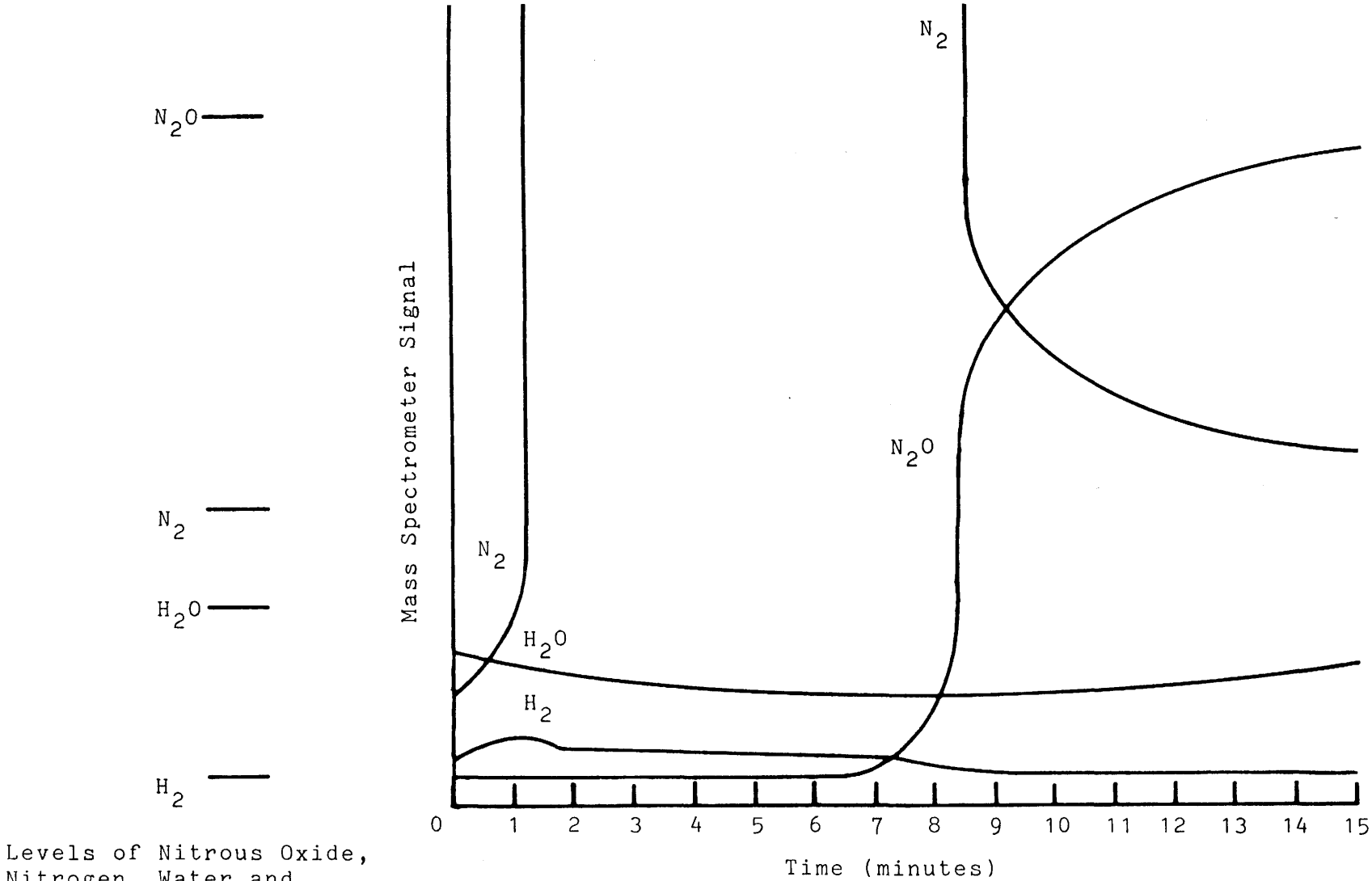

Figure 4.29 Adsorption of Nitrous Oxide on Fully Oxidised $Cu/ZnO/Al_2O_3$ After Treatment with Hydrogen at Ambient Temperature - Levels of Nitrous Oxide, Nitrogen, Water and Hydrogen in Outlet Gas.

CHAPTER FIVE

5. DISCUSSION

The results presented in chapter four show a number of interesting differences between the adsorption of carbon dioxide and the adsorption of carbon monoxide on each of the catalysts used. Whilst the direct monitoring technique as used in the present study, did not permit an absolute comparison of the amounts of the adsorbed species from sample to sample because of minor differences in the counting geometry between different samples, multiple determinations on similar weights of different catalyst samples, indicated an overall variation of ± 10.6%. Nevertheless it is possible, particularly in view of the gross differences in behaviour between the various systems, to draw important conclusions regarding the nature of the adsorbed states of carbon dioxide and carbon monoxide on the $Cu/ZnO/Al_2O_3$ catalyst and its components.

The relative amounts of carbon dioxide and carbon monoxide adsorbed on the various catalysts were investigated by comparison of the surface count rates, standardised to a specific activity of 0.130 mCi $mmol^{-1}$, obtained from the appropriate adsorption isotherms at an arbitrarily chosen gas pressure of 1.50 torr. This particular gas pressure was chosen because it corresponded to the plateau region in the carbon monoxide isotherms and the reduced gradient region in the carbon dioxide isotherms.

5.1 The Adsorption of Carbon Dioxide and Carbon Monoxide on Cu/Al_2O_3

The nature of the sites responsible for the adsorption and subsequent reaction of carbon dioxide and carbon monoxide on $Cu/ZnO/Al_2O_3$ was investigated by probing, initially, the less complex Cu/Al_2O_3 system. Both carbon dioxide and carbon monoxide were found to adsorb on Cu/Al_2O_3 although, under the conditions used in the present study, Al_2O_3 alone adsorbed only carbon dioxide. From the isotherms in Figure 4.12(a), it can be seen that, the adsorption of [14-C]carbon dioxide on Cu/Al_2O_3 exhibits a region of rapid increase in surface concentration with increasing gas pressure followed by a slow increase in concentration of adsorbed species as further aliquots of [14-C]carbon dioxide were admitted to the reaction vessel. Similar results have been reported for carbon dioxide adsorption on various supported palladium (75) and Rh/Al_2O_3 (106) catalysts.

In contrast with [14-C]carbon dioxide, the adsorption isotherms for [14-C]carbon monoxide on Cu/Al_2O_3 (Figure 4.12(b)) show a rapid increase in surface concentration with increasing gas pressure until a plateau is reached. This is the expected behaviour for carbon monoxide adsorption on a metal and similar results have been reported for carbon monoxide adsorption on some Cu/ZnO binary catalysts (62).

From Figures 4.12(a) and 4.12(b), the surface count rates after adsorption of [14-C]carbon dioxide and [14-C]carbon monoxide on Cu/Al_2O_3 at 1.50 torr gas pressure, when

standardised to a specific activity of 0.130 mCi $mmol^{-1}$, were 1740 cpm (0.1714 g) and 3460 cpm (0.1865 g) respectively. Bearing in mind the slightly different weights of catalyst used, approximately twice as much carbon monoxide is adsorbed on Cu/Al_2O_3 as carbon dioxide.

The results from the evacuation experiments (Tables 4.10(a) and 4.10(b)) indicate that a larger fraction of carbon dioxide is strongly adsorbed on Cu/Al_2O_3 than is the case with carbon monoxide, where 90% of the adsorbed material can be evacuated over a period of 10 minutes.

5.2 The Adsorption of Carbon Dioxide and Carbon Monoxide on Reduced $Cu/ZnO/Al_2O_3$

The isotherms for the adsorption of [14-C]carbon dioxide on reduced $Cu/ZnO/Al_2O_3$ (Figure 4.1) are not similar to those observed during the adsorption of this gas on Cu/Al_2O_3 (Section 5.1) where, initially, there is a less rapid increase in concentration of adsorbed species.

Carbon dioxide adsorbs on each of the components of the catalyst. The amounts adsorbed on the various adsorbents studied are summarised in Table 5.1.

Table 5.1 Amount of Carbon Dioxide Adsorbed on Each Adsorbent

Adsorbent	Weight (g)	BET area ($m^2\ g^{-1}$)	Surface count rate* (cpm)
$Cu/ZnO/Al_2O_3$ (60/30/10)	0.2078	67.8	3670
ZnO - A	0.2179	50.2	4853
ZnO - B	0.1979	5.1	723
Al_2O_3	0.1827	308	2484

*These figures were obtained from the appropriate isotherms, at a gas pressure of 1.50 torr and standardised to a specific activity of 0.130 mCi $mmol^{-1}$, the figure for $Cu/ZnO/Al_2O_3$ was taken from isotherm 1 in Figure 4.3.

The percentage of carbon dioxide adsorbed on each component of the catalyst is 53% (copper), 40% (ZnO) and 7% (Al_2O_3). These are obtained by assuming that the BET areas of the individual components of the catalyst, ZnO and Al_2O_3 are the same, respectively, as the ZnO - A and Al_2O_3 catalysts.

The adsorption isotherms for the adsorption of [14-C] carbon dioxide on the individual components of the catalyst, ZnO - A (Figure 4.13(a)), ZnO - B (isotherm 1 in Figure 4.16) and Al_2O_3 (Figure 4.17) are different in shape to those on reduced $Cu/ZnO/Al_2O_3$ (Figure 4.1) in that, in general, the initial sharp rise in concentration of adsorbed species is not present.

Although carbon dioxide adsorbs to a large extent on the copper component of the catalyst, very little evidence

for the adsorption of carbon dioxide on clean copper surfaces is available in the literature. It is likely that residual surface oxygen, left after the reduction procedure (107), enhances the adsorption of carbon dioxide on the copper component. This is in agreement with Stone and Tiley (81) who reported that no appreciable amount of carbon dioxide was adsorbed by a baked-out copper surface. However, after oxygen had been preadsorbed, carbon dioxide was adsorbed immediately.

The adsorption of carbon dioxide on Al_2O_3 is in agreement with results obtained by Solymosi et al. (75) who reported the presence of carbonate bands during the adsorption at 300 - 400K.

By comparison of the results for the evacuation and molecular exchange experiments for carbon dioxide adsorbed on each of the catalysts (Table 5.2) the relative strengths of adsorption of carbon dioxide on each of the catalyst components can be deduced. The molecular exchange results, quoted in Table 5.2, have been corrected for the slow adsorption of [14-C]carbon dioxide using data from Figures 4.5, 4.14 and 4.18, assuming that [12-C]carbon dioxide has no effect on this process.

From Table 5.2, it can be seen that, carbon dioxide exists in both a relatively strongly adsorbed and a relatively weakly adsorbed state on both ZnO and Al_2O_3 components of the catalyst. It is proposed that, in agreement with similar studies of carbon dioxide adsorbed on ZnO (15) and Al_2O_3 (75), the relatively strongly bound species is a carbonate species.

Table 5.2 Summary Table of the Effects of Evacuation and Molecular Exchange (without evacuation) on Carbon Dioxide Adsorbed on the Catalysts

Catalyst	% Evacuated (after 10 minutes)	% Exchanged with [12-C]Carbon Dioxide (after 10 minutes)	(after 12 hours)
$Cu/ZnO/Al_2O_3$	33.6	15	44.4
Cu/Al_2O_3	44.4	-	-
ZnO - A	40.5	60.2	68
ZnO - B	50.0	-	-
Al_2O_3	38.1	14.2	38.2

It is concluded from studies of the adsorption of [14-C]carbon dioxide on reduced $Cu/ZnO/Al_2O_3$, Cu/Al_2O_3, ZnO - A and Al_2O_3 that these processes involve two stages; a fast initial adsorption followed by a slow adsorption or subsequent reaction on the catalyst surface. To check if this slow adsorption, recorded by both the pressure transducer and the G.-M. tubes, is due to pore diffusion, which may be more evident for carbon dioxide than carbon monoxide due to the greater molecular size of the former, the maximum distance travelled by β^- particles emitted from [14]-Carbon in Al_2O_3 is deduced as follows.

E_{max} (for β^- emitted from [14]-Carbon) = 0.156M eV

Range in aluminium = $0.028g\ cm^{2}$ (108)

Distance travelled in aluminium = $\frac{\text{Range}}{\rho} = \frac{0.028g\ cm^{-2}}{2.6798g\ cm^{-2}}$

$= 0.0104cm$

Distance travelled in Al_2O_3 = $\frac{\rho(Al)}{\rho(Al_2O_3)} \times 0.0104cm$

$= 0.104 \times \frac{2.679}{3.970} cm$

$= 7.05 \times 10^{-3} cm$

Minimum particle diameter of catalyst (100 BSS mesh)

$= 150 \times 10^{-6} m$

$= 15 \times 10^{-3} cm$

Therefore, since the maximum distance a β^- particle, emitted from [14]-Carbon, can travel in Al_2O_3, is less than half the diameter of the smallest particle, assuming that the particles are spherical, the slow adsorption process as detected by the G.-M. tubes, cannot be due to pore diffusion. Consequently, the pressure decrease monitored by the pressure transducer is not due to pore diffusion since it correlates with the increase in surface count rate.

The slow adsorption of carbon dioxide on reduced $Cu/ZnO/Al_2O_3$ must occur, at least in part, on the ZnO and Al_2O_3 components since a slow adsorption of [14-C]carbon dioxide was recorded with both ZnO - A and Al_2O_3. In order to estimate the contribution of the individual components to the slow adsorption process, the following calculation has been performed using data from Figures 4.5, 4.14 and 4.18.

Catalyst	Surface count rate (after 4 hours)	Surface count rate (after 24 hours)	% Change
Al_2O_3	1780 cpm	2080 cpm	+ 16.8
ZnO - A	1550 cpm	1670 cpm	+ 7.7
$Cu/ZnO/Al_2O_3$	3350 cpm	4700 cpm	+ 40.3

As discussed earlier, the fraction of carbon dioxide adsorbed on each component is 53%, 40% and 7% for copper, ZnO and Al_2O_3 respectively, therefore, after 4 hours the surface count rate on each component of the $Cu/ZnO/Al_2O_3$ catalyst will be 1775 cpm, 1340 cpm and 235 cpm respectively. Taking into account the predicted increases in surface count rates for the ZnO - A and Al_2O_3 catalysts, quoted above, and assuming these are the same as the ZnO and Al_2O_3 components of the catalyst, the increase in surface count rate on the copper component is deduced as follows.

$$[1775 + (\frac{x}{100} \times 1775)] + [1340 + (\frac{7.7}{100} \times 1340)] + [235 + (\frac{16.8}{100} \times 235)] = 4700$$

$$x = 68$$

Therefore the percentage increase in adsorption of carbon dioxide on each of the components is 68%, 7.7% and 16.8% respectively, for copper, ZnO and Al_2O_3.

Considering first the slow adsorption of carbon dioxide on ZnO - A and Al_2O_3, the results from the evacuation experiments after adsorption of [14-C]carbon dioxide over a period of 4 hours and 25 hours on ZnO - A and over a period

of 4 hours and 23 hours on Al_2O_3 (Table 5.3), indicate that, the adsorption of carbon dioxide over a long time period leads, in both cases, to a more strongly bound species. It is proposed that the slow adsorption of carbon dioxide on these components is carbonate formation which, as postulated earlier, would be irreversible at ambient temperature. This result is in agreement with Bowker et al (15) who concluded that the formation of carbonates from the adsorption of carbon dioxide on ZnO is an activated process.

Table 5.3 Summary Table of the Effects of Evacuation on Carbon Dioxide Adsorbed on ZnO - A and Al_2O_3

Catalyst	% Evacuated after [14-C]carbon dioxide adsorbed over a short time period	% Evacuated after [14-C]carbon Dioxide adsorbed over a long time period
ZnO - A	40	28
Al_2O_3	38	18

However, the slow adsorption of carbon dioxide on the surface of the catalyst, takes place predominantly on the copper component. One of the reactions occurring on this component is the dissociation of carbon dioxide to carbon monoxide and surface oxygen, since traces of carbon monoxide are detected in the gas phase after 24 hours, during the adsorption of carbon dioxide on reduced $Cu/ZnO/Al_2O_3$. The dissociation of carbon dioxide on

Cu (110) has been reported by Wachs and Madix (79) who found that 99% of carbon dioxide adsorbed, dissociated to give carbon monoxide.

As the energy involved in breaking the carbon/oxygen bond in the carbon dioxide molecule is relatively large, 127 kcal mol^{-1}, the dissociation is likely to occur at high energy, corner, ledge or kink sites where a greater surplus of free energy is extant. The relative number of these sites is small and since these high energy sites will be occupied first during the adsorption process, the increase in surface radioactivity cannot be due to the dissociation but rather a subsequent reaction on the surface of the catalyst. The increase in radioactivity on the copper component is likely to be the reaction of carbon dioxide with O(a) from both the dissociation reaction and that left after the reduction process to form a carbonate species, as proposed earlier by Stone and Tiley (81). This is in agreement with isotope exchange studies by Chinchen and Jackson (107), who found that carbon dioxide exchanges with adsorbed oxygen on both $Cu/ZnO/Al_2O_3$ and Cu/Al_2O_3. Subsequently, since very little carbon monoxide is detected in the gas phase despite the large increase in surface radioactivity on the copper component, the carbon monoxide from the dissociation

$$CO_2(g) \rightleftharpoons CO_2(a) \rightleftharpoons CO(a)^* + O(a)$$

is different to that formed from the adsorption of carbon monoxide:- $CO(g) \rightleftharpoons CO(a)$

in that it is strongly adsorbed and perhaps multiply bonded to the surface. Evidence for multiply bonded carbon monoxide has been reported by Solymosi et al. (75). These authors concluded that, in the temperature range 300 - 473K, carbon dioxide adsorbs on a group of palladium atoms and dissociates to give multiply bonded carbon monoxide. In a study of the adsorption of carbon dioxide on Rh(111) and rhodium foil at 300K, the same authors (75) reported that no adsorption takes place on a clean surface, however, boron impurities induce the dissociation at this temperature.

It is proposed that, surface oxygen, which remains after the reduction process enhances the adsorption and dissociation of carbon dioxide on the copper component of the catalyst.

Further evidence for the dissociation of carbon dioxide on reduced $Cu/ZnO/Al_2O_3$ was obtained in the microreactor/ mass spectrometer system at 503K as reported in Section 4.9.1. From Figure 4.24 it can be seen that, when carbon dioxide is passed over reduced $Cu/ZnO/Al_2O_3$ at 503K, the production of carbon monoxide becomes constant. Therefore, at this temperature CO(a) desorbs from the surface as carbon monoxide. Subsequently, as adsorbed oxygen is produced in the process, in order to maintain a steady production of carbon monoxide this too must desorb from the surface or, more likely, be used up in a surface reaction. Evidence in support of the latter conclusion is obtained from studies of the adsorption of carbon monoxide on oxidised $Cu/ZnO/Al_2O_3$ in which carbon dioxide is produced. After adsorption of

carbon dioxide at 503K for $1\frac{1}{2}$ hours, 38% of the copper surface is covered with adsorbed oxygen as revealed by nitrous oxide.

The dissociation of carbon dioxide on the copper component of the catalyst explains the greater decrease in copper surface area, 51%, obtained after [14-C]carbon dioxide is adsorbed on reduced $Cu/ZnO/Al_2O_3$ and treated with helium at 463K compared to the decrease, 22%, recorded in the absence of carbon dioxide. The area loss in the latter case is most likely due to sintering of the copper. However, in the presence of [14-C]carbon dioxide, since treatment with helium removes all of the surface radioactivity, it is likely that O(a) from the dissociation is stable to the helium treatment and consequently, leads to an enhanced loss of copper area.

Both the dissociation and subsequent reaction of carbon dioxide, by the above arguments, will lead, after the slow adsorption process is complete, to a more strongly adsorbed species. This, unfortunately, cannot be confirmed from the results of molecular exchange experiments (Tables 4.3(a) and 4.4) since, as will be discussed later, the molecular exchange between adsorbed and gaseous carbon dioxide involves some sort of complex formation and may therefore, not be an accurate measure of the relative strength of adsorption.

The dissociation and subsequent reaction of carbon dioxide to form a carbonate species explains the unusual shape of isotherms 2 and 3 in Figure 4.3 compared to

isotherm 1. Aliquots of [14-C]carbon dioxide admitted during isotherms 2 and 3 do not encounter a reduced surface but one which is partially oxidised and has carbonate species adsorbed. Consequently, the amount of [14-C] labelled species which can be evacuated decreases from isotherms 1 to 3.

The isotherm for the adsorption of [14-C]carbon monoxide on 0.1569g $Cu/ZnO/Al_2O_3$ (curve 1 in Figure 4.6) is similar to the isotherms for the adsorption of [14-C] carbon monoxide on Cu/Al_2O_3 (Figure 4.12(b)). However, occasionally (curve 2 in Figure 4.6), the plateau region showed a slight positive gradient with increasing gas pressure. This behaviour, which has been observed with carbon monoxide on supported platinum catalysts (109, 110) is characteristic of catalysts which are not fully reduced. It is also characteristic of the adsorption of carbon monoxide on partially oxidised copper surfaces (111). Carbon monoxide is adsorbed relatively quickly (Figure 4.9) with no subsequent slow adsorption or reaction occurring on the catalyst.

In contrast with carbon dioxide, carbon monoxide is not adsorbed on unreduced $Cu/ZnO/Al_2O_3$ and therefore sites for carbon monoxide adsorption are located on the copper component, since no apparent change (reduction) takes place during the reduction of ZnO or Al_2O_3. This conclusion is supported by the fact that no carbon monoxide is adsorbed on either ZnO - B or Al_2O_3 and only a minimal amount is adsorbed on ZnO - A (688 cpm, 0.1890 g). These results are

in agreement with earlier studies by Waugh et al (58). The unusual shape of the isotherms for the adsorption of [14-C]carbon monoxide on ZnO - A (Figure 4.13(b)) suggest that more sites for carbon monoxide adsorption are created as each aliquot of [14-C]carbon monoxide is admitted to the reaction vessel.

The relative strength of adsorption of carbon monoxide on the various catalysts is summarised in Table 5.4.

Table 5.4 Summary Table of the Effects of Evacuation and Molecular Exchange (without evacuation) on Carbon Monoxide Adsorbed on the Catalysts

Catalyst	% Evacuated (after 10 minutes)	% Exchanged with [12-C]Carbon Monoxide (after 10 minutes)	(after 12 hours)
$Cu/ZnO/Al_2O_3$	82.1	40.2	37.6
Cu/Al_2O_3	90.3	-	-
ZnO - A	98.2	0	30.4
ZnO - B	N.A.	-	-
Al_2O_3	N.A.	-	-

From Table 5.4 it can be seen that, since carbon monoxide is reversibly adsorbed on ZnO - A, the copper component of the catalyst adsorbs this gas both reversibly and irreversibly at ambient temperature. Subsequently, irreversible adsorption of carbon monoxide is induced in $Cu/ZnO/Al_2O_3$ since less carbon monoxide is evacuated from this catalyst compared to Cu/Al_2O_3. This may be due to irreversible adsorption

of carbon monoxide on Cu^{I}/ZnO species as proposed by Parris and Klier (62). Alternatively, the differences in strength of adsorption of carbon monoxide may reflect the larger amount of residual surface oxygen after the reduction of $Cu/ZnO/Al_2O_3$, with the greater formation of carbonates via:-

$$CO(a) + O(a) \rightarrow CO_2(a) \xrightarrow{O(a)} CO_3^{2-}(a)$$

The results from the molecular exchange experiments , both with carbon monoxide and carbon dioxide, indicate that these processes are not straightforward displacements but involve complex formation or reaction between the adsorbed and gaseous species since, with exception of carbon monoxide on reduced $Cu/ZnO/Al_2O_3$, the exchange <u>increases</u> with time. Indeed, both with carbon dioxide and carbon monoxide adsorbed on reduced $Cu/ZnO/Al_2O_3$, after evacuation, the relatively strongly held species are capable of molecular exchange (Tables 4.3(b) and 4.6(b)).

Carbon dioxide and carbon monoxide are adsorbed on reduced $Cu/ZnO/Al_2O_3$ in approximately the same amounts [3670 cpm (0.2078 g) and 3807 cpm (0.1747 g) (from the isotherm for the molecular exchange experiment reported in Table 4.6(a)),respectively]. This is in sharp contrast to the ratio of carbon dioxide:carbon monoxide (1:2) adsorbed on Cu/Al_2O_3. Subsequently, this is further evidence that carbon dioxide adsorbs on ZnO but relatively little carbon monoxide is adsorbed by this component of the catalyst. Carbon dioxide is more strongly adsorbed on $Cu/ZnO/Al_2O_3$ than carbon monoxide. This is in agreement with Klier et

al. (63) who reported that carbon dioxide is relatively strongly adsorbed on Cu/ZnO and estimated the adsorption strength of carbon dioxide to be greater than that of carbon monoxide.

The isotherms presented in Figures 4.15(a) and 4.15(b) suggest that carbon dioxide adsorbed on ZnO - A does not prevent the adsorption of carbon monoxide and vice versa. However, as the slow adsorption of [14-C]carbon dioxide will be registered during the adsorption of [14-C]carbon monoxide the results presented in Figure 4.15(a) are misleading. The slow adsorption of [14-C]carbon dioxide accounts for the unusual shape of the isotherm for [14-C]carbon monoxide in this figure, since the Geiger-Müller tube cannot distinguish between the two species.

More quantitative information regarding competition between the adsorbates on ZnO - A is obtained from the results presented in Tables 4.13(a) and 4.13(b). From Table 4.13(a), the increase in surface count rate, 1% after 10 minutes and 27% after 12 hours for the exchange between adsorbed [14-C]carbon dioxide and gas phase [12-C]carbon monoxide, is similar to that predicted for the slow adsorption of [14-C]carbon dioxide in the absence of carbon monoxide, 6% and 19% respectively (from Figure 4.14). Therefore no exchange between adsorbed carbon dioxide and gas phase carbon monoxide takes place on ZnO - A. In sharp contrast, the results presented in Table 4.13(b) show that carbon monoxide adsorbed on ZnO - A is immediately, totally displaced by carbon dioxide in the gas phase. It is

concluded that, carbon dioxide and carbon monoxide compete for sites on the ZnO component of $Cu/ZnO/Al_2O_3$. However, carbon dioxide is more strongly and consequently, preferentially adsorbed.

As with the adsorption of [14-C]carbon dioxide followed by [14-C]carbon monoxide and vice versa on ZnO - A, Figures 4.10(a) and 4.10(b) show that the adsorption of one species on reduced $Cu/ZnO/Al_2O_3$ does not prevent the adsorption of the other. However, Figure 4.10(a) is somewhat misleading as the slow adsorption of [14-C]carbon dioxide is measured during the adsorption of [14-C]carbon monoxide and this accounts for the change in shape of the [14-C]carbon monoxide isotherm.

From Table 4.7, it can be seen that during the exchange between adsorbed [14-C]carbon dioxide and gas phase [12-C] carbon monoxide the increase in surface count rate, 35.5% after 10 minutes, is greater than that predicted (1.4%) from the slow adsorption of carbon dioxide. Therefore carbon monoxide must create sites on the copper component for further carbon dioxide adsorption, since no similar increase is recorded on ZnO - A. This is consistent with the proposal that carbon monoxide titrates residual surface oxygen, present after the reduction process and from the dissociation of carbon dioxide, to form carbon dioxide:-

$$Cu_2^{I}O + CO(a) \longrightarrow CO_2(g) + 2Cu^{o}$$

This leads to the conclusion that carbon dioxide must adsorb on reduced copper. It is important to point out that the

increase in surface radioactivity may disguise any exchange between the two species, although a similar exchange carried out after carbon dioxide had attained surface equilibrium (Table 4.8), indicated a negligible amount of exchange. Table 4.9 shows that the exchange between adsorbed carbon monoxide and gas phase carbon dioxide increases with time, consequently, carbon dioxide has the slightly higher heat of adsorption on copper.

The amount of carbon dioxide adsorbed on reduced $Cu/ZnO/Al_2O_3$, 3670 cpm (0.2083 g) appears to be unaffected by the presence of carbon monoxide 3781 cpm (0.1943 g). It is important to note however, that the process:-

$$CO(a) + O(a) \longrightarrow CO_2(g)$$

which as shown above, creates sites for further carbon dioxide adsorption, may disguise any site blockage by CO(a). In sharp contrast, the amount of [14-C]carbon monoxide adsorbed on reduced $Cu/ZnO/Al_2O_3$, 3807 cpm (0.1747 g), is reduced in the presence of carbon dioxide, 2791 cpm (0.2137g). These results provide further evidence that carbon dioxide is preferentially adsorbed to carbon monoxide on $Cu/ZnO/Al_2O_3$. The adsorption of carbon dioxide and carbon monoxide on reduced $Cu/ZnO/Al_2O_3$ is summarised below.

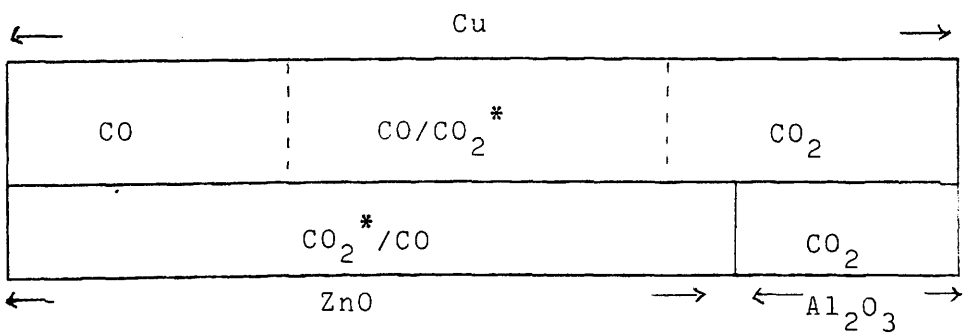

*preferentially adsorbed.

The decrease in pressure recorded during the adsorption of hydrogen on reduced $Cu/ZnO/Al_2O_3$, 0.44 torr, indicates a slow adsorption and/or reaction on the catalyst surface. This process cannot be due to pore diffusion since, as is discussed later, it is affected by the presence of surface oxygen. Hydrogen does not affect the amount of carbon dioxide or carbon monoxide adsorbed on reduced $Cu/ZnO/Al_2O_3$ although the amount of carbon dioxide which is evacuated in the presence of hydrogen, 23%, is less than in its absence (33%). The enhanced strength of adsorption of carbon dioxide in the presence of hydrogen must occur, at least in part, on the ZnO component, since similar results have been obtained on this catalyst.

5.3 The Adsorption of Carbon Dioxide and Carbon Monoxide on Partially Oxidised and Fully Oxidised $Cu/ZnO/Al_2O_3$

Studies of the adsorption of carbon dioxide on fully oxidised $Cu/ZnO/Al_2O_3$ reveal that, adsorption takes place, initially, on the support, the adsorption on fully oxidised copper being a slow process. Table 5.5 shows that, compared to reduced $Cu/ZnO/Al_2O_3$, a 60% decrease in carbon dioxide adsorbed is recorded when the catalyst is fully oxidised with nitrous oxide. This corresponds, within experimental error to that portion, 53% (Section 5.2), which is adsorbed on the copper component. Further evidence that full oxidation prevents the adsorption of carbon dioxide on the copper component is obtained by comparison of Figures

4.19(a) and 5.1. Figure 5.1 shows the isotherm obtained by combining the isotherms for the adsorption of [14-C]carbon dioxide on ZnO - A (Figure 4.13(a)) and Al_2O_3 (Figure 4.17), accounting for the proportion of each of these components in the catalyst. To facilitate the comparison, the isotherm in Figure 5.1 has been standardised to the same specific activity as that in Figure 4.19(a). It can be seen from these figures that the isotherm for the adsorption of [14-C]carbon dioxide on fully oxidised $Cu/ZnO/Al_2O_3$ is very similar to the resultant isotherm for the adsorption of [14-C]carbon dioxide on ZnO - A and Al_2O_3.

Table 5.5 Amounts of and Effects of Evacuation on Carbon Dioxide Adsorbed on Fully Oxidised, Partially Oxidised and Reduced $Cu/ZnO/Al_2O_3$

Catalyst	Weight (g)	Surface count rate (cpm)	% Evacuated (after 10 minutes)
Fully Oxidised $Cu/ZnO/Al_2O_3$	0.2203	1457	+ 26.5
Partially Oxidised $Cu/ZnO/Al_2O_3$	0.2141	4277	- 8.0
Reduced $Cu/ZnO/Al_2O_3$	0.2078	3670	- 33.6

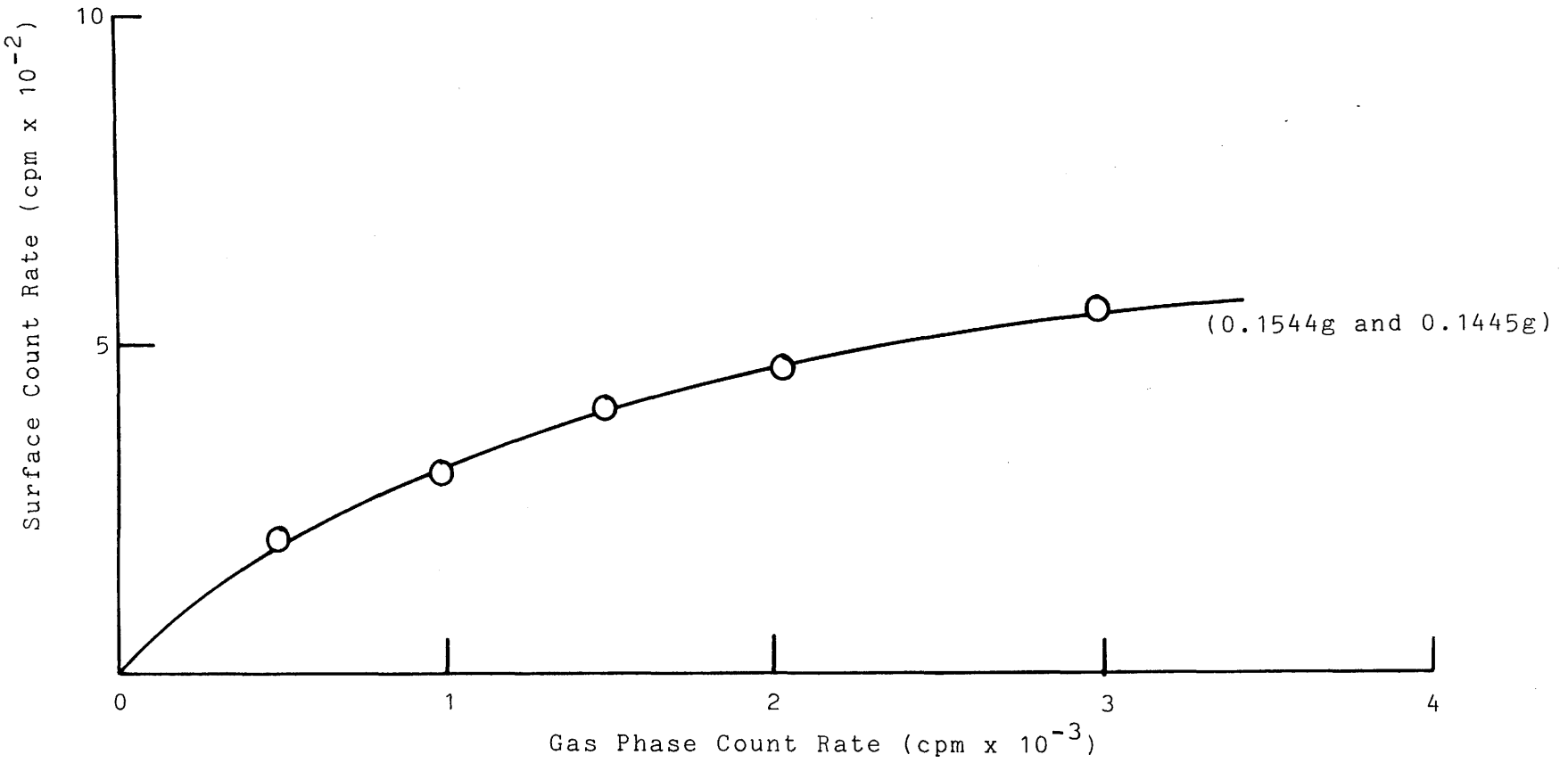

Figure 5.1. Resultant Isotherm for the Adsorption of [14-C]Carbon Dioxide (sp. acty = 0.066 mCi $mmol^{-1}$) on ZnO - A and Al_2O_3.

From Figure 4.21(a), it is deduced, when carbon dioxide is adsorbed on fully oxidised $Cu/ZnO/Al_2O_3$, assuming that the oxidation process does not affect the adsorption of carbon dioxide on the support, that after 24 hours, of the total amount of carbon dioxide adsorbed, 20% is adsorbed on the copper, 67% on the ZnO and 13% on the Al_2O_3. Therefore, the adsorption of carbon dioxide on fully oxidised copper is a very slow process, which is likely to involve the reaction between carbon dioxide and adsorbed oxygen atoms to form carbonate species. From Table 5.5 it can be seen that, the amount of carbon dioxide adsorbed on partially oxidised $Cu/ZnO/Al_2O_3$ is similar to that on reduced $Cu/ZnO/Al_2O_3$. It is likely therefore that, as discussed previously, the reduced catalyst harbours residual surface oxygen. Table 5.5 shows that, as the catalyst becomes more oxidised, more surface species are retained. Indeed it would appear that surface oxygen on the copper component affects the adsorption of carbon dioxide on the support, perhaps at the Cu^I - ZnO interface.

The adsorption of [14-C]carbon monoxide on oxidised $Cu/ZnO/Al_2O_3$ is observed to be different to that on reduced $Cu/ZnO/Al_2O_3$ in that, not surprisingly, carbon dioxide is detected in the gas phase. This presumably accounts for the absence of a plateau region for the adsorption on both partially oxidised $Cu/ZnO/Al_2O_3$ (Figure 4.22(b)) and fully oxidised $Cu/ZnO/Al_2O_3$ (Figure 4.19(b)). The adsorption of carbon monoxide on fully oxidised $Cu/ZnO/Al_2O_3$ (Figure 4.19 (b)) follows an induction period which is reflected in the

shape of the isotherm showing initially, a relatively slow rate of increase in surface radioactivity with increasing gas pressure. As with the adsorption of [14-C]carbon dioxide on fully oxidised $Cu/ZnO/Al_2O_3$ (Figure 4.19(a)) this is likely to be caused by steric hinderance by the adsorbed oxygen atoms.

The amounts and the effects of evacuation on carbon monoxide adsorbed on fully oxidised, partially oxidised and reduced $Cu/ZnO/Al_2O_3$ are summarised in Table 5.6.

Table 5.6 Amounts of and Effects of Evacuation on Carbon Monoxide Adsorbed on Fully Oxidised, Partially Oxidised and Reduced $Cu/ZnO/Al_2O_3$

Catalyst	Weight (g)	Surface count rate (cpm)	% Evacuated (after 10 minutes)
Fully Oxidised $Cu/ZnO/Al_2O_3$	0.2027	5334	- 33.3
Partially Oxidised $Cu/ZnO/Al_2O_3$	0.2115	5603	- 45.3
Reduced $Cu/ZnO/Al_2O_3$	0.1747	3807	- 82.1

The enhanced adsorption of carbon monoxide on oxidised $Cu/ZnO/Al_2O_3$ is likely to be a direct result of the formation and subsequent adsorption of carbon dioxide, formed as a result of the titration of surface oxygen by carbon monoxide. Indeed the amount of adsorbed species which can be evacuated from the surface of the oxidised catalysts reflects the amount

of carbon dioxide produced in each case.

In contrast with reduced $Cu/ZnO/Al_2O_3$, carbon monoxide slowly adsorbs on oxidised $Cu/ZnO/Al_2O_3$. Figure 4.21(b) shows that, during the adsorption of [14- C]carbon monoxide on fully oxidised $Cu/ZnO/Al_2O_3$, equilibrium is not attained until after 10 hours. This slow adsorption is due to the formation and subsequent adsorption of carbon dioxide on the catalyst. Presumably some surface oxygen is relatively unreactive towards carbon monoxide and this accounts, in part, for the slow adsorption of the latter. The formation of carbon dioxide during the adsorption of [14-C]carbon monoxide on fully oxidised $Cu/ZnO/Al_2O_3$ over a long time period is reflected by the amount which is adsorbed on the surface after 10 hours, 7992 cpm (0.2370 g) and the amount which is evacuated, 25%.

5.3.1 The Effects of Hydrogen on the Adsorption of Carbon Dioxide and Carbon Monoxide on Partially Oxidised and Fully Oxidised $Cu/ZnO/Al_2O_3$

The pressure decrease recorded during the adsorption of hydrogen on partially oxidised - and to a lesser extent on fully oxidised - $Cu/ZnO/Al_2O_3$ indicates that a slow adsorption/ reaction takes place on the catalyst surface. Further information regarding the nature of this adsorption is obtained from the microreactor/mass spectrometer studies. The adsorption of hydrogen on fully oxidised (from nitrous oxide) $Cu/ZnO/Al_2O_3$ (Figure 4.26), in the microreactor system, indicates that, after an induction period, hydrogen

is adsorbed but no water is produced. The amount of hydrogen adsorbed varies slightly ($8cm^3$ and $10cm^3$) but is approximately half that of nitrous oxide adsorbed ($16cm^3$), therefore the relationship between surface copper, oxygen and hydrogen atoms is:

$$2Cu : 1O(a) : 1H(a)$$

As a result of the observations below it is concluded that hydrogen adsorbs at Cu^o - Cu^+ sites to produce surface hydroxyl groups:-

$$H_2(g) \longrightarrow H_2(a) \xrightarrow{O(a)} OH(a) + H(a) \qquad (1)$$

(i) Treatment of a fully oxidised catalyst with hydrogen at ambient temperature results in a 68% regeneration of the copper surface area.

(ii) During the adsorption of nitrous oxide on a fully oxidised catalyst in the presence of hydrogen at ambient temperature, a small amount of hydrogen is desorbed from the surface (Figure 4.29). Similar effects are obtained with carbon monoxide (Figure 4.28).

(iii) The thermal desorption spectrum of hydrogen adsorbed on a fully oxidised catalyst (Figure 4.27) shows that, no water is produced until 365K.

(iv) Assuming that O(a) from carbon dioxide is similar to that from nitrous oxide then, in comparison with a fully oxidised catalyst, no induction period is observed with and less hydrogen is adsorbed by a partially oxidised catalyst.

The formation of surface hydroxyl groups on partially

oxidised polycrystalline copper foil at 383K (112) and partially oxidised $Cu/ZnO/Al_2O_3$ at 295K (86) has been reported in the literature.

The hydrogen atoms produced in reaction (1) are likely to be associated with the copper component of the catalyst and are displaced upon admission of nitrous oxide or carbon monoxide. These hydrogen atoms are probably mobile and desorb from the surface during the adsorption of hydrogen. This is concluded since only a small amount of hydrogen is displaced by nitrous oxide or carbon monoxide and the ratio of hydrogen to nitrous oxide adsorbed by the catalyst is ca. 1:2

These results are in agreement with Packer et al. (113) who reported the formation of H(a) on the copper metal phase of a $Cu/ZnO/Al_2O_3$ catalyst by n.m.r. experiments. This species disappeared when hydrogen was pumped from the catalyst.

The isotherm for the adsorption of [14-C]carbon dioxide on fully oxidised $Cu/ZnO/Al_2O_3$ in the presence of hydrogen (Figure 4.20(a)) is comparable to that in the absence of hydrogen (Figure 4.19(a)). Indeed the amounts adsorbed, 1467 cpm (0.1956 g) and 1457 cpm (0.2203 g) respectively, are similar in each case. Since some copper surface area is regenerated upon addition of hydrogen to the fully oxidised catalyst this suggests that carbon dioxide requires an ensemble of copper atoms for adsorption to occur.

In sharp contrast to the behaviour observed with fully oxidised $Cu/ZnO/Al_2O_3$, the presence of hydrogen results in an increase in the amount of carbon dioxide adsorbed on partially

oxidised $Cu/ZnO/Al_2O_3$ [6814 cpm (0.2518 g) cf. 4277 cpm (0.2141 g)] although the amount which is evacuated is similar in each case. This may be interpreted by considering that carbon dioxide forms a complex with surface hydroxyl groups on the copper component, such that the complex requires fewer sites for adsorption than carbon dioxide itself. If carbon dioxide merely adsorbs on the copper sites which are not bonded to surface hydroxyls then the amount which is evacuated would not be comparable to that for the adsorption of [14-C]carbon dioxide on partially oxidised $Cu/ZnO/Al_2O_3$ where the formation of carbonate is proposed.

The proposed mechanism for the formation of a surface complex between adsorbed carbon dioxide and hydroxyl groups is as follows:-

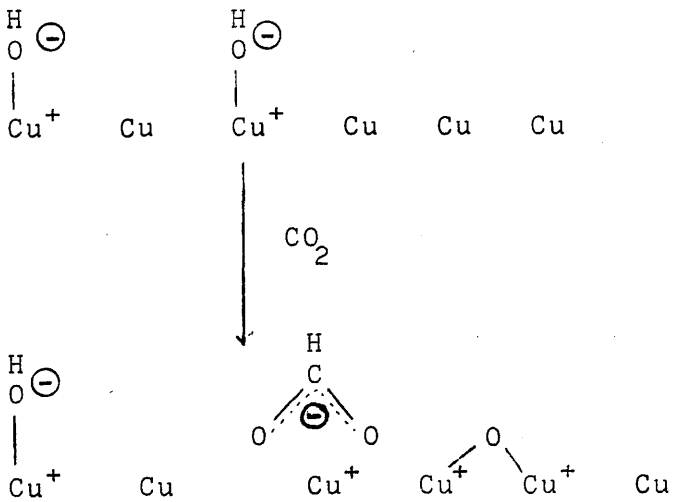

Similar to the adsorption of carbon dioxide on partially oxidised $Cu/ZnO/Al_2O_3$ in the presence of hydrogen, it is likely that during the adsorption of carbon monoxide on both fully oxidised and partially oxidised $Cu/ZnO/Al_2O_3$ in the presence of hydrogen, complex formation occurs.

Studies of the adsorption of carbon monoxide on fully oxidised $Cu/ZnO/Al_2O_3$ in the presence of hydrogen, both in the static and flow systems, revealed that, carbon dioxide is not formed in the gas phase. Indeed this is reflected in the decreased amount of carbon monoxide adsorbed by the fully oxidised catalyst in the presence of hydrogen, 2465 cpm (0.1838 g), relative to that in the absence of hydrogen, 5334 cpm (0.2027 g), although the amounts which can be evacuated are comparable. If carbon monoxide merely adsorbs on the copper sites revealed during hydroxyl formation, the amount which can be evacuated, 25%, should be comparable to that on reduced $Cu/ZnO/Al_2O_3$ (82%).

The amount of carbon monoxide adsorbed on partially oxidised $Cu/ZnO/Al_2O_3$ in the presence of hydrogen (3474 cpm (0.1807 g)) is decreased relative to that in the absence of hydrogen (5603 cpm (2115 g)). By a similar argument to that presented above, complex formation takes place when carbon monoxide is adsorbed on partially oxidised $Cu/ZnO/Al_2O_3$ in the presence of hydrogen since less surface species can be evacuated in this case (24%) compared to the reduced catalyst.

The proposed mechanism for the formation of a surface

complex between adsorbed carbon monoxide and hydroxyl groups, which is similar to part of the mechanistic cycle for the synthesis of methanol as proposed by Vedage et al. (114) is shown below.

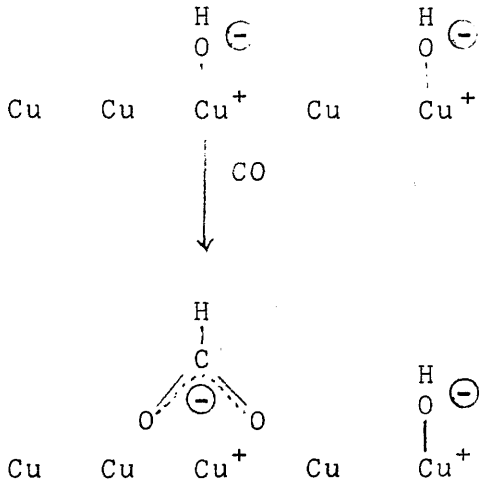

5.4 General Conclusions

It is apparent that during the adsorption of carbon dioxide on reduced $Cu/ZnO/Al_2O_3$ each of the components is actively involved, carbon dioxide being adsorbed in both weak and strong states. On the copper component of the catalyst carbon dioxide dissociates at high energy sites to form carbon monoxide and surface oxygen:-

$$CO_2(g) \rightleftharpoons CO_2(a) \rightleftharpoons CO(a) + O(a)$$

On all the components of the catalyst further slow adsorption of carbon dioxide takes place, possibly with the

formation of carbonate type species. The presence of hydrogen has no substantial effect on the adsorption of this gas on the reduced catalyst.

In the presence of a limited amount of surface oxygen on the copper component of the catalyst, the nature of the adsorbed species is changed in that they are more strongly bonded to the surface, although the amount of carbon dioxide adsorbed remains the same. This suggests that after reduction in hydrogen, some oxygen still remains on the surface of the catalyst.

The fully oxidised $Cu/ZnO/Al_2O_3$ catalyst behaves in a totally different manner to partially oxidised $Cu/ZnO/Al_2O_3$ in that sites for the adsorption of carbon dioxide on the copper component are partially, if not totally, blocked.

Evidence has been obtained for the adsorption of hydrogen on both fully oxidised and partially oxidised $Cu/ZnO/Al_2O_3$ to give hydroxyl groups and weakly adsorbed hydrogen atoms:-

$$H_2(g) \longrightarrow H_2(a) \xrightarrow{O(a)} OH(a) + H(a)$$

During this process some copper surface area is regenerated. It is deduced that an ensemble of copper atoms is required for the adsorption of carbon dioxide since no detectable amount of carbon dioxide adsorbs on the copper component of a fully oxidised catalyst in the presence of hydrogen. In sharp contrast, complex formation takes place during the adsorption of carbon dioxide on the partially oxidised catalyst in the presence of hydrogen. It is proposed that

this complex is $HCO_2^-(a)$.

In contrast with the adsorption of carbon dioxide on reduced $Cu/ZnO/Al_2O_3$, carbon monoxide adsorbs almost exclusively on the copper component of the catalyst as a weakly and reversibly bonded species. Hydrogen has no effect on the adsorption of carbon monoxide on the reduced catalyst.

Oxidation of the copper component, either partially or fully, results in an enhanced adsorption of carbon monoxide on the catalyst as detected by the G.-M. tubes. This is attributed to the formation and subsequent adsorption of carbon dioxide from the reaction between carbon monoxide and surface oxygen:-

$$CO(g) \rightleftharpoons CO(a) \xrightleftharpoons{O(a)} CO_2(a) \rightleftharpoons CO_2(g)$$

Complex formation, possibly $HCO_2^-(a)$, takes place during the adsorption of carbon monoxide on the oxidised (partially or fully) catalyst in the presence of hydrogen.

Carbon dioxide and carbon monoxide compete for sites on the copper component of the reduced catalyst.

The overall mechanism for the adsorption of carbon dioxide, carbon monoxide and hydrogen on reduced $Cu/ZnO/Al_2O_3$ and partially oxidised $Cu/ZnO/Al_2O_3$ is summarised in Figures 5.2 and 5.3 respectively.

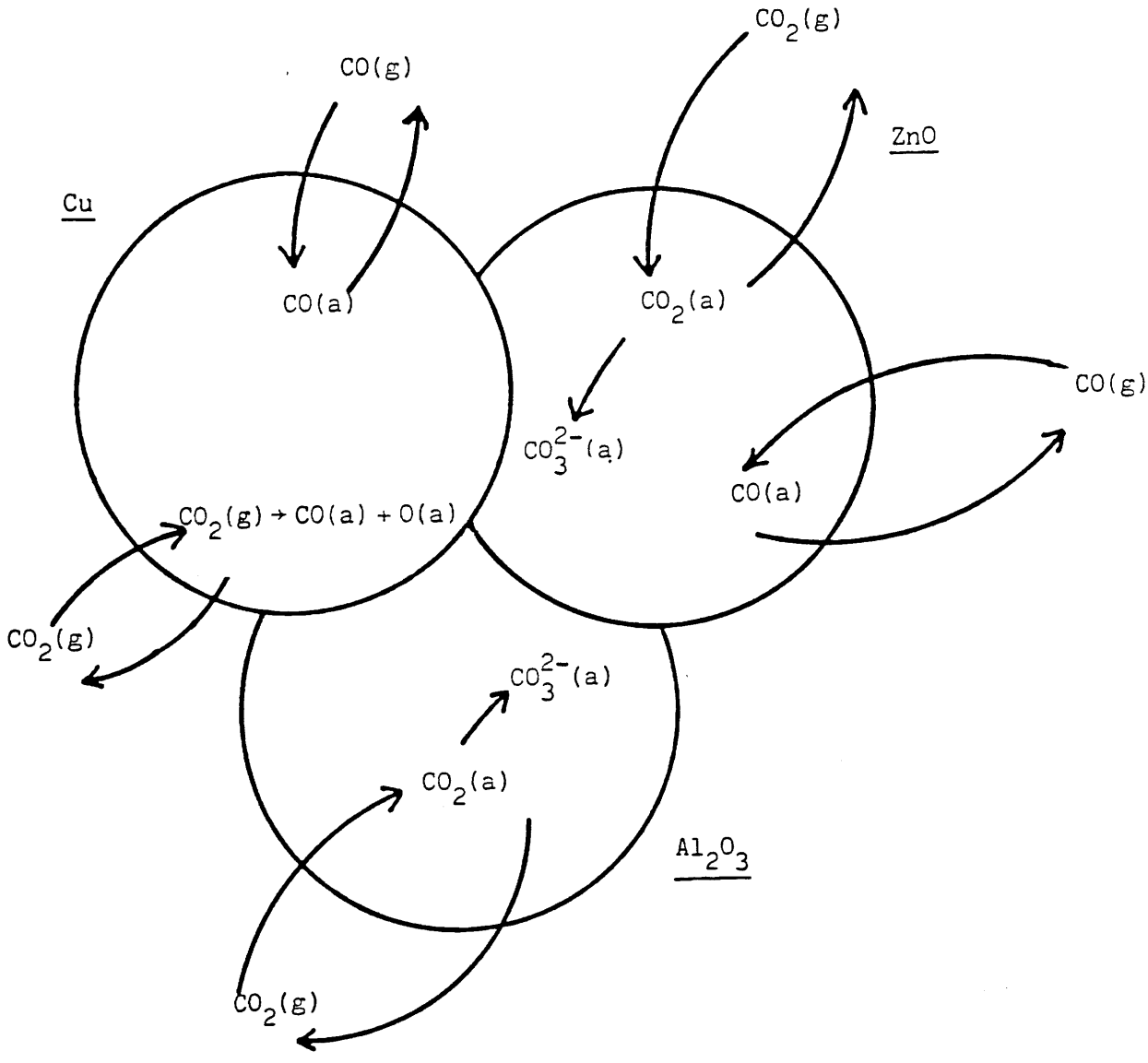

Figure 5.2 Adsorption of Carbon Dioxide and Carbon Monoxide on Reduced $Cu/ZnO/Al_2O_3$ at Ambient Temperature.

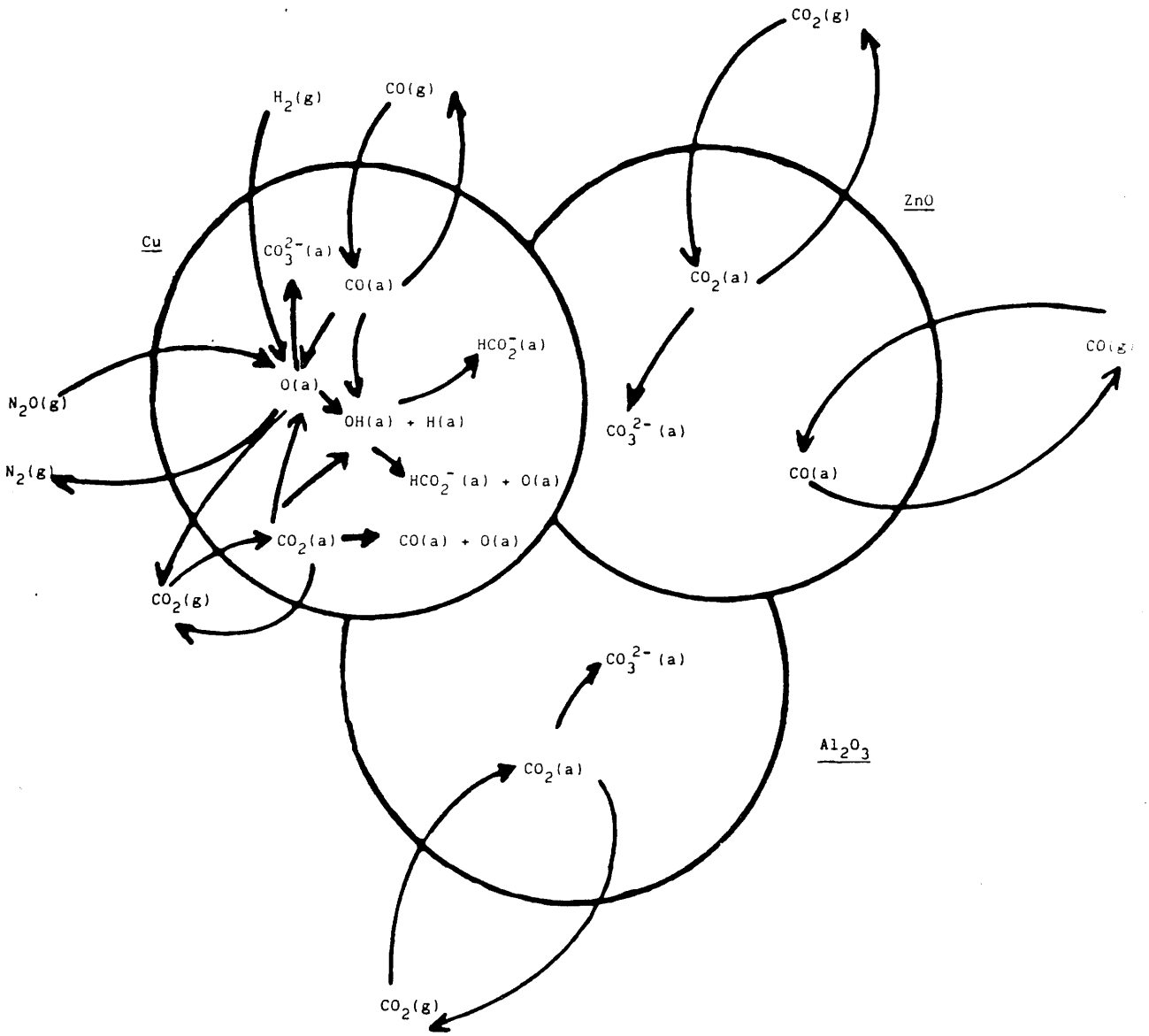

Figure 5.3 Adsorption of Carbon Dioxide, Carbon Monoxide and Hydrogen on Partially Oxidised $Cu/ZnO/Al_2O_3$ at Ambient Temperature.

REFERENCES

1. Chang, C.D., and Silvestri, A.J., J. Catal. 47, 249 (1977).
2. Meisel, S.L., McCullough, J.P., Lenchthaler, C.H. and Weisz, P.B., Chem. Tech. 2, 86 (1976).
3. Ullmann,F. "Enzyclopädie der technischen Chemie", vol VI, p.170, Berlin-Wein, 1930.
4. Hibben, J.H., Ind. Eng. Chem. 46, 1127 (1954).
5. Denny, P.J., and Whan, D.A., Catalysis (London) 2, 46 (1978).
6. Lormand, C., Ind. Eng. Chem. 17, 430 (1925).
7. Natta, G., Catalysis 3, 349 (1955).
8. Patart, M., French Patent 540,343 (Aug. 1921).
9. Audibert, E., and Raineau, A., Ind. Eng. Chem. 20, 1105 (1928).
10. Klier, K., Adv. Catal. 31, 243 (1982).
11. Friedrich, J.B., Wainwright, M.S., and Young D.J., J. Catal. 80, 1 (1983).
12. Natta, G., G. Chim. ind. appl. 12, 13 (1930).
13. Natta, G., Brev. Ital. 267, 698 (1928).
14. Bowker, M., Hyland, J.N.K., Vandervell, H.D., and Waugh, K.C., in Proc. 8th Int. Congr. Catal., 1984 (Verlag Chemie, Weinheim, 1985) vol. II p.35.
15. Bowker, M., Houghton, H., and Waugh, K.C., J. Chem. Soc., Faraday Trans. I, 77, 3023 (1981).

16. Dandy, A.J., J. Chem. Soc. 5, 5956 (1963).

17. Fuderer-Luetić, P., and Sviben, I., J. Catal. 4, 109 (1965).

18. Morelli, F., Giorgini, M., and Tartarelli, R., J. Catal. 26, 106 (1972).

19. Frolich, P.K., Fenske, M.R., Perry, L.R., and Hurd, N.L., J. Am. Chem. Soc. 51, 187 (1929).

20. Kostelitz, O., and Hensinger, G., Chim. Ind. 40, 757, (1939).

21. Dolgov, B.N., Karpinskii, M.H., Khimiya tverd Topl. 3, 559 (1932).

22. Molstad, M.C., and Dodge, B.F., Ind. Eng. Chem. 27, 134 (1935).

23. Lazier, W.A., and Vaughen, J.V., J. Am. Chem. Soc. 54, 3080 (1932).

24. Hüttig, G.F., Strial, K.S., and Kittel, H., Z. Elektrochem. 39, 368 (1933).

25. Hüttig, G.F., Meyer, T., Kittel, H., and Cassirer, S., Z. anorg. allg. Chem. 224, 225 (1935).

26. Hüttig, G.F., and Theimer, H., Z. anorg. allg. Chem. 246, 51 (1941).

27. Hüttig, G.F., and Theimer, H., Kolloid Z. 100, 162 (1942).

28. Kostelitz, O., Hüttig, G.F., Kittel, H., and Radler, H., Naturwiss 20, 640 (1932).

29. Ogino, Y., Oba, M., and Uchida, H., Bull, Chem. Soc. Jpn. 32, 284 (1959).

30. Ogino, Y., and Nakajima, S., J. Catal. 9, 251 (1967).

31. Andrew, S.P.S., 7th Int. Congr. Catal., Post Congr. Symp., Osaka, Plenary Lecture (Paper 12), July 1980.

32. Herman, R.G., Simmons, G.W., and Klier, K., in Proc. 7th Int. Congr. Catal., 1980 (Elsevier, Amsterdam, 1981) vol. A, p 475.

33. Fischer, A., Hosemann, R., Vogel, W., Koutecký, J., Pohl, J., and Rálek, M., in Proc. 7th Int. Congr. Catal., 1980 (Elsevier, Amsterdam, 1981) vol. A, p 341.

34. Kostelitz, O., and Huttig, G.F., Kolloid Z. 67, 265 (1934).

35. Sabatier, P., and Senderens, J.B., Ann. Chim. Phys. 4, 418 (1905).

36. Sabatier, P., and Mailhe, A., C.R. 146, 1376 (1908).

37. Frolich, P.K., Fenske, M.R., and Quiggle, D., Ind. Eng. Chem. 20, 694 (1928).

38. Frolich, P.K., Fenske, M.R., Taylor, P.S., and Southwich, C.A., Ind. Eng. Chem. 20, 1327 (1928).

39. Frolich, P.K., Davidson, R.L., and Fenske, M.R., Ind. Eng. Chem. 21, 109 (1929).

40. Fleury, M., Meml Poud. 24, 10 (1931).

41. Herman, R.G., Klier, K., Simmons, G.W., Finn, B.P., Bulko, J.B., and Kobylinski, T.P., J. Catal. 56, 407 (1979).

42. Mehta, S., Simmons, G.W., Klier, K., and Herman, R.G., J. Catal. 57, 339 (1979).

43. Bulko, J.B., Herman, R.G., Klier, K., and Simmons, G.W., J. Phys. Chem. 83, 3118 (1979).

58. Waugh, K.C., Denny, P.J., and Parker, D., Prepr. Amer. Chem. Soc. Meeting on Activation of Carbon Oxides by Oxides and Metals, Miami Beach (April 1985).

59. Kagan, Yu, B., Rozovskii, A. Ya., Lin, G.I., Slivinskii, E.V., Loktev, S.M., Liberov, L.G., and Bashkirov, A.N., Kinet. Katal. 16, 809 (1975).

60. Rozovskii, A. Ya., Kagan, Yu, B., Lin, G.I., Slivinskii, E.V., Loktev, S.M., Liberov, L.G., and Bashkirov, A.N., Kinet. Katal. 16, 810 (1975).

61. Kagan, Yu, B., Rozovskii, A. Ya., Liberov, L.G., Slivinskii, E.V., Lin, G.I., Loktev, S.M., and Bashkirov, A.N., Dokl. Akad. Nauk SSSR. 224, 1081 (1975).

62. Parris, G.E., and Klier, K., J. Catal. 97, 374 (1986).

63. Klier, K., Chatikavanij, V., Herman, R.G., and Simmons, G.W., J. Catal. 74, 343 (1982).

64. Ruggeri, O., Trifirò, F., Vaccari, A., J. Solid State Chem. 42, 120 (1982).

65. Lui, G., Willcox, D., Garland, M., and Kung, H.H., J. Catal. 96, 251 (1985).

66. Garner, W.E., J. Chem. Soc. 1239 (1947).

67. Winter, E.R.S., Adv. Catal. 10, 196 (1958).

68. John, C.S., Catalysis (London) 3, 169 (1980).

69. Eischens, R.P., Pliskin, W.A., and Low, M.J.D., J. Catal. 1, 180 (1962).

70. Boccuzzi, F., Borello, E., Zecchina, A., Bossi, A., Camia, M., J. Catal. 51, 150 (1978).

71. Roberts, D.L., and Griffin, G.L., Appl. Surf. Sci. 19, 298 (1984).

72. Nagarjunan, T.S., Sastri, M.V.C., and Kuriacose, J.C., J. Catal. 2, 223 (1963).

73. Aharoni, C., and Tompkins, F.C., Trans. Faraday Soc. 66, 434 (1970).

74. Boccuzzi, F., Garrone, E., Zecchina, A., Bossi, A., and Camia, M., J. Catal. 51, 160 (1978).

75. Solymosi, F., Erdőhelyi, A., and Lancz, M., J. Catal. 95, 567 (1985).

76. Cotton, F.A., and Wilkinson, G., "Advanced Inorganic Chemistry", 3rd ed., p. 687, Wiley, New York, 1972.

77. Boccuzzi, F., Ghiotti, G., and Chiorino, A., Surf. Sci. 156, 933 (1985).

78. Hollins, P., and Pritchard, J., Surf. Sci. 134, 91 (1983).

79. Wachs, I.E., and Madix, R.J., J. Catal. 53, 208 (1978).

80. Hierl, R., Knözinger, H., and Urbach, H.P., J. Catal. 69, 475 (1981).

81. Stone, F.S., and Tiley, P.F., Discuss. Faraday Soc. 8, 254 (1950).

82. Garner, W.E., Gray, T.J., and Stone, F.S., Discuss. Faraday Soc. 8, 246 (1950).

83. Habraken, F.H.P.M., Mesters, C.M.A.M., and Bootsma, G.A., Surf. Sci. 97, 264 (1980).

84. Russell, J.N., Gates, S.M. and Yates, J.T., Surf. Sci. 163, 516 (1985).

85. Wachs, I.E., and Madix, R.J., Appl. Surf. Sci., 1, 303 (1978).

86. Mesters, C.M.A.M., Vink, T.J., Gijzeman, O.L.J., and Geus, J.W., Surf. Sci. 135, 428 (1983).

87. Balooch, M., Cardillo, M.J., Miller, D.R., and Stickney, R.E., Surf. Sci. 46, 358 (1974).

88. Cadenhead, D.A., and Wagner, N.J., J. Catal. 21, 312 (1971).

89. Eberhardt, W., Cantor, R., Greuter, F., and Plummer, E.W., Solid State Commun. 42, 799 (1982).

90. Greuter, F., and Plummer, E.W., Solid State Commun. 48, 37 (1983).

91. Mikovsky, R.J., Boudart, M., and Taylor, H.S., J. Am. Chem. Soc. 76, 3814 (1954).

92. Alexander, C.S., and Pritchard, J., J. Chem. Soc., Faraday Trans. I. 68, 202 (1972).

93. Pritchard, J., Catterick, T., and Gupta, R.K., Surf. Sci. 53, 1 (1975).

94. Anderson, A.B., Surf. Sci. 62, 119 (1977).

95. Pritchard, J., Surf. Sci. 79, 231 (1979).

96. Barber, M., Vickerman, J.C., and Wolstenholme, J., J. Chem. Soc.,Faraday Trans. I, 72, 40 (1976).

97. Chatikavanij, V., M.S. Thesis, Lehigh University, 1980.

98. Dell, R.M., Stone, F.S., and Tiley, P.F., Trans. Faraday Soc. 49, 195 (1953).

99. Joyner, R.W., McKee, C.S., and Roberts, M.W., Surf. Sci. 26, 303 (1971).

100. Hollins, P., and Pritchard, J., Surf. Sci. 89, 486 (1979).

101. Grabke, V.H.J., Ber. Bunsenges. phys. Chem. 71, 1067 (1967).

102. Bernstein, R.B., and Taylor, T.I., Science 106, 498 (1947).

103. Narita, K., Takezawa, N., Kobayashi, H., and Toyoshima, I., React. Kinet. Catal. Lett. 19, 91 (1982).

104. Evans, J.W., Wainwright, M.S., Bridgewater, A.J., and Young, D.J., Appl. Catal. 7, 75 (1983).

105. Chinchen, G.C., and Waugh, K.C., private communication to G. Webb.

106. Solymosi, F., Erdöhelyi, A., and Kocsis, M., J. Catal. 65, 428 (1980).

107. Chinchen, G.C., and Jackson, S.D., private communication to G. Webb.

108. Friedlander, G., and Kennedy, J.W., "Nuclear and Radiochemistry", 2nd ed., p.202, Wiley, New York, 1956.

109. Wells, P.B., Appl. Catal. 18, 259 (1985).

110. Arafa, E.A., M.Sc. Thesis, University of Glasgow, 1985.

111. Hadden, R.A., and Webb, G., unpublished results.

112. Roberts, M.W., and Ryder, R., unpublished results.

113. Packer, K.J., Dennison, P., and Spencer, M.S., unpublished results.

114. Vedage, G.A., Pitchai, R., Herman, R.G., and Klier, K., in Proc. 8th Int. Congr. Catal., 1984 (Verlag Chemie, Weinheim, 1985) vol. II p.47.